creative commons
COMMONS DEED

저작자표시-비영리-동일조건변경허락 2.0 대한민국

이용자는 아래의 조건을 따르는 경우에 한하여 자유롭게

- 이 저작물을 복제, 배포, 전송, 전시, 공연 및 방송할 수 있습니다.
- 이차적 저작물을 작성할 수 있습니다.

다음과 같은 조건을 따라야 합니다:

저작자표시. 귀하는 원저작자를 표시하여야 합니다.

비영리. 귀하는 이 저작물을 영리 목적으로 이용할 수 없습니다.

동일조건변경허락. 귀하가 이 저작물을 개작, 변형 또는 가공했을 경우에는, 이 저작물과 동일한 이용허락조건하에서만 배포할 수 있습니다.

- 귀하는, 이 저작물의 재이용이나 배포의 경우, 이 저작물에 적용된 이용허락조건을 명확하게 나타내어야 합니다.
- 저작권자로부터 별도의 허가를 받으면 이러한 조건들은 적용되지 않습니다.

저작권법에 따른 이용자의 권리는 위의 내용에 의하여 영향을 받지 않습니다.

이것은 이용허락규약(Legal Code)을 이해하기 쉽게 요약한 것입니다.

Disclaimer

dCollection

Coupled Map Lattice based Homeostatic Complex Systems

Dharani Punithan
Department of Computer Science & Engineering
Seoul National University

A thesis submitted for the degree of
Doctor of Philosophy
February, 2014

Abstract

Homeostasis is the ability to regulate the essential variables of a complex system within a viability zone in the face of perturbations. It is a core complexity phenomenon for understanding real or artificial life. In this thesis, we explore the interplay between nonlinear system dynamics and complex topologies in such homeostatic (self-regulating) systems.

We investigate the self-causing nature of homeostasis in artificial and real-world complex systems. We analyse planetary and ecological homeostasis using daisyworld system – a cybernetic proof of Gaia hypothesis and apply those principles to demonstrate the social homeostasis in stock market. We reconstruct the formulations of the original daisyworld based on Coupled Map Lattice (CML) which enable us to investigate a wide range of rich features of complex systems covering different arenas such as system science, nonlinear science and network science.

Our study reveals that daisyworld is a self-oganizing system and a reaction-diffusion (activator-inhibitor) system exhibiting an array of fascinating pattern formations – complex patterns, Turing-like structures, cyclic patterns, random patterns and uniform dispersed patterns for different parameter settings. The phenomenon governing the self-organizing pattern formation in our system is observed in biological systems (schooling of fish, animal coat formation, etc.) as well as in non-living systems (Turing's reaction-diffusion system, Belousov-Zhabotinsky reaction, Bénard convection, etc.).

We incorporate evolutionary interactions in our system via replicator-mutator mechanisms. The results underline the importance of balance between ecosystem feedback and ecosystem disturbance in

generating spatially coexistence of domains of dominance among the original daisies and their mutants and adaptants.

We inspect our system based on small-world graphs (complex topologies) embodying realistic couplings via the Watts-Strogatz (WS), Newman-Watts models and Smallest-world (SW) models. We examine our system on an adaptive topology (adding connections with more realistic mechanisms) where there exists a feedback between the local dynamics and the topology. We introduce scale-freeness into our system with high clustering.

We thus perturb our system through system parameters, system topologies and evolutionary changes. In all scenarios, our system self-regulates the environment and thus life persists, and thereby demonstrating robustness. We also introduce metrics Moran's I and permutation entropy to measure the spatio-temporal dynamics of the system.

Our remarkable finding is that by applying the dynamical linking mechanisms to our system on regular lattice can self-organise to a lattice with small-world phenomenon. We observe 'completely coherent (homogeneous) short-lived cyclical dominance' even with a small fraction of long-range couplings in complex and adaptive topologies. This apparent behaviour is seen in social, political and economical realms.

Our system yields profound insights and implications, from which we derive an analogy with stock market. Based on an "Ecosystem Approach", we analyse the feedback between market sentiment and stock price. We collect $\$APPL$ tweets from twitter and stock data from Yahoo finance and demonstrate their homeostatic nature. We compare stock market with other social homeostatic systems in nature such as termite colonies. Thus our study on self-causing systems helps both in understanding existing self-regulating systems and in modelling new artificial homeostatic system.

Keywords: complex systems, system thinking,
nonlinear thinking, network thinking,
collective dynamics, pattern formation,
self-organization, emergence,
reaction-diffusion system,
Turing instabilities, activator-inhibitor system,
Moore neighbourhood, Laplacian diffusion,
logistic growth model (Verhulst model),
chaos, bifurcation, attractors,
Coupled Map Lattice (CML),
Gaia hypothesis, daisyworld,
homeostasis, cybernetics, feedbacks,
graph theory,
small-world network, small-world phenomena,
Watts-Strogatz, Newman-Watts, Smallest-world,
adaptive network, scale-free network,
degree distribution, Poisson distribution,
power law distribution, long-fat-tail distribution,
clustering coefficient, characteristic path length,
proximity ratio,
phase transition and critical phenomenon,
Moran's I, permutation entropy,
replicator-mutator mechanisms,
sentiment analysis, machine learning,
Naive Bayes, Support Vector Machine,
Granger causality,
Engle–Granger two-step method,
Phillips–Ouliaris cointegration test

Student Number: 2008-30708

Contents

Contents v

List of Figures xi

List of Tables xix

1 Introduction 1

1.1 Homeostatic Complex Systems 2
1.2 Daisyworld 3
1.3 Limitations of Daisyworld Models 4
1.4 Motivation 4
1.5 Inspirations from Nature 5
1.6 Contribution 5
1.6.1 Incorporation of Complex Spatio-temporal Dynamics . . 6
1.6.2 Demonstration as Complex Systems 7
1.6.3 Incorporation of Evolutionary Mechanisms 8
1.6.4 Introduction of Spatio-temporal Quantification 9
1.6.5 Incorporation of Complex and Adaptive Topological Properties 9
1.6.6 Applications (Demonstration of Social Homeostasis in Stock Market) 11
1.7 Outline 11

2 Background **13**

2.1 Complexity Science : A Means to Understanding Complex Systems . . . 13

2.1.1 Systems Thinking . . . 14

2.1.2 Nonlinear Thinking . . . 19

2.1.3 Network Thinking . . . 20

2.1.4 Collective Behaviour . . . 25

2.1.5 Pattern Formation . . . 26

2.2 Modelling Tools . . . 28

2.2.1 Daisyworld Model (Life-Environment Bidirectional Feedback Model) . . . 28

2.2.2 Logistic Growth Model (Verhulst Model) . . . 32

2.2.3 Replicator Mutator Model . . . 34

2.2.4 Neighbourhood Models . . . 34

2.2.5 Diffusion Models . . . 35

2.2.6 Spatio-temporal Model – Coupled Map Lattice (CML) . . . 35

2.2.7 Graph (Network) Models . . . 37

2.3 Quantification of Spatio-Temporal Dynamics . . . 42

2.3.1 Permutation Entropy (PE): . . . 42

2.3.2 Moran's I (MI): . . . 43

3 Homeostatic Complex System based on Daisyworld Modelling **45**

3.1 Reconstructed Core Daisyworld Model . . . 46

3.1.1 Solar Insolation . . . 50

3.1.2 Albedo . . . 50

3.1.3 Growth . . . 50

3.1.4 Temperature . . . 51

3.1.5 Population Size . . . 51

3.2 Limiting Similarity (Temperature Overlap) . . . 52

3.3 Incorporation of Complex Topological Properties . . . 54

3.4 Experimental Setup . . . 55

3.4.1 Parameter Settings . . . 55

3.4.2 Initializations . . . 56
3.4.3 Visualisations . . . 56

4 Daisyworld with Local Couplings 57
4.1 Self-Organizing Spatio-temporal Patterns . . . 57
4.1.1 Variable Parameter Settings . . . 58
4.1.2 Self-organized Complex Pattern . . . 58
4.1.3 Turing-like Structure . . . 59
4.1.4 Cyclical Pattern . . . 60
4.1.5 Random Pattern . . . 61
4.1.6 Dispersed Pattern . . . 62
4.1.7 Discussion . . . 62
4.1.8 Summary . . . 65
4.2 Locally Chaotic and Globally Stable Dynamics (Temporal Fluctuations and Spatial Stability) . . . 67
4.2.1 Spatial Stability . . . 70
4.2.2 Temporal Fluctuations . . . 71
4.2.3 Summary . . . 72
4.3 Homeostasis with Evolutionary Dynamics . . . 73
4.3.1 Modification to Core Model . . . 77
4.3.2 Variable Parameter Settings . . . 80
4.3.3 Baseline Scenario: No Mutation . . . 81
4.3.4 Phenotypic Variability – Mutation . . . 85
4.3.5 Adaptation – Exploring New Environments . . . 90
4.3.6 Summary . . . 94
4.4 Quantification of the Daisyworld Model . . . 95
4.4.1 Statistical Measures and Spatio-Temporal Dynamics . . . 95
4.4.2 Parameter Space Analysis of the Daisyworld Model . . . 97

5 Daisyworld with Complex Couplings 99
5.1 Variable Parameter Settings . . . 99
5.2 Benchmark Graph Models . . . 100

5.2.1 Degree Distribution of Benchmark Models 100
5.2.2 Regular Graph 101
5.2.3 Random Graph 102
5.2.4 Fully Connected Graph 102
5.3 Small-world Phenomenon 103
5.3.1 Indentifying the Small-world Regime 105
5.3.2 Degree Distribution of Small-world Models 105
5.3.3 Daisyworld with Static Local and Non-local Couplings . 107
5.3.4 Possible Critical Point of Phase Change 111
5.3.5 Topology and Criticality 113
5.3.6 Without Life-Environment Feedback 116
5.3.7 Summary 117
5.4 Adaptive Couplings 118
5.4.1 Daisyworld with Dynamic Local and Non-local Couplings 119
5.4.2 Topological Properties of NW-CML and Adaptive CML 120
5.4.3 Topological Evolution 122
5.4.4 Summary 125
5.5 Scale-freeness 125
5.5.1 Degree Distribution of Scale-free Graph 126
5.5.2 Daisyworld with Hubs 126
5.5.3 Summary 127
5.6 Behaviour Study 127
5.6.1 Daisyworld Behaviour in Complex and Adaptive Topologies 127
5.6.2 Social Collective Behaviour 128
5.6.3 Analogies with Popular Metaphors 129
5.6.4 A Comparative Study 129

6 Applications – Demonstration of Social Homeostasis in Stock Market 139
6.1 Introduction 139
6.2 Daisyworld - Stock Market Analogy 140

6.2.1 Daisyworld Behaviour . . . 141
6.2.2 Stock Market Behaviour . . . 141
6.2.3 Comparison of Behaviours – An Ecosystem Approach . 142
6.3 Background . . . 142
6.3.1 Sentiment Analysis and Microblogging Services . . . 142
6.3.2 Supervised Classification . . . 143
6.3.3 Twitter API . . . 145
6.4 Sentiment Analysis on Apple ($*AAPL*) Stock Market Tweets . 145
6.4.1 Data Collection . . . 145
6.4.2 Tweet Text Pre-Processing . . . 146
6.4.3 Training the Classifier . . . 147
6.4.4 Sentiment Score . . . 148
6.5 Demonstration of Social Homeostasis . . . 148
6.6 Discussion . . . 149
6.6.1 Social Mood Trends - A Psychological Perspective . . . 149
6.6.2 Stock Market - A Termite Colony . . . 150
6.7 Summary . . . 151

7 Conclusion **153**
7.1 Summary . . . 153
7.2 Conclusion . . . 156
7.3 Future Directions . . . 156

Bibliography **159**

List of Figures

2.1 Linear Cause-and-Effect : A system consisting of components A, B and C 14

2.2 Circular Cause-and-Effect : A system consisting of components A, B and C 14

2.3 System with Feedback Mechanisms 15

2.4 Reinforcing Process 15

2.5 Balancing Process 15

2.6 Adaptive Network (Source : [Gross and Blasius, 2008]) 24

2.7 Neighbourhood Models 34

3.1 Overlap of Growth Curves of Black and White Daisies 53

4.1 Maze like Organization for 10% Overlap, $D_c = 0.001$, $D = 0.2$, $r = 1$ and NL= 0.001 in 2D 100×100 Lattice 59

4.2 Local Dynamics of Maze : 10% Overlap, $D_c = 0.001$, $D = 0.2$, $r = 1$ and NL= 0.001 in 2D 100×100 Lattice 60

4.3 Global Dynamics of Maze : 10% Overlap, $D_c = 0.001$, $D = 0.2$, $r = 1$ and NL= 0.001 in 2D 100×100 Lattice 61

4.4 Turing-like Structure for 100% Overlap, $D_c = 0.01$, $D = 0.2$, $r = 1$, $NL = 1$ in 2D 100×100 Lattice 62

4.5 Local Dynamics of Turing-like Structure : 100% Overlap, $D_c = 0.01$, $D = 0.2$, $r = 1$ and NL= 1 in 2D 100×100 Lattice 63

4.6 Global Dynamics of Turing-like Structure : 100% Overlap, $D_c = 0.01$, $D = 0.2$, $r = 1$ and NL= 1 in 2D 100×100 Lattice 64
4.7 Cyclical Pattern : 10% overlap, $D_c = 0.2$, $D = 0.2$, $r = 1$ and NL= 0.05 in 2D 100×100 Lattice 65
4.8 Local Dynamics of Cyclical Pattern : 10% overlap, $D_c = 0.2$, $D = 0.2$, $r = 1$ and NL= 0.05 in 2D 100×100 Lattice 66
4.9 Global Dynamics of Cyclical Pattern : 10% overlap, $D_c = 0.2$, $D = 0.2$, $r = 1$ and NL= 0.05 in 2D 100×100 Lattice 67
4.10 Random Pattern : 10% Overlap, $D_c = 0$, $D = 0.2$, $r = 1$ and $NL = 0.01$ in 2D 100×100 Lattice 68
4.11 Local Dynamics of Random Pattern : 10% Overlap, $D_c = 0$, $D = 0.2$, $r = 1$ and $NL = 0.01$ in 2D 100×100 Lattice 69
4.12 Global Dynamics of Random Pattern : 10% Overlap, $D_c = 0$, $D = 0.2$, $r = 1$ and $NL = 0.01$ in 2D 100×100 Lattice 70
4.13 Uniformly Dispersed Pattern : Overlap=10%, $D_c = 0$, $D = 0.2$, $r = 1$ and $NL = 0.5$ in 2D 100×100 Lattice 71
4.14 Local Dynamics of Uniformly Dispersed Pattern : 10% Overlap, $D_c = 0$, $D = 0.2$, $r = 1$ and $NL = 0.5$ in 2D 100×100 Lattice . 72
4.15 Global Dynamics of Uniformly Dispersed Pattern : 10% Overlap, $D_c = 0$, $D = 0.2$, $r = 1$ and $NL = 0.5$ in 2D 100×100 Lattice 73
4.16 Bifurcation Diagram of Daisyworld – Black Daisy Population . 74
4.17 Bifurcation Diagram of Daisyworld – White Daisy Population . 74
4.18 Population Dynamics in 100×100 2D CML with 10% Overlap, $D_c = 0.01$, $D = 0.2$, $r = 1$ and $NL = 1$ 75
4.19 Global Dynamics of Daisyworld in 100×100 2D CML with 10% Overlap, $D_c = 0.01$, $D = 0.2$, $r = 1$ and $NL = 1$ 76
4.20 Local Dynamics at a specific location (row 54 and column 54) with 10% Overlap, $D_c = 0.01$, $D = 0.2$, $r = 1$ and $NL = 1$ . . . 77
4.21 Cobweb Plot of Local Dynamics at a specific location (row 54 and column 54) with $D_c = 0.01$, $D = 0.2$, $r = 1$ and $NL = 1$ over 5000 Steps 77

4.22 Population abundance without mutation : $D_c = 0.2$, $D = 0.2$, $r = 1$ and $NL = 0.05$ 81
4.23 Local dynamics at habitat (55, 41) without mutation and $NL = 0.05$ 82
4.24 Global dynamics without mutation, $NL = 0.05$ 82
4.25 Population abundance without mutation : $D_c = 0.2$, $D = 0.2$, $r = 1$ and $NL = 3$ 82
4.26 Local dynamics at habitat (55, 50) without mutation, $NL = 3$. 83
4.27 Global dynamics without mutation, $NL = 3$ 83
4.28 Population abundance without mutation : $D_c = 0.2$, $D = 0.2$, $r = 1$ and $NL = 5$ 83
4.29 Local dynamics at habitat (56, 50) without mutation, $NL = 5$. 84
4.30 Global dynamics without mutation, $NL = 5$ 84
4.31 Population abundance with Grey daisies : $D_c = 0.2$, $D = 0.2$, $r = 1$ and $NL = 0.05$ 85
4.32 Local dynamics at habitat (57, 49) with Grey and $NL = 0.05$. 86
4.33 Global dynamics with Grey, $NL = 0.05$ 86
4.34 Population abundance with Grey daisies : $D_c = 0.2$, $D = 0.2$, $r = 1$ and $NL = 2$ 87
4.35 Local dynamics at habitat (54, 43) with Grey and $NL = 2$ . . . 87
4.36 Global dynamics with Grey, $NL = 2$ 88
4.37 Population abundance with Grey daisies : $D_c = 0.2$, $D = 0.2$, $r = 1$ and $NL = 3$ 88
4.38 Local dynamics at habitat (51, 53) with Grey and $NL = 3$ . . . 89
4.39 Global dynamics with Grey, $NL = 3$ 89
4.40 Population abundance without feedback : $D_c = 0.2$, $D = 0.2$ and $r = 1$ at epoch 5000 90
4.41 Population abundance with Warm Black and Cool White daisies : $D_c = 0.2$, $D = 0.2$, $r = 1$ and $NL = 0.05$ 91
4.42 Local dynamics at habitat (51, 50) with Warm Black and Cool White, $NL = 0.05$ 92
4.43 Global dynamics with Warm Black and Cool White, $NL = 0.05$ 92

4.44 Population abundance with Warm Black and Cool White daisies : $D_c = 0.2$, $D = 0.2$, $r = 1$ and $NL = 2$ 92
4.45 Local dynamics at habitat (57, 55) with Warm Black and Cool White, $NL = 2$ 93
4.46 Global dynamics with Warm Black and Cool White, $NL = 2$. 93
4.47 Population abundance with Warm Black and Cool White daisies : $D_c = 0.2$, $D = 0.2$, $r = 1$ and $NL = 3$ 94
4.48 Local dynamics at habitat (52, 61) with Warm Black and Cool White, $NL = 3$ 94
4.49 Global dynamics with Warm Black and Cool White, $NL = 3$. 95
4.50 Moran's I (section 4.2) 96
4.51 Moran's I and PE on 100×100 2D CML with 10% overlap and $r = 1$ 98

5.1 2-lattice Benchmark Models (with $k = 8$ except for fully-connected graph). We omit periodic boundary conditions for clarity, and also show some connections superimposed.
(a) Regular graph ($p = 0$) (b) Random graph ($p = 1$) (c) Fully-connected graph 101
5.2 Degree Distribution of Benchmark Models 101
5.3 Regular CML ($p = 0$) : Overlap=10%, $D_c = 0.2$, $D = 0.2$, $r = 1$ and $NL = 0.001$ in 2D 100×100 102
5.4 Random Lattice($p = 1$) : Overlap=10%, $D_c = 0.2$, $D = 0.2$, $r = 1$ and $NL = 0.001$ in 2D 100×100 103
5.5 Fully Connected Lattice : Overlap=10%, $D_c = 0.2$, $D = 0.2$, $r = 1$ and $NL = 0.001$ in 2D 100×100 103
5.6 2-lattice Small-world Models
(a) Watts-Strogatz (WS) ($p = 0.05$) (b) Newman-Watts (NW) ($p = 0.05$) (c) Smallest World (SW) ($p = 0.05$) 104
5.7 Watts-Strogatz model in 2D 100×100 lattice: Clustering Coefficient, Characteristic Path Length and Proximity Ratio . . . 106

5.8 Newman-Watts model in 2D 100×100 lattice: Clustering Coefficient, Characteristic Path Length and Proximity Ratio . . . 106
5.9 Smallest World model in 2D 100×100 lattice: Clustering Coefficient, Characteristic Path Length and Proximity Ratio . . . 107
5.10 Degree Distribution of Small-world Models . . . 107
5.11 Watts-Strogatz Model ($p = 0.05$) : Overlap=10%, $D_c = 0.2$, $D = 0.2$, $r = 1$ and $NL = 0.001$ in 2D 100×100 Small-world Lattice . . . 108
5.12 Newman-Watts ($p = 0.05$) : Overlap=10%, $D_c = 0.2$, $D = 0.2$, $r = 1$ and $NL = 0.001$ in 2D 100×100 Small-world CML . . . 109
5.13 Smallest-World Model ($p = 0.05$) : Overlap=10%, $D_c = 0.2$, $D = 0.2$, $r = 1$ and $NL = 0.001$ in 2D 100×100 Small-world Lattice . . . 109
5.14 WS close to phase change : Overlap=10%, $D_c = 0.2$, $D = 0.2$, $r = 1$ and $NL = 0.001$ in 2D 100×100 Small-world Lattice ($p = 0.01$) . . . 112
5.15 NW close to phase change : Overlap=10%, $D_c = 0.2$, $D = 0.2$, $r = 1$ and $NL = 0.001$ in 2D 100×100 Small-world Lattice ($p = 0.01$) . . . 112
5.16 SW close to phase change : Overlap=10%, $D_c = 0.2$, $D = 0.2$, $r = 1$ and $NL = 0.001$ in 2D 100×100 Small-world Lattice at epoch $5,000$ . . . 112
5.17 Regular without life-environment feedback: $p = 0$, $D = 0.2$ and $NL = 0.001$ in 2D 100×100 . . . 116
5.18 WS without life-environment feedback: $D = 0.2$ and $NL = 0.001$ in 2D 100×100 Small-world Lattice ($p = 0.05$) . . . 116
5.19 NW without life-environment feedback: $D = 0.2$ and $NL = 0.001$ in 2D 100×100 Small-world Lattice ($p = 0.05$) . . . 116
5.20 SW without life-environment feedback: $D = 0.2$ and $NL = 0.001$ in 2D 100×100 Small-world Lattice ($p = 0.05$) . . . 117
5.21 Adapted Reciprocal Couplings . . . 119

5.22 Adaptive CML : Overlap=10%, $D_c = 0.2$, $D = 0.2$, $r = 1$ and $NL = 0.001$ in 2D 100×100 120
5.23 Degree Distribution 121
5.24 Adapted Reciprocal Couplings 122
5.25 Degree Distribution 123
5.26 Global Temperature dynamics : Overlap=10%, $D_c = 0.2$, $D = 0.2$, $r = 1$ and $NL = 0.001$ 123
5.27 Quick Adaptation : Overlap=10%, $D_c = 0.2$, $D = 0.2$, $r = 1$ and $NL = 0.001$ in 2D 100×100 124
5.28 Slow Adaptation : Overlap=10%, $D_c = 0.2$, $D = 0.2$, $r = 1$ and and $NL = 0.001$ in 2D 100×100 124
5.29 Scale-free Graph 125
5.30 Scale-free Degree Distribution 126
5.31 $D = 0.2$ and $NL = 0.001$ in 2D 100×100 Scale-free CML . . . 126
5.32 Regular CML : Temperature dynamics; $p = 0$, Overlap=10%, $D_c = 0.2$, $D = 0.2$, $r = 1$ and $NL = 0.001$ in 2D 100×100 . . . 131
5.33 Regular CML: Local population dynamics at habitat (57, 50); $p = 0$, Overlap=10%, $D_c = 0.2$, $D = 0.2$, $r = 1$ and $NL = 0.001$ in 2D 100×100 131
5.34 Regular CML : Global population dynamics; $p = 0$, Overlap=10%, $D_c = 0.2$, $D = 0.2$, $r = 1$ and $NL = 0.001$ in 2D 100×100 . . . 131
5.35 Random Lattice: Temperature dynamics; $p = 1$, Overlap=10%, $D_c = 0.2$, $D = 0.2$, $r = 1$ and $NL = 0.001$ in 2D 100×100 . . . 132
5.36 Random Lattice: Local population dynamics at habitat (53, 53); $p = 1$, Overlap=10%, $D_c = 0.2$, $D = 0.2$, $r = 1$ and $NL = 0.001$ in 2D 100×100 132
5.37 Random Lattice: Global population dynamics; $p = 1$, Overlap=10%, $D_c = 0.2$, $D = 0.2$, $r = 1$ and $NL = 0.001$ in 2D 100×100 . . . 132
5.38 Fully Connected Lattice: Temperature dynamics; Overlap=10%, $D_c = 0.2$, $D = 0.2$, $r = 1$ and $NL = 0.001$ in 2D 100×100 . . . 133

5.39 Fully Connected Lattice: Local population dynamics at habitat (50, 46); Overlap=10%, $D_c = 0.2$, $D = 0.2$, $r = 1$ and $NL = 0.001$ in 2D 100×100 133

5.40 Fully Connected Lattice: Global population dynamics; Overlap=10%, $D_c = 0.2$, $D = 0.2$, $r = 1$ and $NL = 0.001$ in 2D 100×100 . . . 133

5.41 Watts-Strogatz Model ($p = 0.05$): Temperature dynamics; Overlap=10%, $D_c = 0.2$, $D = 0.2$, $r = 1$ and $NL = 0.001$ in 2D 100×100 . . . 134

5.42 Watts-Strogatz Model ($p = 0.05$): Local population dynamics at habitat (53, 62); Overlap=10%, $D_c = 0.2$, $D = 0.2$, $r = 1$ and $NL = 0.001$ in 2D 100×100 134

5.43 Watts-Strogatz Model ($p = 0.05$): Global population dynamics; Overlap=10%, $D_c = 0.2$, $D = 0.2$, $r = 1$ and $NL = 0.001$ in 2D 100×100 134

5.44 Newman-Watts CML ($p = 0.05$): Temperature dynamics; Overlap=10%, $D_c = 0.2$, $D = 0.2$, $r = 1$ and $NL = 0.001$ in 2D 100×100 . . . 135

5.45 Newman-Watts CML ($p = 0.05$): Local population dynamics at habitat (52, 58); Overlap=10%, $D_c = 0.2$, $D = 0.2$, $r = 1$ and $NL = 0.001$ in 2D 100×100 135

5.46 Newman-Watts CML ($p = 0.05$): Global population dynamics; Overlap=10%, $D_c = 0.2$, $D = 0.2$, $r = 1$ and $NL = 0.001$ in 2D 100×100 135

5.47 Smallest-World Model ($p = 0.05$): Temperature dynamics; Overlap=10%, $D_c = 0.2$, $D = 0.2$, $r = 1$ and $NL = 0.001$ in 2D 100×100 . . . 136

5.48 Smallest-World Model ($p = 0.05$): Local population dynamics at habitat (54, 44); Overlap=10%, $D_c = 0.2$, $D = 0.2$, $r = 1$ and $NL = 0.001$ in 2D 100×100 136

5.49 Smallest-World Model ($p = 0.05$): Global population dynamics; Overlap=10%, $D_c = 0.2$, $D = 0.2$, $r = 1$ and $NL = 0.001$ in 2D 100×100 136

5.50 Adaptive CML: Temperature dynamics; Overlap=10%, $D_c = 0.2$, $D = 0.2$, $r = 1$ and $NL = 0.001$ in 2D 100×100 137

5.51 Adaptive CML: Local population dynamics at habitat (56, 57); Overlap=10%, $D_c = 0.2$, $D = 0.2$, $r = 1$ and $NL = 0.001$ in 2D 100×100 137
5.52 Adaptive CML: Global population dynamics; Overlap=10%, $D_c = 0.2$, $D = 0.2$, $r = 1$ and $NL = 0.001$ in 2D 100×100 . . . 137
5.53 Scale-free CML ($p = 0.05$): Temperature dynamics; Overlap=10%, $D_c = 0.2$, $D = 0.2$, $r = 1$ and $NL = 0.001$ in 2D 100×100 . . . 138
5.54 Scale-free CML ($p = 0.05$): Local population dynamics at habitat (52, 58); Overlap=10%, $D_c = 0.2$, $D = 0.2$, $r = 1$ and $NL = 0.001$ in 2D 100×100 138
5.55 Scale-free CML ($p = 0.05$): Global population dynamics; Overlap=10%, $D_c = 0.2$, $D = 0.2$, $r = 1$ and $NL = 0.001$ in 2D 100×100 . . . 138

6.1 Self-causing Feedback in Daisyworld 140
6.2 Self-causing Feedback in Stock Market 140
6.3 Supervised Classification (Source : [Bird et al., 2009]) 143
6.4 Sentiment Vs. Price 148

List of Tables

3.1 Basic Equations 48
3.2 Daisyworld Model Equation Set 48
3.3 Optimal Temperature (of black and white daisies with respect to overlap) 53
3.4 Daisyworld Parameter Settings (last six rows are variable parameters, others are fixed) 55

4.1 Variable Parameter Settings 58
4.2 Optimal temp. and albedo of original daisies and their mutants 80
4.3 Evolutionary Dynamics : Representative Parameter Set 81
4.4 Permutation Entropy Regimes 95
4.5 Moran's I Regimes 96
4.6 Local PE (section 4.2) 96
4.7 Global PE (section 4.2) 97

5.1 Representative Parameter Set 100
5.2 $\bar{C}$, $\bar{L}$ and μ; $p = 0.05$ is qualitatively compared with $p = 1$ and quantitatively compared with μ 108
5.3 Possible Critical Point (p) 111
5.4 Spatial Emergence and Std. Dev. of States 113
5.5 Temporal Dynamics and Permutation Entropy 113
5.6 Spatio-temporal Patterns 113

5.7 The range of std. dev. of states and PE of daisies for 25 realizations . . . 114
5.8 Typical Clustering Coefficients and Characteristic Path Lengths 120
5.9 Average($\pm Std.Dev.$) Clustering Coefficients and Characteristic Path Lengths . . . 121
5.10 Adaptation : Clustering Coefficients and Characteristic Path Lengths . . . 122
5.11 Scale-free Graph : Clustering Coefficient and Characteristic Path Length . . . 126

6.1 Parametric Analogy of Daisyworld and Stock Market . . . 141
6.2 p-values of Granger Causality Analysis . . . 149
6.3 p-values of Cointegration Tests . . . 149

Chapter 1

Introduction

> "I think the next century will be the century of complexity."
> Stephen Hawking, *San Jose Mercury News, January 2000*

> "...the nations and people who master the new sciences of complexity will become the economic, cultural, and political superpowers of the next century."
> Heinz Pagels, *The Dreams of Reason: The Computer and the Rise of the Sciences of Complexity(1988)*

In recent decades, the complex system studies have revealed the paradigm shift in our worldviews [Bar-Yam, 2003; Mitchell, 2009] from linear thinking to complexity thinking. Before the world was described by command and control, linear cause-and-effect, centralised control, etc. But today the fundamental nature of the world is described by instability, disorder, chaos theory, bifurcations, turbulence, tipping points, butterfly effects, etc.

Traditional science focuses on simple cause-and-effect relationships – linear worldview in which the output of a system is proportional to its input. For example, the ideal gas law, $PV = nRT$ where P is the pressure of the gas, V is the volume of the gas, n is the amount of substance of gas, T is the temperature of the gas and R is the ideal gas constant. This reductionist approach of an "additive model", where "the composite whole is the sum of its component parts", enables us to predict the outcome based on the initial

conditions. For instance, the ideal gas law enables us to predict pressure given the initial temperature, volume, and quantity of a gas.

But our complex world is dynamic and unpredictable, exhibiting nonlinear patterns. Examples include unpredictability of weather, epidemics, economic, political and cultural behaviours of societies, stock price movement, etc. Complexity science reframes our worldview as "holistic" – where "the whole is more than the sum of the parts" [Von Bertalanffy, 1968]. The logistic equation $x_{t+1} = rx_t(1 - x_t)$ where x is a dynamical variable, r is bifurcation parameter and t is time. This simple (nonlinear) equation, when iterated, results in very complex forms – logistic map. By altering the value of r in the logistic equation, we can generate a variety of complex patterns, including fixed-point attractors, periodic attractors (bifurcations), and strange (chaotic) attractors [May, 1976].

Complexity emerge from simple rules and feedback mechanisms. Examples include climate change, stock market behaviour, human immune system, World Wide Web, Wood Wide Web, human brain, termite colony, etc. Complexity is an approach to problems in many diverse disciplines including artificial intelligence, artificial life, agent-based modelling, computer science, economics, evolutionary computation, sociology, etc.

1.1 Homeostatic Complex Systems

Complex system comprises of a network of nonlinear interactions involving multiple positive and negative feedback loops among huge number of lower-level components (agents) resulting in a higher-level emergence which is manifested as collective behaviours, self-organization and self-regulation [Mitleton-Kelly, 2003; Prigogine, 1997]. Complex systems can evolve towards homeostasis [Tregonning and Roberts, 1979] where the complex dynamics rest on balance between positive and negative feedbacks. Examples of such cybernetic systems include daisyworld, stock market, predator-prey system, etc. In this thesis, we investigate daisyworld where self-regulation of the physical environment emerge by the influence of biota.

1.2 Daisyworld

Daisyworld[Watson and Lovelock, 1983] model imitates the real feedback structure of the earth and captures the characteristic behaviour especially self-regulation. It provides mathematical justification for Lovelock's well-known Gaia hypothesis [Lovelock, 1972]. It is an imaginary planet where only two types of species live – black and white daisies. These biotic components interact stigmergically via an abiotic component – temperature. The different colours of the daisies influence the albedo (reflectivity) – environment-altering trait – of the planet.

In the beginning, the atmosphere of the daisyworld is cooler and only black daisies thrive as they absorb all the energy. As the black daisy population expands, it warms the planet. When it is too warm for black daisies to survive, white daisies start to bloom since they reflect all the energy back into space. As the white daisy cover spreads, it cools the planet. When it is too cold for the survival of white daisies, again black daisies thrive. This emergence leads to an infinite dance of black and white daisies. This endless cycle, owing to the bi-directional feedback loop between life and the environment, self-regulates the temperature and thereby allows life to persist.

Thus, it demonstrates the emergence of homeostasis as a consequence of the feedback loop between life and its environment. This ecosystems model has subsequent application in a number of fields (refer 2.2.1). The original daisyworld was modelled on a one-point (0D) world. It was subsequently extended to a one-dimensional (1D) world by Adams et al. [2003], to a flat two-dimensional (2D) world by von Bloh et al. [1997] and to a curved 2D world by Ackland et al. [2003] and Ackland and Wood [2010]. We have taken daisyworld as our base model and reconstruct formulations to incorporate complex dynamical features.

1.3 Limitations of Daisyworld Models

- All 2D spatial extension of Daisyworld in the literature are based on Cellular Automata [Ackland et al., 2003; Ackland and Wood, 2010; Lenton and Van Oijen, 2002; von Bloh et al., 1997]. In these, the new state of a cell is determined by a set of predetermined local rules and previous state of the randomly chosen cell in the neighbourhood.

- The original paper on Daisyworld pays only limited attention to population dynamics. But population dynamics may also lead to the regulation of resources and population.

- Stable coexistence of species in Daisyworld can be achieved either by temporal fluctuations or by spatial extension. Von Bloh and others used only spatial extensions for their study and not temporal fluctuations.

- The regular 1D or 2D lattice is not a real-world topology. In particular, non local dispersion or diffusion has not yet been studied in Daisyworld.

- The species diffusion approach used in Daisyworld modelling in the literature is not realistic, because the previous state of the neighbourhood alone determines the new state of a cell. There is no reflection of population density, and hence limited possibility to study population diffusion effects based on density gradient.

- The principles underlying complex systems are not deeply analysed with daisyworld.

1.4 Motivation

Future engineering systems are to be designed with long-term self-maintenance and self-organization which implies that the systems have to be homeostatic – they have to self-regulate their internal states by themselves to cope up with their changing environment without any external intervention. This urges

us to investigate self-regulating systems. If our systems implement the self-regulating principles of nature, they will be more close to nature and more reliable. Otherwise they will be alienated from nature and we have to engineer our systems again and again endlessly. By analysing homeostatic principles based on nature will give complete understanding of our problems.

Daisyworld is the mathematical proof of Gaia hypothesis [Lovelock, 1972] which illustrates how our earth works. Daisyworld model demonstrates the emergence of homeostasis (by and for the biosphere) as a consequence of the feedback loop between life and its environment. Identifying the feedback mechanisms which lead to homeostasis in a system is a very challenging research area. We apply daisyworld principles in deriving the analogies with stock market and we demonstrate social homeostasis.

1.5 Inspirations from Nature

Our behavioural studies of our daisyworld system is based on the following listed inspirations from nature.

- Life-environment Feedback Systems (Rock formation of bacteria)
- Complex Interacting Self-organizing Systems (Schooling of fish)
- Reaction-Diffusion Systems (Animal coats)
- Connections (Wood Wide Web)
- Super-organism (Termite colonies)
- Adaptive Networks (Brain)

1.6 Contribution

We analyse daisyworld as a paradigm shift from a mechanistic world view to a holistic ecological view. To study the complexity phenomena in daisyworld, we reconstruct some of the daisyworld formulations based on Coupled Map

Lattice (CML)(refer the chapter 3). We examine the emergence of complexity phenomena. We also incorporate complex and adaptive topological changes to our system. We observe the cyclical coexisting dominance of daises in complex and adaptive systems exemplifying behaviours of social, political and economical systems. We perceive the analogy between daisyworld and stock market as they both are complex systems giving rise to homeostatic behaviour (self-regulation, self-organization, self-causing, etc.).

1.6.1 Incorporation of Complex Spatio-temporal Dynamics

1.6.1.1 Coupled Map Lattice (CML) Modelling

Most 2D spatial extensions of daisyworld (life-environmental feedback system) in the literature are based on Cellular Automata (CA) [Ackland et al., 2003; Ackland and Wood, 2010; Lenton and Van Oijen, 2002; von Bloh et al., 1997]. In these CA based models, the new state of each cell is determined by a set of predetermined local rules and previous state of the randomly chosen cell in the neighbourhood. The discrete set of state values represents the presence or absence of a species at a cell.

In almost any real ecosystem, the population dynamics include both temporal reproduction processes and spatial diffusion processes. Hence we propose Coupled Map Lattices (CML) based spatio-temporal computational modelling tool which is convenient for simulation, interpretation of results, and analysis of spatio-temporal dynamics [Kaneko and Tsuda, 2001]. CML (also known as continuous cellular automata) are dynamical models in which discrete space and time are combined with a continuous state. The new state of a cell is updated with difference equations (maps) which depend on the current value of the cell itself, and a coupling (diffusion) term, which depends on the neighbourhood values. CMLs are CA in which the states of the cells are real values in [0, 1], and the update rule is in the form of a real function. Thus, they differ from CA primarily in the state value representations. In CA, each variable at a lattice point represents a microscopic state; in contrast, in CML, each variable represents a semi-macroscopic (mesoscopic) state. In this research,

we analyse the daisyworld dynamics through such mesoscopic modelling.

The basic CML incorporates both a nonlinear local map for temporal fluctuations, and a discretised diffusion process for spatial extension; due to these combined effects, it displays rich local and global dynamics.
(Publication : Punithan et al. [2012])

1.6.1.2 Detailed Population Dynamics

Daisyworld models in the literature lack detailed population dynamics, owing to their primary focus on environmental regulation. But population dynamics, with density dependent factors such as resource limitation and influence, crowding, dispersion, competition, disease, predation, etc., may lead to homeostasis at an ecosystem level. The regulation due to density dependence is a well known emergent ecological phenomenon.

This research studies the detailed symbiotic population dynamics of daisyworld in CML, in an alternative approach reconstructing some of the mathematical equations of the original Daisyworld models [von Bloh et al., 1997; Watson and Lovelock, 1983] adapted to coupled maps. The ecological homeostasis of our system is determined by the biotic and abiotic components of the system and the density-dependent nature of the growth due to overcrowding. These two regulatory mechanisms shape the dynamics and behaviour of our daisyworld model.
(Publication : Punithan et al. [2012])

1.6.2 Demonstration as Complex Systems

Based on our computations, we exemplify daisyworld as a complex dynamical system, self-organizing system and reaction-diffusion system. A large scale of identical habitats (components) in a 2D daisyworld interact with their neighbours produce complex and robust global behaviour. Our system combines spatial Laplacian diffusion, nonlinear local dynamics via logistic growth equation, noisy fluctuations in influencing the physiological, behavioural rules and physical constraints which cause a wide range of patterns formation such as

complex patterns, Turing-like structures, cyclic patterns, random patterns and uniform dispersed patterns emerge from our system. The emergence of such complex behaviours from our model serve to illuminate the complex mosaic of patterns that we observe in real-world biosystems.

1.6.2.1 Complex Dynamical System

From our results at a one point world, we infer daisyworld – a system with life-environment feedback – exerts stationary, periodic and strange attractors. (refer sub-section 4.1.7)

1.6.2.2 Self-organizing System

The combined effect of positive and negative feedback couplings result in a negative feedback loop, which stabilises the physiological processes and leads to homeostasis. We observe that life and their environment together organize themselves.
(Publications : Punithan and McKay [2012b] and Punithan et al. [2012])

1.6.2.3 Reaction-diffusion (Activator-inhibitor System)

In our nonlinear reaction-diffusion system, symmetry-breaking is induced by species dispersion, temperature diffusion and noise. Same as morphogens in Turing's experiments [Turing, 1952], black and white daisies locally react and spatially diffuse to give rise to complex behaviours and pattern formation.
(Publications : Punithan and McKay [2012b] and Punithan et al. [2012])

1.6.3 Incorporation of Evolutionary Mechanisms

We introduce replicator-mutator mechanisms from evolutionary dynamics into our core two-dimensional daisyworld model, thereby coupling evolutionary change with daisyworld's bi-directional feedback between biota and environment. Daisyworld continues to self-regulate in the presence of these evolutionary forces. The most interesting behaviours, exhibiting a complex and dynamic

dance through space and time in species' abundance, emerges through the introduction of additive spatio-temporal random perturbations in the form of thermal noise. The balance between ecosystem feedback and fluctuations in the ecosystem determines the spatial coexistence of dominance between daisy species and their mutants or adaptants.
(Publication : Punithan and McKay [2012a])

1.6.4 Introduction of Spatio-temporal Quantification

We introduce metrics for quantifying the behaviour of daisyworld, and used them to analyse the spatio-temporal dynamics: Permutation Entropy to measure the temporal dynamics, standard deviation to measure the scale of fluctuation, and Moran's I to measure the spatial auto correlation and pattern formation. PE and MI quantify the spatio-temporal dynamics accurately, demonstrating their reliability in quantifying a wide range of dynamics.
(Publication : Punithan et al. [2012])

1.6.5 Incorporation of Complex and Adaptive Topological Properties

1.6.5.1 Small-world Phenomena

All 2D versions of daisyworld [Ackland et al., 2003; Ackland and Wood, 2010; Lenton and Van Oijen, 2002; von Bloh et al., 1997] are of regular lattice structure – in which all neighbourhoods are isomorphic – with fixed numbers of nearest neighbours. However, in planetary ecodynamics, some species may have a mix of local and global dispersal patterns – for example, coconuts [Perera et al., 2000] or shellfish [White et al., 2010] – which can dramatically alter their ecological behaviour. This motivates us to study the effects of global interactions on daisyworld.

We study the dynamics of daisyworld using 2D versions of the Watts-Strogatz (WS) model [Watts and Strogatz, 1998] – in which a small fraction of the existing edges are rewired as random couplings, of the Newman-Watts (NW) model [Newman and Watts, 1999] – in which a few new random edges

are added and of Smallest-World (SW) model [Dorogovtsev and Mendes, 2002] – in which new nodes and random edges from them are added. These rewired or added edges are known as 'shortcuts', and they give rise to the small-world properties in which even a quite small numbers of shortcuts can dramatically change many characteristics of the network behaviour and can exhibit dramatic effect on the system dynamics.

We recognize that even a few long-range connections dramatically affect the population dynamics of daisyworld, but it is still able to self-regulate the environment (temperature) and thus sustain life (daisies). The introduction of non-local long-range connectivities into a highly locally structured daisy population lattice permits the rapid and homogeneous spread of a dominant daisy type, invading the whole coexisting daisyworld. Although the proportion of long-range connections is small, the pattern of interaction is changed from entirely local to almost entirely global.

If a system exhibits such a dramatic change in its characteristic properties under the perturbations of small changes in some of its model parameters, the system is said to have changed phase. Such phase transitions are very common in physical, social and technical systems. For example, a magnet exhibits magnetism up to a critical temperature, above which the magnetic properties are suddenly destroyed. In the same way, when we perturb the connectivity of our daisyworld graph while leaving all other parameters fixed, it exhibits periodic behaviour while the unaltered system forms static self-organised patterns.
(Publications : Punithan et al. [2011] and [Punithan and McKay, 2013b])

1.6.5.2 Topology-Dynamics Feedback (Adaptive Graphs)

We investigate the behaviour of the daisyworld on an adaptive graph [Gross and Blasius, 2008; Gross and Sayama, 2009] – a class of dynamical graphs whose topologies and states coevolve, comparing it to previous studies on a fixed topology grid, and a fixed small-world graph. Here, we consider the small-world graph based on Newman-Watts (NW) model as baseline for com-

parison. The adaptive graphs eventually generate topologies with small-world phenomenon behaving similarly to the NW model – and radically different from the grid world. Under the same parameter settings, static but complex patterns emerge in the grid world. In the NW model, we see the emergence of completely coherent periodic dominance. In the adaptive-topology world, the systems may transit through varied behaviours, but can self-organise to a small-world graph structure with similar cyclic behaviour to the NW model. (Publication : Punithan and McKay [2013a])

1.6.5.3 Scale-freeness (Power law or Fat-tailed Distribution)

We incorporate scale-freeness into our system possessing power law distribution, high clustering and small-world effect. The daisyworld dynamics exert the homeostatic emergent property even with the presence of additional topological properties. The system is shown to be able to precisely coordinate behaviour with internal dynamics.

1.6.6 Applications (Demonstration of Social Homeostasis in Stock Market)

We derive the parametric and functional analogies between daisyworld and stock market. The life-environment feedback mechanisms in daisyworld self-regulate the planet. The very same way the feedback between market sentiment (investors' opinion) and stock price cause the self-regulation in stock market. We apply our analysis from daisyworld (an imaginary world) to real-world stock market.

1.7 Outline

First we describe the background materials in the chapter 2. In chapter 3, we present our reconstructed mathematical modelling of daisyworld that is developed based on Coupled Map Lattice (CML) and other modelling tools provided in the background materials, and we detail our experimental set-up

that we use for our investigations. In the chapter 4, we analyse daisyworld in CML with only local couplings. In chapter 5, we examine daisyworld in CML with complex couplings based on small-world phenomenon, scale-freeness and adaptive networks. In chapter 6, we demonstrate stock market as a collective social homeostatic system by analysing stock tweets and stock price. Finally, we conclude by summarising our contribution and findings in the chapter 7.

Chapter 2

Background

In this chapter, we provide the background materials on complex systems (section 2.1), modelling tools (section 2.2) – that we use for our modelling, and quantifiers (section 2.3) – that we use to analyse the spatio-temporal dynamics of our model.

2.1 Complexity Science : A Means to Understanding Complex Systems

By etymology, the term complex roots from Latin *plectere*, which means interwoven. That implies a complex system is inseparable due to the interactions and the interdependencies between their the components. A complex system is a large network of components interacting according to simple rules and exhibit an emergent complex behaviour, adaptation via learning or evolution; or non-trivial information without central control. Complex systems covers many core areas such as system theory, nonlinearity theory, network theory, game theory, evolution and adaptation, collective behaviour and pattern formation, etc. There are numerous examples of complex systems in nature, society, man made technological systems– human brain (neurons), stock market (investors), insect colonies (termites), the internet (computers) and World Wide Web (pages), social networks (humans or animals), etc.

2.1.1 Systems Thinking

A system consists of components, interconnections, and a function or purpose [Wright and Meadows, 2012] – a set of interacting, interrelated or interdependent components interconnected to produce a specific pattern of behaviour over time. The system maintains its existence through the mutual interactions of its parts [Von Bertalanffy, 1968]. Example include societies, ecosystem, nervous system, etc.

Systems thinking is the science of how things are connected. It emphasizes the relationships among a system's parts rather than the parts themselves. It provides a way of thinking based on whole and relationship rather than parts. A system is more than sum of its parts that may exhibit adaptive, dynamic, self-regulating and evolutionary behaviour. In traditional thinking, a problem is broken into a set of simpler sub-problems and solving each of them individually. In contrast, systems thinking emphasizes the interconnections between parts of a system and external environment. Systems thinking signifies circular feedback (Figure 2.2) rather then linear cause and effect (Figure 2.1).

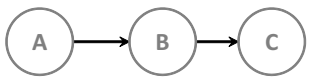

Figure 2.1: Linear Cause-and-Effect : A system consisting of components A, B and C

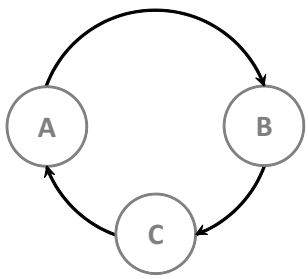

Figure 2.2: Circular Cause-and-Effect : A system consisting of components A, B and C

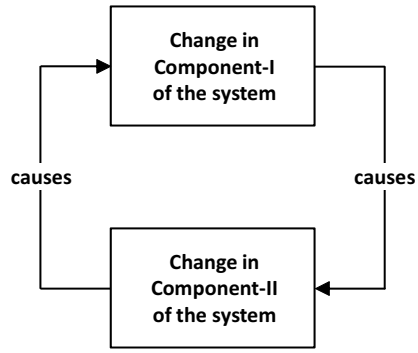

Figure 2.3: System with Feedback Mechanisms

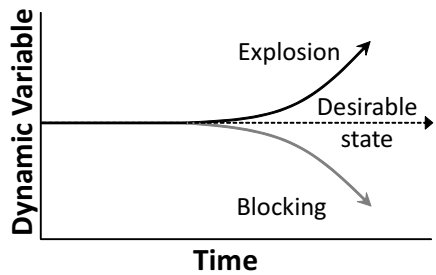

Figure 2.4: Reinforcing Process

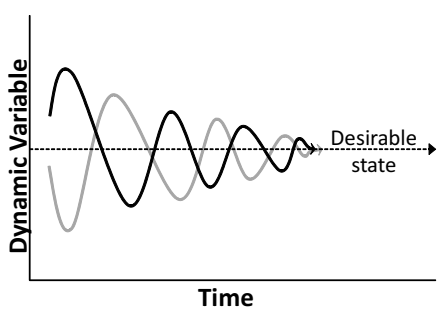

Figure 2.5: Balancing Process

Interactions : The *interactions* lead to shift from perception of objects to perception of relationships [Capra, 2004]. They play a vital rule in the system and can generate novel dynamics. Interactions trigger complexity in the system. When interactions of the system are dependent, feedback enters the system and alters the dynamics of the system (Figure 2.3). With the positive coupling, changes get amplified leading to instability. With the negative coupling, changes get quickly absorbed and the system gain stability. Thus the system behaviour is described by both reinforcing and balancing processes – bipolar feedback couplings.

Driving Positive Coupling Positive coupling (runaway or amplifying or escalating) is self-reinforcing. It generates exponential growth (virtuous) or collapse (vicious) (Figure 2.4). This brings changes (difference or innovation) in the system. If there is no positive coupling, the system will be monotonous and uninteresting. Examples include fashion crazes, reproduction cycle, etc.

Regulating Negative Coupling Negative Coupling (homeostatic or self-maintaining or dampening) is balancing – self-correct (Figure 2.5). It controls (counters) the change and exhibit self-maintenance, robustness and stability. Examples include thermostat, immune system, etc.

Dynamical Systems : Dynamical systems are systems that change over time. Examples include brain, heart, stock market, global economy, global climate, etc. Dynamical systems theory characterises the system behaviour in terms of attractors, bifurcations and universal properties of the ways systems can change.

Cybernetics : Cybernetics (from the Greek word for *steersman*) is the study of complex systems and processes, their modelling, feedback, control, information, communication and purpose. Examples include robots (technological), human body temperatures (biological), Gaia hypothesis-daisyworld (environmental), stock market (economical), etc. Artificial intelligence, artificial life,

neural networks are the offsprings of cybernetics.

Homeostasis - Adapting to change :

> "... a form of behaviour is **adaptive** if it maintains the essential variables within physiological limits"
> Ashby, W.R, *Design for a Brain: The Origin of Adaptive Behaviour, 1952*

Homeostasis is derived from the word *homoios* (Greek) meaning same, like, resembling and *stasis* (Greek) meaning to stand, posture. The term homeostasis was introduced by Claude Bernard, who founded the principle of the internal environment [Bernard, 1878]. Cannon suggested homeostasis as the coordinated physiological processes which maintain most of the steady states in the organism [Cannon, 1929]. Ashby stated that the process of homeostasis is directly related to intelligence [Ashby, 1952].

A well known example of homeostasis is the regulation of body temperature. Homeostasis is a fundamental property of living systems which tends to maintain the internal conditions of living organisms stable (within a normal range), regardless of the external environment. These internal conditions include body temperature, blood pressure, pH level, glucose level, etc. Hence it is essential for survival.

Adaptation is the maintenance of system variables within predetermined (normal) limits either by evolutionary changes, physiological reactions, sensory adjustment, or by learning novel behaviours. Hence adaptive behaviour is equivalent behaviour of a stable system. Homeostasis is the ability of a system to adapt to a continuously changing and unpredictable environment. It corresponds to an adaptive reaction to maintain "essential states" within a range [Ashby, 1952].

Through adaptation, a system or an organism functions within a "viability zone" – the lower and upper bounds of the essential states. When perturbations or environmental changes occur, the system adapts to face the changes within the viability zone, i.e. without the system "breaking" [Ashby, 1947]. The system remain in the viability zone owing to homeostasis. It is the active

regulation which differs from mere inertia – stagnant state. It also emphasises on the resistance to the change.

Homeostatic systems (either living or technical) maintain the balance through complex interacting feedback control processes. For instance, the brain keeps the living organisms in physical and emotional balance by its highly intricated physical, chemical and neurological processes. In order to understand real or artificial life, it is necessary to understand the conceptual framework and basic mechanisms of homeostasis [Dyke and Harvey, 2006]. The corrective behaviour in a system can be innate (pre-programmed) or learned. Hence, homeostasis is an important tool for adaptation in dynamic environments.

Homeostasis can exist at any scale of biological organization–from the cellular to the biospheric. Individual organisms can exhibit homeostasis and the assemblages of organisms can also co-operate to maintain the dynamic orderliness that is characteristic of life [Turner, 2009a]. Homeostatic systems provide high levels of stability, adaptation, coordination, self-organization, robustness, survivability, viability, sustainability, corrective behaviour, etc. Some of different forms of homeostasis are listed below.

Organismal Homeostasis The cells of an organism coordinate their activities to regulate the body's internal environment.

Ecological Homeostasis Ecosystem has the power of self-maintenance and self-regulation. Ecological homeostasis is referred as balance of nature. The ecological balance is maintained by the number of factors. The carrying capacity is one among them. The ecosystem also exhibits organism-like behaviours.

Social Homeostasis Social homeostasis is a phenomenon of social insect colonies. The environment of the colony is regulated by the collective activities of the colony's inhabitants. The colony is a superorganism [Turner, 2009b]. Examples include termite colony, bee hive, etc.

2.1.2 Nonlinear Thinking

In linear systems (proportional), the behaviour of the whole is the sum of the behaviour of its parts, while in nonlinear systems, the behaviour of the whole is more than the sum of its parts. Recursion (iterations) and feedback loops cause nonlinear effect.

Linear system obeys the principle of superposition and homogeneity. Any system that does not satisfy these properties is nonlinear. Linear system can be understood by analysing its parts in isolation. While nonlinear system can be understood by analysing the interactions between parts, rather than parts themselves [Langton et al., 1989]. Examples include our nervous system, laws of ecology, immune response of patients, viral population dynamics, human psychology, etc [Strogatz, 2003].

In nonlinear systems, cause and effect are disproportionate because of feedback loops. Interactions among the components are nonlinear and hence a very small perturbations or fluctuations can become amplified into gigantic, structure-breaking waves Prigogine et al. [1985]. These systems are of tipping points (systems tip from one state to another), stable regimes that collapse, butterfly effects, avalanches, etc. But linear systems are incapable of rich behaviour [Strogatz, 2003].

Dynamical Behaviours : The dynamics of the systems can evolve towards single stable steady state, multistability (several stable steady states), limit cycles (sustained oscillations), chaos (strange attractors), etc. Bistability (a particular case of multistability) is the coexistence of two steady states. Bistability plays a critical role in biological systems (genetic switch, memory effect, etc) and limit cycle in biological rhythms. The system can exhibit complex behaviours (such as chaos– multiple instability mechanisms) due to multiple feedback loops. Other complex behaviours include quasi-periodic oscillations, bursting (alternance between oscillatory and non-oscillatory phases), synchronization, and excitability.

Chaos : If the trajectories of the two realizations of the same dynamical system with an infinitesimal difference in the initial conditions diverge exponentially, then the system has sensitive dependence on initial conditions. "Chaos is aperiodic long-term behaviour in a deterministic system that exhibits sensitive dependence on initial conditions" [Strogatz, 2001]. In a chaotic system small disturbances grow exponentially, causing long-term prediction drastically inaccurate [Lorenz, 1963]. This is known as butterfly effect. An appropriate system of this sort of behaviour of is stock market. As the value of a stock rises or falls, people make their decisions to buy or sell that stock. This in turn further affects the price of the stock, causing it to rise or fall chaotically. Chaos has been observed in electronic circuits, cardiac disorders, etc.

Iterative Systems : The logistic map is the most popular equation in the science of dynamical systems and chaos, which exhibits the fundamental properties of complex systems in nature. This extremely simple nonlinear iterative system is astounding. The behaviours of such iterative systems are characterized by bifurcations, attractors and universal properties such as period-doubling route to chaos and Feigenbaum's constant is same for all unimodal maps. Other nonlinear iterative systems are growth and decay of biological populations, predator-prey interactions, spread of communicable diseases, etc.

2.1.3 Network Thinking

> "Whenever we look at life, we look at networks."
> Fritjof Capra, *The Web of Life*

> "Networks are present everywhere. All we need is an eye for them."
> Albert-László Barabasi, *Linked*

"Networks are prerequisite for describing any complex system, indicating that complexity theory must inevitably stand on the shoulders of network" [Barabasi, 2003]. Thinking networks is about how networks emerge, what they look like, and how they evolve [Barabasi, 2003]. The components of

living systems–organisms, parts of organisms, and communities of organisms–are arranged in network fashion [Capra, 1997]. Network thinking focuses on the relationships or connections or interactions among entities rather than the entities themselves.

The key features of networks are pattern of organization (holistic view), interconnectivity, nonlinearity, unpredictability, contingency, etc.

Random Networks : Paul Erdos and Alferd Renyi made first breakthrough in network science. They modelled networks by selecting n number of nodes and connecting every pair of nodes with a probability p – Poisson random network or Bernoulli network [Bollobás, 2001]. These random networks exhibits small-world effect but fail to display other topological characteristics of real world networks. One of the most characteristic of social networks that random networks cannot model is social cliques.

Small-world Complex Networks : Watts and Strogatz [1998] in their seminal paper proposed that real-world networks lie between regular and random networks and are usually highly locally clustered (cliquish), as in regular lattices, yet have low characteristic path lengths, in which they resemble random networks. These properties are found across a wide spectrum of sciences – in social, biological and technological networks such as neural networks, electronic power grids, networks of movie actors [Watts and Strogatz, 1998], the world wide web [Albert et al., 1999], scientific collaborations networks [Newman, 2001], and so on.

The small-world property was first investigated in the pioneering empirical work of social psychologist Milgram [1967]. He showed that any two randomly chosen people on the planet were likely to be linked by a chain of six intermediate acquaintances. His notion has been widely accepted, and is referred to as the "small-world phenomenon" (more popularly known as the "six degrees of separation"). More precisely, the underlying social network is a superposition of high local clustering and short global chains, possessing the small-world property.

Watts and Strogatz [1998] (WS) in their ground-breaking work first modelled the small-world phenomenon by randomly rewiring a fraction of the connections of regular networks. These 'shortcuts' drastically decreased the diameter of the network (the longest shortest path between two nodes) and created the small-worlds. The measure of connectedness of a network is the average minimum path length between any two points. This is known as degree of separation. Due to the shortcuts, networks have low degrees of separation and thus they make small-world small. They are highly connected as fully-connected network (one degree of separation).

Other variants exhibiting the small-world phenomenon include the Newman-Watts (NW) model of Newman and Watts [1999] and the Smallest World (SW) model of Dorogovtsev and Mendes [2002].

Since a small-world network realises both high local clustering and high connectivity simultaneously, it exhibits properties from regular lattices and random networks: with regular lattices, it shares local coherence, while with random networks, it shares rapid diffusion. Thus it shares interesting properties of two opposed topologies.

In turn, the structural properties of networks exhibiting small-world phenomenon can have dramatic effect on the dynamics of systems acting on them. Well known examples include the dynamics of epidemics, biological evolution and of diffusion processes. For further reading, see Boccaletti et al. [2006].

Scale-free Complex Networks : Watts and Strogatz model does not capture all topological properties of real networks. In WS model, each node begins with the same number of links and are rewired with a uniform distribution. The distribution of the number of links that a node has follow a peaked distribution. Albert-Laszlo Barabasi found that the distribution of links in real world networks follow a power law or fat-tailed distribution. Majority of nodes have very few links while a few have majority of links. Barabasi referred to these popular (high degree) nodes as hubs and coined complex networks exhibiting power law distribution as scale-free networks as they exhibit self-similarity (parts of network show the same statistical properties at many

scales) or a fractal. No single node can characterize the population of nodes and thus there is no scale in these networks. Hubs are exceptionally massive nodes in terms of the number of other nodes they are connected to. Hubs ('keystone species' in ecology and 'connectors' in sociology) are nodes with an anomalously large number of links. They present in very diverse complex systems ranging from economy to a cell. The emergence of hubs allows the small-world effect to occur.

"90% of all documents on the web have 10 or fewer links pointing to them, while a few, about 3, are referenced by close to a million other pages" [Barabasi, 2003].

Most real networks are formed by just a few nodes and a few links. The original links may be random or may not, but as the network grows – more and more links are added. However, they are not added completely randomly or at least not uniformly. Barabasi hypothesized that they are added with preferential attachment. ie., each link would be more likely to be added to those nodes which already have more links (older more established (popular) nodes). This allows the rich to get richer – "Matthew effect". The combination of allowing a network to grow and allowing it to grow with preferential attachment, forms the power distribution characteristic of scale-free networks.

There are two kinds of small-world networks :
egalitarian (those without hubs) and aristocratic (those with hubs) or also called scale-free networks [Buchanan, 2003]. In egalitarian networks, most of the nodes have approximately the same number of connections. Examples are synchronising fireflies, human brain and road, rail and air networks.

In aristocratic networks a few nodes (hubs) have a disproportionally large number of connections. Examples are the Internet, WWW, ecosystems, food webs, the networks of airline companies, citation networks, etc.

Adaptive Complex Networks (dynamics *on* the network interacting with dynamics *of* the network) : The key features in network theory are topologies and dynamics. The complex networks in nature, society and technology are adaptive and dynamic, in that they exhibit feedback between

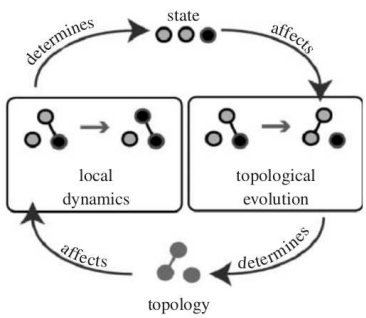

Figure 2.6: Adaptive Network (Source : [Gross and Blasius, 2008])

the local dynamics of nodes (state) and the evolution of the topological structure (Figure 2.6). Examples include genetic, neural, immunity, ecological, economic, organic, social networks, complex game interactions, etc.

Dynamics has two meanings:
"The first meaning is what we might call dynamics of the network. In this sense of the word, dynamics refers to the evolving structure of the network itself, the making and breaking of network ties. ... A dynamical view of networks, claims that existing structure can only be properly understood in terms of the nature of the processes that led to it. The second meaning, is what we might call dynamics on the network. From this perspective, we can imagine the network as a fixed substrate linking a population of individuals, but now the individuals are doing something – the outcome of which is influenced by what their neighbors are doing and, therefore, the structure of the network. ... In the real world, both kinds of dynamics are going on all the time. ... The structure of the network could change, but so could the pattern of activity on the network" [Watts, 2004].

In most real-world networks, the topology itself is a dynamical system which changes in time and in response to the dynamics of the states of the nodes (dynamics *of* the network). The evolved topology in turn influences the dynamics of the states of the nodes (dynamics *on* the network), creating a feedback loop between the dynamics of the nodes and the evolution of the topology. Networks exhibiting such a feedback loop (mutual evolution of struc-

ture and state values) are called adaptive or coevolutionary networks [Gross and Blasius, 2008; Gross and Sayama, 2009].

In road networks, the topology of the road influences the traffic flow, while traffic congestion influences the construction of new roads. In the vascular system, the topology of the blood vessels controls blood flow, while restrictions in blood flow influence the formation of new arteries (arteriogenesis). The internet respond to the addition and removal of nodes by re-routing messages via new nodes. The neuroplastic brain compensates the brain damage by re-routing, rewiring and with the growth of new neurons. Thus complex adaptive networks are intelligent.

2.1.4 Collective Behaviour

A collective behaviour (bottom-up behaviour or decentralization) is a fascinating phenomenon, in which the low-level components have the ability to self-organize themselves and emerge into a higher-level system of sophistication and intelligence [Johnson, 2012]. Examples include ant colonies, social web (a disorganized entity self-organize itself into a bottom-up intelligence), Linux open-source software (intelligent crowd in action), etc.

Self-Organization : The components comprising the system are able to self-organize and the interaction of the components comprising the system can exhibit emergence. In other words, self-organization is a processes, which exhibits emergences at global scale due to the short-range local interactions of the system, with no external intervention [Camazine et al., 2003]. A wide range of pattern formation processes have been observed in fields from chemistry (Turing's reaction-diffusion system [Turing, 1952], Belousov-Zhabotinsky reaction [Belousov, 1958]) and fluid dynamics (Bénard convection cells [Bénard, 1900]) to biology (patterns on animals' coats [Murray, 2008]). A large numbers of relatively simple entities organize themselves, without any central control, into a collective whole as patterns, information, learning and evolution.

Self-organizing systems produce global pattern from the interaction of their components. Classic examples include flocking of birds, colony of insects,

schooling of fishes, etc. A dynamical system can exhibit self-organizing property as they tend to attractors.

Emergence : The emergence is a phenomenon whereby well-formulated aggregate behaviour arises from localised individual behaviour. It is the property observed only at high scale and is not present at the lower scale. For example, the colour, conductivity, malleability of gold is not present in the properties of gold atoms [Anderson et al., 1972]. The properties of a system are emergent if they are not present in their components.

Phase Transition and Critical Phenomenon : Lev Landau invented theory of phase transition – how substances of all kinds change their forms – by focusing on the abstract elements of molecular and atomic organization. His visionary idea leads modern physics about discovering the law of forms in networks of interacting things and not the matter. The interacting things are not only atoms and molecules, but also bacteria and people. The small-world idea is just a part of this larger theory of networks – a collection of interacting elements often has properties that depend no crucial way on the nature of the elements themselves [Ball, 2004; Buchanan, 2003].

When solid ice melts into liquid or dry ice turns into smoky vapour – substances change from one form to another, the atoms or molecules remain the same. Only the collective organization of the atoms or molecules changes. The modern version of Landau's theory is called the theory of critical phenomena. When water is neither liquid nor vapour, it is in critical state. The new form of Landau's theory applies not only to changes in organization but also to the changes in the activity. Nothingness (static) changes to dynamism is called tipping point.

2.1.5 Pattern Formation

Positive and negative feedback are the two basic modes of interactions among components of self-organizing systems [Camazine et al., 2003]. Self-enhancing

positive feedback coupled with antagonistic negative feedback leads to the formation of striking patterns in nature (ripples in sand dunes, schooling of fish, flocking of birds, coat of animals). A stationary state becomes unstable due to amplification, and this provokes pattern in the system. Since amplification purely in one direction leads to destruction, negative feedback takes control of the system and plays a critical role in inhibiting amplification and shaping the process and pattern, for example in colonial nesting of male bluegill sunfish [Camazine et al., 2003].

Turing instabilities : Turing instability of a homogeneous steady state in a two-species reaction-diffusion system provides theoretical mechanisms for pattern formation. Generally diffusion is perceived as an homogenising process. By contrast, Turing, in his remarkable paper(1952 [Turing, 1952]), demonstrated that a simple system of coupled reaction-diffusion equations could give rise to spatial patterns in chemical concentrations, through a process of chemical instability. The chemicals (morphogens or species), characterised as activator and inhibitor, react and diffuse throughout the tissue, and due to this physico-chemical process patterns such as spots and stripes can form in an animal's coat. These spatial patterns emerge from a homogeneous equilibrium state, due to symmetry-breaking via diffusion. This diffusion-driven instability forms the basis of pattern formation in physics, chemistry and biology. A wide spectrum of complex self organized patterns such as stationary, waves, spirals or turbulence emerge from reaction-diffusion systems.

Turing pattern formation in activator-inhibitor systems forms the paradigm of self-organization [Nakao and Mikhailov, 2010], and provides a theoretical explanation of animal coat patterns [Murray, 2008]. The activator and inhibitor species destabilize the homogeneous state of the system due to diffusion, and lead to the spontaneous emergence of spatial patterns.

2.2 Modelling Tools

A mathematical model is the simplified representation of a real world principle or a phenomenon. We study nature through modelling tools. In this chapter, we describe the background material on computational modelling tools.

2.2.1 Daisyworld Model (Life-Environment Bidirectional Feedback Model)

Gaia Hypothesis :

> "Living organisms and their material environment are tightly coupled. The coupled system is a superorganism, and as it evolves there emerges a new property, the ability to self-regulate climate and chemistry ."
> James Lovelock, *The Ages of Gaia, 1988*

> ...[Gaia can be defined] as a complex entity involving the Earths biosphere, atmosphere, oceans, and soil; the totality constituting a feedback of cybernetic systems which seeks an optimal physical and chemical environment for life on this planet." James Lovelock, *Gaia - A New Look at Life on Earth*

The Gaia hypothesis, was conceived by James E lovelock, posits that earth and its biological systems behave as a huge single entity. This entity comprises of closely controlled self-regulatory negative feedback loops that keep the conditions on the plant within the boundaries that are favourable to life. The self-regulation of physical variables around a narrow range and resistance to perturbation via cybernetic feedback loops leads the earth to be homeostatic. This new perception of global ecology differs from the classical ecology owing to the biological response to physical conditions [Jrgensen and Fath, 2010].

A wide range of fascinating examples have been observed in nature, portraying the influence of life on its environment. Examples include the formation of lakes, dams and canals by those so-called ecosystem engineers, beavers; chemical changes in soil by earthworms; cloud formation by marine phytoplankton; carbon sinks in terrestrial plants via photosynthesis and in the

oceans via physicochemical and biological processes; stromatolite formation by microbial mats, etc.

Daisyworld Model : Hutton et al. [1987], father of modern geology, emphasised that the Earth was a superorganism and its study should be viewed as physiology. Lamarck, Goethe, Humboldt, and Suess espoused similar holistic system views [Capra, 1997; Harding, 2006]. Vernadski and McMenamin [1998], influenced by Y. Korolenko, hypothesized that life is the geological force that shapes the earth and popularised the term 'biosphere'. Lotka [1925] recognised that species and environment are inseparable. However Lovelock and Margulis were the first to explore the self-regulating earth beyond these preliminary speculative ideas [Harding, 2006]. Watson and Lovelock [1983] devised a model known as 'daisyworld', which demonstrates homeostasis by and for the biosphere.

Daisyworld is a cybernetic model which demonstrates that a biosphere can regulate a planetary environment without external guidance, providing mathematical justification for Lovelock's well-known Gaia hypothesis [Lovelock, 1972]. This simple self adaptive system consists of two dominant life forms (absorptive black and reflective white daisies) and an environmental variable (surface temperature). The petal colour (phenotype) of the daisies influences the environment-altering trait, albedo (i.e. the reflectivity of the surface) of the planet, and thus the temperature which in turn determines the daisy cover; thus life and environment are tightly coupled in this model. The homeostasis emerges from the biosphere's tuning of the planetary albedo. The daisies do not interact with each other directly but via the temperature of the environment. Thus the biotic components (black and white daisies) interact stigmergically via an abiotic component (temperature).

In the beginning, the planet is lifeless, cold ($278K$) and equally seeded with black and white daisies(=agents). At this lower temperature, black daisies are favoured as they absorb more sun light. As the growth of black daisies increases, it lowers the surface albedo (negative coupling). The decrease in surface albedo cause an increase in the surface temperature (negative coupling).

The increase in temperature increases the growth (positive coupling).This positive feedback amplifies the growth and daisyworld becomes hotter. Eventually highly reflective white daisies are favoured to prevent the system from overheating as they are good at reflecting the sunlight. As the growth of white daisies increases, it increases the surface albedo (positive coupling) which in turn decreases the surface temperature (negative coupling). The decrease in temperature increases the growth (negative coupling). Due to this positive feedback, daisyworld becomes cooler and black take advantage, re-warming the system. This cycle goes on continuously.

The behaviour of one type of daisies modifies the temperature, which affects the behaviour of the other, and vice versa. In general, increased growth of a particular type of daisy alters the temperature in a direction which is unfavourable for itself, but suitable to the other type. When black daisies start spreading more, the local temperature rises. Conversely, when white daisies spread, the temperature drops.

Due to the complementary tendencies of the species, the planet remains in homeostasis, the temperature is self-regulated and hence the planet remains habitable without any explicit mechanism for cooperation. This is the key emergent property of the system.

Daisyworld as Deep Ecological System Deep ecology, as introduced in Naess [1973], is a contemporary ecological view emphasising the interdependence and connectedness of organisms within ecosystems, and ecosystems within the biosphere. Capra [1983] emphasised that the planetary ecosystem is an integrated web of living and nonliving forms, and encouraged a paradigm shift from a mechanistic world view to a holistic ecological view. Anima Mundi [Harding, 2006], a similar perspective, emphasised the intrinsic connection between all living things on the planet. Daisyworld reflects all these perspectives and recognises life and environment as a single coupled, self-regulating and self-organising system.

Daisyworld Models in Literature : This mathematical model has inspired interpretations and analogies in many fields such as social science, politics, religion etc. There have been many offshoots to other area of science, including ecology [Wilkinson, 2003], food web theory [Ackland and Gallagher, 2004; Harding, 1999], evolutionary theory[Lenton and Lovelock, 2000, 2001; Lenton et al., 1998; Lovelock, 1992], physiology [Saunders et al., 1998, 2000], maximum entropy production [Dewar, 2003, 2005; Ozawa et al., 2003], artificial life [Harvey, 2004], cybernetics [Andrew, 1996], earth system science [Ford, 1999; Kump et al., 2010; McGuffie and Henderson-Sellers, 2005] and Information Technology. Daisyworld has been applied in information technology and robotics [Dyke and Harvey, 2005, 2006] and inherent rein control mechanism [Saunders et al., 1998, 2000].

Variants of Daisyworld on Spatial Structures : The original model was based on a zero-dimensional world. It was extended to a one-dimensional (1D) world by Adams et al. [2003], to a two-dimensional (2D) world by von Bloh et al. [1997] and to a curved 2D world by [Ackland et al., 2003; Ackland and Wood, 2010].

Adams et al. [2003] examined a 1D Daisyworld with curvature on a spherical planet. The global regulatory properties of the original model are retained. The introduction of heat diffusion destabilizes the coexistence equilibrium of the two daisy types. As a result, a striped pattern consisting of blocks of all black or all white daisies emerges. Because of curvature, this model exhibits desert formation, the equatorial or polar regions being denuded of biota.

von Bloh et al. [1997] extended the Daisyworld to a 2D Cellular Automata (CA). This is the most studied and basic 2D model and includes multiple daisy types with regrowth rules as follows: At a given time step, one cell is chosen at random. If the neighbouring cell is empty, there is no colonization. If the neighbouring cell is vegetated, the chosen cell is colonized with growth rate. During successful colonization the albedo of the colonizing vegetation is allowed to mutate by a small random change.

A two-dimensional Daisyworld model with curvature was developed by Ack-

land et al. [2003]; Ackland and Wood [2010] to further study spatial effects. They found that catastrophic collapse of life can occur under gradual forcing of environmental feedback. This model predicts that large desert formation will be a sudden phenomenon, foreshadowed by large but temporary fluctuations, rather than the gradual growth of a small, expanding desert.

Daisyworld Applications : Although Daisyworld was originally introduced as an ecosystems model, it has seen subsequent application in a number of fields.

The regulation of some human physiological systems is analogous to Daisyworld. For example in the blood glucose regulation analogy, black and white daisies are replaced by the hormones insulin and glucagon, and temperature is replaced with blood glucose. Saunders et al. [1998] used this analogy to predict salient feature of type I and type II diabetes. Saunders et al. [2000] extended this to model the control of ionized calcium by parathyroid hormone and calcitonin.

Harvey used Daisyworld to model a sensing system [Harvey, 2004]. A circular body agent rotates around its centre by a force from a tentacle with sensor. Many tentacles on the surface work cooperatively and rotate the agent towards a light source over a range of positions just as daisies maintain global temperature over a range of luminosities.

Having intrinsic self-regulating behaviour, daisyworld system concept can be applied to a wide range of problems especially decision making under changing environmental conditions such as stock market, autonomous robot navigation, smart vehicles, etc. For further reading on daisyworld literature and applications, please see Wood et al. [2008].

2.2.2 Logistic Growth Model (Verhulst Model)

Populations grow at geometric or exponential (Malthusian) rates in unconstrained ecological systems. In realistic worlds, this cannot continue indefinitely. Verhulst proposed an extension of the Malthusian growth model with

an additional negative quadratic term $-r\frac{P^2}{\kappa}$, which decreases the population growth due to over-crowding. An Euler discretisation of Verhulst's equation (equation 2.1), also known as the discrete logistic equation, is key to theoretical population ecology. This density dependent population growth also models a form of ecological homeostasis.

$$P_{(t+1)} = P_t \left[1 + r\left(1 - \frac{P_t}{\kappa}\right)\right]; \quad r > 0, \kappa > 0 \tag{2.1}$$

where $P \in [0, \kappa]$ is the population size (at times t and $t+1$), and ranges from 0 (extinction) to κ (maximum conceivable population); r is the intrinsic rate of natural increase (growth coefficient) or bifurcation parameter; κ is the carrying capacity: the maximum sustainable population beyond which P cannot increase; and $\left(1 - \frac{P_t}{\kappa}\right)$ is known as the 'biotic resistance'. The parameter r enhances the growth (positive coupling) and the component $[1 - \frac{P_t}{\kappa}]$ dampens the growth (negative coupling), with their combined effect regulating the population.

The logistic map was originally studied in the context of population dynamics. May [1976], through his pioneering studies, showed that deterministic chaos emerges in population dynamics due to non-linearity and density-dependence. He proved that the above simple, density-dependent, non-linear, iterative, discrete map gives rise to a wide range of complex dynamics. It exhibits three types of attractors, namely static or fixed point attractors, limit cycles or periodic attractors, and chaotic or strange attractors. Although this equation has a built in regulatory mechanism based on κ, it forms the paradigm for the period-doubling bifurcation route to deterministic chaos, the basis of modern chaos theory.

2.2.3 Replicator Mutator Model

Replicator-mutator (aka selection-mutation) dynamics are embodied in the RME (equation 2.2):

$$\dot{P}_c = \sum_{c'=1}^{\mathfrak{n}} P_{c'} \mathfrak{f}_{c'} \mathfrak{q}_{c'c} - \phi P_c, c = 1, ..., \mathfrak{n} \tag{2.2}$$

Here P_c is the population proportion of type c, $\mathfrak{n}$ is the total species, $\mathbb{Q} = [\mathfrak{q}_{cc'}]$ is the mutation matrix, $\mathfrak{f}_{c'}$ defines the selection dynamics $\mathfrak{f}_{c'} = \mathfrak{f}_0 + \sum_{c'} \mathfrak{a}_{c'c} P_{c'}$ and $\phi = \sum_c P_c \mathfrak{f}_c$ is the average fitness. $\mathfrak{f}_0$ is the intrinsic fitness and $\mathbb{A} = [\mathfrak{a}_{cc'}]$ is a reward matrix.

In addition to biological evolution [Bürger, 1998], RME has been used to model evolution in language [Nowak et al., 2001], culture, behaviour in social networks [Olfati-Saber, 2007] and evolutionary game theory [Brenner, 1998].

2.2.4 Neighbourhood Models

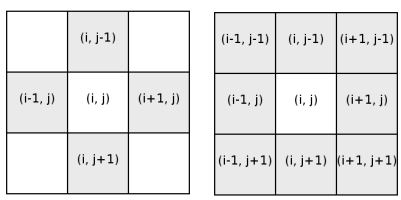

(a) von Neumann (b) Moore

Figure 2.7: Neighbourhood Models

The choice of neighbourhood models can be von Neumann (right, left, up, down); refer sub figure 2.7(a) or Moore (orthogonal (right, left, up, down) and diagonal vertices); refer sub figure 2.7(b). In the sub figures of Figure 2.7, the shaded grey cells indicate the neighbours of the central cell (i, j).

2.2.5 Diffusion Models

Spatial effects come into play in any system via diffusion, and this coupling effect is defined by the neighbourhood structure. In our model, we use the discretised version of the Laplacian operator. This is simple passive diffusion, requiring no catalyst. Diffusion is one of the key ingredients in our system to break symmetry and spread effects to the entire system. In the absence of diffusion, the ecosystem is uncoupled, and each habitat functions independently leading to an unrealistic world. Unlike other models, we do not have an explicit reseeding mechanism; instead the dispersal of daisies achieves the same function implicitly. Dispersal also reduces the likelihood of global extinction of daisies.

2.2.6 Spatio-temporal Model – Coupled Map Lattice (CML)

The Coupled Map Lattice (CML), introduced by Kaneko [1985], is one of the most widely used models for investigating the non linear dynamics of a spatially extended system. CML incorporates discrete time evolution (map) in a discrete space (lattice or network) as in cellular automata (CA), but can take arbitrary state values in the range $[0, 1]$ as in partial differential equation (PDE) models. In our model, we permit a range of population size from $[0, \kappa]$, where κ is the carrying capacity at a particular habitat (cell), for population dynamics and a range of temperature values from $[270, 330]K$ in the case of planetary energy dynamics.

The dynamics of a CML is governed by two terms: the temporal nonlinear reaction (maps - difference equation - f) and the spatial diffusion (coupling - ϵ). The evolution rules for a system in two-dimensional space with periodic conditions are defined as follows. The local variables $x_{(i,j,t)}$ diffuse to their neighbours, and the local weighted average value after diffusion is iterated over a local map.

Discrete Laplacian diffusion model is defined by:

$$x'_{(i,j,t)} = (1-\epsilon)x_{(i,j,t)} + \frac{\epsilon}{k}\sum_{<l,m>}^{n} x_{(l,m,t)} \tag{2.3}$$

where $x_{(i,j,t)}$ is the spatio-temporal distribution of a dynamical variable, t is the time step: $t \in \mathbb{Z}$; (i,j) indicates a 2D lattice point: $i,j \in \mathbb{Z}$; x is a dynamical variable: $x_{(i,j,t)} \in \mathbb{R}$; $x'_{(i,j,t)}$ is an intermediate local value after diffusion; $\epsilon \in [0,1]$ is the coupling parameter (diffusion rate); and k is the coordination number, specifying the number of interacting neighbours. It is derived from the neighbourhood model, in which $< l,m >$ ranges over the immediate neighbours of (i,j).

Discrete Laplacian diffusion in a regular graph with Moore neighbourhoods $(k=8)$ is formulated as:

$$\begin{aligned} x'_{(i,j,t)} = (1-\epsilon)x_{(i,j,t)} + \frac{\epsilon}{8}\Big[&x_{(i+1,j,t)} + x_{(i-1,j,t)} + x_{(i,j+1,t)} + x_{(i,j-1,t)} \\ &+x_{(i-1,j-1,t)} + x_{(i+1,j-1,t)} + x_{(i-1,j+1,t)} + x_{(i+1,j+1,t)}\Big] \end{aligned} \tag{2.4}$$

The local map function is defined as: $f(x)$ can be any nonlinear function of a dynamical variable. In our work, we use logistic maps.

Combining local reaction and spatial diffusion terms

$$x_{(i,j,t+1)} = f\Big(x'_{(i,j,t)}\Big) \tag{2.5}$$

where f is the local non-linear function – logistic map in the case of population dynamics and temperature update function in the case of planetary energy dynamics.

Equation 2.5 can be rewritten as:

$$\begin{aligned} x_{(i,j,t+1)} = f\Big((1-\epsilon)x_{(i,j,t)} + \frac{\epsilon}{8}\Big[&x_{(i+1,j,t)} + x_{(i-1,j,t)} + x_{(i,j+1,t)} + x_{(i,j-1,t)} \\ &+x_{(i-1,j-1,t)} + x_{(i+1,j-1,t)} + x_{(i-1,j+1,t)} + x_{(i+1,j+1,t)}\Big]\Big) \end{aligned} \tag{2.6}$$

And is simplified as :

$$x_{(i,j,t+1)} = f\Big((1-\epsilon)x_{(i,j,t)} + \frac{\epsilon}{k}\sum_{<l,m>}^{k} x_{(l,m,t)}\Big) \tag{2.7}$$

CML is a widely used tool in numerous fields such as physics, biology, mathematics, ecology and engineering; specific simulation of phenomena include convection [Yanagita and Kaneko, 1993], chemical waves [Kaneko, 1993], formation of sand dunes [Nishimori and Ouchi, 1993] and cloud formation [Yanagita and Kaneko, 1997]. CML has also been used as an alternative to other spatially explicit models such as IBM [Brännström and Sumpter, 2005].

2.2.7 Graph (Network) Models

A graph is a compact mathematical representation of the connectivity topology of complex systems. It consists of an ordered pair of disjoint sets $G = \langle V(G), E(G)\rangle$ such that $V(G) \neq \phi$ and $E(G) \subseteq \{\{u, v\} : u \neq v \in V(G)\}$, i.e. $E(G)$, the edge set, is a subset of the set of the unordered pairs of a nonempty vertex set $V(G)$ [Bollobás, 1979], implying that $|E(G)| \leq \binom{n}{2}$; $n = |V(G)|$[1].

G is called *regular (k-regular)* if each of its vertices has the same degree (k). It is *fully connected* ($k = n - 1$) if $|E(G)| = \binom{n}{2}$ and *random* if $kn/2$ out of all possible $\binom{n}{2}$ edges are chosen uniformly randomly with equal probability [Bollobás, 2001].

Structural properties : The most commonly used metrics to characterise structural properties of graphs are the characteristic path length and the clustering coefficient.

Characteristic path length ($\bar{L}$) The characteristic path length is a measure of the global structure of a graph (how well connected a graph is). In general, a path (a walk in which no vertex is visited more than once) from

[1] In graph theory, the size of the graph is generally denoted by $|E(G)|$ and the order of the graph by $|V(G)|$; however in complex systems theory, the size usually refers to the vertex set $|V(G)|$.

a vertex u to another vertex v in a graph G is a sequence of edges that are traversed from u to v with no edge traversed more than once (trail). There may exist more than one path from u to v in G. The length of a path is the number of edges. The shortest path (or geodesic) between two vertices u and v is the path between them with the smallest length. The Characteristic Path Length is the length of the shortest path $d_{uv} = \min_{l \in \text{paths}(u,v)} \text{length}(l) : u, v \in V(G)$ between any two vertices u and v, averaged over all pairs of vertices:

$$\bar{L} = \frac{1}{\binom{n}{2}} \sum_{u=1}^{n} \sum_{v>u}^{n} d_{uv} \tag{2.8}$$

where n is the order of the graph.

Clustering coefficient ($\bar{C}$) The clustering coefficient [Watts and Strogatz, 1998] is a measure of local graph structure – the "cliquishness" of a neighbourhood (how locally clustered a graph is). The open neighbourhood of a vertex v is $\Gamma_v = \{u \mid d(u,v) = 1\} \setminus \{v\}$, i.e. the set of vertices directly connected to v, but excluding v itself. The clustering coefficient of vertex v is the ratio of the actual number of edges realised in Γ_v to the number of possible edges:

$$C_v = \frac{|E(\Gamma_v)|}{\binom{k_v}{2}} \tag{2.9}$$

where $C_v \in [0,1]$, Γ_v is the neighbourhood of the vertex v, $|E(\Gamma_v)|$ is the number of actual edges in the neighbourhood of v, k_v is the number of vertices in the subgraph Γ_v (or equivalently $|\Gamma_v|$) and $\binom{k_v}{2}$ is the number of possible edges in Γ_v since a vertex v with k_v neighbours can have have at most $k_v(k_v-1)/2$ edges between them (the fully connected graph). $C_v = 1$ if every vertex in the neighbourhood of v is connected to every other vertex in the neighbourhood of v. $C_v = 0$ if no vertices in the neighbourhood of v are connected.

The clustering coefficient of the graph G, ($\bar{C}$) is the average neighbourhood clustering coefficient, or equivalently, the number of actual edges normalised

by number of possible edges and averaged over all the vertices $v \in V(G)$:

$$\bar{C} = \frac{1}{n} \sum_{v=1}^{n} C_v \tag{2.10}$$

where $\bar{C} \in [0, 1]$, n is the order of the graph and C_v is the clustering coefficient of vertex v in graph G.

For a complete graph we have $(k = n - 1)$, $\bar{C} = 1$, and for an empty graph $(k = 0)$, $\bar{C} = 0$ [Watts, 1999].

Proximity ratio Walsh [1999] introduced a quantitative measure of "small-worldliness" known as the proximity ratio, defined as the ratio $\bar{C}(p)/\bar{L}(p)$ normalised by $\bar{C}(1)/\bar{L}(1)$:

$$\mu = \frac{\bar{C}(p)}{\bar{L}(p)} \frac{\bar{L}(1)}{\bar{C}(1)} \tag{2.11}$$

where $\bar{L}(1)$ and $\bar{C}(1)$ are the characteristic path length and clustering coefficient of random graphs and $0 < p < 1$ is the randomness probability which introduces long range edges in the graph. Random graphs have a proximity ratio of 1, while lattice graphs have smaller proximity ratios. For graphs with a small world effect, $\mu \gg 1$.

Degree Distribution The degree of a node is the number of neighbours it is connected to. The degree distribution is defined as the normalised frequency distribution of degrees over the whole network. The degree distribution of a network is a simple property which helps to classify networks. The regular network with Moore neighbourhoods have the same degree $(k = 8)$ for all the nodes. The degree distribution of small-world networks (p in the small-world regime [Punithan and McKay, 2013b] follows a Poisson distribution with exponential tail. Networks in which most nodes have approximately the same number of neighbours are known as "egalitarian" networks [Buchanan, 2003].

Regular graphs have high local clustering ($\bar{C} \approx 3/4$ for $k \gg 2d$; where d is the dimension of the graph), but large global separation ($\bar{L} \approx n/2k$) [Watts, 1999, 2003]. Random graphs have low local clustering ($\bar{C} \approx k/n$) and short paths ($\bar{L} \approx \ln(n)/\ln(k)$) [Watts, 1999, 2003]. Fully connected (all-to-all) graphs have the maximum clustering coefficient of 1 and no spatial relations. Although fully connected graphs have large $\bar{C}$ and small $\bar{L}$, they are not sparse, with the number of edges being quadratic in the number of vertices. But real world graphs typically have the properties of high local clustering (large $\bar{C}$) as in regular graphs, and low characteristic path length (small $\bar{L}$) as in random or fully connected graphs. In addition, they are sparse: the number of edges is comparable to the number of vertices.

Small-world graph : Many real-world graphs are characterised by large size ($n \gg 1$), sparseness ($|E(G)| \ll \binom{n}{2}$), decentralisation ($n \gg k_{max} \gg 1$ – where k_{max} is the maximal degree over all vertices), and rich local clustering ($\bar{C} \gg \bar{C}_{random}$), but still show short paths ($\bar{L} \approx \bar{L}_{random}$) between pairs of vertices [Watts, 1999, 2003]. This structure derives from the existence of a few non-local long range connections. Such a graph is said to exhibit the 'small-world phenomenon'.

Small-world graphs can be created in a multitude ways. We use three methods: randomly rewiring the edges of a regular graph (WS), adding new edges to a regular graph (NW) and adding both new vertices and random edges to a regular graph (SW). In more detail:

Watts-Strogatz model The existing edges between the vertices in a d-dimensional k-regular graph are rewired uniformly randomly with probability $p \in [0, 1]$; that is, approximately $pnk/2$ edges are randomly removed, and the same number of new edges are added, where n is order of the graph and k is the number of neighbours. When the existing edge from a vertex is removed, a new edge is added from the same vertex to a randomly chosen vertex in the graph. After the rewiring process, each vertex has a varying number of edges (degree). The random rewiring does not change the size of the graph,

maintaining it as $nk/2$. Though this WS procedure preserves the number of connections in the original graph, it suffers from one deficiency: it does not guarantee that the resulting graph is connected.

As p increases, the properties of the graph change. When $p = 0$, no existing edge has been rewired, so the graph remains a regular graph. For small values of p, the graph remains highly clustered and highly connected. When $p = 1$, all the existing edges have been rewired, and the graph is similar to a random graph. In the WS model, the connectivity topology can be set anywhere between a completely regular graph and a random graph, through tuning the rewiring probability p.

Newman-Watts model Newman and Watts adapted the WS model to guarantee connectivity, by introducing a variant in which instead of rewiring the edges, additional long range edges are added with probability $p \in [0, 1]$ between randomly chosen vertices in the regular graph with k neighbours. In contrast to WS, no edges are removed, which means the local connectivity is not altered. After the addition of the extra edges, the number of neighbours at each vertex may vary, but it remains at least k. Thus we can guarantee that there are no disjoint vertices. This process changes the size of the graph.

When $p = 0$, no non local connections are added. When $p = 1$, k extra non local edges are added to each vertex in the graph. When p is between 0 and 1, [0, k] edges are added. Thus the linkage density increases over that for $p = 0$. With 0 or small values of p, the graph will be close to a regular graph. When $p = 1$ and $k = n - 1$, the resultant graph is fully connected.

Smallest-World model In this model, (np) new vertices are added and are connected to randomly chosen (k) vertices in the initial graph. No edges are deleted from the initial lattice. This process changes both the order and size of the graph. When $p = 0$, no new vertices and edges are added. When $p = 1$, n new vertices are added and nk edges are added.

The rewired or added edges are built independent of their spatial locations. As more are added, so-called small-world properties emerge; the region in which this occurs is known as the small-world regime. Within this regime, the graph is ordered locally but randomised globally.

Adaptive graph : The adaptive nature of the system is modelled via Dynamic Linking (DL), which is the key feature of adaptive networks and can be modelled in a number of ways:

1. Active vertices grow and inactive vertices lose edges
2. Active vertices lose edges and inactive vertices grow them
3. Vertices never lose edges; the graph evolves by either:
   (a) Adding new edges to active vertices from inactive vertices
   (b) Adding new edges to inactive vertices from active vertices
   (c) Adding reciprocal edges between vertices and inactive vertices

2.3 Quantification of Spatio-Temporal Dynamics

2.3.1 Permutation Entropy (PE):

Bandt and Pompe [2002] introduced Permutation Entropy (PE) as a measure to detect stationary, periodic, chaotic and random behaviour of a complex time series. Other metrics, for example the Lyapunov exponent, have been used to characterise a chaotic time series; we chose PE due to its conceptual simplicity and computational efficiency. Importantly, it is robust to noise and does not require any preprocessing of the data such as noise elimination. The PE of order $q \geq 2$ is defined as:

$$H_p(q) = -\sum p(\pi) \ln p(\pi) \tag{2.12}$$

where the sum is over all $q!$ permutations π of order q.

A normalised form, H_p, can be computed by:

$$0 \leq H_p = \frac{H_p(q)}{\ln(q!)} \leq 1 \tag{2.13}$$

where the lower bound denotes regularity in a time series and the upper bound represents a completely random system. In general, smaller values of q, such as 1 or 2, are not appropriate due to the small number of distinct states and larger values of q, such as 12 or 15, are also inappropriate since the aim is to detect the changes in the system [Cao et al., 2004]. Bandt and Pompe used $q = 3, ..., 7$ in their experiments. Hence we have chosen 7 as the order in our experiments.

2.3.2 Moran's I (MI):

Moran's I [Moran, 1950] is a measure of spatial autocorrelation, and is also used to analyse spatial patterns. It is defined as:

$$I = \frac{U}{\sum_i \sum_j w_{ij}} \frac{\sum_i \sum_j w_{ij}(P_i - \bar{P})(P_j - \bar{P})}{\sum_i (P_i - \bar{P})^2} \tag{2.14}$$

where U is the number of spatial units, indexed by i and j; P is the population size; $\bar{P}$ is the mean population; and w_{ij} is a spatial weight matrix. In our work, we use a binary weight matrix with $w_{ij} = 1$ if i and j are neighbours and 0 otherwise. The Moran's I value ranges from -1 to $+1$. Positive values indicate high spatial autocorrelation, while negative values indicate negative spatial autocorrelation, with 0 indicating no spatial correlation. In the context of pattern analysis, negative, 0 and positive values indicate spatially dispersed, random, and clustered patterns respectively.

Chapter 3

Homeostatic Complex System based on Daisyworld Modelling

Homeostasis is resistance to change. The most studied homeostatic systems are Ashby's homeostat [Ashby, 1962] (physical device) and Lovelock's daisyworld (a planetary mathematical model). Homeostat demonstrated ultrastability by maintaining the essential variables within a viability ranges in the face of externally imposed perturbations. Daisyworld model demonstrated homeostatic regulation of the environment by the biota. Daisyworld is an approach to design and analyse robust artificial homeostatic systems. Hence we take daisyworld as our base model for further investigations.

In this chapter, we reconstruct the original daisyworld model [Watson and Lovelock, 1983] based on Coupled Map Lattice (CML). We model life-environment feedback in diffusively coupled logistic systems in a 2D tordoidal regular lattice with chaotic local dynamics. Then we incorporate small-world phenomenon, scale-freeness and topology-dynamics feedback.

Our model differs from previous work [Wood et al., 2008, section 3] primarily in the following areas:

- Previous work generally used only presence/absence of daisies in a cell (hence the population model functioned as a form of cellular automaton). We use a finite population with a logistic carrying capacity model, permitting more detailed examination of population dynamics and of diffusion effects using Coupled Map Lattice(CML).
- As a result, previous work extending daisyworld spatially could only observe boom and bust temporal behaviour; because of the more detailed population dynamics in our model, we can observe other kinds of temporal fluctuations (including chaos) arising from spatial extension, and can analyse new and interesting spatio-temporal interactions in daisyworld.
- Previous work analysed the dynamics of daisyworld qualitatively. We use statistical quantifiers to measure the spatio-temporal dynamics of the daisyworld.
- We study the variation of the spatio-temporal dynamics with changes in the model parameters both qualitatively and quantitatively.
- We allow limiting similarity (sub section 3.2).
- Previous work are only based on regular lattice, we incorporate characteristics of complex and adaptive networks (sub section 3.3), such as
  - Small-world phenomenon
  - Adaptiveness
  - Scale-freeness

3.1 Reconstructed Core Daisyworld Model

Our version of daisyworld is a 2-lattice graph $G_{N,N}$ ($N = 100$ is the lattice length) of coupled dynamic units. We first construct a square regular lattice in a two-dimensional Euclidean space ($N \times N$) of unit-distance, each vertex having the same degree k. The k vertices are based on the Moore neighbourhood model ($k = 8$) and hence our graph is sufficiently sparse ($k \ll N * N$)

and also sufficiently dense ($k \gg 1$). We enforce periodic boundary conditions in this lattice to eliminate edge effects by wrapping the edges around, resulting in a torus.

Each vertex in the lattice represents a habitat (dynamical unit) and is constrained with a maximum vegetation (carrying capacity κ) of $10,000$ daisies to avoid unbounded behaviours, while each edge supports interactions between the units – the neighbourhood connectivities. There are k habitats in the neighbourhood Γ. Each such habitat (*discrete space*) contains real-valued attributes ($0 < P_b, P_w < 10,000$ and $278 < T < 313$K; P_b, P_w and T are *continuous states* representing black and white daisy population size and temperature respectively). The states are updated in *discrete time* by real-valued functions. Thus our constructed system is a complex dynamic system in which the continuous state habitats diffusively interact with their neighbours (coupled), evolve in discrete time (map) and are distributed on a discrete space (lattice) – a Coupled Map Lattice (CML). The attribute values evolve according to deterministic rules, depending both on their own value and those of their neighbours.

Each habitat (interating component) in our ecosystem is a system. The elements such as life (black and white daisies) and environment (temperature) are interconnected and interdependent via reinforcing and balancing feedback loops. The interaction rules among these system components are based only on local information (microscopic level) and not on the global emergence (macroscopic level). The black and white daisies, along with the temperature, diffuse around the world via their neighbourhood. At each succession of a habitat, we compute the population of black and white daisies, and the temperature, based on equation 2.7.

Our daisyworld model has two terms:

- A *reaction term* describing the growth of daisies and temperature change at a particular habitat
- A *coupling term* describing the dispersion of daisies and diffusion of temperature in their neighbourhood

These local components and their interaction rules at the microscopic level give rise to global emergence at the system level.

Table 3.1: Basic Equations

Name of the equation	**Equation**
Energy balance	$\sigma_B T^4 = SL(1-A)$
Logistic population growth	$P_{(t+1)} = P_t \left[1 + r\left(1 - \frac{P_t}{\kappa}\right)\right]$
Logistic population growth with temperature feedback	$P_{(t+1)} = P_t \left[1 + r\left(\beta(T) - \frac{P_t}{\kappa}\right)\right]$
Discrete Laplacian diffusion	$x'_{(i,j,t)} = (1-\epsilon)x_{(i,j,t)} + \frac{\epsilon}{k}\sum_{<l,m>}^{k} x_{l,m,t)}$
Reaction diffusion of a dynamic variable (x)	$x_{(i,j,t+1)} = f\left(x'_{(i,j,t)}\right)$
Reaction diffusion extended form	$x_{(i,j,t+1)} = f\left((1-\epsilon)x_{(i,j,t)} + \frac{\epsilon}{k}\sum_{<l,m>}^{k} x_{l,m,t)}\right)$

Table 3.2: Daisyworld Model Equation Set

Parameter Name	**Equation**
Albedo	$A_{(i,j,t)} = A_b(\alpha_b)_{(i,j,t)} + A_w(\alpha_w)_{(i,j,t)} + A_g(\alpha_g)_{(i,j,t)}$
Growth rate	$\beta_c(T_{(i,j,t)}) = \max\left(1 - \left[\frac{(T_{\mathrm{opt}_c} - T_{(i,j,t)})^2}{17.5^2}\right], 0\right)$
Temperature	$T_{(i,j,t+1)} = g\left((1-D)T_{(i,j,t)} + \frac{D}{k}\sum_{<l,m>}^{k} T_{(l,m,t)}\right)$ $g\left(T'_{(i,j,t)}\right) = T'_{(i,j,t)} + \left[\frac{\left(SL(1-A_{(i,j,t)}) - \sigma_B (T'_{(i,j,t)})^4\right)}{C}\right] + \xi$
Population size	$P_{c(i,j,t+1)} = h\left((1-D_c)P_{c(i,j,t)} + \frac{D_c}{k}\sum_{<l,m>}^{k} P_{c(l,m,t)}\right)$ $h\left(P'_{c(i,j,t)}\right) = P'_{c(i,j,t)}\left[1 + r\left(\beta_c(T_{(i,j,t)}) - \frac{P'_{c(i,j,t)}}{\kappa}\right)\right]$

Reaction Term

Population Dynamics The local population dynamics at each location is computed using Verhulst dynamics (logistic equation with carrying capacity); it is of interest due to its chaotic behaviour over a specific range of bifur-

cation parameter values. The logistic population growth model with carrying capacity can lead to a density dependent population regulation (equation 2.1).

We also incorporate the temperature feedback effect in the logistic equation. The computation of population size with temperature feedback uses a difference equation based on Maddock [1991]:

$$P_{(t+1)} = P_t \left[1 + r\left(\beta(T) - \frac{P_t}{\kappa}\right)\right] \tag{3.1}$$

where $\beta(T)$ is temperature feedback; refer equation 3.4.

Temperature Dynamics The emitted radiation is defined by the Stefan-Boltzmann law as $E_{out} = \sigma_B T^4$ where σ_B is the Stefan-Boltzmann constant, and T is the temperature. The absorbed energy is computed as $E_{in} = SL(1 - A)$ where S is the solar constant, L is the luminosity and A is the albedo. At equilibrium, absorbed and emitted radiation follows Kirchhoff's law. Thus we can compute the temperature change at each location based on the planetary energy balance equation [McGuffie and Henderson-Sellers, 2005]:

$$\sigma_B T^4 = SL(1 - A) \tag{3.2}$$

Coupling Term

The interaction pattern of daisyworld is determined by the neighbourhood and the diffusion model.

Neighbourhood Model Since cliques are not captured in an open von Neumann neighbourhood, we choose Moore neighbourhoods. In any ecosystem, both species and temperature of our model diffuse around the world via their neighbourhood.

Diffusion Model We use a Laplacian diffusion model (or Turing diffusion). The diffusion model is detailed in the section 2.2.6.

The population and temperature update functions in our daisyworld model are based on the above basic equations (equation 3.1 and equation 3.2) from population dynamics and thermodynamics combining the spatio-temporal modelling (equations in the section 2.2.6). The basic set of equations is tabulated in Table 3.1.

3.1.1 Solar Insolation

Let us assume that there is no life in a Daisyworld. In this case, the albedo of the planet is that of bare ground, i.e. 0.5. The desired environmental temperature is $295.5K$ with solar luminosity 1.0. Substituting these values in equation 3.2 (energy balance), the required solar insolation is $864.65Wm^{-2}$; we use this value in all our experiments.

3.1.2 Albedo

The albedo (A) at a lattice point (i, j) and at time (t) is

$$A_{(i,j,t)} = A_b\alpha_{b_{(i,j,t)}} + A_w\alpha_{w_{(i,j,t)}} + A_g\alpha_{g_{(i,j,t)}} \tag{3.3}$$

i.e. the average of the albedos A_b of ground covered by black daisies, A_w of ground covered by white daisies and A_g of bare ground, weighted by $\alpha_b, \alpha_w, \alpha_g (= 1 - \alpha_w - \alpha_b) \in [0, 1]$, the relative areas occupied by black, white daisies and bare ground at time t. We assume that $A_w > A_g > A_b$, with corresponding values of 0.75, 0.5, 0.25. In our experiments, bare ground is completely occupied within the first few epochs.

3.1.3 Growth

The growth curve of daisies (β_c) is an inverted parabola:

$$\beta_c(T_{(i,j,t)}) = \max\left(1 - \left[\frac{(T_{\text{opt}_c} - T_{(i,j,t)})^2}{17.5^2}\right], 0\right) \tag{3.4}$$

$T_{(i,j,t)}$ is the local temperature and T_{opt_c} is the optimal temperature of the species. The optimal temperature of the daisies depends on their petal colour 'c' (phenotype). The optimal temperature for black daisies is lower than for white; the mean optimal temperature is assumed to be $295.5K$.

3.1.4 Temperature

The temperature $(T_{(i,j,t+1)})$ is computed as the sum of temperature after Laplacian diffusion $(T'_{(i,j,t)})$, the difference between solar absorption and heat radiation incorporating $T'_{(i,j,t)}$, and Gaussian white noise:

$$T_{(i,j,t+1)} = g\Big((1-D)T_{(i,j,t)} + \frac{D}{k}\sum_{<l,m>}^{k} T_{(l,m,t)}\Big) \tag{3.5}$$

where $T_{(i,j,t)}$ is local temperature , $< l, m >$ represents the set of neighbours of (i, j) and $D = D_T/C$ is the thermal diffusion constant normalised by heat capacity C. $g(T'_{(i,j,t)})$ is the temperature update function [Wood et al., 2008], in which $T'_{(i,j,t)}$ is the temperature after diffusion:

$$g\Big(T'_{(i,j,t)}\Big) \quad = \quad T'_{(i,j,t)} + \left[\frac{\Big(SL(1-A_{(i,j,t)}) - \sigma_B(T'_{(i,j,t)})^4\Big)}{C}\right] + \xi \tag{3.6}$$

where S is the solar constant, L is the luminosity, $A_{(i,j,t)}$ is the albedo, σ_B is the Stefan-Boltzmann constant and ξ is additive Gaussian white noise (with mean 0 and standard deviation 1.0) multiplied by the noise level (NL).

3.1.5 Population Size

The local population update depends on dispersion, density-dependant growth rate and the feedback coefficient:

$$P_{c_{(i,j,t+1)}} = h\Big((1-D_c)P_{c_{(i,j,t)}} + \frac{D_c}{k}\sum_{<l,m>}^{k} P_{c_{(l,m,t)}}\Big) \tag{3.7}$$

where $P_{c_{(i,j,t)}}$ is the population size at location (i, j) and time step t, D_c is the fraction of the population being dispersed to its neighbours, c stands for colour of daisies and k is number of neighbours. $h(P'_{c_{(i,j,t)}})$ is the population growth function and $P'_{c_{(i,j,t)}}$ is population size after dispersion:

$$h\left(P'_{c_{(i,j,t)}}\right) = P'_{c_{(i,j,t)}}\left[1 + r\left(\beta_c(T_{(i,j,t)}) - \frac{P'_{c_{(i,j,t)}}}{\kappa}\right)\right] \tag{3.8}$$

where r is population increase rate, $\beta_c(T_{(i,j,t)})$ is the feedback due to temperature and κ is the carrying capacity. Thus the population density at a habitat is controlled by the density dependence at that location and dispersal to its nearest neighbours. In general simulations, deterministic chaos is observed only at high values for the increase rate. But deterministic chaos can also be induced by diffusion, so our system does not require high intrinsic growth rates to exhibit interesting behaviours.

The above set of equations (from 3.3 to 3.8) from thermodynamics and population dynamics integrate well and generate the couplings between life and the environment. Daisy population size (P) depends on the growth rate (β) which depends on the environmental variable temperature (T) which depends on the environment altering trait albedo (A) which is influenced by the daisy cover (P). These interdependencies among the physical variables of interest form a tightly coupled system with an endless feedback loop. The computation of these variable are tabulated in the Table 3.2 for easy understanding.

3.2 Limiting Similarity (Temperature Overlap)

Limiting similarity defines a level of overlap between any two species that allows them to coexist. The range of temperature regimes in which daisies can survive is the viability constraint of our model, and is based on the overlap between the optimal temperatures of black and white daisies as in Table 3.3. We define the optimal temperature of black daisies within the range $[278, 295.5]K$

Table 3.3: Optimal Temperature (of black and white daisies with respect to overlap)

Overlap(%)	**Opt. temp. (K) black daisies**	**Opt. temp. (K) white daisies**
0	278	313
10	284.5	306.5
25	288	303
50	291.5	299.5
100	295.5	295.5

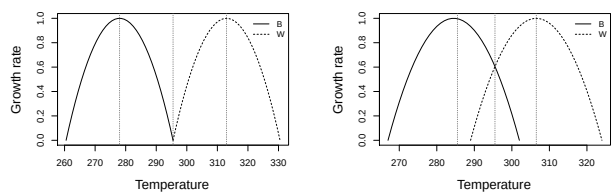

(a) Overlap0

(b) Overlap10

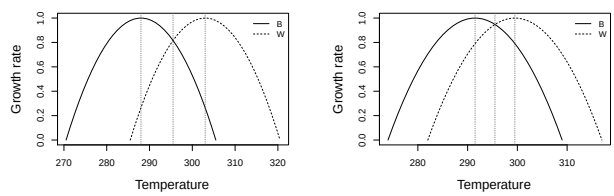

(c) Overlap25

(d) Overlap50

Figure 3.1: Overlap of Growth Curves of Black and White Daisies

and of white in the range $[295.5, 313]K$ so as to have an overlap in the range $[0, 100]\%$ (Figure 3.1). When the overlap is 100%, the two growth curves superimpose on each other.

3.3 Incorporation of Complex Topological Properties

We have investigated daisyworld phenomenon in regular (chapter 4 and sub section 5.2.2), random (sub section 5.2.3), fully-connected (sub section 5.2.4), small-world (section 5.3), adaptive topologies (section 5.4) and scale-free (section 5.5). The changes to the underlying topology (regular) are described in their corresponding chapters.

1. We start with an ecosystem where habitats are only locally connected (regular CML with Moore neighbourhood). The experiments described in the chapter 4 are based on regular lattice.

2. We rewire or add random non-local couplings to the underlying regular lattice, which introduces small-world effects in system (Watts-Strogatz model, Newman-Watts model and Smallest World model in CML). The experiments described in the section 5.3 incorporate small-world phenomenon.

3. Each frozen vertex in the underlying regular lattice is dynamically and reciprocally coupled to a randomly chosen active vertex (adaptive CML). The experiments described in section 5.4 are adaptivly acquire connections based on the local dynamics.

4. Each vertex in the lattice reciprocally connected to hub vertices or to local vertices or to non-local vertices. The experiments described in section 5.5 incorporate scale-freeness.

In complex and adaptive topologies, species (black and white daisies) –through the mix of local and long range couplings– can disperse quickly around the daisyworld but temperature diffuses only via the local neighbours to other parts of the world. The inclusion of even a few long-range interactions in the underlying topology leads to highly interconnected dynamical units, exhibiting a significant effect on daisyworld dynamics.

3.4 Experimental Setup

3.4.1 Parameter Settings

Table 3.4: Daisyworld Parameter Settings (last six rows are variable parameters, others are fixed)

Parameter	**Value(s)**
Fixed	
Number of cells ($N \times N$)	100×100
Bare ground Albedo (A_g)	0.5
Albedo of black daisies (A_b)	0.25
Albedo of white daisies (A_w)	0.75
Heat capacity (C)	2500 $Wm^{-2}K^{-1}$
Diffusion constant (D_T)	500 $Wm^{-2}K^{-1}$
Stefan-Boltzmann constant (σ_B)	5.67 $E^{-8}Wm^{-2}K^{-4}$
Solar constant (S)	$864.65Wm^{-2}$
Luminosity (L)	1
Mean growth temperature	$295.5K$
Carraying capacity (κ)	10000
Time step (t)	1
Horizontal grid size (i)	1
Vertical grid size (j)	1
Variable	
Opt. temp. of black daisies (T_{opt_b})	$[278, 295.5]K$
Opt. temp. of white daisies (T_{opt_w})	$[295.5, 313]K$
Diffusion rate of black daisies (D_b)	$[0, 1]$
Diffusion rate of white daisies (D_w)	$[0, 1]$
Noise level (NL)	$[0, 10]K$
Natural rate of increase (r)	$[1, 4]$

The model parameters for the simulation are shown in Table 3.4. They are adapted from the parameter values used in the wider daisyworld literature, modified to fit a CML model [von Bloh et al., 1997; Watson and Lovelock, 1983]. The last six rows in Table 3.4 are variable parameters, while the rest are the fixed parameters. As we have a huge parameter space, we have restricted

our experiments to an increase rate of $r = 1$. We have used the same diffusion constant for both black and white daisies in all our experiments. We have limited our focus to studying the effects of species diffusion (which influences the species distribution) and noise (which influences the temperature) in detail. The range of temperatures in which daisies can survive is the viability constraint of our model, and is based on the overlap between the optimal temperatures of black and white daisies as in Table 3.3. We define the optimal temperature of black daisies within the range $[278, 295.5]$K and of white in the range $[313, 295.5]$K so as to have an overlap in the range $[0, 100]\%$. The variable parameter differs for different set of experiments and are tabulated in their corresponding chapters.

3.4.2 Initializations

All habitats in the lattice are randomly initialised with a population size in $[0, 100]$ for both black and white daisies. The temperature is initialised randomly depending on the overlap between the optimal temperatures of black and white daisies (Table 3.3).

3.4.3 Visualisations

We capture snapshots from the evolution of daisyworld to inspect its spatio-temporal dynamics. Each snapshot represents the population structure of the ecosystem at the particular epoch. As it is impractical to show all the snapshots over $5,000$ epochs, we plot the temporal dynamics of daisy populations and temperature at a particular habitat as well as the temporal dynamics of the average daisy populations and temperature of the whole ecosystem. These plots reflect the local and global behaviours of the daisyworld. In the visualisations, a habitat is shown as black if black daisies alone occupy that habitat and correspondingly for white. If both daisies coexist at a habitat but black dominates, it is shown as dark grey; if white dominates, it is presented as light grey; and if the populations are equal, it is represented as medium grey.

Chapter 4

Daisyworld with Local Couplings

In this chapter, we investigate two-dimensional (2D) CML based daisyworld with only local couplings. In the section 4.1, we analyse daisyworld as self-organizing system, reaction-diffusion system (activator-inhibitor system), complex dynamical system and pattern formation system based on biological inspirations from nature. In section 4.2, we investigate local chaoticity and global stability dynamics of daisyworld. We examine the evolutionary dynamics of daisyworld in the section 4.3. In section 4.4, we introduce methods to analyse a huge parameter space with spatio-temporal quantifiers.

4.1 Self-Organizing Spatio-temporal Patterns

In this section, we examine self-organized, spatio-temporal patterns from our 2D CML based daisyworld with only local couplings. We investigate the self-organizing properties of daisyworld, and qualitatively analyse pattern formation in daisyworld. We also quantify the emergence of vegetation patterns using a statistical measure, Moran's I. We show that the surface temperature of planet is self-regulated around the mean 295.5K by the daisyworld dynamics regardless of the varied self-organized pattern formations.

In our daisyworld model, depending on model parameter values we observe a variety of behaviours, such as 1) complex patterns, 2) Turing-like structures, 3) cyclical patterns, 4) random patterns and 5) uniformly dispersed patterns.

4.1.1 Variable Parameter Settings

Table 4.1: Variable Parameter Settings

Parameter	**Value**
Overlap	$\{0, 5, 10, 25, 50, 100\}\%$
Natural rate of increase (r)	$[1, 4]$
Noise level (NL)	$\{0, 0.001, 0.005, 0.01, 0.05,$ $0.1, 0.2, 0.5, 1, 2.5, 5, 7.5, 10\}$
Temperature diffusion (D)	$\{0, 0.05, 0.1, 0.2, 0.3, 0.5, 1\}$
Dispersion rate (D_c)	$\{0, 0.001, 0.01, 0.1, 0.2, 0.5, 1\}$

We have run over $15,000$ experiments on this CML based daisyworld model, with each experiment running for 5000 epochs. The ranges for the various parameters are shown in Table 4.1. The results presented in the following sub sections are samples from over 15,000 experiments with different variable parameter settings. We have examined the results for the emergence of interesting patterns both qualitatively (by capturing snapshots of each experiment and inspecting visually and by plotting cobwebs) and quantitatively (using the value of Moran's I).

4.1.2 Self-organized Complex Pattern

A maze-like self-organizing pattern (Figure 4.1) emerge from our system with a temperature overlap of 10%, species dispersion rate of 0.001, and a noise level of 0.001. After some cyclical behaviour, the system finally converged to a stationary maze-like structure. The global spatial behaviour is plotted in the Figure 4.3. The sub Figure 4.3 (a) shows that the global temperature fluctuates initially, but converges to $295.5K$ and the sub Figure 4.3 (b) displays a static average population of black and white daisies, exhibiting a stationary

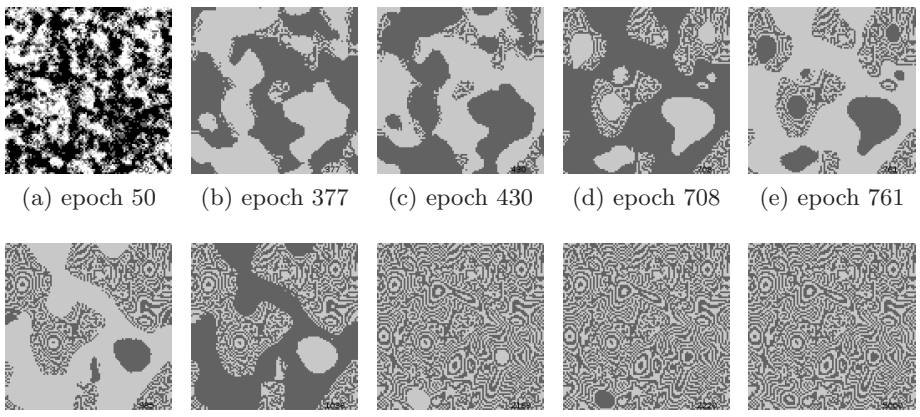

(a) epoch 50 (b) epoch 377 (c) epoch 430 (d) epoch 708 (e) epoch 761

(f) epoch 985 (g) epoch 1036 (h) epoch 2169 (i) epoch 2220 (j) epoch 5000

Figure 4.1: Maze like Organization for 10% Overlap, $D_c = 0.001$, $D = 0.2$, $r = 1$ and NL= 0.001 in 2D 100×100 Lattice

pattern formation. Initially the Moran's I is very high (sub Figures 4.3 (c) and 4.3 (d)), indicating the formation of very large clusters, but it finally drops below 0, indicating a uniformly dispersed pattern. In between, the fluctuations show complex dynamics. The local behaviours at a particular habitat is depicted in the Figure 4.2. The local temperature (sub Figure 4.2 (a)) and population (sub Figure 4.2 (b)) confirms stationary dynamics. The straight lines in coweb plots 4.2 (c) and 4.2 (d) also indicate the static dynamics (stationarity) of black and white daisy populations.

4.1.3 Turing-like Structure

Turing-like patterns emerge with a diffusion constant of 0.01 for both species, a noise level of 1 and an overlap of 100% – refer to Figure 4.4. This clearly shows self-organized pattern emerge with time. The patterns which emerge look like an animal's coat (e.g. Holstein cow). The corresponding global dynamics are plotted in Figure 4.6. The fluctuations in global temperature in sub Figure 4.6 (a) shows the dynamicity (non-stationary) of pattern formation. The sub Figure 4.6 (b) depicts the global population dynamics. The high

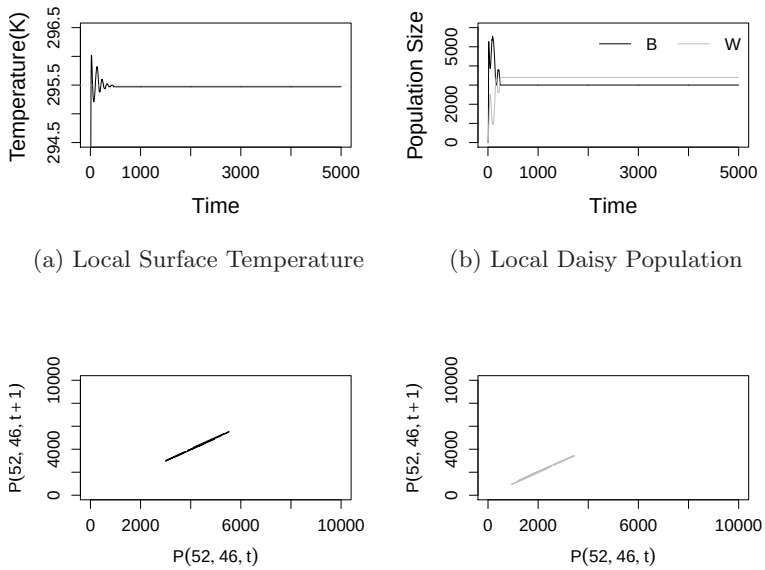

(a) Local Surface Temperature

(b) Local Daisy Population

(c) Local Black Daisy Cobweb

(d) Local White Daisy Cobweb

Figure 4.2: Local Dynamics of Maze : 10% Overlap, $D_c = 0.001$, $D = 0.2$, $r = 1$ and NL= 0.001 in 2D 100×100 Lattice

Moran's I throughout the run (except the initial transitions) corresponds to the emergence of large clusters in the patterns (sub Figures 4.6 (c) and 4.6 (d)). The local dynamics can be observed in the Figure 4.5. The cowebs displays chaoticity within the range $[4000, 6000]$ – population size.

4.1.4 Cyclical Pattern

Cyclical patterns are formed (Figure 4.7) from the system with a temperature overlap of 10%, dispersion rate of 0.2 for both the species, and noise level of 0.05. The corresponding global dynamics are plotted in Figure 4.9. The cycles in the global temperature (sub Figure 4.9 (a)) indicate the cyclical dynamics of the daisy population (sub Figure 4.9 (b)). Except for the initial states, Moran's I is high throughout the run, confirming the formation of large clusters (sub

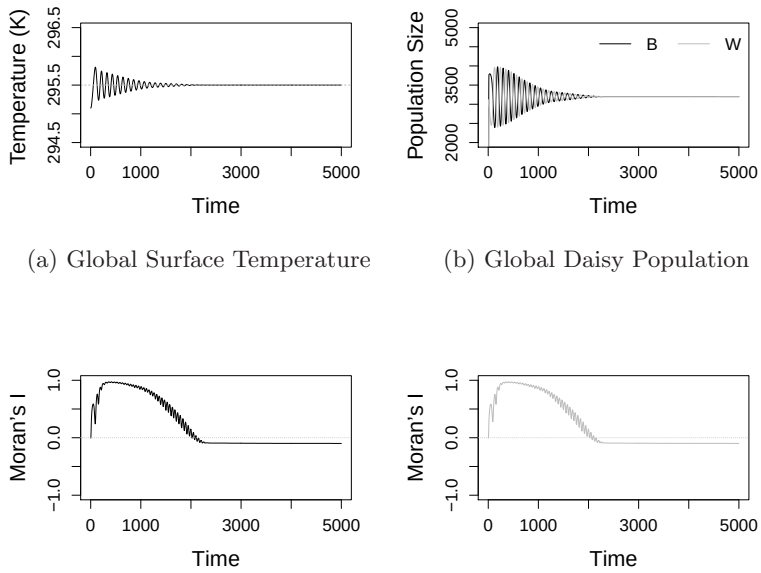

(a) Global Surface Temperature

(b) Global Daisy Population

(c) MI Black Daisy

(d) MI White Daisy

Figure 4.3: Global Dynamics of Maze : 10% Overlap, $D_c = 0.001$, $D = 0.2$, $r = 1$ and NL= 0.001 in 2D 100×100 Lattice

Figures 4.9 (c) and 4.9 (d)). The local dynamics are plotted in the Figure 4.8. The cobweb plots 4.8 (c) and 4.8 (d) depict cyclical abundance of black and white daisies. The cycles seen in local temperature and population plots (sub Figures 4.8 (a) and 4.8 (b)) confirm the cyclical pattern formation.

4.1.5 Random Pattern

Figure 4.10 depicts the global dynamics of random pattern formation in the daisyworld system for a noise level of 0.01 and with no species dispersion. The global temperature dynamics is shown in sub Figure 4.12 (a) and corresponding daisy abundance is plotted in sub Figure 4.12 (b). The near-zero value of Moran's I in sub Figures 4.12 (c) and 4.12 (d) confirm the formation of random patterns. The local dynamics are plotted in the Figure 4.11.

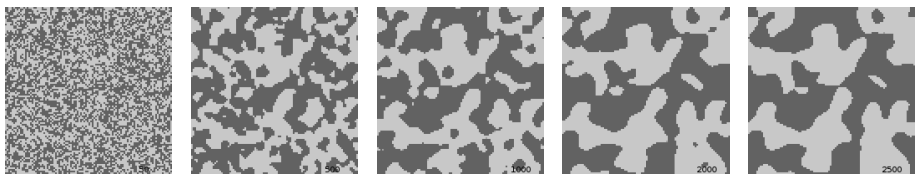

(a) epoch 50 (b) epoch 500 (c) epoch 1000 (d) epoch 2000 (e) epoch 2500

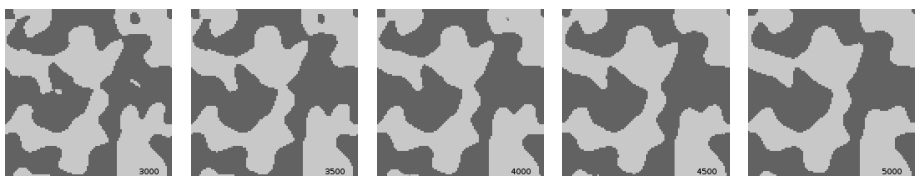

(f) epoch 3000 (g) epoch 3500 (h) epoch 4000 (i) epoch 4500 (j) epoch 5000

Figure 4.4: Turing-like Structure for 100% Overlap, $D_c = 0.01$, $D = 0.2$, $r = 1$, $NL = 1$ in 2D 100×100 Lattice

4.1.6 Dispersed Pattern

Uniformly dispersed patterns emerge at a of noise level 0.5 with no species diffusion (Figure 4.13); the corresponding global dynamics are depicted in Figure 4.15. Moran's I in sub Figures 4.15 (c) and 4.15 (d) lie below zero, indicating dispersed patterns. Interestingly, we do see the emergence of a hint of a large scale grid in this setting, presumably resulting from the effects of temperature diffusion. The local dynamics are depicted in the Figure 4.14.

4.1.7 Discussion

Global Emergence: The behavioural rules in the system specify that black daisies grow better in colder temperatures, while white daisies grow better in hotter temperatures, both diffusing to their nearest neighbours. These simple components at the local level generate complicated dynamics at the global level due to the collective behaviour of the whole system, without the influence of any external forces. The interaction pattern is determined by the neighbourhood topology and the diffusion term. The key ingredients leading to global emergence are the local nonlinear interactions among the components,

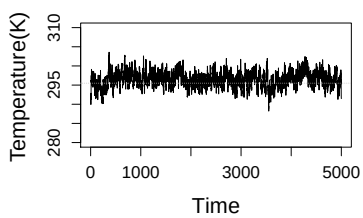

(a) Local Surface Temperature

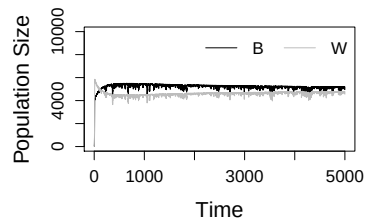

(b) Local Daisy Population

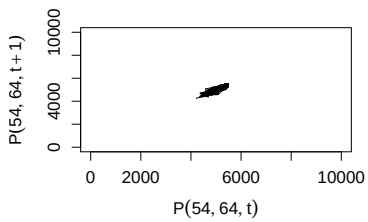

(c) Local Black Daisy Cobweb

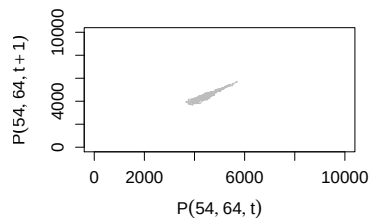

(d) Local White Daisy Cobweb

Figure 4.5: Local Dynamics of Turing-like Structure : 100% Overlap, $D_c = 0.01$, $D = 0.2$, $r = 1$ and NL= 1 in 2D 100×100 Lattice

physiological and behavioural rules, and physical constraints. The inhibition of self-growth can also arise from the physical constraints, due to the self-limiting factor of carrying capacity.

Daisyworld as a Dynamical System We examine our formulation at a point with NL=0.1 and 100% overlap. The corresponding bifurcation plots in the Figures 4.16 and 4.17 illustrate that the reconstructed daisyworld system is a dynamical system. The plots show fixed point attractors, bifurcations and strange attractors.

Daisyworld as Self-organizing System In daisyworld, an initial growth of black daisies, due to positive feedback, increases the temperature of system

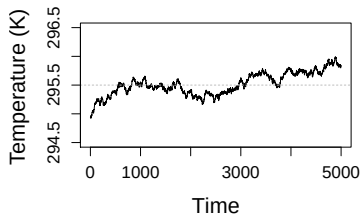

(a) Global Surface Temperature

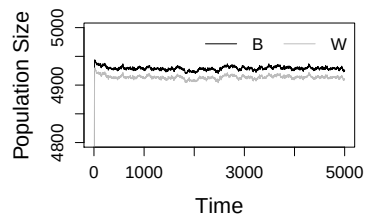

(b) Global Daisy Population

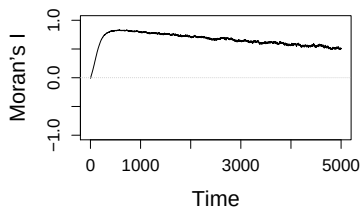

(c) MI Black Daisy

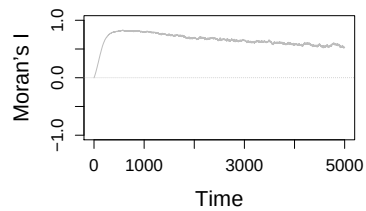

(d) MI White Daisy

Figure 4.6: Global Dynamics of Turing-like Structure : 100% Overlap, $D_c = 0.01$, $D = 0.2$, $r = 1$ and NL= 1 in 2D 100×100 Lattice

and thus reinforces the change in the same direction. Hence it has the potential to explode the system. But in daisyworld, at a higher temperature, white daisies bloom and keep the positive feedback under control. In the same manner, the growth of white daisies, due to positive feedback, decreases the temperature in the same direction. But at a colder temperature, black daisies bloom and inhibit the system behaviour. The initial growth of daisies promotes new changes in the system state but on the other hand, increased growth counteracts the changes. The combined effect of positive and negative feedback couplings result in a negative feedback loop, which stabilises the physiological processes and leads to homeostasis. Due to this behaviour, we can see that daisyworld is a self-organizing system.

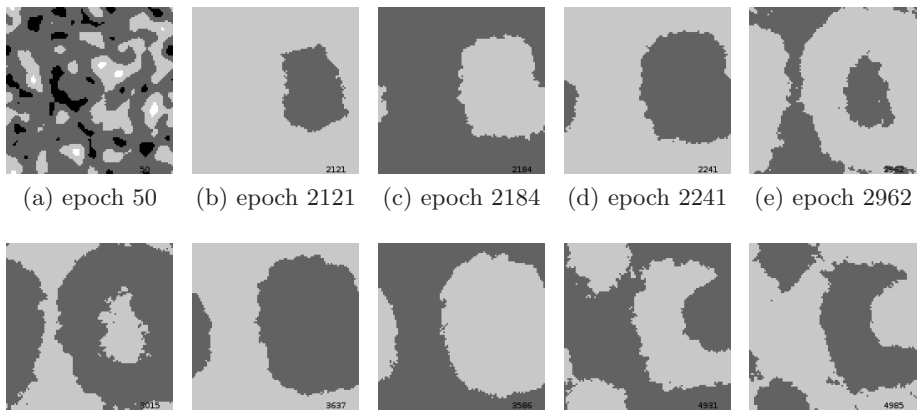

(a) epoch 50 (b) epoch 2121 (c) epoch 2184 (d) epoch 2241 (e) epoch 2962

(f) epoch 3015 (g) epoch 3637 (h) epoch 3586 (i) epoch 4931 (j) epoch 4985

Figure 4.7: Cyclical Pattern : 10% overlap, $D_c = 0.2$, $D = 0.2$, $r = 1$ and NL= 0.05 in 2D 100×100 Lattice

Daisyworld as Reaction-Diffusion System We can view daisyworld as a Turing reaction-diffusion system of two morphogens: black and white daisies. In cooler temperatures, black daisies absorb the available sun light and amplify their growth, functioning as activators (autocatalysis) because they activate their own production. But further increase in black daisies increases the surface temperature to the level at which cooler white daisies grow well, thereby acting as an inhibitor (self-suppression) because they inhibit their own production. This process is reversed for white daisies. Depending on the temperature, black and white daisies act both as inhibitor and as activator. Here, the diffusion of the two species, coupled by nonlinear local rules, result in the generation of patterns and spatial self-organization due to symmetry-breaking instability.

4.1.8 Summary

The results in this section illustrate that the underlying dynamics of daisyworld are not restricted to stationary patterns but extend to periodic and chaotic behaviour. We see stability as well as complexity emerge. The fig-

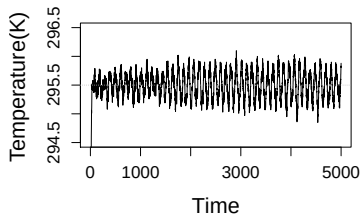

(a) Local Surface Temperature

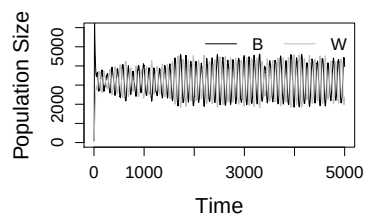

(b) Local Daisy Population

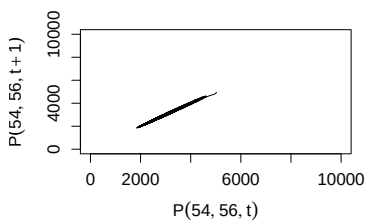

(c) Local Black Daisy Cobweb

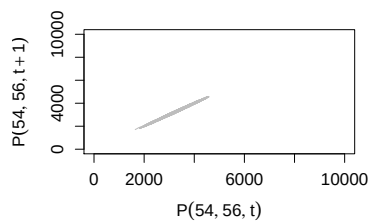

(d) Local White Daisy Cobweb

Figure 4.8: Local Dynamics of Cyclical Pattern : 10% overlap, $D_c = 0.2$, $D = 0.2$, $r = 1$ and NL= 0.05 in 2D 100×100 Lattice

ures clearly show the spatial patterns and temporal behaviour of daisyworld. Moran's I quantifies the pattern formation accurately, demonstrating its reliability in spatially quantifying a wide spectrum of patterns. The global temperature in all cases is self-regulated around $295.5K$.

The localised interaction of species (black and white daisies) in our daisyworld model generate an array of fascinating spatio-temporal patterns, due to endogenous self-organization resulting from "symmetry-breaking instability". In our nonlinear reaction-diffusion system, symmetry-breaking is induced by species dispersion, temperature diffusion and noise. A low species dispersion rate combined with noise leads to complex self-organized patterns (Figure 4.1). As species dispersion and noise increase, periodic (Figure 4.7) and dynamic chaotically evolving patterns (Figure 4.4) emerge. In the absence of species

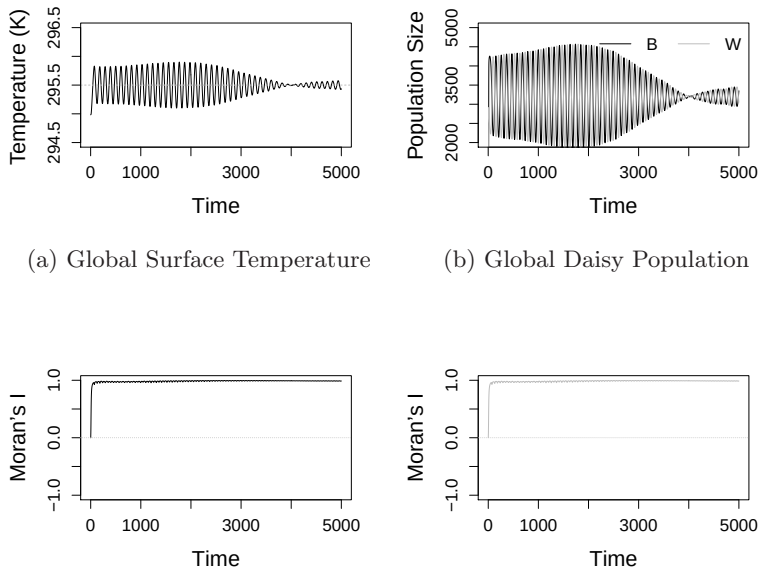

(a) Global Surface Temperature

(b) Global Daisy Population

(c) MI Black Daisy

(d) MI White Daisy

Figure 4.9: Global Dynamics of Cyclical Pattern : 10% overlap, $D_c = 0.2$, $D = 0.2$, $r = 1$ and NL= 0.05 in 2D 100×100 Lattice

dispersion, random (Figure 4.10) and dispersed (Figure 4.13) patterns emerge. We thus see the constructive roles of spatial diffusion, nonlinear local rules and noisy fluctuations in influencing the physiological, behavioural rules and physical constraints and thereby self-organizing the daisyworld. In addition, we have also demonstrated that our system as dynamical system and reaction-diffusion (activator-inhibitor) system.

4.2 Locally Chaotic and Globally Stable Dynamics (Temporal Fluctuations and Spatial Stability)

We first visually inspect the spatial dynamics of the system. We have collected snapshots from the evolution of Daisyworld in order to characterise the

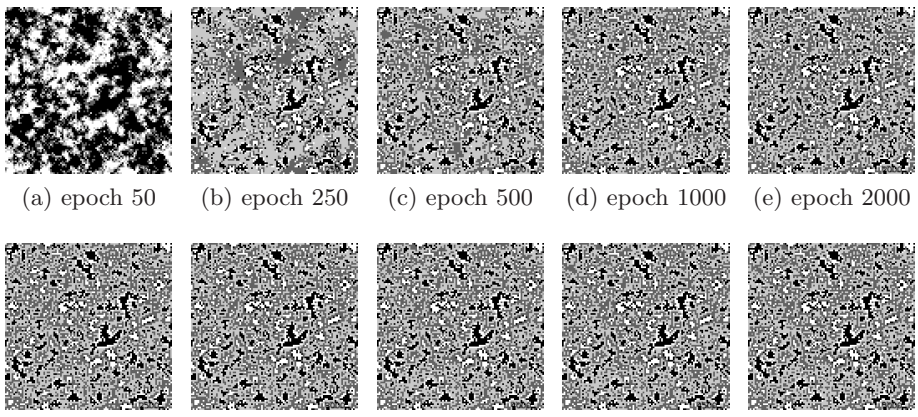

(a) epoch 50 (b) epoch 250 (c) epoch 500 (d) epoch 1000 (e) epoch 2000

(f) epoch 2500 (g) epoch 3000 (h) epoch 4000 (i) epoch 4500 (j) epoch 5000

Figure 4.10: Random Pattern : 10% Overlap, $D_c = 0$, $D = 0.2$, $r = 1$ and $NL = 0.01$ in 2D 100×100 Lattice

dynamics. For illustration purposes, we show the state of the Daisyworld at time step 1 (initial), 500 (i.e. after the system's behaviour has stabilised from any initial behaviours), 1000 (so that the system's behaviour can be compared over a long period), 1010 (so that we can see any short-term dynamicity), 2000, 2500, 3000, 3500 and 4000 (as intermediate epochs) and 5000 (the limit of the epochs).

Figure 4.18 depicts a typical succession of the ecosystem over time. We observe that black or white daisies form individual dominant clumped/patchy clusters, and coexistence of black and white occurs only at the boundaries. These boundary zones expand and contract depending on the local temperature and local population density of each daisy type. This is an example of a community that has a distinct boundaries which are driven by physical conditions that influence them. The boundaries of the daisy populations form patterns, and these patterns define the community structures. The communities are dynamic, changing over time. Though the initial frame appears greyish, the system breaks symmetry and evolves to more spatially heterogeneous coexisting dissipative patches, due to the recolonisation of the population from neighbouring patches via short-range dispersal.

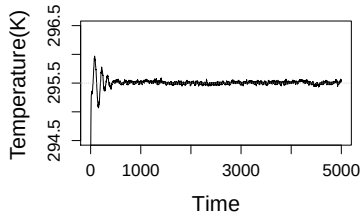

(a) Local Surface Temperature

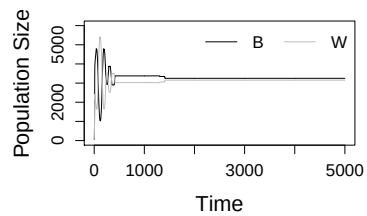

(b) Local Daisy Population

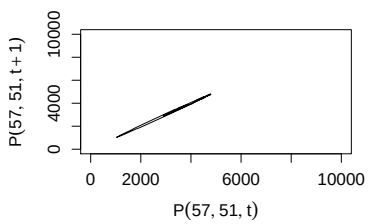

(c) Local Black Daisy Cobweb

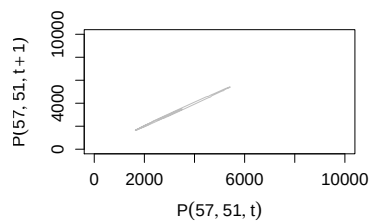

(d) Local White Daisy Cobweb

Figure 4.11: Local Dynamics of Random Pattern : 10% Overlap, $D_c = 0$, $D = 0.2$, $r = 1$ and $NL = 0.01$ in 2D 100×100 Lattice

Once daisies start germinating at a location, they spread to the neighbourhood, and hence the neighbouring environment is modified and a set of micro-environments is formed. Thus the daisy population creates a form of distributive patchy landscape, separating the habitable sites and inhospitable sites, due to environmental heterogeneity. These microclimates are then modified by the increased growth of a particular type of daisy. Such mosaic occurrence of species in patchy environments is an ubiquitous feature in ecological communities.

The changes appear essentially random to the naked eye. While there is persistence over short timespans (epochs 1000 and 1010 closely resemble each other), there is essentially no persistence over long timespans (it is difficult to detect any hint of previous clusters from a particular epoch when one examines

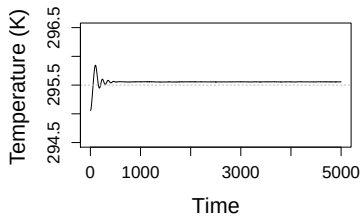

(a) Global Surface Temperature

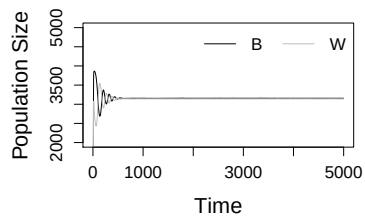

(b) Global Daisy Population

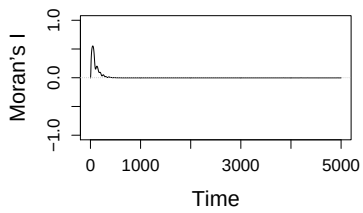

(c) MI Black Daisy

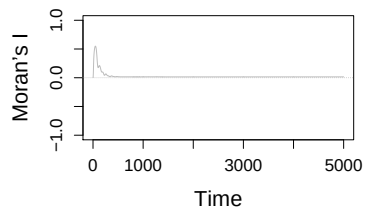

(d) MI White Daisy

Figure 4.12: Global Dynamics of Random Pattern : 10% Overlap, $D_c = 0$, $D = 0.2$, $r = 1$ and $NL = 0.01$ in 2D 100×100 Lattice

the population 500 epochs later).

4.2.1 Spatial Stability

To fill in the gaps between the spatial snapshots, we show the temporal trajectory of global dynamics (the temperature averaged over all lattice points) over the 5000 epochs in Figure 4.19 (a). The figure clearly captures the emergence of temperature self-regulation by the daisy population. The global temperature is regulated around the mean temperature ($295.5K$), ideal for daisy growth. This self-regulation of surface temperature arises from, but also gives rise to, a globally stable daisy population (average black or white population of the whole ecosystem), an emergent property of daisyworld, as seen in Figure 4.19 (b). In these figures, we discard the first 20 epochs (which would

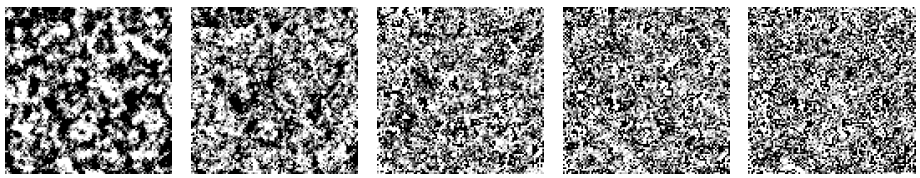

(a) epoch 50 (b) epoch 100 (c) epoch 200 (d) epoch 300 (e) epoch 500

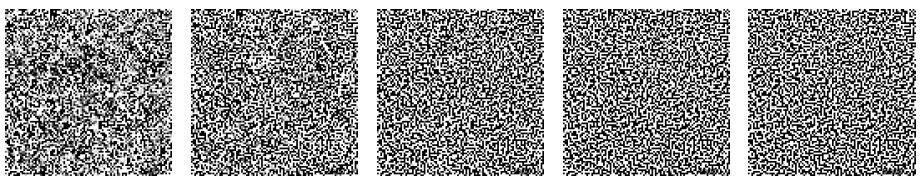

(f) epoch 1000 (g) epoch 2000 (h) epoch 3000 (i) epoch 4000 (j) epoch 5000

Figure 4.13: Uniformly Dispersed Pattern : Overlap=10%, $D_c = 0$, $D = 0.2$, $r = 1$ and $NL = 0.5$ in 2D 100×100 Lattice

otherwise generate off-scale behaviours) to concentrate on the long-term behaviour.

4.2.2 Temporal Fluctuations

The environmental fluctuations arise from temporal heterogeneity: different environmental conditions occur at different times at the same habitat. Figure 4.20 plots the local temporal series of temperature 4.20 (a), black 4.20 (b) and white 4.20 (c) daisies at a specific location (arbitrarily chosen as row 54 and column 54), showing the aperiodic dynamics arising from the deterministic chaos of the system. Although we used an increase rate of 1 (which in a non-diffusive world would not generate such dynamics), we observe deterministic temporal chaos. This is induced by the diffusion, an alternate route to chaos. Thus the network topologies and neighbourhood (structural properties) play a key role in determining the ecosystem complexity.

Figure 4.21 presents the cobweb plots (Verhulst diagrams) corresponding to Figure 4.20. In these, the value at a particular location (54, 54) and time step (x-axis) is plotted against the value at the same location but the next

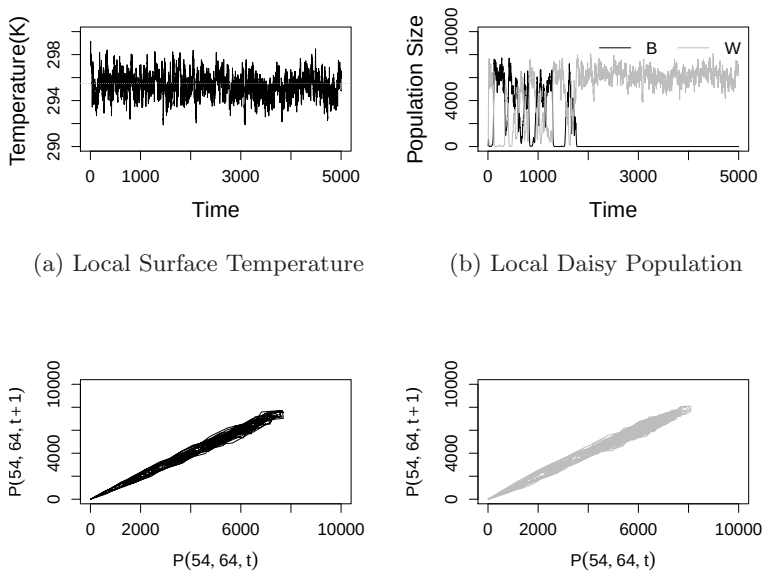

(a) Local Surface Temperature

(b) Local Daisy Population

(c) Local Black Daisy Cobweb

(d) Local White Daisy Cobweb

Figure 4.14: Local Dynamics of Uniformly Dispersed Pattern : 10% Overlap, $D_c = 0$, $D = 0.2$, $r = 1$ and $NL = 0.5$ in 2D 100×100 Lattice

time step (y-axis). We show plots for surface temperature 4.21 (a), black daisies 4.21 (b) and white daisies 4.21 (c). We clearly see the fluctuating but chaotic, aperiodic behaviour of the temporal dynamics in these plots.

4.2.3 Summary

The daisyworld model exhibits local temporal aperiodicity and global spatially-stabilised dynamics. We also see that spatial heterogeneity and temporal heterogeneity create a set of microclimates, which determine the existence of daisies. In our model, daisies' spread in a patchy environment is influenced by various factors such as overlap, dispersion, noise level and increase rate.

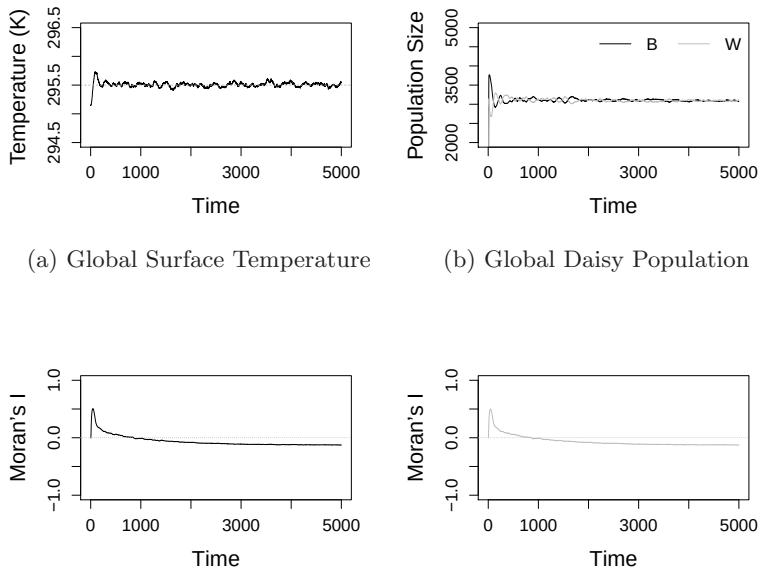

(a) Global Surface Temperature

(b) Global Daisy Population

(c) MI Black Daisy

(d) MI White Daisy

Figure 4.15: Global Dynamics of Uniformly Dispersed Pattern : 10% Overlap, $D_c = 0$, $D = 0.2$, $r = 1$ and $NL = 0.5$ in 2D 100×100 Lattice

4.3 Homeostasis with Evolutionary Dynamics

Evolutionary studies have highlighted the importance of biota-environment feedback in evolutionary dynamics, for example, niche construction [Odling-Smee et al., 2003], extended phenotypes [Dawkins, 1999]. Biota-environment feedback is inherent in daisyworld models, so we have chosen to extend the basic daisyworld model with evolutionary dynamics based on the replicator-mutator equation (RME) [Hofbauer and Sigmund, 2003].

The three fundamental factors in Darwinian evolution are replication (entities reproducing themselves), mutation (producing small variations in transforming to a new entity) and selection (passing the fitter entities to later generations). These factors determine the population dynamics: changes in population size and evolution of new populations. Populations are the funda-

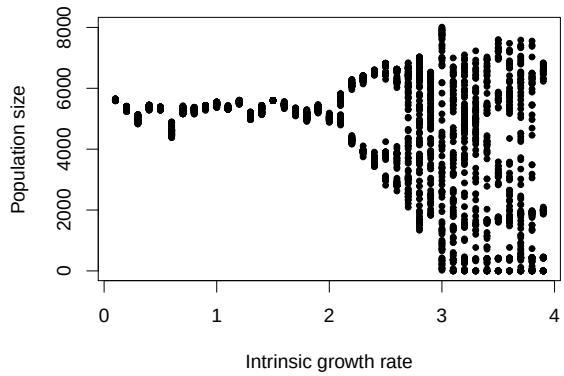

Figure 4.16: Bifurcation Diagram of Daisyworld – Black Daisy Population

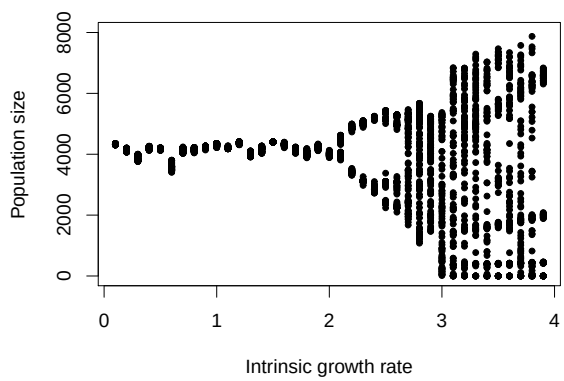

Figure 4.17: Bifurcation Diagram of Daisyworld – White Daisy Population

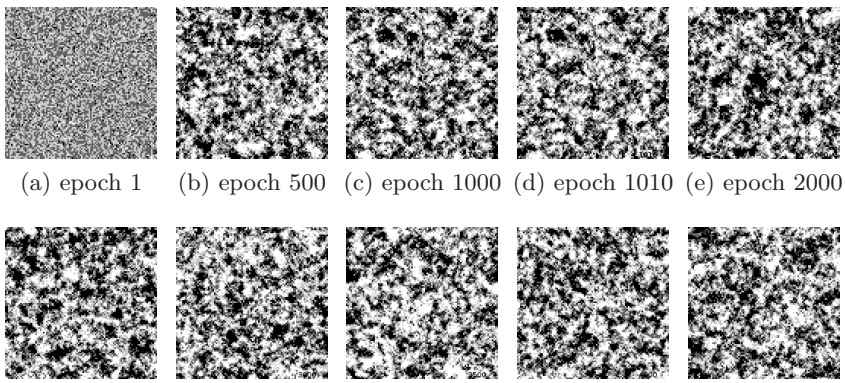

(a) epoch 1 (b) epoch 500 (c) epoch 1000 (d) epoch 1010 (e) epoch 2000

(f) epoch 2500 (g) epoch 3000 (h) epoch 3500 (i) epoch 4000 (j) epoch 5000

Figure 4.18: Population Dynamics in 100×100 2D CML with 10% Overlap, $D_c = 0.01$, $D = 0.2$, $r = 1$ and $NL = 1$

mental basis of evolution; individuals can change over time, but only populations evolve [Nowak, 2006]. We focus our attention on population dynamics in daisyworld with evolutionary change.

Generally, selection arises as a consequence of competition, commonly due to prey-predator relationships or resource limits. In the daisyworld of Watson and Lovelock [1983], daisies compete for space and hence for light. Daisyworld also incorporates a feedback mechanism: different daisy species affect the temperature, and the temperature in turn affects daisy survival, and hence selection. Thus the classic daisyworld realises the competition and natural selection of an evolutionary framework.

What is less studied in classical Darwinian evolution is the global feedback between biota and environment; conversely, the components that are omitted in the original daisyworld model are mutation and adaptation. In this field, it is common to distinguish between evolution of the daisies in ways which change their effect on the environment (in this case, albedo), which is referred to simply as mutation; and evolution of the daisies in ways which change their response to the environment (growth curve with temperature), generally referred to as adaptation. Thus a simple evolutionary daisyworld can incor-

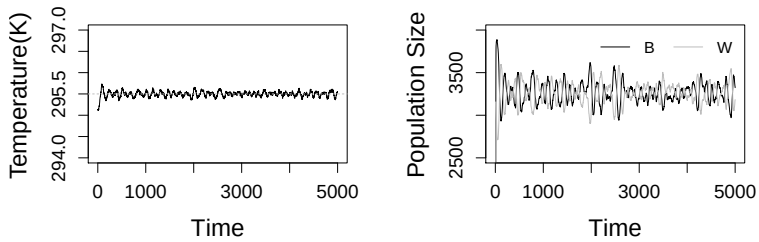

(a) Average Surface Temperature of all habitats

(b) Average Daisy Population of all habitats

Figure 4.19: Global Dynamics of Daisyworld in 100×100 2D CML with 10% Overlap, $D_c = 0.01$, $D = 0.2$, $r = 1$ and $NL = 1$

porate all these factors, through 1) influence of temperature on daisies, 2) influence of daisies on temperature, 3) mutation of daisies and 4) adaptation of daisies to the temperature.

A number of researchers have studied evolution in daisyworld. Mutation was introduced into daisyworld by Lovelock [1992] and expanded by Lenton and Lovelock [2001]; Lenton et al. [1998]. Adaptation in daisyworld was studied by Lenton and Lovelock [2000]. For a more detailed survey, please see Wood et al. [2008, section 4].

In this section, we model the population dynamics of daisies using the replicator-mutator equation (RME) of evolutionary dynamics, in a diffusively coupled logistic lattice of daisyworld - a model which has not been studied previously. RME has the advantage of expressing replication, mutation and selection mechanisms within a single framework; these evolutionary changes can be influenced by external environment factors such as temperature or abundance of species. Also, the interaction with the environment affects the survival of daisies and changes their adaptive fitness.

We have analysed the population dynamics of our daisyworld model through allowing a range of fluctuations in temperature, studying its effects on the evolutionary behaviour of the daisyworld. We have done this by introducing

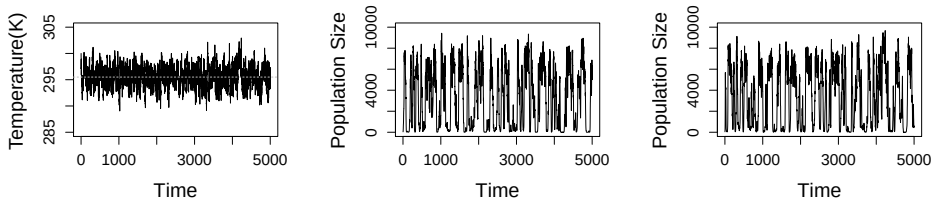

(a) Surface Temperature (b) Black Daisy Population (c) White Daisy Population

Figure 4.20: Local Dynamics at a specific location (row 54 and column 54) with 10% Overlap, $D_c = 0.01$, $D = 0.2$, $r = 1$ and $NL = 1$

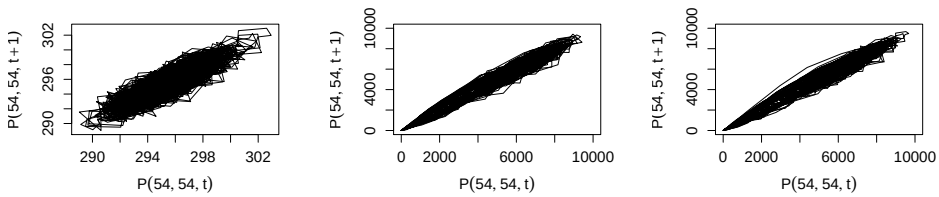

(a) Surface Temperature (b) Black Daisy Population (c) White Daisy Population

Figure 4.21: Cobweb Plot of Local Dynamics at a specific location (row 54 and column 54) with $D_c = 0.01$, $D = 0.2$, $r = 1$ and $NL = 1$ over 5000 Steps

ecosystem disturbance in the form of additive spatio-temporal Gaussian white noise [García-Ojalvo and Sancho, 1999]. The scale of fluctuation is controlled by the noise level.

4.3.1 Modification to Core Model

Patch Temperature: Daisies at a location (i, j) are divided (by species) into patches, whose temperature may vary from the local temperature $T_{(i,j,t)}$. The albedo of the daisies in the patch determines the patch temperature:

$$T_{c_{(i,j,t)}} = q(A_{(i,j,t)} - A_{c_{(i,j,t)}}) + T_{(i,j,t)} \tag{4.1}$$

where $T_{c_{(i,j,t)}}$ is the patch temperature of a habitat (i, j) at time t; c (phenotype) is the color of the daisies, $q = 20$ is a constant; refer [Lovelock, 1992], $A_{(i,j,t)}$ is the albedo of a habitat (i, j) at time t, $A_{c_{(i,j,t)}}$ is the albedo of each daisy type 'c' of a habitat (i, j) at a time t and $T_{(i,j,t)}$ is the local temperature of a habitat at a time t.

Density Dependent Fitness: We use absolute numbers for population size (P) rather than the relative frequencies of the classical form (equation 2.2). To prevent unrealistic exponential growth or decay, we formulated our fitness $(\mathfrak{f})$ based on a carrying capacity (κ) such that $\mathfrak{f} < 0$ for $P > \kappa$ and $\mathfrak{f} > 0$ for $P < \kappa$. The death rate of each daisy type is dependent on the total density of daisies. The corresponding fitness function is (equation 4.2):

$$\mathfrak{f}_{c_{(i,j,t)}} = \beta_{c_{(i,j,t)}} * \left(1 - \frac{P_{c_{(i,j,t)}}}{\kappa}\right) - \gamma * \left(\frac{P_{c_{(i,j,t)}}}{\kappa}\right) \tag{4.2}$$

β is the growth rate from equation 3.4, $\gamma = 0.3$ is the death rate, P is total population size and κ the carrying capacity.

Population Size: The local population abundance is based on replicator-mutator dynamics. We start from a variant of the discrete form [Page and Nowak, 2002] of RME (equation 2.2) shown in equation 4.3:

$$P\prime_{c(i,j,t)} = \frac{\sum_{c'=1}^{\mathfrak{n}} P_{c'(i,j,t)} \mathfrak{f}_{c'(i,j,t)} \mathfrak{q}_{c'c}}{\phi}, c = 1, ..., \mathfrak{n} \tag{4.3}$$

where P_c is the proportion of the population of type c, (i, j) represents a spatial location, $\mathfrak{n}$ is the number of phenotypes, and $\mathfrak{f}_{c'}$ defines the selection dynamics. Rather than separate reward (payoff) and mutation matrices, we use a combined replicator-mutator matrix $\mathbb{Q} = [\mathfrak{q}_{cc'}]$ – a doubly stochastic matrix – defining the evolutionary properties and satisfying $\sum_c \mathfrak{q}_{cc'} = \sum_{c'} \mathfrak{q}_{cc'} = 1$. The diagonal of the matrix defines the replication rate, while other entries

defines the mutation rates. $\phi = \sum_c P_c \mathfrak{f}_c$ is the average fitness, and is used as a normalisation term to ensure the population doesn't exceed its bounds.

Since our fitness function is density dependent and directly ensures the orbits are bounded in the region $P \leq \kappa$, the term ϕ is not needed. However we need to incorporate diffusion of individuals. Combining this, we can define the change in population as in equation 4.4:

$$h\left(P'_{c_{(i,j,t)}}\right) = P'_{c_{(i,j,t)}} + \sum_{c=1}^{\mathfrak{n}} P_{c_{(i,j,t)}} \mathfrak{f}_{c_{(i,j,t)}} \mathfrak{q}_{cc} + \sum_{c' \neq c}^{\mathfrak{n}} P_{c'_{(i,j,t)}} \mathfrak{f}_{c'_{(i,j,t)}} \mathfrak{q}_{c'c} \tag{4.4}$$

D is the Laplace-diffused population. Since we don't use a reward matrix, the discrete time fitness (selection coefficient) is just the intrinsic fitness, leading to equation 4.2.

The fitness of a particular type of daisies changes, depending on the abundance of both itself and the other species because of the life-environment feedback. Here, $\mathfrak{f}$ affects P and depends on β which depends on T which depends on A which in turn depends on P, thus forming a tightly coupled system with an indefinite feedback loop. The model incorporates two types of feedback: from the life-environment effect of daisyworld and from the density-dependent nature of population dynamics. This model covers all the main ingredients of evolutionary population dynamics – reproduction, mutation, selection and spatial dispersion – with a bi-directional life-environment feedback effect.

Importance to Study Noise Modelling nonlinear dynamics in a noisy world is very common in population ecology. The two key factors in studying population dynamics are the internal feedback which inhibits the exploding population and the external environmental (abiotic) variability which determines the population fluctuations [Begon et al., 1996]. In our model, the first factor (internal feedback) results from the imposition of a carrying capacity and the second (external variability) from Gaussian noise. These external perturbations can cause the system to deviate from equilibrium. The noise level controls the scale fluctuations in the environment. Noise helps to intro-

duce sufficient nonlinearity to observe complex dynamics such as limit cycles, quasi-periodicity and chaos (nonlinear attractors). Diffusion of temperature and dispersion of daisies also allow the system to break symmetry and generate interesting patterns in daisyworld [Punithan and McKay, 2012b]. In this section, we focus on the evolutionary population dynamics of daisyworld, so we study the impact of the external variability in detail. In the absence of noise, the dynamics of the world is stationary (static attractor). But with the imposition of noise, we observe evolving patterns of life – so long as there is not too much. With higher levels, noise completely dominates the feedback, and the behaviour becomes random and uninteresting.

4.3.2 Variable Parameter Settings

We analyse the changes in dominance by specific phenotypes (petal colour) under the effect of environmental perturbations (temperature). In our experiments, the optimal temperature and albedo of the original black, white daisies, their mutants and adaptants are tabulated in the Table 4.2; please refer Lenton and Lovelock [2001], and other parameter settings are tabulated in the Table 4.3. In all analyses, we first examine the spatio-temporal population patterns (using snapshots of the system status over the 5000 epochs). We focus on the local dominance of species. We plot the local (temporal) behaviour at a single habitat, and the global dynamics (average temporal behaviour of the whole ecosystem).

Table 4.2: Optimal temp. and albedo of original daisies and their mutants

	T_{opt}(K)	Albedo	Colours in Figures
Black	295.5	0.25	black
White	295.5	0.75	white
Grey	295.5	0.5	grey
Warm Black	300.5	0.25	dark grey
Cool White	290.5	0.75	light grey

Table 4.3: Evolutionary Dynamics : Representative Parameter Set

Parameter	**Value**
Diffusion rate of black daisies (D_b)	0.2
Diffusion rate of white daisies (D_w)	0.2
Noise Level (NL)	$[0, 3]$
Natural Rate of Increase (r)	1

4.3.3 Baseline Scenario: No Mutation

In this subsection, we present the behaviour of the system with no evolutionary change, as a baseline for comparisons. Since the level of noise is an important control in determining the effect of evolutionary change, we present results for different levels of noise.

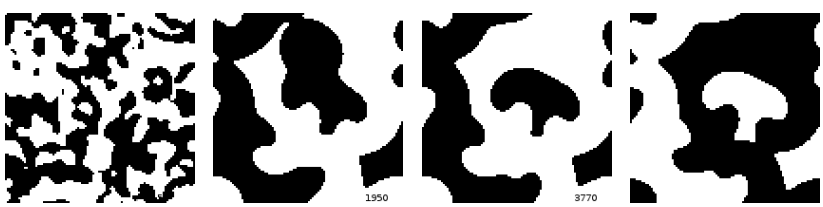

(a) epoch 50 (b) epoch 1950 (c) epoch 3770 (d) epoch 4885

Figure 4.22: Population abundance without mutation : $D_c = 0.2$, $D = 0.2$, $r = 1$ and $NL = 0.05$

Noise Level $= 0.05$ With low noise levels ($NL = 0.05$), periodic behaviour emerges from the system (Figure 4.22). The cycles in the local dynamics (Figure 4.23) for both patch temperature and population confirm this. At the global level, the temperature (Figure 4.24) is regulated around $295.5K$.

Noise Level $= 3$ With increased noise, rough turing like structures form – Figure 4.25, and the periodic behaviour becomes less regular – Figures 4.26 and 4.27.

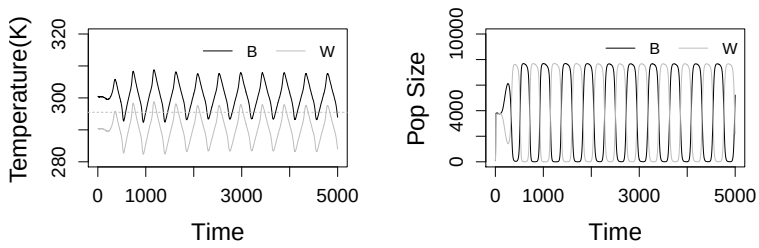

(a) Patch Temperature (b) Population abundance

Figure 4.23: Local dynamics at habitat (55, 41) without mutation and $NL = 0.05$

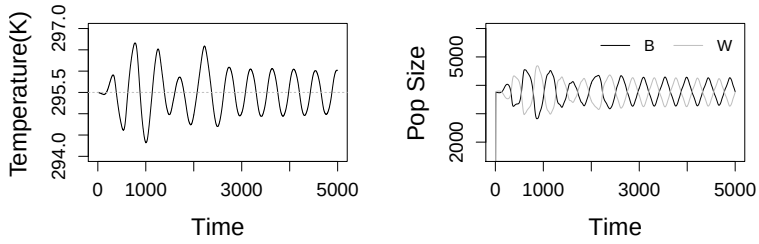

(a) Surface Temperature (b) Population abundance

Figure 4.24: Global dynamics without mutation, $NL = 0.05$

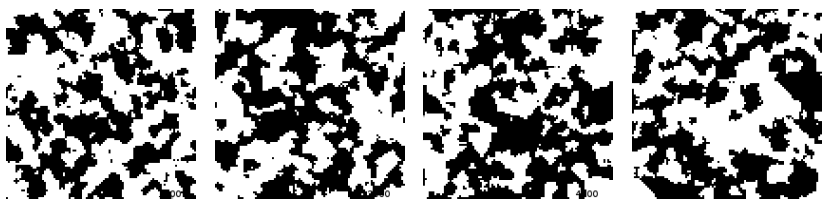

(a) epoch 1000 (b) epoch 2000 (c) epoch 4000 (d) epoch 5000

Figure 4.25: Population abundance without mutation : $D_c = 0.2$, $D = 0.2$, $r = 1$ and $NL = 3$

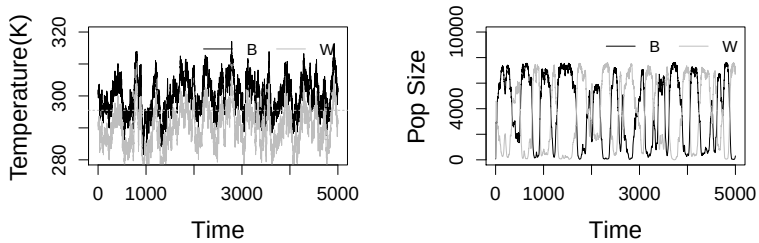

(a) Patch Temperature (b) Population abundance

Figure 4.26: Local dynamics at habitat (55, 50) without mutation, $NL = 3$

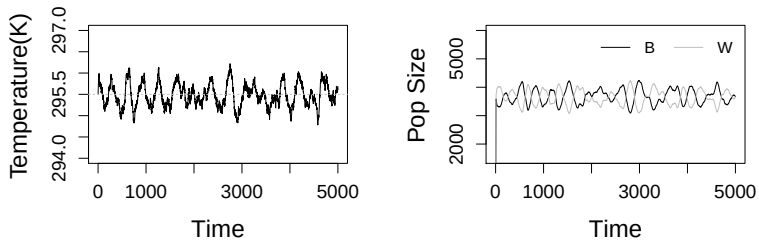

(a) Surface Temperature (b) Population abundance

Figure 4.27: Global dynamics without mutation, $NL = 3$

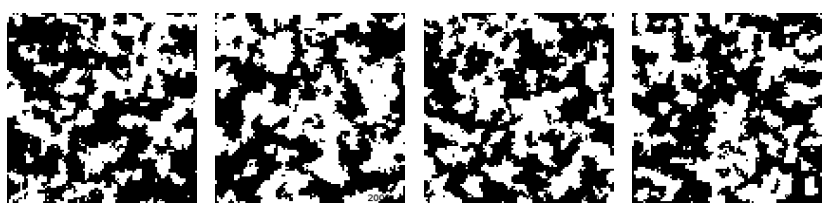

(a) epoch 1000 (b) epoch 2000 (c) epoch 4000 (d) epoch 5000

Figure 4.28: Population abundance without mutation : $D_c = 0.2$, $D = 0.2$, $r = 1$ and $NL = 5$

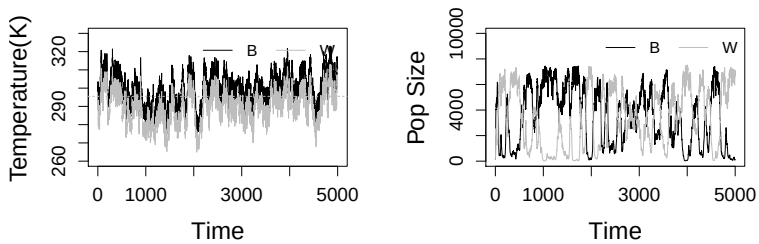

(a) Patch Temperature (b) Population abundance

Figure 4.29: Local dynamics at habitat (56, 50) without mutation, $NL = 5$

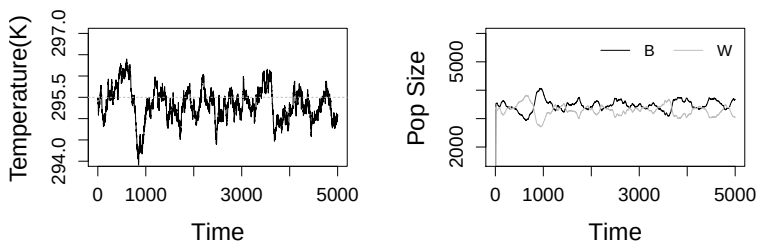

(a) Surface Temperature (b) Population abundance

Figure 4.30: Global dynamics without mutation, $NL = 5$

Noise Level = 5 With further increase in noise, rough clusters ceaselessly form and dissolve (Figure 4.28), and the periodic behaviour almost entirely disappears as in Figures 4.29 and 4.30. We have reached the less interesting region in which noise dominates the environmental feedback; behaviours in this region are little affected by other parameters, so we omit it from consideration in the rest of the section.

4.3.4 Phenotypic Variability – Mutation

The ability of mutations to generate new phenotypes is one of the hallmarks of Darwinian evolution. The black and white daisies in the model undergo random mutation, introducing a new phenotypic state – grey daisies (T_{opt} = 295.5 and albedo = 0.5). The evolutionary relationships between the species are defined in the replicator-mutator matrix (μ is the rate of random mutation and B, W, G denote Black, White and Grey daisies):

$$Q = \begin{array}{c} \\ B \\ W \\ G \end{array} \begin{array}{c} \begin{array}{ccc} B & W & G \end{array} \\ \begin{pmatrix} (1-0.1\mu) & 0 & 0.1\mu \\ 0 & (1-0.1\mu) & 0.1\mu \\ 0.1\mu & 0.1\mu & (1-2(0.1\mu)) \end{pmatrix} \end{array}$$

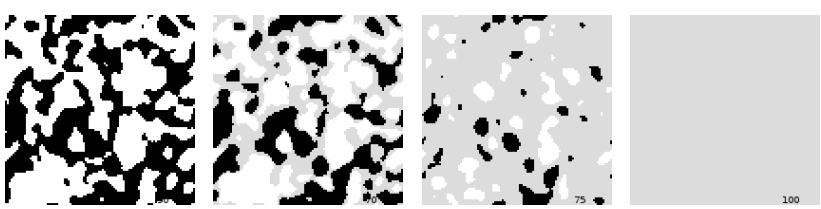

(a) epoch 50 (b) epoch 70 (c) epoch 75 (d) epoch 100

Figure 4.31: Population abundance with Grey daisies : $D_c = 0.2$, $D = 0.2$, $r = 1$ and $NL = 0.05$

Noise Level = 0.05 Grey daisies quickly dominate (Figure 4.31) when the noise level is very low ($NL = 0.05$). Both local (Figure 4.32 (b)) and global (Figure 4.33 (b)) populations of the original black and white daisies drop very low, almost disappearing. This happens because the patch temperatures of

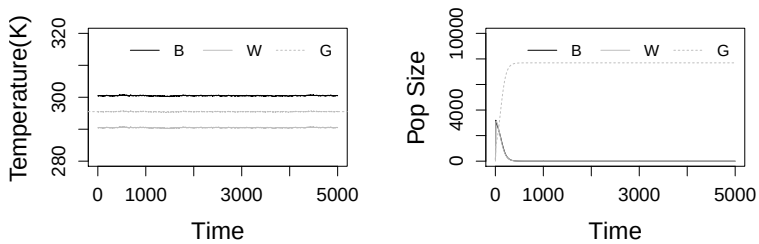

(a) Patch Temperature (b) Population abundance

Figure 4.32: Local dynamics at habitat (57, 49) with Grey and $NL = 0.05$

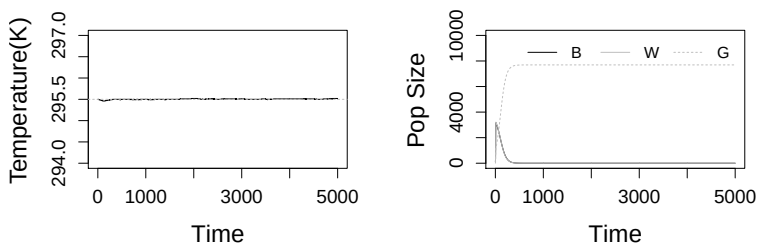

(a) Surface Temperature (b) Population abundance

Figure 4.33: Global dynamics with Grey, $NL = 0.05$

black and white daisies are almost constant, above and below $295.5K$, so the growth of grey daisies is favoured: refer to Figure 4.32 (a). Since there is not much fluctuation in the local temperature due to the low noise level, grey daisies dominate the whole space. The temperature is regulated to $295.5K$ (Figure 4.33 (a)).

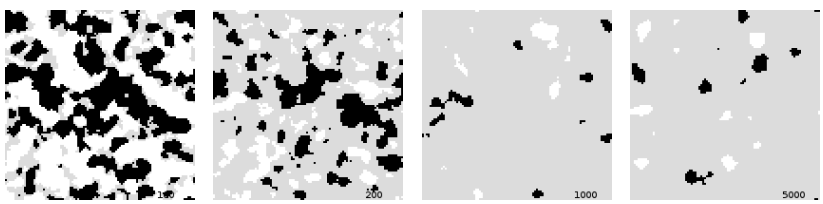

(a) epoch 100 (b) epoch 200 (c) epoch 1000 (d) epoch 5000

Figure 4.34: Population abundance with Grey daisies : $D_c = 0.2$, $D = 0.2$, $r = 1$ and $NL = 2$

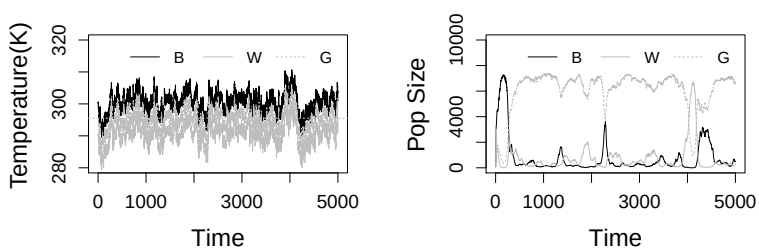

(a) Patch Temperature (b) Population abundance

Figure 4.35: Local dynamics at habitat (54, 43) with Grey and $NL = 2$

Noise Level = 2 When the noise level increases to 2, although the world is still rapidly dominated by grey daisies, the original black and white species can form distinct groups and dominate smaller regions (Figure 4.34). All three species coexist locally as well as globally, mainly to due the patch temperatures. Black patches mostly fluctuate above $295.5K$, and white mostly below,

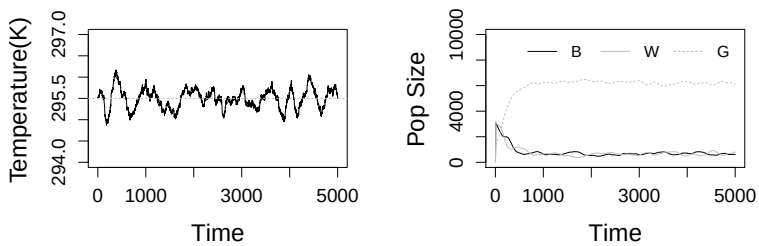

(a) Surface Temperature (b) Population abundance

Figure 4.36: Global dynamics with Grey, $NL = 2$

with only grey fluctuating around the favoured $295.5K$ (Figure 4.35 (a)). The global temperature is regulated around $295.5K$ (Figure 4.36 (a)) with coexisting populations (Figures 4.35 (b) and 4.36 (b)) but a majority of grey.

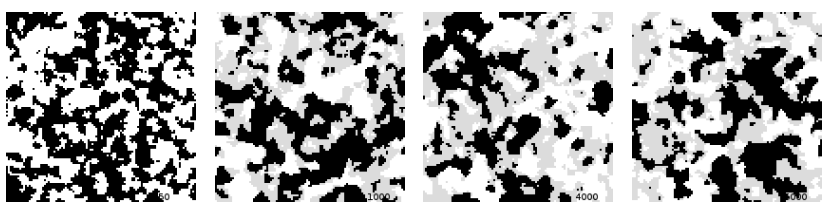

(a) epoch 50 (b) epoch 1000 (c) epoch 4000 (d) epoch 5000

Figure 4.37: Population abundance with Grey daisies : $D_c = 0.2$, $D = 0.2$, $r = 1$ and $NL = 3$

Noise Level = 3 Further increasing the noise level to 3 results in all species dominating local regions, with highly evolving and dynamic (Figure 4.37) behaviours. The local patch temperatures fluctuate widely around the mean $295.5K$ (Figure 4.38 (a)). The global temperature is regulated to around $295.5K$ (Figure 4.39 (a)) with all species coexisting locally (Figure 4.38 (b)) and globally (Figure 4.39 (b)).

To summarise, the grey mutant form dominates the whole ecosystem when

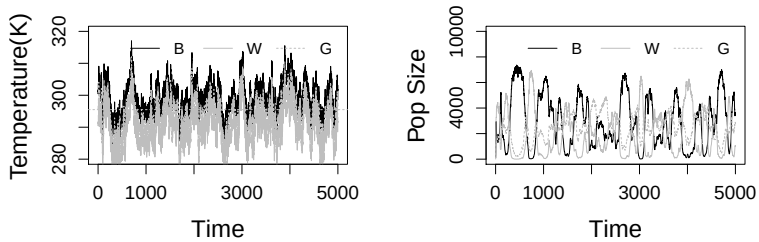

(a) Patch Temperature (b) Population abundance

Figure 4.38: Local dynamics at habitat (51, 53) with Grey and $NL = 3$

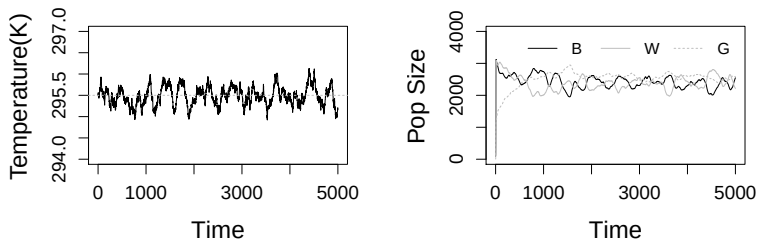

(a) Surface Temperature (b) Population abundance

Figure 4.39: Global dynamics with Grey, $NL = 3$

there are small temperature fluctuations ($NL = 0.05$). As the noise level increases to ($NL = 2$), the black and white daisies form distinct population groups. Further increase in noise level ($NL = 3$), allow all three species to dominate locally, and they coexist both locally and globally. Thus we see the determination of evolutionary dominance through environmental influences.

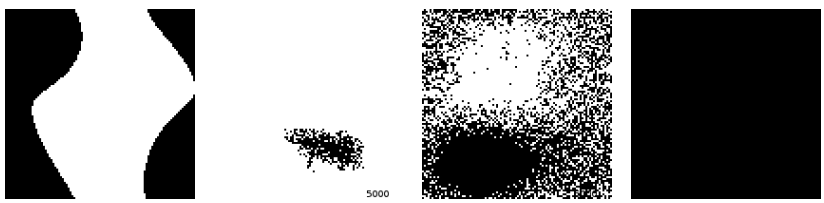

(a) $NL = 0$ (b) $NL = 2$ (c) $NL = 3$ (d) $NL = 5$

Figure 4.40: Population abundance without feedback : $D_c = 0.2$, $D = 0.2$ and $r = 1$ at epoch 5000

Mutation without Life-Environment Feedback We observed population spatial structures with mutation but excluding life-environment feedback (i.e. temperature is not influenced by the daisies at all) for different noise levels (Figure 4.40). When we compare these snapshots (no grey dominance) with Figures 4.31 and 4.37, we can see that the balance between feedback and noise plays a vital role in the coexistence of dominance of the original daisies and their mutants. The dynamics we see, for example, in Figure 4.37 is due to the interplay of noise and feedback, rather than either alone.

4.3.5 Adaptation – Exploring New Environments

In the absence of other species, black daises will generate a very hot environment unsuited to them. Instead of mutating to reduce their environmental effect, they can also adapt to tolerate these higher temperatures, generating "warm black daisies". Similarly, white daisies may adapt to a cold environment, giving "cool white daisies". We explore the effects of warm black ($T_{opt} = 300.5$, $albedo = 0.25$) and cool white daisies ($T_{opt} = 290.5$,

albedo = 0.75). In all patch temperature plots, the patch temperature trajectories of black and warm black daisies superimpose and similarly for white and cool white – inevitably, because the originals and their adaptants have the same albedo.

The evolutionary properties are by the following replicator-adapter matrix (WB and CW stand for warm black and cool white daisies):

$$Q = \begin{array}{c} \\ B \\ W \\ WB \\ CW \end{array} \begin{array}{c} \begin{array}{cccc} B & W & WB & CW \end{array} \\ \begin{pmatrix} (1-0.1\mu) & 0 & 0.1\mu & 0 \\ 0 & (1-0.1\mu) & 0 & 0.1\mu \\ 0.1\mu & 0 & (1-0.1\mu) & 0 \\ 0 & 0.1\mu & 0 & (1-0.1\mu) \end{pmatrix} \end{array}$$

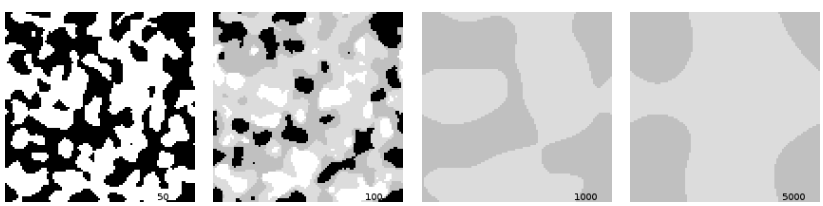

(a) epoch 50 (b) epoch 100 (c) epoch 1000 (d) epoch 5000

Figure 4.41: Population abundance with Warm Black and Cool White daisies : $D_c = 0.2$, $D = 0.2$, $r = 1$ and $NL = 0.05$

Noise Level = 0.05 When the noise level is low (0.05), the original daisies almost disappear (Figures 4.42 (b) and 4.43 (b)) and the warm black and cool white self-organise, forming patterns with huge clusters that dominate the ecosystem (Figure 4.41). The global surface temperature is regulated to 295.5K (Figure 4.43 (a)). Though the patch temperatures of black and warm black are identical (also for white and cool white) (Figure 4.42 (a)), the adaptants are superior to the existing phenotypes, and rapidly dominate.

Noise Level = 2 At a noise level of 2, both warm black and cool white, self-organise to form Turing-like patterns, while the originals, black and white, dominate in smaller regions here and there (Figure 4.44). The local and global dynamics are shown in Figures 4.45 and 4.46.

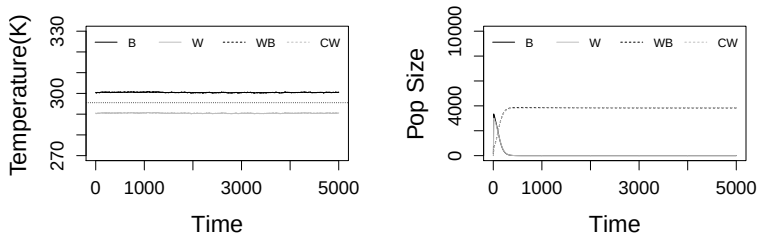

(a) Patch Temperature (b) Population abundance

Figure 4.42: Local dynamics at habitat (51, 50) with Warm Black and Cool White, $NL = 0.05$

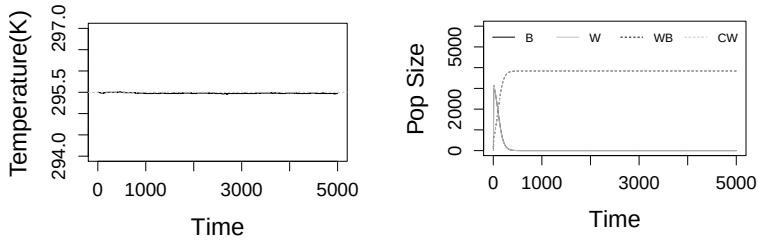

(a) Surface Temperature (b) Population abundance

Figure 4.43: Global dynamics with Warm Black and Cool White, $NL = 0.05$

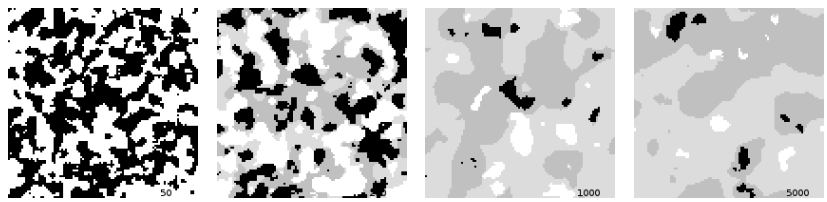

(a) epoch 50 (b) epoch 200 (c) epoch 1000 (d) epoch 5000

Figure 4.44: Population abundance with Warm Black and Cool White daisies : $D_c = 0.2$, $D = 0.2$, $r = 1$ and $NL = 2$

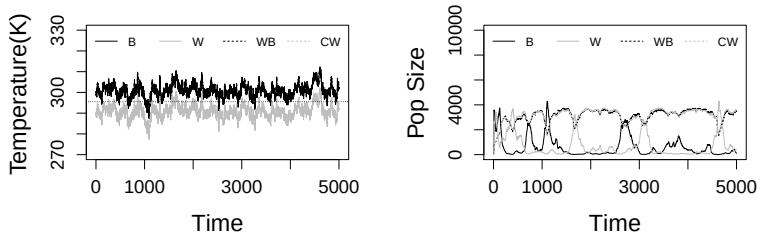

(a) Patch Temperature (b) Population abundance

Figure 4.45: Local dynamics at habitat (57, 55) with Warm Black and Cool White, $NL = 2$

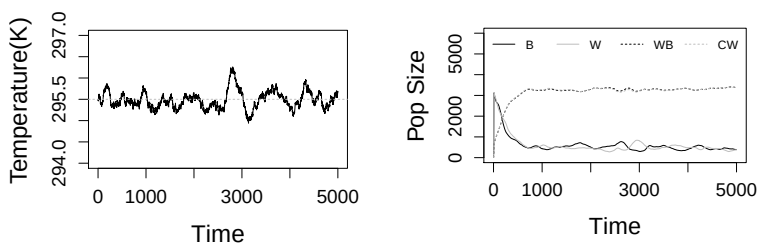

(a) Surface Temperature (b) Population abundance

Figure 4.46: Global dynamics with Warm Black and Cool White, $NL = 2$

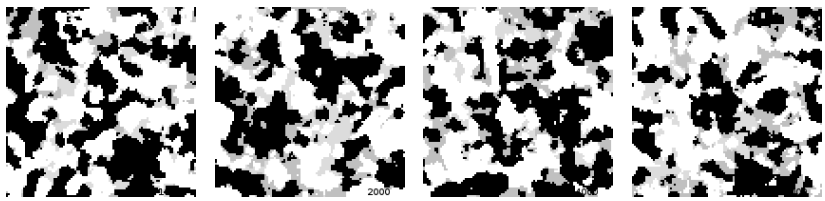

(a) epoch 1000 (b) epoch 2000 (c) epoch 4000 (d) epoch 5000

Figure 4.47: Population abundance with Warm Black and Cool White daisies : $D_c = 0.2$, $D = 0.2$, $r = 1$ and $NL = 3$

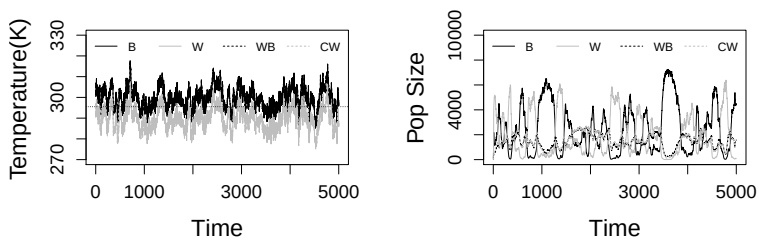

(a) Patch Temperature (b) Population abundance

Figure 4.48: Local dynamics at habitat (52, 61) with Warm Black and Cool White, $NL = 3$

Noise Level = 3 All four phenotypes coexist, each dominating the ecosystem locally (Figure 4.47). The overall behaviour is revealed in Figures 4.48 and 4.49.

4.3.6 Summary

The evolutionary daisyworld model – replication with mutation and adaptation – presented in this section illustrates global surface temperature regulation around $295.5K$ as in the original models. Thus demonstrating its robustness in homeostatic self-regulation in scenarios such as evolution of the environment altering trait (albedo) and adaptive evolution of optimal temperature. Tem-

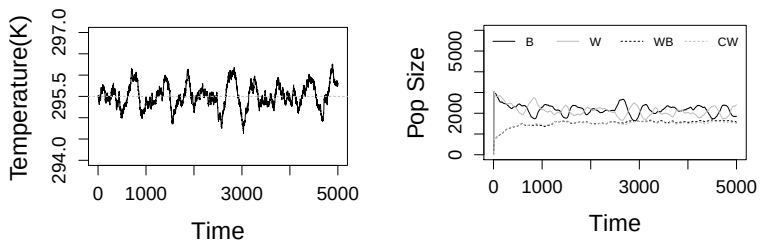

(a) Surface Temperature

(b) Population abundance

Figure 4.49: Global dynamics with Warm Black and Cool White, $NL = 3$

poral fluctuation in temperature, due to ecosystem disturbance, introduces nonlinearity into the daisyworld, leading to the most interesting behaviours. With very low noise, we observe monotonous life (quiescent daisy dominance states). Without feedback or with very high noise, we observe suppression of mutants. Thus, these results underline the importance of balance between ecosystem feedback and ecosystem disturbance in generating spatially coexistence of domains of dominance among the original daisies and their mutants.

4.4 Quantification of the Daisyworld Model

4.4.1 Statistical Measures and Spatio-Temporal Dynamics

Table 4.4: Permutation Entropy Regimes

Temporal Dynamics (Local or Global)	**PE value**
Static	< 0.1
Periodic	$[0.1, 0.2]$
Chaotic	$[0.3, 0.7]$
Random	near 1

We analyse the temporal and spatial dynamics of our daisyworld model us-

Table 4.5: Moran's I Regimes

Global Spatial Distribution	**MI value**
Uniform	$-ve$
Random	0
Clustered	$+ve$

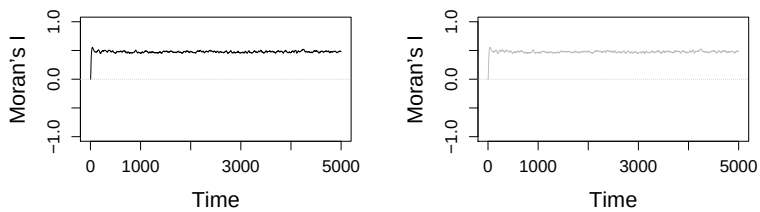

(a) MI Black Daisy (b) MI White Daisy

Figure 4.50: Moran's I (section 4.2)

ing Permutation Entropy (PE) and Moran's I (MI) (defined in subsection 2.3), along with standard deviation metrics. We are particularly interested in settings which lead to a chaotically stable (locally chaotic and globally stable (section 4.2)) system with self-regulation and interesting spatio-temporal dynamics, so we aim to characterise the values of PE and MI at which we are likely to find such behaviours. We have studied over $15,000$ experiments delineated in subsection 3.4.1, to find suitable regimes for local and global dynamics. The dynamics of our interest (chaotic stability with evolving patches) are observed for systems with local dynamics (dynamics at a specific habitat in the ecosystem) characterised by a local permutation entropy (PE computed

Table 4.6: Local PE (section 4.2)

	Local PE	Std Dev
Black Population	0.435	2783
White Population	0.424	2800

Table 4.7: Global PE (section 4.2)

	Global PE	Std Dev
Black Population	0.365	132
White Population	0.365	130

on temporal trajectory of daisies at a specific habitat in the ecosystem) in the range $[0.3, 0.7]$ with high standard deviation, and global dynamics (mean population dynamics of the whole ecosystem) characterised by Moran's I in the range $[0.4, 0.9]$ and global permutation entropy (PE computed on temporal trajectory of mean daisy populations of the whole ecosystem) in the range $[0.3, 0.7]$ with low standard deviation. We also observe that large clumped/patchy patterns tend to emerge as Moran's I increases towards $+1$. The overall regimes of PE and MI that we observed are shown in Tables 4.4 and 4.5. However these are not enough to characterise the dynamics. We use the standard deviation to measure the scale of fluctuation in both local and global dynamics. For example, a given value of PE for both local and global dynamics tells us only about the shape of fluctuations, not their scale. We use the standard deviation to measure the range of fluctuation. If it is high, the behaviour is characterised as chaotic, otherwise not.

As an example of such an analysis, consider the daisyworld presented in the section 4.2. The figure 4.50 shows the time evolution of MI (4.50 (a) and 4.50 (b)) of daisy population. The global permutation entropy and standard deviation of daisy population are listed in the table 4.7. The local permutation entropy and standard deviation of daisy population are tabulated in the table 4.6. Although the global PE would indicate a globally chaotic world, the small standard deviation indicates instead a stable world.

4.4.2 Parameter Space Analysis of the Daisyworld Model

Two of the most influential factors on daisyworld behaviour are the noise level (which influences temperature) and the dispersion rate of daisies (which influences the distribution of daisies). In this section, we study the effects

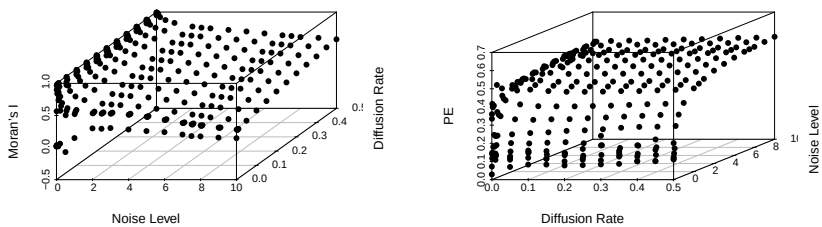

(a) (b)

Figure 4.51: Moran's I and PE on 100×100 2D CML with 10% overlap and $r = 1$

of noise and diffusion rate on our two key metrics; Moran's I (average of Moran's I of the whole ecosystem over 5000 epochs) and permutation entropy (average of permutation entropy of N randomly selected habitats with their neighbours (ecological aggregate), from the ecosystem of $N \times N$ habitats, over 5000 epochs).

From sub Figure 4.51 (a), we observe low MI values when both the dispersion rate of species and noise are very low, indicating the formation of uniform (MI < 0) and random (MI is nearly 0) patterns. The noise level has the largest overall effect, especially at very low values where we see very high MI values (even as high as 1), indicating the formation of huge patches. As noise increases and diffusion decreases, we see the MI values decrease, indicating the formation of patches of decreasing size.

The diffusion rate has almost no effect on the permutation entropy (sub Figure 4.51 (b)). However the effect of noise level is very substantial. Low noise results in very low PE (less than 0.1), indicating static attractors. With little increase in noise, PE also increases in the range $[0.1, 0.2]$, indicating periodic attractors. PE rises rapidly with increasing noise level at first, but saturates from noise levels of around 4. High PE in $[0.3, 0.7]$ indicates strange attractors.

Chapter 5

Daisyworld with Complex Couplings

In this chapter, we investigate two-dimensional (2D) CML based daisyworld with local couplings and non-local couplings (added either statically or dynamically). In section 5.2, daisyworld dynamics in different baseline graph models such as regular, random and fully-connected graphs are discussed which we use to compare other complex and adaptive topologies in the following sections 5.3, 5.4 and 5.5. In section 5.3, we introduce and examine the small-world phenomenon in daisyworld. In section 5.4, we examine adaptive topology of the system based on the local daisyworld dynamics. We study scale-freeness in daisyworld in section 5.5. In section 5.6, we discuss the behaviour study of the daisyworld with the additional connections (added either statically or dynamically).

5.1 Variable Parameter Settings

The parameter settings for the experiments described in this chapter are shown in Table 5.1 to have consistency for analyses. We have chosen a low noise level, increase rate and overlap so that we can study topological effect on the system behaviour without undue influences from other model system parameters.

Table 5.1: Representative Parameter Set

Parameter	**Value**
Opt. temp. of black daisies (T_{opt_b})	$284.5K$
Opt. temp. of white daisies (T_{opt_w})	$306.5K$
Diffusion rate of black daisies (D_b)	0.2
Diffusion rate of white daisies (D_w)	0.2
Noise Level (NL)	0.001
Natural Rate of Increase (r)	1

In the daisyworld literature [Wood et al., 2008, section 3], the connectivities for both species (black and white), and for the environmental resource (temperature), are the same – local connections. In our system, we use different connectivity topologies for species and the resource. Black and white daisies disperse via both local and long-range connections (by water, air, animal pollinator transport etc.), while temperature diffuses only locally. All the rewired or added connections are reciprocal.

5.2 Benchmark Graph Models

We have taken regular (sub Figure 5.1 (a)) and random graphs (sub Figure 5.1 (b)) as our benchmarks, as the interactions are purely local in former and purely global in the latter. For completeness, we also compare with fully-connected graphs (sub Figure 5.1 (c)) in which there is no notion of spatial relationship.

5.2.1 Degree Distribution of Benchmark Models

The degree distributions of regular graph having constant degree distribution (sub Figure 5.2 (a)) and random graph having Poisson distribution (sub Figure 5.2 (b)) are depicted in the Figure 5.2. Both graphs are constructed in 100×100 lattice.

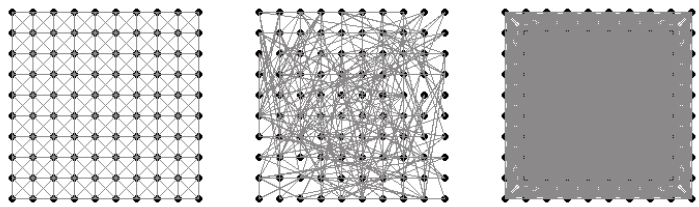

(a) (b) (c)

Figure 5.1: 2-lattice Benchmark Models (with $k = 8$ except for fully-connected graph). We omit periodic boundary conditions for clarity, and also show some connections superimposed.
(a) Regular graph ($p = 0$) (b) Random graph ($p = 1$) (c) Fully-connected graph

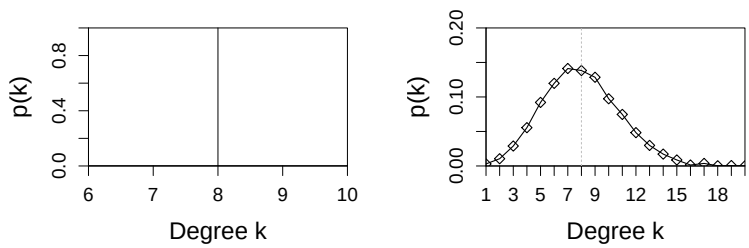

(a) Regular (b) Random

Figure 5.2: Degree Distribution of Benchmark Models

5.2.2 Regular Graph

With only local couplings, we observe the formation of complex static patterns. The whole ecosystem freezes after epoch 1710. This scenario is clearly seen in the snapshots (Figure 5.3), in global population dynamics (Figure 5.34) and in global temperature dynamics (sub Figure 5.32 (b)). The local population dynamics (Figure 5.33) and local temperature (sub Figure 5.32 (a)) at a typical habitat $(57, 50)$ shows that the dynamics freezes even quicker (epoch 1055). All trajectories show initial fluctuations but evolve to complete stationarity.

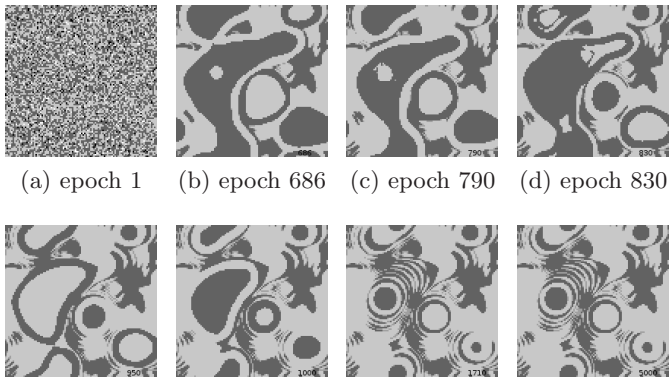

(a) epoch 1 (b) epoch 686 (c) epoch 790 (d) epoch 830

(e) epoch 950 (f) epoch 1000 (g) epoch1710 (h) epoch5000

Figure 5.3: Regular CML ($p = 0$) : Overlap=10%, $D_c = 0.2$, $D = 0.2$, $r = 1$ and $NL = 0.001$ in 2D 100×100

5.2.3 Random Graph

In the random connectivity case, $N^2k/2$ random connections are made, independent of the spatial structure. We observe a periodic behaviour. Both daisy types coexist, both locally and globally. But one type homogeneously dominates the world for some epochs, while the other type takes over completely for others. The transition from one type to the other is extremely rapid – see epoch numbers in the visuals (Figure 5.4). The top row shows a change from dark grey (coexistence dominated by black daisies) to light grey (coexistence dominated by white daisies); the bottom row shows the reverse. The periodic behaviour is confirmed by the local and global temperature dynamics (Figure 5.35) and by the local (Figure 5.36) and global (Figure 5.37) population dynamics.

5.2.4 Fully Connected Graph

We see a similar behaviour to a random lattice (Figure 5.5). The cycles in the local population dynamics (Figure 5.39), global population dynamics (Figure 5.40) and temperature dynamics (Figure 5.38) reflect the periodicity.

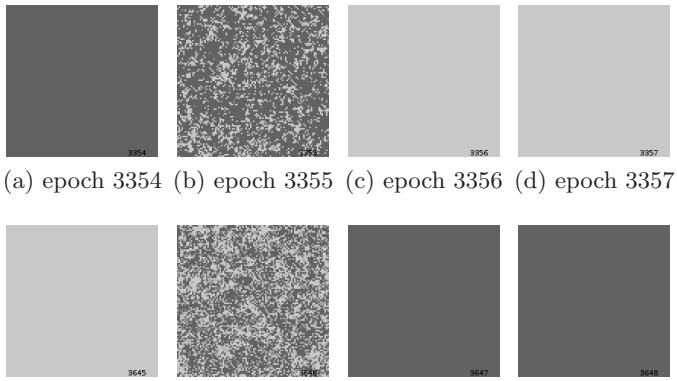

(a) epoch 3354 (b) epoch 3355 (c) epoch 3356 (d) epoch 3357

(e) epoch 3645 (f) epoch 3646 (g) epoch 3647 (h) epoch 3648

Figure 5.4: Random Lattice($p = 1$) : Overlap=10%, $D_c = 0.2$, $D = 0.2$, $r = 1$ and $NL = 0.001$ in 2D 100×100

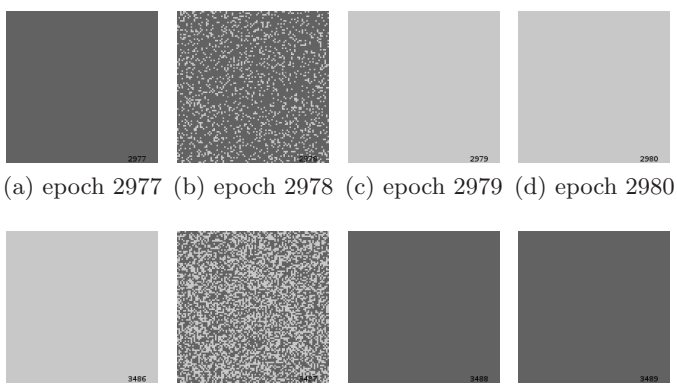

(a) epoch 2977 (b) epoch 2978 (c) epoch 2979 (d) epoch 2980

(e) epoch 3486 (f) epoch 3487 (g) epoch 3488 (h) epoch 3489

Figure 5.5: Fully Connected Lattice : Overlap=10%, $D_c = 0.2$, $D = 0.2$, $r = 1$ and $NL = 0.001$ in 2D 100×100

5.3 Small-world Phenomenon

Small-world graphs can be modelled in various ways – Watts and Strogatz [1998] (WS) model, Newman and Watts [1999] (NW) model, Dorogovtsev and Mendes [2002] (SW) model, etc. We introduce small-world effects to the underlying 2-lattice graph by applying either the WS, NW or SW model to

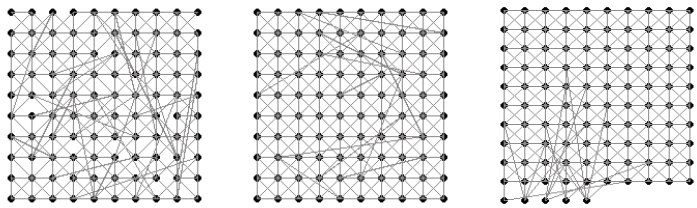

(a) (b) (c)

Figure 5.6: 2-lattice Small-world Models
(a) Watts-Strogatz (WS) ($p = 0.05$) (b) Newman-Watts (NW) ($p = 0.05$)
(c) Smallest World (SW) ($p = 0.05$)

introduce non-local long-range shortcuts. These processes may change the size and order of the neighbourhood (Γ) of each vertex depending on a random probability $0 < p < 1$. WS maintains the order ($N * N$) and size ($N * N * k/2$) of the graph, NW changes the size of the graph but not the order and SW alters both the size and order of the graph. Hence in the visualisations, the snapshots of the smallest-world (SW) lattice are a little taller than for WS and NW because its order (and size) grow with increasing randomness. The newly added habitats are shown at the bottoms of the snapshot.

WS model In the WS model, for each edge (u, v) in the underlying square lattice with k-sized neighbourhood (sub Figure 5.1 (a)), the selected edge is rewired with probability p. In other words, a new edge (u, w) is added to a randomly chosen vertex $w \notin (u \cup \Gamma(u))$ in the rest of the lattice, and the existing edge (u, v) is removed (sub Figure 5.6 (a)). When $p = 1$, the graph is completely rewired into a random graph (sub Figure 5.1 (b)).

NW model In the NW model, for each edge (u, v) in the underlying square lattice with k nearest neighbours (sub Figure 5.1 (a)), an extra short cut (u, w) is added, joining u to a randomly chosen vertex $w \notin (u \cup \Gamma(u))$ with probability p (sub Figure 5.6 (b)).

SW model In the SW model, N^2p new vertices (V') are added and are connected to k randomly chosen vertices in the initial regular lattice (sub Figure 5.6 (c)).

The small-world graphs generated from the above models conform to simple graph properties. ie., the added or rewired edges are undirected without self loops ($(v, v) \notin E$) and without parallel edges (multiple or duplicate). In WS, re-created copies of previously removed edges are discarded. The three models exhibit the small-world effect to varying degrees but they are generally connected (there is a path between any two distinct vertices) with short paths and have low average vertex degree ($k \ll n$ and $k \gg 1$) with high degrees of clustering.

5.3.1 Indentifying the Small-world Regime

The small world regime is identified as the region where $\bar{L}(p) \gtrsim \bar{L}(1)$ and $\bar{C}(p) \gg \bar{C}(1)$, or in other words where the proximity ratio $\mu \gg 1$. Starting from randomness probability $p = 0$, the average path length rapidly drops with increasing p for all three models, as can be observed in Figures 5.7, 5.8 and 5.9.[1] In the small world regime (the shaded regions in these Figures), the observed structural properties of the graphs are similar to real-world topologies – we see a coexistence of small path length and high cliquishness.

5.3.2 Degree Distribution of Small-world Models

The Figure 5.10 shows the degree distribution of small-world graphs (in 100×100 lattice) generated via WS (5.10 (a)), NW (5.10 (b)) and SW (5.10 (c)) models. All possessing Poisson distribution with tails reaching 0.

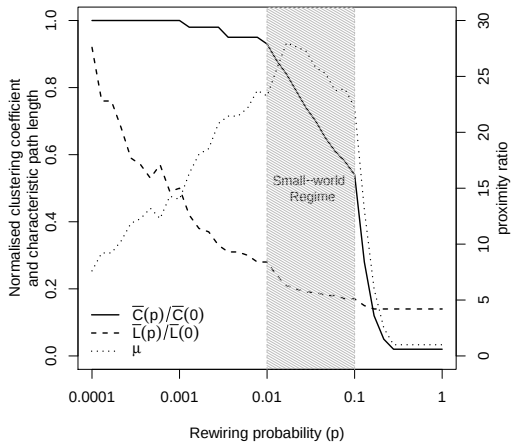

Figure 5.7: Watts-Strogatz model in 2D 100×100 lattice: Clustering Coefficient, Characteristic Path Length and Proximity Ratio

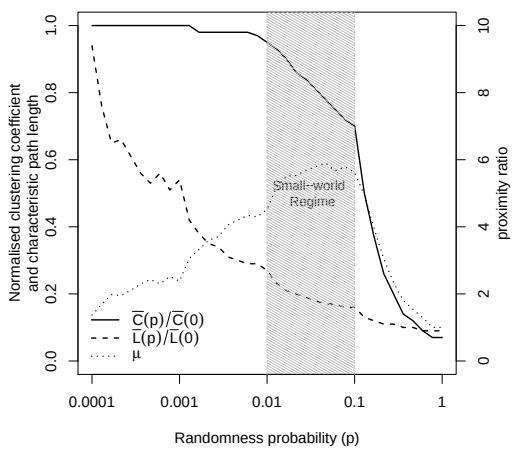

Figure 5.8: Newman-Watts model in 2D 100×100 lattice: Clustering Coefficient, Characteristic Path Length and Proximity Ratio

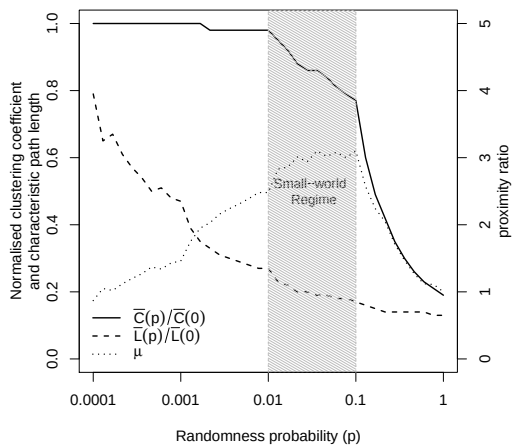

Figure 5.9: Smallest World model in 2D 100×100 lattice: Clustering Coefficient, Characteristic Path Length and Proximity Ratio

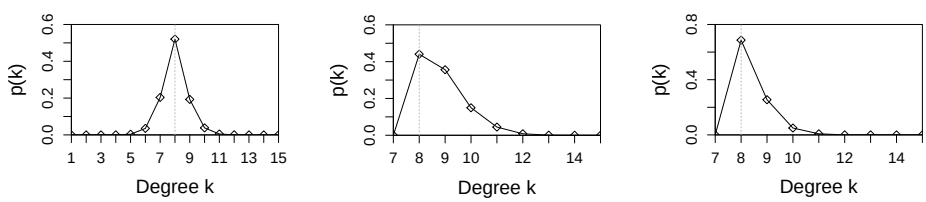

(a) WS (b) NW (c) SW

Figure 5.10: Degree Distribution of Small-world Models

5.3.3 Daisyworld with Static Local and Non-local Couplings

We observe a phase change in daisy population dynamics, from static self-organised patterns to periodic behaviour, when small-world effects are introduced by any of the three models – WS, NW, SW.

[1]In these Figures, the values of $\bar{L}(p)$ and $\bar{C}(p)$ are normalised by the respective values of a regular lattice $\bar{L}(0)$ and $\bar{C}(0)$.

Table 5.2: $\bar{C}$, $\bar{L}$ and μ; $p = 0.05$ is qualitatively compared with $p = 1$ and quantitatively compared with μ

	$\bar{L}(0.05)$	$\bar{L}(1)$	$\bar{C}(0.05)$	$\bar{C}(1)$	$\mu(0.05)$
WS	0.19	0.14	0.74	0.02	27.26
NW	0.19	0.09	0.84	0.07	5.68
SW	0.2	0.13	0.86	0.19	2.94

We fix 0.05 as the randomness probability for all the three models (WS, NW and SW) in our experiments for easy comparison. At $p = 0.05$, we have tabulated the corresponding values of characteristic path length, clustering coefficient and proximity ratio for all models (Table 5.2). We can conclude that all graphs exhibit small-world effects. The μ values for NW and SW greatly differ from those for WS for the obvious reasons: WS maintains the graph size and order even up to probability ($p = 1$), whereas the other models do not.[1]

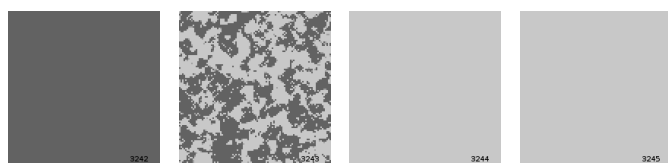

(a) epoch 3242 (b) epoch 3243 (c) epoch 3244 (d) epoch 3245

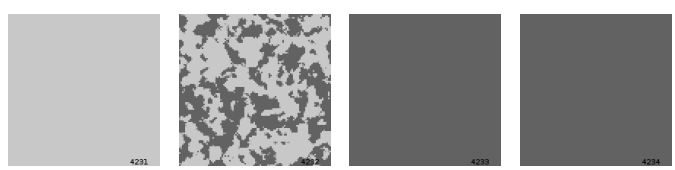

(e) epoch 4231 (f) epoch 4232 (g) epoch 4233 (h) epoch 4234

Figure 5.11: Watts-Strogatz Model ($p = 0.05$) : Overlap=10%, $D_c = 0.2$, $D = 0.2$, $r = 1$ and $NL = 0.001$ in 2D 100×100 Small-world Lattice

[1]We picked the probability $p = 0.05$ by inspecting the visuals and by analysing the results of quantifiers; please see section 5.3.4 for more details.

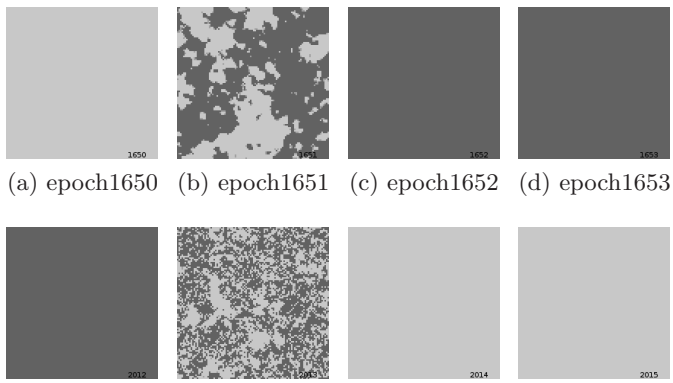

(a) epoch1650 (b) epoch1651 (c) epoch1652 (d) epoch1653

(e) epoch2012 (f) epoch2013 (g) epoch2014 (h) epoch2015

Figure 5.12: Newman-Watts ($p = 0.05$) : Overlap=10%, $D_c = 0.2$, $D = 0.2$, $r = 1$ and $NL = 0.001$ in 2D 100×100 Small-world CML

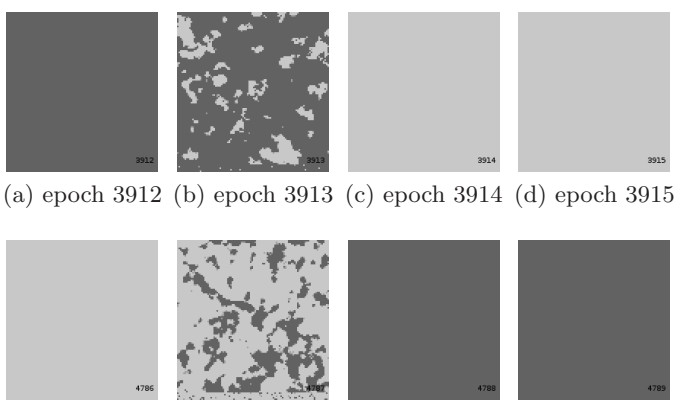

(a) epoch 3912 (b) epoch 3913 (c) epoch 3914 (d) epoch 3915

(e) epoch 4786 (f) epoch 4787 (g) epoch 4788 (h) epoch 4789

Figure 5.13: Smallest-World Model ($p = 0.05$) : Overlap=10%, $D_c = 0.2$, $D = 0.2$, $r = 1$ and $NL = 0.001$ in 2D 100×100 Small-world Lattice

Watts-Strogatz (WS) model: We observe that the periodic behaviour we saw in random and fully connected graphs is also exhibited in WS-based small-world graphs (Figure 5.11). The transition between the daisy type dominance is also very rapid (see the epoch numbers in the visuals), even though most connectivities are still local. The periodicity in the daisyworld dynamics

is confirmed by the temporal trajectories of the local population abundance (Figure 5.42), global population abundance (Figure 5.43) and temperature dynamics (Figure 5.41).

Newman-Watts (NW) model: Each dynamic unit (habitat) is coupled through a small-world topology initialised through the NW mechanism. The topology remains static but the states of the habitats change dynamically. This ecosystem exhibits a periodic behaviour (Figure 5.12). The cyclic behaviour is understood by observing the trajectories in temperature dynamics (Figure 5.44), local population dynamics (Figure 5.45) and global population dynamics (Figure 5.46). This shows that a small change in the underlying topology drastically influences the dynamical properties of the ecosystem, and the transition is very abrupt. Within a single time frame, black dominance may change to white dominance, or vice versa (Figure 5.12).

Smallest-World (SW) model: Periodic behaviour again emerges from the small-world SW lattice (Figure 5.13), and we see similar periodicity in local population (Figure 5.48), global population (Figure 5.49) and temperature dynamics (Figure 5.47).

The result section 5.3.3 illustrates the collective dynamic behaviour (behaviour in a large system of similar interacting units) of a set of coupled life-environmental feedback oscillators with direct short-cuts chosen randomly between oscillators by either WS or NW or SW. Due to the introduction of the non-local connections, the range of interaction grows. But even a small degree of randomness in topological connectivity plays a constructive role in determining the dynamics of the system. This can be understood clearly by comparing the spatio-temporal trajectories of our daisyworld with only local connectives (Figures 5.32, 5.33 and 5.34) and daisyworld with both local and few non-local connectives by WS (Figures 5.41, 5.42 and 5.43), NW (Figures 5.44, 5.45 and 5.46) and SW (Figures 5.47, 5.48 and 5.49). The trajectories in regularly connected daisyworld are static with initial fluctuations

and the ones in smallworld-daisyworld are periodic in nature, which is obviously due to the random perturbation in connectivity, as in trajectories of fully connected daisyworld (Figures 5.38, 5.39, and 5.40).

In general, though the overall dynamics looks the same for random, fully-connected and small-world lattices, a detailed examination shows some differences. If we observe the transition frames, those between black dominance and white dominance or vice versa, they differ depending on the nature of the connectivity. However the main conclusion we can draw is that even quite low levels of long-range connection make daisyworld behave like a fully-connected world: the static emergent patterns of the grid world depend on the almost complete absence of long-range connections. With short-cuts, the emergent spatio-temporal pattern of the daisyworld is completely coherent in space and periodic in time. This sort of behavioural patterns can be observed in nature, for example in firing pattern of neurons [Goel and Ermentrout, 2002], flashing of fire flies [Mirollo and Strogatz, 1990], etc.

5.3.4 Possible Critical Point of Phase Change

Table 5.3: Possible Critical Point (p)

Model	**Probability** p
WS	0.02
NW	0.02
SW	0.04

If there is a phase transition in daisyworld behaviour between grid-like worlds ($p = 0$) and small-world graphs ($p = [0.01, 1]$), then it is of interest to examine the critical point: the point at which the new behaviour emerges. In this context, the relevant parameter is that controlling graph randomness, the probability parameter p (often known as the rewiring probability, as that is its role in the original WS model). The possible critical points for WS, NW and SW are tabulated in Table 5.3.

We examined the behaviour in the transition region of the small-world

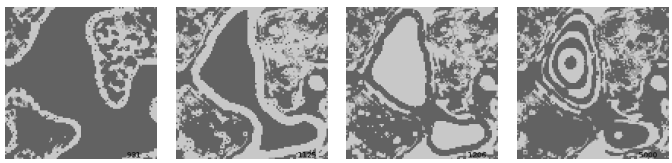

(a) epoch 931 (b) epoch 1125 (c) epoch 1206 (d) epoch 5000

Figure 5.14: WS close to phase change : Overlap=10%, $D_c = 0.2$, $D = 0.2$, $r = 1$ and $NL = 0.001$ in 2D 100×100 Small-world Lattice ($p = 0.01$)

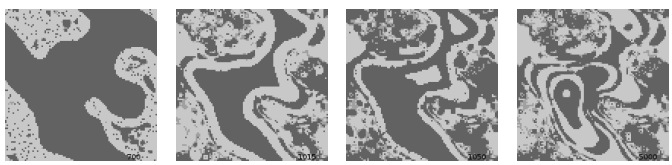

(a) epoch 700 (b) epoch 1015 (c) epoch 1050 (d) epoch 5000

Figure 5.15: NW close to phase change : Overlap=10%, $D_c = 0.2$, $D = 0.2$, $r = 1$ and $NL = 0.001$ in 2D 100×100 Small-world Lattice ($p = 0.01$)

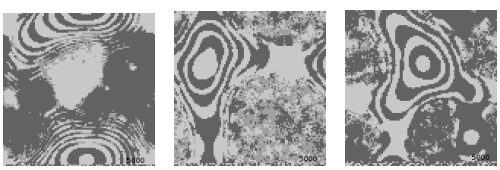

(a) p=0.01 (b) p=0.02 (c) p=0.03

Figure 5.16: SW close to phase change : Overlap=10%, $D_c = 0.2$, $D = 0.2$, $r = 1$ and $NL = 0.001$ in 2D 100×100 Small-world Lattice at epoch $5,000$

effect regime for each of the three small-world mechanisms. In each case, we see a mix of self-organised patterns (as in regular lattices) and partially collapsed patterns (as in random or fully-connected graphs). We show the dynamics for WS (Figure 5.14) and NW (Figure 5.15) at ($p = 0.01$). For SW, we show only the final system state, but at different probability parameter values ($p = 0.01, 0.02, 0.03$ – Figure 5.16). The coexistence of order and disorder indicates that the system behaviour is in transition. The small dots or patches

that we see in the visuals are due to the shortcuts, which tend to destroy the static patterns that we see in regular lattice.

Table 5.4: Spatial Emergence and Std. Dev. of States

Spatial emergence	**Std. dev.**
Mix of states	> 0.25
Dominance of a state	< 0.25

Table 5.5: Temporal Dynamics and Permutation Entropy

Temporal dynamics	**PE**
Static	< 0.1
Periodic	$[0.1, 0.2]$

Table 5.6: Spatio-temporal Patterns

Patterns	**Std. dev.**	**PE**
Self-organised	> 0.25	< 0.1
Static distorted	> 0.25	< 0.1
Periodic distorted	> 0.25	$[0.1, 0.2]$
Periodic complete dominance	< 0.25	$[0.1, 0.2]$

5.3.5 Topology and Criticality

Topology explains how the habitats of the ecosystem are connected and criticality explains how the ecosystem behaves. The topological connectivity affects the critical behaviour of the ecosystem. Since identifying the critical points by inspecting the visuals is laborious, we computed the standard deviation of the local states (spatial dynamics; refer Table 5.4) and permutation entropy (PE) (temporal dynamics; refer Table 5.5). We also used standard deviation of states and PE to analyse the spatio-temporal pattern formation in our daisyworld – (1)static complex self-organised or (2)periodic complete dominance or (3)static distorted patterns or (4)periodic distorted patterns; re-

Table 5.7: The range of std. dev. of states and PE of daisies for 25 realizations

Model	p	**Std. dev.**	**PE**
WS	0.01	$[0.474, 0.649]$	$[0.062, 0.086]$
WS	0.02	$[0.028, 0.595]$	$[0.116, 0.073]$
WS	0.03	$[0.019, 0.589]$	$[0.119, 0.058]$
WS	0.04	$[0.015, 0.504]$	$[0.117, 0.074]$
WS	0.05	$[0.011, 0.563]$	$[0.118, 0.035]$
NW	0.01	$[0.462, 0.647]$	$[0.126, 0.080]$
NW	0.02	$[0.032, 0.618]$	$[0.116, 0.068]$
NW	0.03	$[0.018, 0.586]$	$[0.119, 0.058]$
NW	0.04	$[0.015, 0.516]$	$[0.116, 0.067]$
NW	0.05	$[0.011, 0.524]$	$[0.117, 0.058]$
SW	0.01	$[0.556, 0.682]$	$[0.071, 0.095]$
SW	0.02	$[0.514, 0.691]$	$[0.062, 0.101]$
SW	0.03	$[0.415, 0.647]$	$[0.146, 0.068]$
SW	0.04	$[0.035, 0.646]$	$[0.116, 0.058]$
SW	0.05	$[0.024, 0.622]$	$[0.116, 0.059]$

fer 5.6. Daisyworlds with only local connections exhibit self-organised patterns (Figure 5.3). Periodic complete dominance patterns emerge from daisyworld with local and a few long range connections at critical points (Figures 5.11, 5.12 and 5.13) and from fully connected daisyworld (Figure 5.5). In the transition regions, we observe static or periodic distorted patterns (Figures 5.14, 5.15 and 5.16).

Though we see a collective behaviour of the whole ecosystem (a snapshot) in the visuals, each habitat falls into one of the six states of life. They are (1) no life (dead state) (2) only the presence of black daisies (complete black dominance state) (3) only the presence of white daisies (complete white dominance state) (4) presence of both black and white daisies in equal numbers (coexistence state with equality) (5) presence of both but with black abundance (coexistence state with black abundance) and (6) presence of both but with white abundance (coexistence state with white abundance). In our experiments, the states (1) and (4) are rare; the other four states indicate the

dominance of a particular daisy type with coexistence or otherwise.

If we analyse the states of all habitats and compute their standard deviation, we can understand the behaviour of the ecosystem spatially at a particular epoch – mix of states or a dominance of a particular state. If we compute the standard deviation of states for all the $5,000$ epochs, we can understand the behaviour of the system over a period of time. Obviously the standard deviation of states is 0 if all the habitats in the ecosystem have the same state – dominance of a particular state. Hence if the average standard deviation of the whole ecosystem over $5,000$ epochs is very low in the range $[0, 0.25]$, our daisyworld system exhibits complete dominance patterns. In our experiments, we see values are little over 0 because the computation includes the initial and transition epochs.

We used permutation entropy (PE) to measure the periodicity in the temporal trajectory of both black and white daisies of a habitat (with its ecological aggregates) in the ecosystem. We sampled N out of $N * N$ habitats and compute PE for each of the sample and then averaged them. If the averaged PE is in the range $[0.1, 0.2]$, it indicates the presence of periodic attractors in the temporal series of daisies (population size).

A configuration of an experiment is defined how a small-world graph is constructed – by which of the mechanisms (WS or NW or SW) and which randomness probability $p = [0.01, 0.05]$ is used. All other parameters such as $D = 0.2$ and $NL = 0.001$ are same for all the configurations. For each of the topological configurations, we run 25 realizations. The spatio-temporal behaviour for each realization of the same configuration can be different due to the randomness in the connectivity and ecosystem disturbance in the form of additive spatio-temporal Gaussian white noise controlled by the noise level. If any one of 25 realizations of a configuration has both the standard deviation of the states in $[0, 0.25]$ and PE in $[0.1, 0.2]$, we consider that p as the critical point for that configuration. The range of standard deviation of states and permutation entropy values are listed in Table 5.7 with the corresponding small-world construction model and p for all the 25 realizations.

The standard deviation of states and PE for the configurations WS($p =$

0.01), NW($p = 0.01$), SW($p = 0.01, 0.02, 0.03$) and for all their 25 realizations (Table 5.7) are not in the specified ranges (Tables 5.4 and 5.5). Hence, the possible critical points are chosen as listed in Table 5.3.

5.3.6 Without Life-Environment Feedback

(a) epoch 50 (b) epoch 1000 (c) epoch 3000 (d) epoch 5000

Figure 5.17: Regular without life-environment feedback: $p = 0$, $D = 0.2$ and $NL = 0.001$ in 2D 100×100

(a) epoch 50 (b) epoch 1000 (c) epoch 5000 (d) epoch 10000

Figure 5.18: WS without life-environment feedback: $D = 0.2$ and $NL = 0.001$ in 2D 100×100 Small-world Lattice ($p = 0.05$)

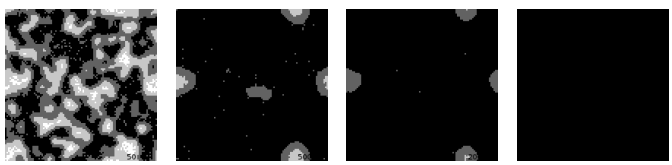

(a) epoch 50 (b) epoch 5000 (c) epoch 20000 (d) epoch 35175

Figure 5.19: NW without life-environment feedback: $D = 0.2$ and $NL = 0.001$ in 2D 100×100 Small-world Lattice ($p = 0.05$)

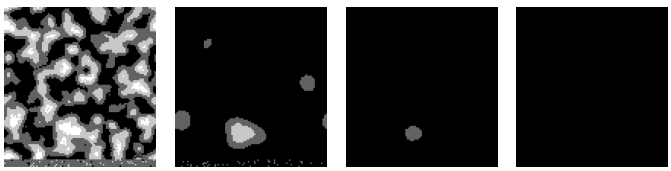

(a) epoch 50 (b) epoch 5000 (c) epoch 50000(d) epoch 61010

Figure 5.20: SW without life-environment feedback: $D = 0.2$ and $NL = 0.001$ in 2D 100×100 Small-world Lattice ($p = 0.05$)

In this section, we validate the system dynamics with no closed loop. To investigate this, we disrupt the feedback: the environment still influences the life (daisies' growth depends on temperature), but there is no feedback from the life to the environment, the daisies do not influence the temperature. We examine the dynamics of system without such feedback in a regular lattice (Figure 5.17) and in small-world lattices – WS (Figure 5.18), NW (Figure 5.19), SW (Figure 5.20). We observe that there is no dynamicity in the behaviour, simply a steady increase in the black daisy cover. The feedback from ecosystem to environment is essential to the rich dynamics of daisyworld, and in the absence of feedback, the qualitative behaviours of regular and small-world lattices are similar. However the long-distance connectivities do change the quantitative behaviour: small-world networks take far longer to converge to a completely black cover (see the epoch numbers in sub Figures 5.18 (d), 5.19 (d) and 5.20 (d) – the final frame is sampled soon after the first emergence of a complete black cover for each model).

5.3.7 Summary

We have explored the implications of small-world phenomena in two-dimensional coupled map daisyworld – a superposition of regular and random graphs. The small fraction of introduced fluctuations in the daisyworld grid structure dramatically affects the dynamics of the system. Proportionally, fewer connections are required for almost full interconnectivity. A few random long range connections to the underlying regular lattice (with high degree of separation)

improves the overall connectivity. Thus adding more and more connections will not increase the connectivity of the lattice. We see an emergence of collective dynamical behaviours, exemplified by homogeneous invasion of a particular daisy type. The daisyworld system in a small-world graphs evolves toward a critical state, where small perturbation are amplified and affect the whole system.

With changes in the level of random connections, we noted a phase transition in the daisyworld, from a self-organised static world to a periodic (seasonal) world in which black or white daisies spread rapidly dominating the whole world. Small alterations to the local structure of daisyworld heavily impact the global emergence. Nevertheless, despite these great variations in behaviour, the temperature is still regulated around 295.5K even in the presence of external perturbations to its connectivity.

5.4 Adaptive Couplings

We examine connectivity changes in a complex adaptive ecosystem based on the daisyworld model, combining coupled map lattice (CML) and complex adaptive graph models. Daisyworld topologies in the literature are static, with only local connections [Wood et al., 2008]. In the previous section 5.3, we have investigated ecological homeostasis in preconstructed static topologies with local and non-local long range couplings –small-world graphs [Punithan et al., 2011; Punithan and McKay, 2013b]. But complex topologies in nature and society are adaptive, in that they exhibit feedback between the local dynamics of nodes (state) and the evolution of the topological structure [Gross and Blasius, 2008; Gross and Sayama, 2009]. Examples include genetic, neural, immunity, ecological, economic and social graphs, complex game interactions etc.

The topology of our ecosystem evolves in response to local habitat states, and the evolved topology in turn impacts the habitat states. Our adaptive and self-maintaining ecosystem, based on CML consists of a set of diffusively coupled habitats incorporating logistic growth of life with bi-directional biota-

environment influences. Thus our ecosystem incorporates three kinds of feedback:

1. Life-environment feedback via the daisyworld model
2. State-topology feedback via an adaptive graph model
3. Density-growth feedback via a logistic growth model

The topology of the our ecosystem evolves with a simple local rule – a frozen habitat is reciprocally linked to an active habitat – and self-organises to complex topologies with small-world effect. In this section, we focus on the emergent collective phenomena and properties that arise in egalitarian small-world ecosystems, constructed from a large number of interacting adaptively linked habitats.

5.4.1 Daisyworld with Dynamic Local and Non-local Couplings

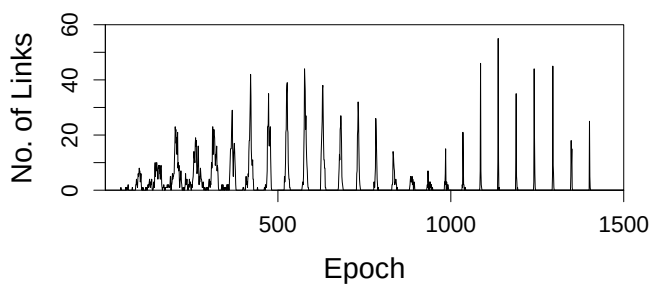

Figure 5.21: Adapted Reciprocal Couplings

The local dynamical linking rule (when a node becomes frozen, we allow that habitat to reciprocally connect to a random active habitat) generates topologies with small-world effect (low characteristic path length (CP)) – here we show topologies with high clustering coefficient (CC) (approximately 50% of runs) to compare to NW-CML ($p = 0.05$). It can also generate topologies with

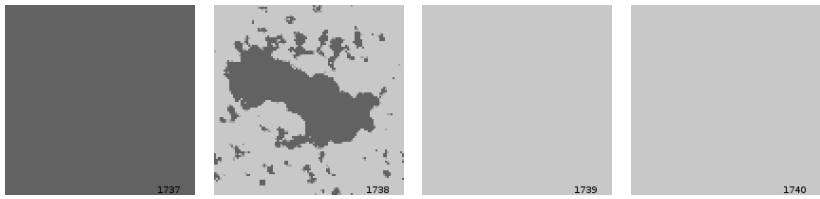

(a) epoch1737 (b) epoch1738 (c) epoch1739 (d) epoch1740

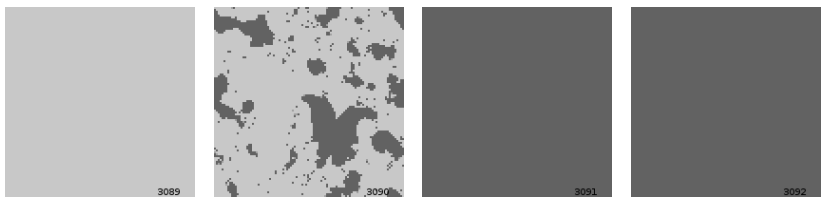

(e) epoch3089 (f) epoch3090 (g) epoch3091 (h) epoch3092

Figure 5.22: Adaptive CML : Overlap=10%, $D_c = 0.2$, $D = 0.2$, $r = 1$ and $NL = 0.001$ in 2D 100×100

low CC. It depends on the random initialization of the temperature of each habitat and random dynamic linking. Typically we observe periodic behaviour (Figure 5.22) similar to NW-CML. In the corresponding time series plots, the dynamics of both local and global temperature (Figure 5.50), local population (Figure 5.51) and global population (Figure 5.52) exhibit cyclic behaviour. The dynamically adapted reciprocal links are shown in Figure 5.21.

5.4.2 Topological Properties of NW-CML and Adaptive CML

Table 5.8: Typical Clustering Coefficients and Characteristic Path Lengths

Model	$\bar{C}(p)/\bar{C}(0)$	$\bar{L}(p)/\bar{L}(0)$
NW-CML	0.837	0.185
Adaptive CML	0.837	0.189

We saw very similar limit behaviours from CML based small-worlds (section 5.3 and adaptive CML (sub section 5.4.1). For comparison and analysis, we take NW-CML results with adptive CML. We can gain understanding

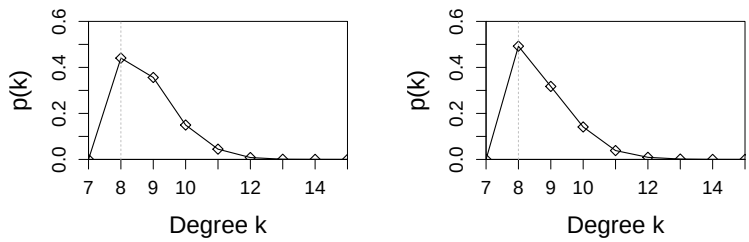

(a) NW-CML (b) Adaptive CML

Figure 5.23: Degree Distribution

through analysing the topological quantifiers (degree distribution, clustering coefficient and characteristic path length) for their network topologies.

The degree distribution of the small-world CML constructed via the NW model in sub section 5.3.3 ranges over $[8, 14]$ and has an exponential tail reaching zero, as shown in the Figure 5.10 (b). The degree distribution reached by adaptive CML in sub section 5.4.1, which dynamically linked with reciprocal links, also ranges over $[8, 14]$ and has an exponential tail reaching zero as shown in the Figure 5.23 (b).

The CC for NW-CML, and that for the final epoch of adaptive CML are almost the same, as are CPs. Figure 5.23 and Table 5.8 show the results. The finally-converged adaptive CML is an egalitarian small-world network. This is why we observe a drastic change in the dynamics of the system compared to the regular lattice. It also shows that the topology, constructed statically or dynamically, influences the collective behaviour of the system: relatively small changes in the linkage structure can generate vastly different dynamics.

Table 5.9: Average($\pm Std.Dev.$) Clustering Coefficients and Characteristic Path Lengths

Model	$\bar{C}(p)/\bar{C}(0)$	$\bar{L}(p)/\bar{L}(0)$
NW-CML	0.8412 ± 0.0024	0.1868 ± 0.001
Adaptive CML	0.8928 ± 0.0639	0.2204 ± 0.0392

The sub section 5.3.3 and sub section 5.4.1 illustrate typical scenarios of NW-CML and adaptive CML. Table 5.9 shows averages over 25 realisations of adaptive CML model and 25 of NW-CML ($p = 0.05$) model. We ran 100 realizations of adaptive CML and picked 25 that fell in small-world regime [Punithan and McKay, 2013b] for comparison purposes – CC in $[0.98, 0.7]$ and CP in $[0.3, 0.16]$. CC and CP are normalised by the values for a regular lattice as proposed in [Watts and Strogatz, 1998].

5.4.3 Topological Evolution

Table 5.10: Adaptation : Clustering Coefficients and Characteristic Path Lengths

Adaptation	$\bar{C}(p)/\bar{C}(0)$	$\bar{L}(p)/\bar{L}(0)$
Quick	0.977	0.295
Slow	0.837	0.238

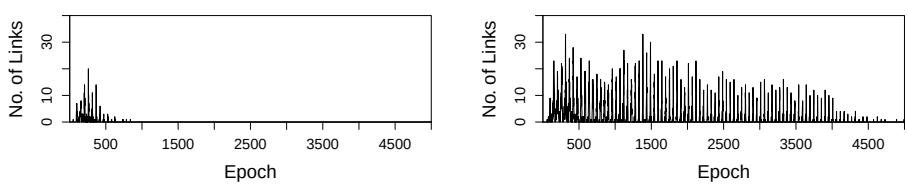

(a) Quick Adaption

(b) Slow Adaptation

Figure 5.24: Adapted Reciprocal Couplings

The evolution of the topology continues until the stationary attractor (frozen local dynamics) of all habitats reach a dynamical attractor – here a limit cycle. Some samples adapt quickly, reaching a stable topology around the 500th epoch (Figure 5.24 (a) – Quick Adaptation), while a few evolve almost until the 5000th epoch (Figure 5.24 (b) – Slow Adaptation). Their degree distribution (Figure 5.25), clustering coefficient and characteristic path (Ta-

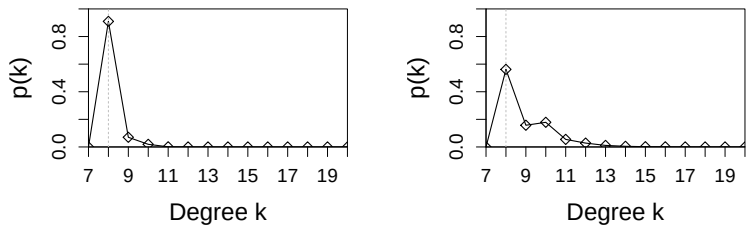

(a) Quick Adaption (b) Slow Adaptation

Figure 5.25: Degree Distribution

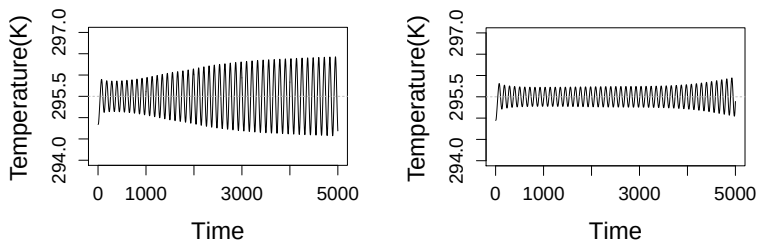

(a) Quick Adaptation (b) Slow Adaptation

Figure 5.26: Global Temperature dynamics : Overlap=10%, $D_c = 0.2$, $D = 0.2$, $r = 1$ and $NL = 0.001$

ble 5.10) show that both evolve to small-world networks, although at different rates.

The collective dynamics in both quick and slow adaptations (Figures 5.27 and 5.28) show the shift in dominance is not so abrupt as in Figures 5.12 and 5.22 (see epoch nos.). The emergent property – the temperature cycles – depicted in Figure 5.26 (in both adaptations) have different limit ranges. In sub Figure 5.26 (b), the shift in dominance takes more time initially, eventually speeding up owing to the increasing limit height. The abruptness is clear in the corresponding global temperature plots – compare the limits in sub

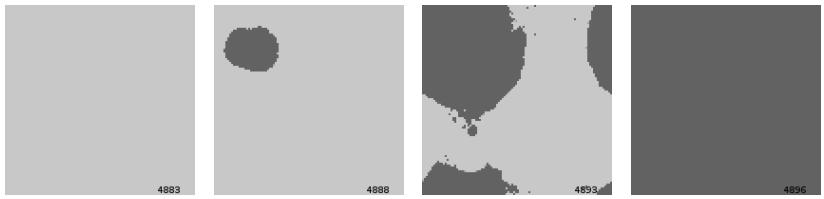

(a) epoch4883 (b) epoch4888 (c) epoch4893 (d) epoch4896

(e) epoch4942 (f) epoch4947 (g) epoch4951 (h) epoch4954

Figure 5.27: Quick Adaptation : Overlap=10%, $D_c = 0.2$, $D = 0.2$, $r = 1$ and $NL = 0.001$ in 2D 100×100

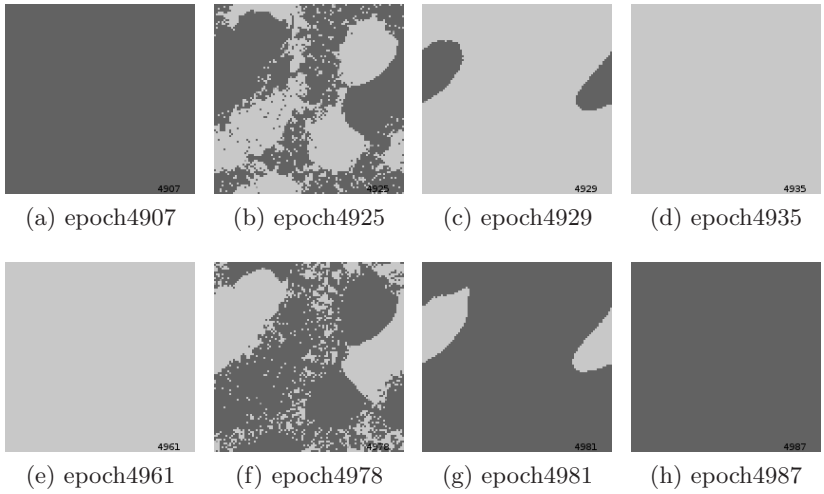

(a) epoch4907 (b) epoch4925 (c) epoch4929 (d) epoch4935

(e) epoch4961 (f) epoch4978 (g) epoch4981 (h) epoch4987

Figure 5.28: Slow Adaptation : Overlap=10%, $D_c = 0.2$, $D = 0.2$, $r = 1$ and and $NL = 0.001$ in 2D 100×100

Figures 5.44 (b), 5.50 (b), 5.26 (a) and 5.26 (b). The degree distribution shows that relatively few reciprocal links are added (sub Figure 5.25 (a)).

This confirms even a few long-distance links – if they are the right links – lead to drastic behaviours changes.

5.4.4 Summary

We have analysed the connectivity changes in a complex adaptive ecosystem combining life-environment, state-topology and density-growth feedback loops. The results illustrate the capacity of the adaptive ecosystem to self-organise to a complex ecosystem (small-world network) through a simple dynamical rule – frozen habitats (nodes) gain reciprocal non-local neighbours (links). Though the collective dynamics change in varying ways, we still observe the emergent property – self-regulation of the temperature at around $295.5K$.

5.5 Scale-freeness

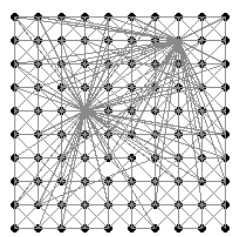

Figure 5.29: Scale-free Graph

We incorporate scale-freeness by pre-defining a set of hub nodes. A node, in a 2-lattice, is assigned a set of $k = 8$ neighbours. The neighbours are added either to local nodes or to hub nodes or to a non-local long-range nodes. Each node is added to any of the hub nodes with probability p, to non-local nodes with probability q and the remaining are added to the local neighbours (Figure 5.29).

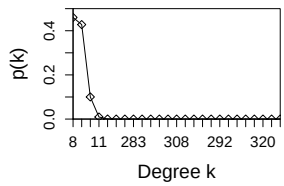

Figure 5.30: Scale-free Degree Distribution

5.5.1 Degree Distribution of Scale-free Graph

Figure 5.30 depicts the degree distribution of the constructed scale-free graph which has a long tail.

5.5.2 Daisyworld with Hubs

Table 5.11: Scale-free Graph : Clustering Coefficient and Characteristic Path Length

$\bar{C}(p)/\bar{C}(0)$	0.79
$\bar{L}(p)/\bar{L}(0)$	0.115

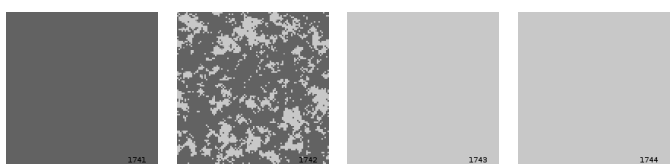

(a) epoch1741 (b) epoch1742 (c) epoch1743 (d) epoch1744

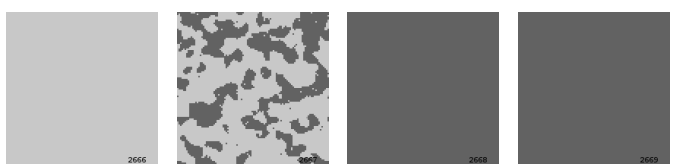

(e) epoch2666 (f) epoch2667 (g) epoch2668 (h) epoch2669

Figure 5.31: $D = 0.2$ and $NL = 0.001$ in 2D 100×100 Scale-free CML

Cyclical behaviour emerges from the lattice with scale-freeness (Figure 5.31), and we see cycles in local population (Figure 5.54), global population (Figure 5.55) and temperature dynamics (Figure 5.53). The degree distribution has a long-tail (Figure 5.30). The corresponding clustering coefficient and characteristic path length are represented in the Table 5.11.

5.5.3 Summary

The results in this section show that the temperature is regulated around $295.5K$ with the hubs and high clustering coefficient. The system behaviour is very similar to daisyworld with small-world phenomenon – 'completely coherent (homogeneous) short-lived cyclical dominance'.

5.6 Behaviour Study

5.6.1 Daisyworld Behaviour in Complex and Adaptive Topologies

Each habitat in the grid daisyworld is confined to a local environment. The inclusion of a few long-range connections, generating a small world networks, brings the whole world close: information is able to disseminate rapidly (ie., dispersion of both daisy types is very rapid). The presence of this global information at a local scale significantly affects the dynamics of daisyworld. Daisyworld with small-world shortcuts in a locally structured networks greatly speeds up the migration of the daisy populations, overcoming the formation of static patterns. The population dynamics in a small-world daisyworld is similar to that of a fully-connected world: just a few long-range connections rapidly disseminating information can completely change the behaviour of the daisyworld. Even a small perturbation in connections are enough for the transition of the system state from a static patterns to dynamic recurrent homogeneous dominance. This recurrent global emergence of complete domination of a particular type of daisies leads to analogies not just in ecosystems dynamics, but in real-world scenarios such as social collective behaviour.

5.6.2 Social Collective Behaviour

In sociology, collective behaviour is defined as "...voluntary, often spontaneous activity that is engaged in by a large number of people and typically violates dominant-group norms and values" [Kendall, 2012]. A contemporary example of collective social behaviour is "flash mobs". Rumours and gossip, crazes and mania, mass hysteria and panic, fads and fashions, public opinion and propaganda are different forms of mass (collective) behaviour [Kendall, 2012; Macionis, 2009] – a dispersed "collective behaviour among people spread over a wide geographic area" [Macionis, 2009]. Fashions are accepted "cultural forms but are periodically subject to change" such as clothing and hair styles, furniture styles, cars, sports, dog breeds, etc. Among varied mass behaviour forms, fads, crazes and mania are similar to fashion but have more extreme rise and fall in their behavioural pattern – a large group of people catch on and adopt very quickly but also give up abruptly.

Fads ("unconventional social patterns" [Macionis, 2009]) emerge out of nowhere and abruptly vanish as fast they appeared. Sometimes, fads that have disappeared reappear and are embraced enthusiastically by a large number of people, even though they are not in one another's immediate vicinity. This phenomenon presumably results from nostalgia. For example, disco music originally emerged in the 1970s and re-emerged in the late 1990s [Malnig, 2008]. Hula hoop, yo-yos, pokemon cards [Andersen and Taylor, 2007] are other examples of the rise and fall of fads from pop culture – reappearing from time to time [Macionis, 2009]. This is due to 'bandwagon effect' – a form of the psychological phenomenon known as 'groupthink'.

Economic bubbles are similar to fads, but profit is the motivator. An example is the high-tech stock boom of the late 1990s, with the corresponding "bubble burst" in the early 2000s. The boom and the burst phases of the economic bubble are result from positive feedback. In dot-com frenzy, a large number of investors purchased technology and e-commerce stocks in the hope of a short-term profit (herd mentality). The stocks reached a higher price than could be supported by the fundamental market value, and subsequently

crashed in value. The Dutch tulip mania, the British south sea bubble and nineteenth century railroad manias are other examples of economic bubbles in history [Mackay, 2004].

Both these examples, the quasi-manic behaviour of fads, with their rapid rise and fall and the boom and bust cycles of markets exhibit similar dynamics, often analogised by a simple model, periodic ups and downs of hemlines. Their behavioural patterns consist of four phases – a rising transition, a positive peak, a falling transition and a negative peak – a behaviour we see clearly modelled in daisyworld.

In the past, with few or no long-distance connections, fads and bubbles were localised, so that a spatially stabilised equilibrium could be reached. Thus tulip mania dramatically affected the Netherlands, but had limited effect on other economies; crinolines could cripple the women of Europe without in the least affecting fashion in East Asia. Nowadays, mass behaviour can propagate beyond physical proximity via telecommunications, viral emails, social media, etc. Hence, the observed behavioural pattern of our small-word daisyworld model – recurrent dominance of black and white daisies and sudden emergence followed by sudden collapse – is reminiscent of more globalised fads and crazes.

5.6.3 Analogies with Popular Metaphors

This "small cause, large effect" behaviour draws analogies with popular metaphors black swan (low probable but high-impact events) [Taleb, 2010], butterfly effect (sensitive dependence on initial conditions) [Hilborn, 2004] and tipping point (little things make a big difference) [Gladwell, 2006].

5.6.4 A Comparative Study

This ecosystem exhibits similar behaviour to contagion systems such as memes or virus – cyclic behaviours – without any external intervention, requiring only the adding of new reciprocal connections under certain locally-defined conditions. Even a small change in the connectivity, with almost no effect on the mean degree of the ecosystem, leads to a drastic behaviour change from

the grid network. It is much more like the real-world behaviour we see in social systems (seasonal rise and fall of fads), economic systems (cyclical booms and busts) etc.. A Flash crash is the quick drop and recovery in stock prices – few recent crashes are May 6, 2010 flash crash and April 23, 2013 flash crash.

The high interconnectivity (same as fully-connected network), owing to the addition of extra connections, of the small-world networks cause the butterfly effect and tipping points. The shortcuts are both change-propagating and change-restraining. Mathematical physics guarantees that there is always a sharp tipping point [Buchanan, 2003] (phase transitions or critical points) – implying that there are always conditions under which a group of social agents or an ecosystem is susceptible to change. When a system goes beyond a threshold, changes occur – a breakthrough or a breakdown. A cascade (contagion or chain-reaction or domino-effect) propagates the effect of the new change across the network. Thus, the individuals in the group act as a coherent mass [Watts, 2004]. This spread can be very rapid and become universal. Example market bubble burst, epidemic of disease, fads, memes, etc.

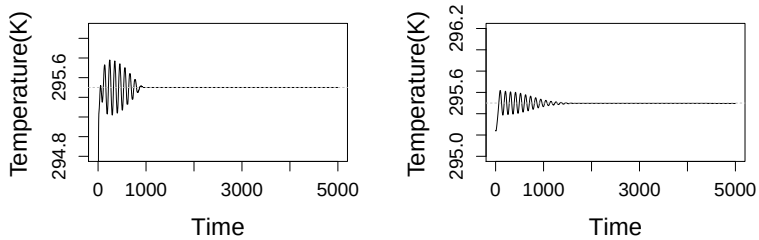

(a) Local Temp. at habitat (57, 50) (b) Global Surface Temp.

Figure 5.32: Regular CML : Temperature dynamics; $p = 0$, Overlap=10%, $D_c = 0.2$, $D = 0.2$, $r = 1$ and $NL = 0.001$ in 2D 100×100

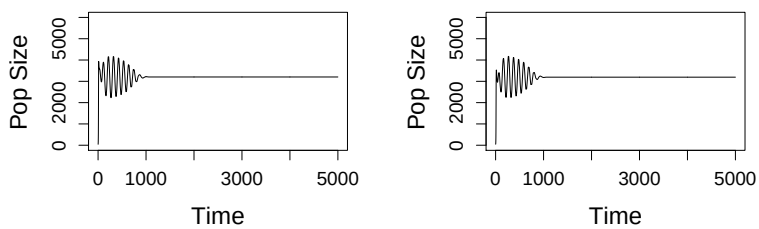

(a) Black Daisy Population (b) White Daisy Population

Figure 5.33: Regular CML: Local population dynamics at habitat (57, 50); $p = 0$, Overlap=10%, $D_c = 0.2$, $D = 0.2$, $r = 1$ and $NL = 0.001$ in 2D 100×100

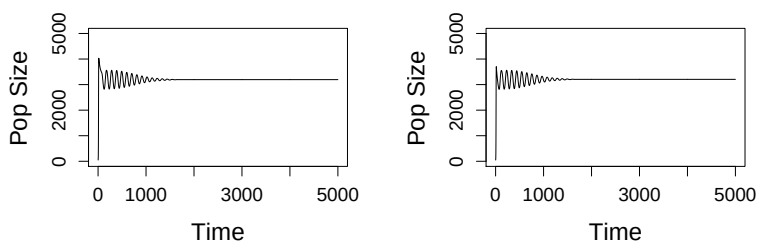

(a) Black Daisy Abundance (b) White Daisy Abundance

Figure 5.34: Regular CML : Global population dynamics; $p = 0$, Overlap=10%, $D_c = 0.2$, $D = 0.2$, $r = 1$ and $NL = 0.001$ in 2D 100×100

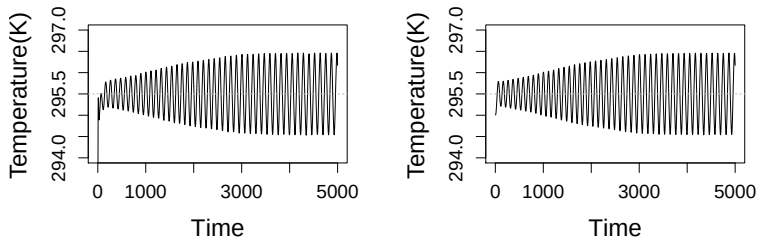

(a) Local Temperature at habitat (53, 53)

(b) Global Surface Temperature

Figure 5.35: Random Lattice: Temperature dynamics; $p = 1$, Overlap=10%, $D_c = 0.2$, $D = 0.2$, $r = 1$ and $NL = 0.001$ in 2D 100×100

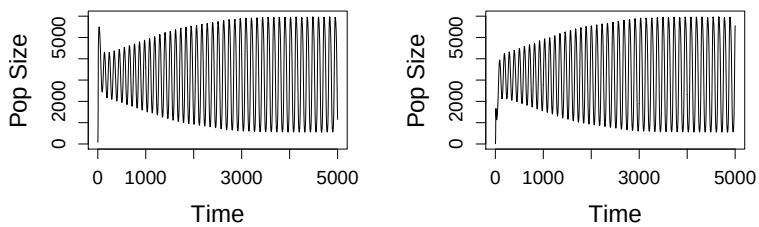

(a) Black Daisy Population

(b) White Daisy Population

Figure 5.36: Random Lattice: Local population dynamics at habitat (53, 53); $p = 1$, Overlap=10%, $D_c = 0.2$, $D = 0.2$, $r = 1$ and $NL = 0.001$ in 2D 100×100

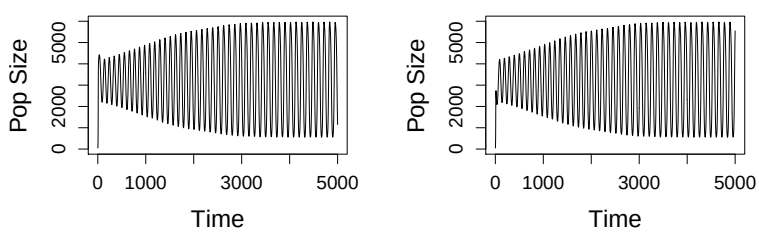

(a) Black Daisy Abundance

(b) White Daisy Abundance

Figure 5.37: Random Lattice: Global population dynamics; $p = 1$, Overlap=10%, $D_c = 0.2$, $D = 0.2$, $r = 1$ and $NL = 0.001$ in 2D 100×100

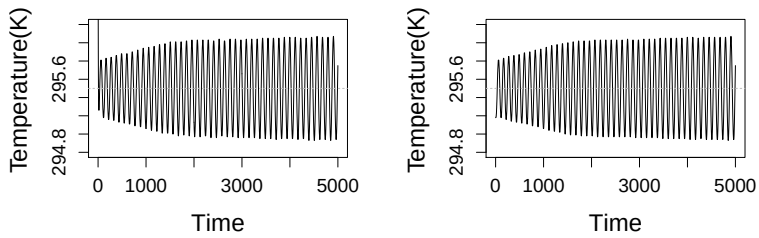

(a) Local Temperature at habitat (50, 46)

(b) Global Surface Temperature

Figure 5.38: Fully Connected Lattice: Temperature dynamics; Overlap=10%, $D_c = 0.2$, $D = 0.2$, $r = 1$ and $NL = 0.001$ in 2D 100×100

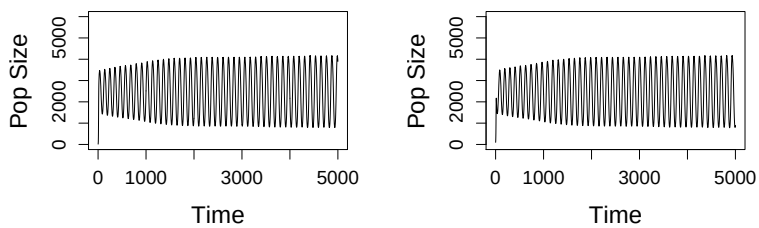

(a) Black Daisy Population

(b) White Daisy Population

Figure 5.39: Fully Connected Lattice: Local population dynamics at habitat (50, 46); Overlap=10%, $D_c = 0.2$, $D = 0.2$, $r = 1$ and $NL = 0.001$ in 2D 100×100

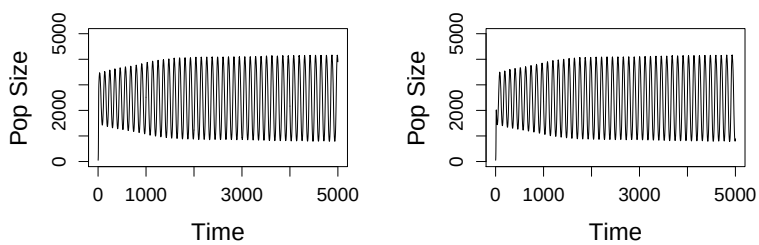

(a) Black Daisy Abundance

(b) White Daisy Abundance

Figure 5.40: Fully Connected Lattice: Global population dynamics; Overlap=10%, $D_c = 0.2$, $D = 0.2$, $r = 1$ and $NL = 0.001$ in 2D 100×100

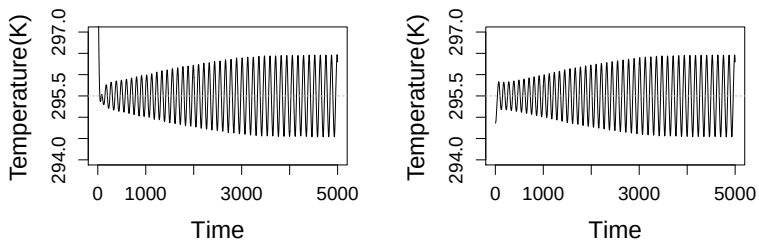

(a) Local Temperature at habitat (53, 62)

(b) Global Surface Temperature

Figure 5.41: Watts-Strogatz Model ($p = 0.05$): Temperature dynamics; Overlap=10%, $D_c = 0.2$, $D = 0.2$, $r = 1$ and $NL = 0.001$ in 2D 100×100

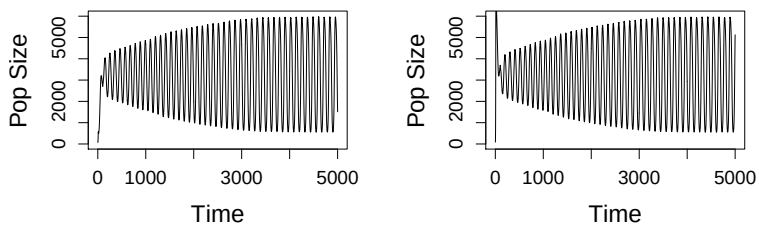

(a) Black Daisy Population

(b) White Daisy Population

Figure 5.42: Watts-Strogatz Model ($p = 0.05$): Local population dynamics at habitat (53, 62); Overlap=10%, $D_c = 0.2$, $D = 0.2$, $r = 1$ and $NL = 0.001$ in 2D 100×100

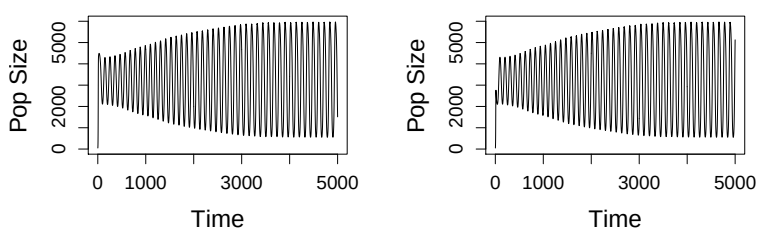

(a) Black Daisy Abundance

(b) White Daisy Abundance

Figure 5.43: Watts-Strogatz Model ($p = 0.05$): Global population dynamics; Overlap=10%, $D_c = 0.2$, $D = 0.2$, $r = 1$ and $NL = 0.001$ in 2D 100×100

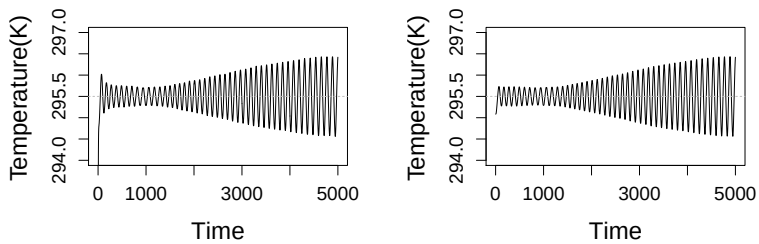

(a) Local Temp. at habitat (52, 58) (b) Global Surface Temp.

Figure 5.44: Newman-Watts CML ($p = 0.05$): Temperature dynamics; Overlap=10%, $D_c = 0.2$, $D = 0.2$, $r = 1$ and $NL = 0.001$ in 2D 100×100

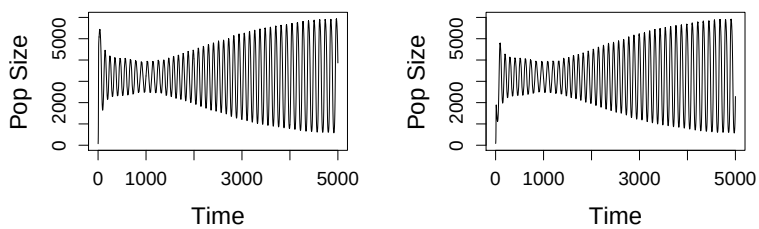

(a) Black Daisy Population (b) White Daisy Population

Figure 5.45: Newman-Watts CML ($p = 0.05$): Local population dynamics at habitat (52, 58); Overlap=10%, $D_c = 0.2$, $D = 0.2$, $r = 1$ and $NL = 0.001$ in 2D 100×100

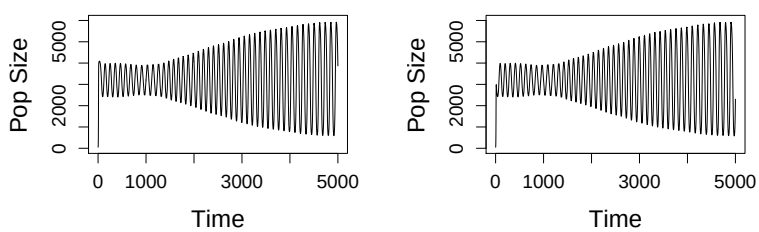

(a) Black Daisy Abundance (b) White Daisy Abundance

Figure 5.46: Newman-Watts CML ($p = 0.05$): Global population dynamics; Overlap=10%, $D_c = 0.2$, $D = 0.2$, $r = 1$ and $NL = 0.001$ in 2D 100×100

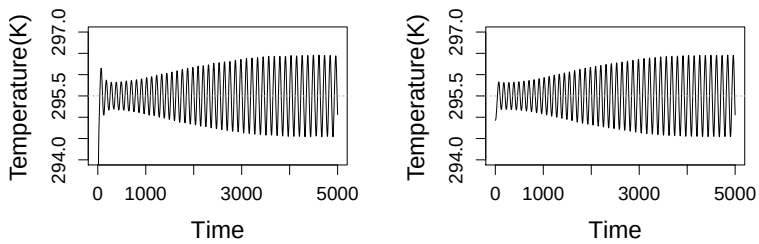

(a) Local Temperature at habitat (54, 44)

(b) Global Surface Temperature

Figure 5.47: Smallest-World Model ($p = 0.05$): Temperature dynamics; Overlap=10%, $D_c = 0.2$, $D = 0.2$, $r = 1$ and $NL = 0.001$ in 2D 100×100

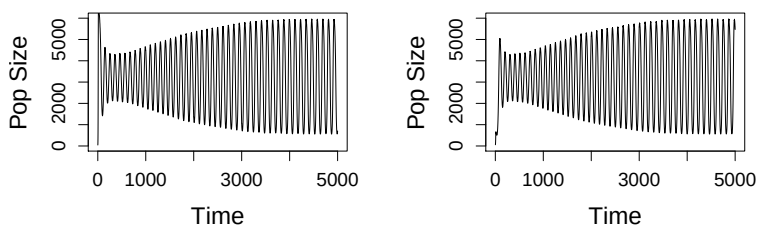

(a) Black Daisy Population

(b) White Daisy Population

Figure 5.48: Smallest-World Model ($p = 0.05$): Local population dynamics at habitat (54, 44); Overlap=10%, $D_c = 0.2$, $D = 0.2$, $r = 1$ and $NL = 0.001$ in 2D 100×100

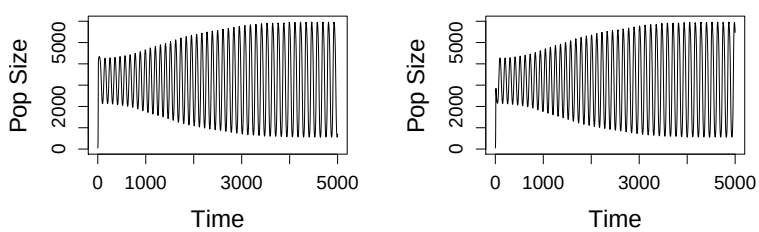

(a) Black Daisy Abundance

(b) White Daisy Abundance

Figure 5.49: Smallest-World Model ($p = 0.05$): Global population dynamics; Overlap=10%, $D_c = 0.2$, $D = 0.2$, $r = 1$ and $NL = 0.001$ in 2D 100×100

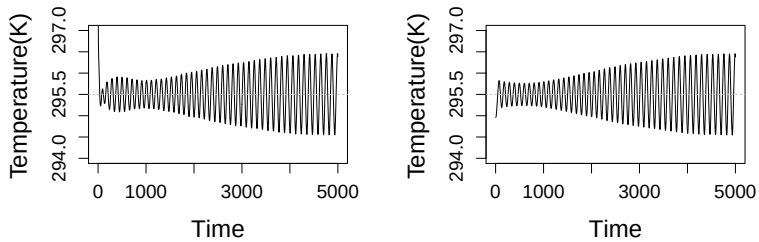

(a) Local Temp. at habitat (56, 57) (b) Global Surface Temp.

Figure 5.50: Adaptive CML: Temperature dynamics; Overlap=10%, $D_c = 0.2$, $D = 0.2$, $r = 1$ and $NL = 0.001$ in 2D 100×100

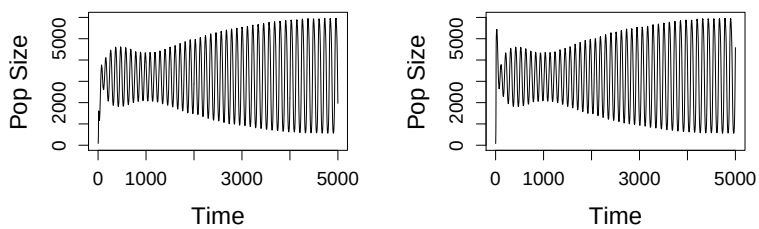

(a) Black Daisy Population (b) White Daisy Population

Figure 5.51: Adaptive CML: Local population dynamics at habitat (56, 57); Overlap=10%, $D_c = 0.2$, $D = 0.2$, $r = 1$ and $NL = 0.001$ in 2D 100×100

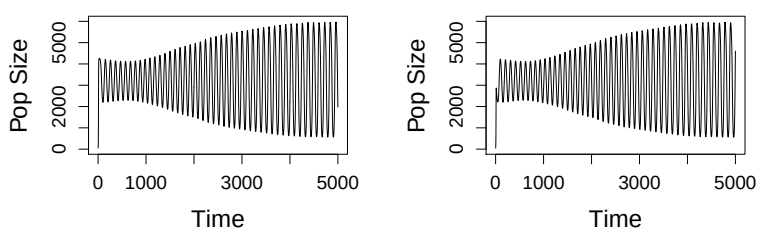

(a) Black Daisy Abundance (b) White Daisy Abundance

Figure 5.52: Adaptive CML: Global population dynamics; Overlap=10%, $D_c = 0.2$, $D = 0.2$, $r = 1$ and $NL = 0.001$ in 2D 100×100

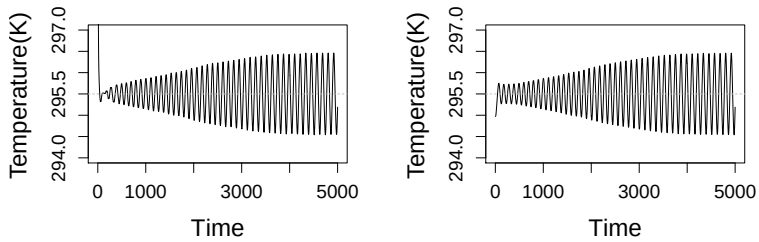

(a) Local Temp. at habitat (52, 58) (b) Global Surface Temp.

Figure 5.53: Scale-free CML ($p = 0.05$): Temperature dynamics; Overlap=10%, $D_c = 0.2$, $D = 0.2$, $r = 1$ and $NL = 0.001$ in 2D 100×100

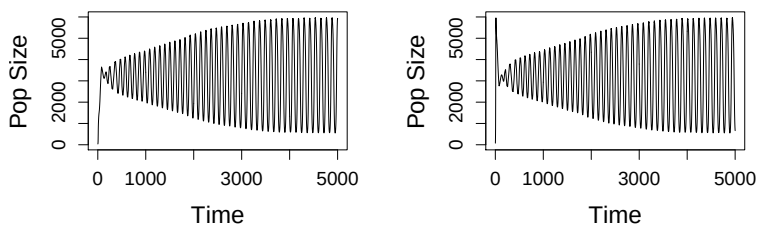

(a) Black Daisy Population (b) White Daisy Population

Figure 5.54: Scale-free CML ($p = 0.05$): Local population dynamics at habitat (52, 58); Overlap=10%, $D_c = 0.2$, $D = 0.2$, $r = 1$ and $NL = 0.001$ in 2D 100×100

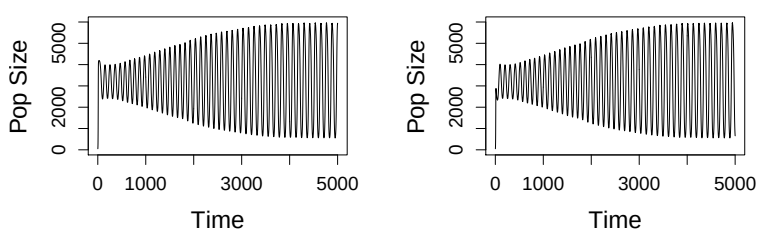

(a) Black Daisy Abundance (b) White Daisy Abundance

Figure 5.55: Scale-free CML ($p = 0.05$): Global population dynamics; Overlap=10%, $D_c = 0.2$, $D = 0.2$, $r = 1$ and $NL = 0.001$ in 2D 100×100

Chapter 6

Applications – Demonstration of Social Homeostasis in Stock Market

6.1 Introduction

Stock market is one of the examples of homeostatic complex system. This is one such system whose response is fedback autonomously into the system as a new cause. The (self-interested) investors' opinion affect the stock price, also the price causes investors to make those very same decision. Thus, the price is self-generated (self-affinity). This produces a feedback loop which is governed by an unconscious social nature of the investors [Frost and Prechter, 2005].

The nobel laureate, Herbert A. Simon, emphasises that most people are only partly rational and partly emotional/irrational in making their decisions [Simon, 1957]. This implies investors' emotions that are expressed can influence their fellow investors.

In this contemporary world, investors express their mood via social media such as Twitter. The tweets posted by the investors reflect their emotions and mood which affect stock price and vice versa. The opinions and emotional expressions are reflected by other traders involved in the market. Eventually,

the wax and wane of the emotions are reflected in the stock price. The stock price urges the traders to monitor themselves. The community feeds off its own emotion and thus self-maintains the stock price. This self-organizing behaviour of markets is called as "invisible hand" [Smith, 2008] which arises from the microscopic decisions of individual investors.

The investors' collective action (response) influence the stock price. The very same way stock price also influences the investors' decision (mood or opinion or sentiments). Thus, investors and stock price influence each other reciprocally. The stock price reflects and affects the pulse of investors. This scenario is very similar to organismic view of society, ecosystem, etc. In this chapter, we analyse the tweets (which reflects traders' emotions) and the stock price movement with the insights from daisyworld.

6.2 Daisyworld - Stock Market Analogy

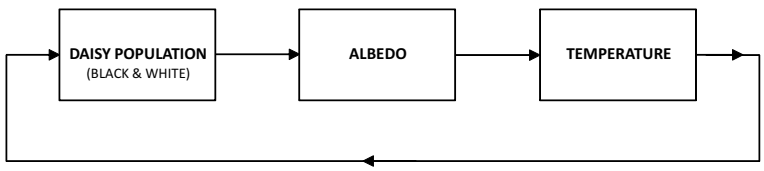

Figure 6.1: Self-causing Feedback in Daisyworld

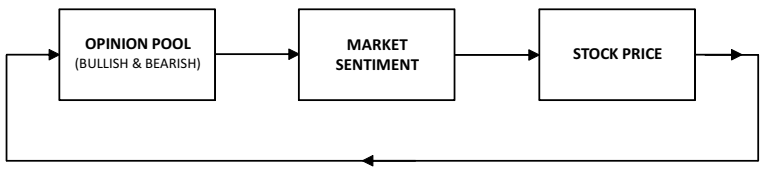

Figure 6.2: Self-causing Feedback in Stock Market

Daisyworld emphasises on reciprocal influence between living organisms and their environment, exemplifying deep ecology principles. The very same way, collective stock market investors' opinion and stock price influence each

Table 6.1: Parametric Analogy of Daisyworld and Stock Market

	Daisyworld	**Stock Market**
Species	Black and White Daisies	Bull and Bear Opinions
Environment	Temperature	Stock Price
Environment Altering Trait	Albedo (reflectivity)	Market Sentiment

other reciprocally. Each investor (at the microscopic level) buys the stocks by learning others' behaviour which pushes the price up in bull market or down in bear market as a whole (on the macroscopic level), and thereby self-organize themselves.

6.2.1 Daisyworld Behaviour

Initially daisyworld is cold and hence black daisies start to grow by absorbing the heat. An initial growth of black daisies increases the temperature of the system (positive coupling). But at a higher temperature, white daisies bloom and keep the positive feedback under control (negative coupling).

The growth of white daisies decreases the temperature further and further (positive feedback). But at a colder temperature, black daisies bloom and inhibit the system behaviour (negative coupling).

This cycle goes on and on demonstrating it as a homeostatic system – keeping the temperature in the viable range of the daisies.

6.2.2 Stock Market Behaviour

When stocks rise, the investors tempt to buy more stocks – bull market. The aggregate behaviour of traders gets amplified and the net buying lifts the prices up and higher (positive coupling). But the increased price of the stocks indicates a peak after which the market will fall and deter buyers (negative coupling).

Once the market begins to fall, investors refrain from buying and are induced to sell – bear market. The net selling pushes prices down and lower (positive coupling). But some may buy because stocks become more and more of a bargain (negative coupling).

Thus, the aggregate behaviour produces a cyclical trend consisting of accelerating growth and accelerating decline.

6.2.3 Comparison of Behaviours – An Ecosystem Approach

We can view stock market as an ecosystem, consisting of a collection of stock investors' bullish and bearish opinions as its biotic component (black and white daisies in daisyworld), stock price as its abiotic component (temperature in daisyworld) and market sentiment as environmental changing trait (albedo in daisyworld – influence factor). Refer Figures 6.1 and 6.2 for comparison. The parametric analogy is provided in Table 6.2. We also perceive stock market as a "superorganism" with "collective intelligence" where social homeostasis emerges similarly to termite colony, bee hives, etc.

6.3 Background

6.3.1 Sentiment Analysis and Microblogging Services

Microblogging is one of the popular contemporary communication tools. A large-scale of data is generated via microblogging web-sites such as Twitter, Tumblr, Facebook, etc. Internet users post their personal views on variety of topics. This huge collection of posts from online microblogging service can be used for social studies. In other words, microblogging is a rich source of data for opinion mining and sentiment analysis. Sentiment analysis detects the public's opinion – polarity (positive or negative) about a given topic in the corresponding document collection. Opinion mining and sentiment analysis on user created contents is relatively recent and a growing research field [Asur and Huberman, 2010; Bollen et al., 2011; Das and Chen, 2007; Gruhl et al., 2005; Mishne and Glance, 2006; Nofsinger, 2005]. Pang and Lee [2008] present

a wide overview of the existing work.

Recently, Twitter – the most popular microblogging platform – is used for sentiment analysis where the users create status messages (called "tweets"). A huge amount of tweets (over 400 million) are transmitted per day via Twitter. Each tweet has maximum of 140 characters and hence 56 billion characters are generated and transmitted via Twitter alone. An individual tweet may not be useful and interesting. But aggregation – collection of tweets – reflects the public mood (opinion) and sentiment of tweeples (people who use twitter.com).

In this chapter, we focus on Apple stock tweets for analysing the sentiments of the stock traders with the stock price fluctuations. By Twitter convention, developed by the users, $ symbol is used with the stock tickers to post the stock related tweets. For instance, $\$AAPL$ represents Apple stocks.

6.3.2 Supervised Classification

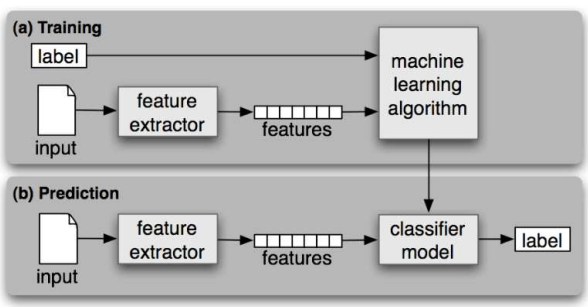

Figure 6.3: Supervised Classification (Source : [Bird et al., 2009])

Classification predicts the appropriate class label for a given input. A classifier is supervised if it is constructed on training corpora which contain correct label for each input. The framework used by supervised classification is depicted in the Figure 6.3. In this framework, features (domain specific words) play the key role. A feature extractor converts each input to a feature set. The feature sets and their corresponding labels are used to build the model. The model is built using the training corpora containing the label for each input

and thus the classifier learns from the training data. The same extractor is also used to convert unseen inputs to feature sets. These feature sets are fed into the model which predicts the possible labels [Bird et al., 2009].

6.3.2.1 Naive Bayes Classifier

A naive Bayes classifier assumes that the presence or absence of a particular feature is unrelated to the presence or absence of any other feature, given the class variable. It considers each of the features to contribute independently to the probability in choosing the class type, regardless of the presence or absence of the other features. The underlying probability model is an "independent feature model". Naive Bayes classifier calculates the prior probability of each label based on the frequency of each label occurring in the training data. The contribution from each feature is then combined with this prior probability, to get a likelihood estimate for each label. The label whose likelihood estimate is the highest is then assigned to the input value.

$$P(label|features) = \frac{P(label) * P(features|label)}{P(features)} \tag{6.1}$$

6.3.2.2 Support Vector Machine (SVM)

Given a training set of features-label pairs $(\mathbf{x}_i, y_i)$ where $i = 1, ..., l$, $\mathbf{x}_i \in R^n$ and $\mathbf{y} \in \{1, 1\}^l$, the support vector machine (SVM) solves the optimization problem:

$$\begin{aligned} \min_{\mathbf{w},b,\xi} \quad & \frac{1}{2}\mathbf{w}^T\mathbf{w} + C\sum_{i=1}^{l}\xi_i \\ \text{subject to} \quad & y_i(\mathbf{w}^T\phi(\mathbf{x}_i) + b) \geq 1 - \xi_i, \\ & \xi_i \geq 0. \end{aligned} \tag{6.2}$$

The training vectors $\mathbf{x}_i$ are mapped into a higher dimensional space by the function ϕ. SVM finds a linear separating hyperplane with the maximal

margin in this higher dimensional space. $C > 0$ is the penalty parameter of the error term. $K(\mathbf{x}_i, \mathbf{x}_j) \equiv \phi(\mathbf{x}_i)^T \phi(\mathbf{x}_j)$ is called the kernel function. The basic kernel functions are linear, polynomial, radia basis function (RBF) and sigmoid. We use linear kernel function: $K(\mathbf{x}_i, \mathbf{x}_j) = \mathbf{x}_i^T \mathbf{x}_j$.

6.3.3 Twitter API

We can collect tweets either via Streaming API or Search API.

Streaming API The Streaming API allows real-time access to tweets based on the input query – in our case, it is apple stock ticker symbol $\$AAPL$. We need to get authenticated and request for a connection to the stream of tweets from the server. After the server opens the streaming connection, the tweets are streamed.

Search API The Search API is a REST API which allows us to request specific queries of only the recent (last 6 days) tweets.

6.4 Sentiment Analysis on Apple ($\$AAPL$) Stock Market Tweets

We form the corpus for sentiment analysis from the tweets collected from Twitter. We use machine learning techniques in acquiring positive and negative sentiments of the tweet corpus. We mine the stock tweets using Twitter's search API and pre-process them for further analysis. We use Naive Bayes classification and Support Vector Machine machine learning techniques to determine the sentiment of the tweets. Then we carry out causality analyses between sentiment score and stock price collected from Yahoo finance.

6.4.1 Data Collection

Collection of Stock Market Domain Specific Words We have collected nearly 1200 stock market specific words. This is a very essential step in sen-

timent analysis. These words are used as features in the analysis. Domain specific words will improve the accuracy of the model.

Stock Data We have collected stock data from July, 2013 to October, 2013 from Yahoo finance data feed.

Training Dataset We form the training dataset by collecting the tweets using Twitter API. We use streaming API to collect the tweets. We have hand classified 1000 tweets as bullish and 1000 tweets as bearish. Each instance in the training dataset contains a tweet (collection of words) and its corresponding class label ("target value") – bullish or bearish. We used the tweets during June, 2013 as our training dataset.

Test Dataset We have streamed $\$AAPL$ tweets from July, 2013 to October, 2013 to form our test dataset.

6.4.2 Tweet Text Pre-Processing

We remove the extraneous words which do not affect the sentiment of the tweet. They are URLs, hash tags (#), user name (@), retweet notation (RT) etc. We pre-process the tweets by following the steps below :

1. converting the tweets to lower case
2. replacing urls with URL
3. replacing @username with AT_USER
4. replacing #hashtag with HASH_WD
5. removing punctuations at the start and at the end of the tweet
6. removing additional white spaces

6.4.3 Training the Classifier

The first step of creating a classifier is collecting the relevant features of the tweets. The feature extractor builds a dictionary containing relevant features in the given tweet. We first tokenize the tweets to list of words. Then we clean up the words, filter unnecessary words and then finally extract the relevant features.

Feature Extraction Feature extraction is the process of transforming a list of words into a feature set that is used by the classifier in learning and predicting. We have collected the domain (stock market) specific bullish and bearish words. The presence/absence of these words in a tweet are the features. Each tweet is splitted into words and each of those words are added to the feature vector. Before adding the words, we need to filter some unnecessary words which don't make any impact on the sentiment. Otherwise the feature vector will explode. We use the following procedure to filter the words:

1. removing stop words
2. removing repeating letters. Eg., woooow as wow
3. converting words starting with an alphabet and containing only alphabets
4. removing punctuation ' " ‘ ? , . ! : ; -

Model Generation The goal of classifiers is to generate a model based on the training data (labelled feature set) which predicts the target values of the unseen (test) tweet (unlabelled feature set) given only the features of the test tweet. We use the machine learning classifiers Naive Bayes Classifier (NB) and Support Vector Machines (SVM) to classify each of tweets. We use Natural Language Toolkit (nltk) [Bird et al., 2009] and LIBSVM [Chang and Lin, 2001] libraries to implement these classifiers.

6.4.4 Sentiment Score

In our approach, we measure the reflectivity of stock investors' mood by a sentiment score. After we classify each day's tweets, we compute the sentiment score on daily basis.

$sentiment = \frac{NumOfBulls - NumOfBears}{NumOfBulls + NumOfBears}$

6.5 Demonstration of Social Homeostasis

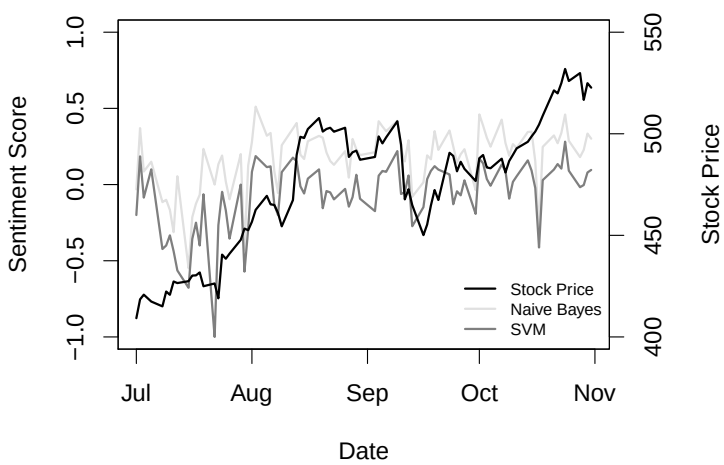

Figure 6.4: Sentiment Vs. Price

In the Figure 6.4, we have plotted the stock price (black line), sentiment score based on Naive Bayes classification (lighter grey line) and sentiment score based on SVM classification (darker grey line). These hemlines show that they are non-stationary time series. We observe that the peaks and troughs in all the three time series have common drifts.

Table 6.2: p-values of Granger Causality Analysis

	Naive Bayes	**SVM**
price causes sentiment	0.03788	0.00452
sentiment causes price	0.01109	0.04421

Causality Analysis The p-values in the Granger causality analysis for lag=1 show that stock price and sentiments cause each other reciprocally.

Table 6.3: p-values of Cointegration Tests

	Naive Bayes and Price	**SVM and Price**
Engle-Granger	0.01	0.01
Phillips-Ouliaris	0.04271	0.03024

Cointegration Tests Two or more time series are cointegrated if they share a common stochastic drift. We have performed Engle-Granger two-step method and Phillips-Ouliaris cointegration tests (Table 6.3). The p-values in the tests show that the time series are cointegrated.

6.6 Discussion

6.6.1 Social Mood Trends - A Psychological Perspective

Band wagon effect is a cognitive bias (tendencies to think in certain way). People tend to do (or believe) something because many other people do (or believe) the same. Herding mentality (gregarious behaviour) and group think are similar biases. This bias affects social, political and economic decisions and belief formation – human behaviour in general.

The evolutionary biologist Richard Dawkins suggests that as genes pass from generation to generation, memes also do the same – genes propagate themselves in the gene pool by leaping body to body via sperm or eggs and

memes propagate themselves in the meme pool by leaping brain to brain via imitation [Dawkins, 2006]. The neuron "mirrors" the behaviour of the others. Vilayanur S. Ramachandran (Marco Polo of neuroscience as called by Richard Dawkins) has speculated that role of mirror neurons will help explain a variety of human mental capacities such as empathy, imitation learning, and the evolution of language.

Human activity can be viewed as collections of many interacting agents (same fluid of interacting atoms or molecules) from which decision-making, learning and adaptation arise [Ball, 2004; Buchanan, 2008]. Then the decision or the innovation diffuses in the social system [Rogers, 2010]. The innovation must be widely adopted in order to self-sustain. Within the rate of adoption, there is a point at which an innovation reaches critical mass [Ball, 2004; Granovetter, 1978].

Herding in stock market is a collective irrationality of investors. Individual investors join the crowd to make decision (buy or sell). This unconscious herding impulse impels social mood trends and is reflected in the stock price. Though stock market face crashes, the system soon recovers due to sentiments of the investors on the stock price. Thus, owing to reflexism, investors act and reinforce and at criticality market crash occurs.

6.6.2 Stock Market - A Termite Colony

Colonies of social insects is the most mysterious complex system in nature. Every termite functions based on set of low level rules and feedback from its neighbours. We have analysed the emergence of stock price by applying the five fundamental principles as illustrated by Johnson [2012]. Here, we compare termites to investors and stock market to the termite colonies – both exhibiting social homeostasis.

More is different: A huge number of termites construct the colonies. Just one tweet does not contribute much to sentiment analysis. But an aggregation of tweets makes the stock market decision.

Ignorance is Useful: Each termite is not intelligent. Each investor does not required to be intelligent. The masses can be smarter than the solitary expert [Surowiecki, 2005]. Hence investor can be a mediocre.

Encourage random encounters: Termites use the feedback from encountering the activities of other termites to usefully modify their behaviour. The very same way investors watch their fellow investors to make their decisions.

Look for Patterns in the Signs: Termites follow trails of pheromones left by other termites. Investors follow the emotions left by other investors.

Pay Attention to Your Neighbours: Termites alter their behaviour by noticing a large number of other fellow termites. The investors in the stock market pay attention to other investors and express their emotions.

To sum up, "**Local information leads to global wisdom**" [Johnson, 2012].

6.7 Summary

The investors' emotions expressed via tweets can influence their fellow investors. This mass action is reflected by the stock price and affects the same. This cause is endogenous. We see a common drift both in the stock price movement and social sentiment trends. Thus Stock price movement is not random but nonlinear due to sentiments. We have analysed this self-causing nature using Granger causality analysis and cointegration tests. We have also touched upon the psychological reasons behind the price trends. We have demonstrated the social homeostasis in stock market is similar to social homeostasis in termite colonies.

Chapter 7

Conclusion

7.1 Summary

In our computational model presented (CML based daisyworld system), life undergoes fluctuations as local nonlinear chaotic oscillators, influenced by the ecological disturbance (noise) and the intrinsic increase rate; this effect is spread throughout the system via diffusion, and then amplified and controlled by the internal feedback mechanisms. We have noticed that the system self-organize itself owing to the combined effect of positive and negative couplings resulting in negative feedback loops, giving rise to the emergence of temperature self-regulation and sustainable population dynamics. This typical behaviour emerge without any tuning of the system from the outside. While the tuning happens from the internal mechanisms, ie., albedo (reflectivity) tunes the temperature (environment).

Thus the dynamics of life, together with temperature feedback, regulate the global temperature of the daisyworld homeostatically in our CML based daisyworld, as in the earlier CA versions. This regulatory behaviour emerges even in the presence of perturbations. The results envisage that daisyworld coordinate complex behaviours and has potential to cope up with disruptions with huge parameter space. Regardless of the varied and complex dynamical response of our system, depending on the parameter settings, the simplify-

ing aspect is that the homeostatic property is exhibited by the system in all scenarios.

The daisyworld models based on both CA and CML are spatially extended bottom-up approaches, in which globally emergent behaviours are generated by the local rules and bounded interactions. In the former model, daisy populations exhibit boom and bust local behaviour at a particular habitat in the ecosystem, and in the latter, chaotic local behaviour. CML represents mesoscopic daisy states, while deterministic CA represents the microscopic states of the daisies.

We have investigated that our system has exerted the following complexity features: • interconnected and interdependent components • simple rules of interaction • positive and negative feedbacks • nonlinearity • sensitivity to initial conditions • structured randomness • neighbour interactions • decentralized control • self-organization • self-regulation • pattern formation • co-evolution • adaptive dynamics

We have analysed life-environment feedback system (daisyworld) from different angles and aspects of complex system's phenomena. We have illustrated that our system exhibits stationary attractors, bifurcations and strange attractors and thereby signifying it as a dynamical system. Our system generates a wide spectrum of striking spatio-temporal patterns deriving insights from biological systems and non-living systems. In our nonlinear reaction-diffusion system, symmetry-breaking is induced by species dispersion, temperature diffusion and noise, which paves the pattern formation.

We have introduced metrics for quantifying the behaviour of daisyworld, and used them to analyse the spatio-temporal dynamics: Permutation Entropy to measure the temporal dynamics, standard deviation to measure the scale of fluctuation, and Moran's I to measure the spatial auto correlation and pattern formation. As we have seen in the analyses, PE and MI quantify the spatio-temporal dynamics accurately, demonstrating their reliability in quantifying a wide range of dynamics.

We have incorporated evolutionary mechanisms via replication with mutation and adaptation into our system which displays the robustness in self-

regulation. Noise plays vital in the system exhibiting different life forms – monotonous (quiescent daisy dominance states), suppression of mutants, etc.

We have explored the implications of topological effects in our system. Under the same parameter settings, the additional random connections to the grid, generating a small-world, destroys the heterogeneous static behaviour of grid to a homogeneous cyclical short-lived behaviours. The system (possessing small-world phenomena) evolves toward a critical state, where a small perturbation is amplified and affects the whole system. Even a small change in one part of the network propagate via the shortcuts, gets amplified (self-reinforcing feedback) and cause huge changes in the whole system. But the self-maintaining feedback counters the effect and the cycle start over. In spite of these variations, the system persists homeostasis.

In addition to life-environment and density-growth feedback loops, we have added up state-topology feedback (adaptive networks). This addition enables the capacity of grid to self-organize to complex topology (small-world) via simple dynamical linking rule – frozen habitats (nodes) gain reciprocal non-local neighbours (links). When the threshold of adding new connections is crossed, the system is switched from one network architecture (organization) to another and hence the behaviour changes. The system displays homogeneous cyclical short-lived behaviours and still self-regulates its environment.

We have incorporated scale-freeness into our system possessing power law distribution. The outcome shows similar behaviours as that of small-world and adaptive networks.

The complex and adaptive networks display 'completely coherent (homogeneous) short-lived cyclical dominance'. Our system represents social phenomena as in spread of memes, epidemics, etc. These behaviours are also seen in stock market – a man made complex adaptive system, which has led us to analyse the social homeostasis in stock market. We have collected $\$APPL$ stock tweets from twitter and stock data from Yahoo finance and examined that the sentiment causes the price reciprocally. We have analysed the chain of causality between investors' sentiment and stock price movement.

7.2 Conclusion

We have detailed how we have reconstructed the computational modelling of our life-environmental, self-regulating system and quantified its spatio-temporal behaviours. We have showed the robustness of our system in self-regulating its environment for the sustainability of life in the presence of various perturbations – parameter change, topological change and evolutionary change. We have analysed our system in different perspective of complexity phenomena. We have demonstrated our system as a complex dynamical system, self-organizing system and reaction-diffusion system. We have acquired insights from natural complex systems such as schooling of fish, flocking of birds, synchronization of fireflies, animal coat to understand the pattern formation principles in our system. Our system, with complex or adaptive topological properties, has displayed a dynamical phase transition both in system dynamics and network structures with significant emergent properties exhibiting interesting analogies with the dynamics of social, political and economical systems. We have related daisyworld behaviour to stock market behaviour. With our application of our behaviour study and its relation in sentiment analysis of stock tweets and stock price movement, we have manifested stock market as complex adaptive man-made system exhibiting social homeostasis. We have also explored the psychological and sociological reasons behind such apparent behaviours. We have compared stock market with other super-organism exhibiting social homeostasis – a termite colony. Thus, we have illustrated our system's utility in understanding self-regulating, self-causing and self-designed principles and systems.

7.3 Future Directions

- Further development of daisyworld model include :
  - Introducing one more feedback loop in the topology of the daisyworld system which dampens the growth of hubs and amplifies the growth of smaller nodes. For instance, we can observe this pattern

in citation networks where the first paper in any new area becomes richer and richer (gets more and more references). But after some time, when a review paper is published, researchers start citing to the new review paper.

- Investigating fractal attractors in the dynamics of daisyworld dynamics.

- The potential directions in sentiment analysis of stock market include :
  - Technical analysis of stock market trends using Elliott wave principle [Frost and Prechter, 2005].
  - Fractals and Fibonacci sequence analysis of human mentation for investigating their social mood swings.

The **theory of Universality** emphasises on fractal patterns to explain much of the world around us [Ward, 2002]. Hence, we are interested in exploring daisyworld model and sentiment analysis of stock market tweets based on fractals.

Bibliography

Ackland, G., Gallagher, I., 2004. Stabilization of large generalized lotka-volterra foodwebs by evolutionary feedback. Physical Review Letters 93 (15), 158701. 31

Ackland, G. J., Clark, M. A., Lenton, T. M., 2003. Catastrophic desert formation in daisyworld. Journal of theoretical biology 223 (1), 39–44. 3, 4, 6, 9, 31

Ackland, G. J., Wood, A. J., 2010. Emergent patterns in space and time from daisyworld: a simple evolving coupled biosphere-climate model. Philosophical Transactions of the Royal Society A: Mathematical, Physical and Engineering Sciences 368 (1910), 161. 3, 4, 6, 9, 31, 32

Adams, B., Carr, J., Lenton, T. M., White, A., 2003. One-dimensional daisyworld: spatial interactions and pattern formation. Journal of Theoretical Biology 223 (4), 505–513. 3, 31

Albert, R., Jeong, H., Barabási, A. L., 1999. The diameter of the world wide web. Arxiv preprint cond-mat/9907038. 21

Andersen, M. L., Taylor, H. F., 2007. Sociology: Understanding a diverse society. Wadsworth Publishing Company. 128

Anderson, P. W., et al., 1972. More is different. Science 177 (4047), 393–396. 26

Andrew, A. M., 1996. The challenge of daisyworld. Kybernetes 25 (7/8), 94–99. 31

Ashby, W. R., 1947. Iii.the nervous system as physical machine: With special reference to the origin of adaptive behaviour. Mind 56 (221), 44–59. 17

Ashby, W. R., 1952. Design for a brain. 17

Ashby, W. R., 1962. Principles of the self-organizing system. Principles of Self-organization, 255–278. 45

Asur, S., Huberman, B. A., 2010. Predicting the future with social media. In: Web Intelligence and Intelligent Agent Technology (WI-IAT), 2010 IEEE/WIC/ACM International Conference on. Vol. 1. IEEE, pp. 492–499. 142

Ball, P., 2004. Critical mass: How one thing leads to another. Macmillan. 26, 150

Bandt, C., Pompe, B., 2002. Permutation entropy: A natural complexity measure for time series. Physical Review Letters 88 (17), 174102. 42

Bar-Yam, Y., 2003. Dynamics of complex systems. 1

Barabasi, A.-L., 2003. Linked: How everything is connected to everything else and what it means. 20, 23

Begon, M., Harper, J. L., Townsend, C. R., 1996. Ecology: individuals, populations, and communities. Blackwell. 79

Belousov, B. P., 1958. A periodic reaction and its mechanism. Sbornik Referatov po Radiatsonno Meditsine (Medgiz, Moscow), 145–147 (in Russian). 25

Bénard, H., 1900. Les tourbillons cellulaires dans une nappe liquide. Revue générale des Sciences pures et appliquées 11, 1261–1271 and 1309–1328. 25

Bernard, C., 1878. Leçons sur les phénomènes de la vie commune aux animaux et aux végétaux. Baillière. 17

Bird, S., Klein, E., Loper, E., 2009. Natural language processing with Python. O'reilly. xviii, 143, 144, 147

Boccaletti, S., Latora, V., Moreno, Y., Chavez, M., Hwang, D. U., 2006. Complex networks: structure and dynamics. Physics reports 424 (4), 175–308. 22

Bollen, J., Mao, H., Zeng, X., 2011. Twitter mood predicts the stock market. Journal of Computational Science 2 (1), 1–8. 142

Bollobás, B., 1979. Graph theory, an introductory course. Springer-Verlag, New York, Heidelberg, Berlin. 37

Bollobás, B., 2001. Random graphs. Vol. 73. Cambridge university press. 21, 37

Brännström, Å., Sumpter, D., 2005. Coupled map lattice approximations for spatially explicit individual-based models of ecology. Bulletin of Mathematical Biology 67 (4), 663–682. 37

Brenner, T., 1998. Can evolutionary algorithms describe learning processes? Journal of Evolutionary Economics 8, 271–283. 34

Buchanan, M., 2003. Nexus: small worlds and the groundbreaking theory of networks. WW Norton. 23, 26, 39, 130

Buchanan, M., 2008. The social atom: Why the rich get richer, cheaters get caught, and your neighbor usually looks like you. Bloomsbury Publishing USA. 150

Bürger, R., 1998. Mathematical properties of mutation-selection models. Genetica 102-103, 279–298. 34

Camazine, S., Deneubourg, J.-L., Franks, N. R., Sneyd, J., Theraula, G., Bonabeau, E., 2003. Self-organization in biological systems, 2nd Edition. Princeton University Press. 25, 26, 27

Cannon, W. B., 1929. Organization for physiological homeostasis. Physiological Reviews 9 (3), 399–431. 17

Cao, Y., Tung, W., Gao, J., Protopopescu, V., Hively, L., 2004. Detecting dynamical changes in time series using the permutation entropy. Physical Review-Series E- 70 (4; PART 2), 46217–46217. 43

Capra, F., 1983. The Turning Point: Science, Society, and the Rising Culture. Bantam. 30

Capra, F., 1997. The Web of Life: A New Scientific Understanding of Living Systems. Anchor. 21, 29

Capra, F., 2004. The hidden connections: A science for sustainable living. Random House Digital, Inc. 16

Chang, C., Lin, C., 2001. Libsvm – a library for support vector machines. URL http://www.csie.ntu.edu.tw/~cjlin/libsvm/ 147

Das, S. R., Chen, M. Y., 2007. Yahoo! for amazon: Sentiment extraction from small talk on the web. Management Science 53 (9), 1375–1388. 142

Dawkins, R., 1999. The extended phenotype: The long reach of the gene. Oxford University Press, USA. 73

Dawkins, R., 2006. The selfish gene. Oxford university press. 150

Dewar, R., 2003. Information theory explanation of the fluctuation theorem, maximum entropy production and self-organized criticality in non-equilibrium stationary states. Journal of Physics A: Mathematical and General 36 (3), 631. 31

Dewar, R. C., 2005. Maximum entropy production and the fluctuation theorem. Journal of Physics A: Mathematical and General 38 (21), L371. 31

Dorogovtsev, S. N., Mendes, J. F. F., 2002. Evolution of networks. Advances in physics 51 (4), 1079–1187. 10, 22, 103

Dyke, J., Harvey, I., 2005. Hysteresis and the limits of homeostasis: from daisyworld to phototaxis. In: Advances in Artificial Life. Springer, pp. 241–251. 31

Dyke, J., Harvey, I., 2006. Pushing up the daisies. 18, 31

Ford, F. A., 1999. Modeling the environment: an introduction to system dynamics modeling of environmental systems. Island press. 31

Frost, A. J., Prechter, R. R., 2005. Elliott wave principle: key to market behavior. Elliott Wave International. 139, 157

García-Ojalvo, J., Sancho, J. M., 1999. Noise in spatially extended systems. Springer. 77

Gladwell, M., 2006. The tipping point: How little things can make a big difference. Little, Brown. 129

Goel, P., Ermentrout, B., 2002. Synchrony, stability, and firing patterns in pulse-coupled oscillators. Physica D: Nonlinear Phenomena 163 (3), 191–216. 111

Granovetter, M., 1978. Threshold models of collective behavior. American journal of sociology, 1420–1443. 150

Gross, T., Blasius, B., 2008. Adaptive coevolutionary networks: a review. Journal of the Royal Society Interface 5 (20), 259–271. xi, 10, 24, 25, 118

Gross, T., Sayama, H., 2009. Adaptive networks. Adaptive Networks, 1–8. 10, 25, 118

Gruhl, D., Guha, R., Kumar, R., Novak, J., Tomkins, A., 2005. The predictive power of online chatter. In: Proceedings of the eleventh ACM SIGKDD international conference on Knowledge discovery in data mining. ACM, pp. 78–87. 142

Harding, S., 1999. Food web complexity enhances community stability and climate regulation in a geophysiological model. Tellus B 51 (4), 815–829. 31

Harding, S., 2006. Animate Earth: Science, Intuition and Gaia. Chelsea Green. 29, 30

Harvey, I., 2004. Homeostasis and rein control: From daisyworld to active perception. In: Proceedings of the Ninth International Conference on the Simulation and Synthesis of Living Systems, ALIFE. Vol. 9. pp. 309–314. 31, 32

Hilborn, R. C., 2004. Sea gulls, butterflies, and grasshoppers: A brief history of the butterfly effect in nonlinear dynamics. American Journal of Physics 72, 425. 129

Hofbauer, J., Sigmund, K., 2003. Evolutionary game dynamics. Bulletin of the American Mathematical Society 40 (4), 479 – 519. 73

Hutton, J., Library, E. U., Society, E. G., 1987. The 1785 Abstract of James Hutton's Theory of the Earth. Scottish Academic Press.
URL http://books.google.co.kr/books?id=2WE7AQAAMAAJ 29

Johnson, S., 2012. Emergence: The connected lives of ants, brains, cities, and software. Simon and Schuster. 25, 150, 151

Jrgensen, Sven Erik, ., Fath, B. D., 2010. Global ecology : a derivative of Encyclopedia of ecology / editor-in-chief, Sven Erik Jrgensen ; associate editor-in-chief, Brian D. Fath. Amsterdam ; Boston : Elsevier/Academic Press, "Material in the text originally appeared in the Encyclopedia of ecology, edited by Sven Eric Jrgenson (Elsevier B.V. 2008)"–T.p. verso. 28

Kaneko, K., 1985. Spatiotemporal intermittency in coupled map lattices. Progress of Theoretical Physics 74 (5), 1033–1044. 35

Kaneko, K., Tsuda, I., 2001. Complex systems: chaos and beyond: a constructive approach with applications in life sciences. Springer Verlag. 6

Kaneko, K. *Ed.*, 1993. Theory and Applications of Coupled Map Lattices. John Wiley & Sons. 37

Kendall, D., 2012. Sociology in our times. Wadsworth Publishing Company. 128

Kump, L. R., Kasting, J. F., Crane, R. G., 2010. The Earth System, 3rd Edition. Prentice Hall. 31

Langton, C. G., et al., 1989. Artificial life. Addison-Wesley Publishing Company Redwood City, CA. 19

Lenton, T., Van Oijen, M., 2002. Gaia as a complex adaptive system. Philosophical Transactions of the Royal Society of London. Series B: Biological Sciences 357 (1421), 683. 4, 6, 9

Lenton, T. M., Lovelock, J. E., 2000. Daisyworld is darwinian: constraints on adaptation are important for planetary self-regulation. Journal of Theoretical Biology 206 (1), 109–114. 31, 76

Lenton, T. M., Lovelock, J. E., 2001. Daisyworld revisited: quantifying biological effects on planetary self-regulation. Tellus B 53 (3), 288–305. 31, 76, 80

Lenton, T. M., et al., 1998. Gaia and natural selection. Nature 394 (6692), 439–447. 31, 76

Lorenz, E. N., 1963. Deterministic nonperiodic flow. Journal of the atmospheric sciences 20 (2), 130–141. 20

Lotka, A. J., 1925. Elements of physical biology. Williams & Wilkins Baltimore. 29

Lovelock, J., 1992. A numerical model for biodiversity. Philosophical Transactions of the Royal Society of London. Series B: Biological Sciences 338 (1286), 383. 31, 76, 78

Lovelock, J. E., 1972. Gaia as seen through the atmosphere. Atmos. Environ. 6, 579–580. 3, 5, 29

Macionis, J. J., 2009. Sociology. Prentice Hall. 128

Mackay, C., 2004. Extraordinary popular delusions and the madness of crowds. Barnes & Noble Publishing. 129

Maddock, L., 1991. Effects of simple environmental feedback on some population models. Tellus B 43 (3), 331–337. 49

Malnig, J., 2008. Ballroom, boogie, shimmy sham, shake: a social and popular dance reader. University of Illinois Press. 128

May, R. M., 1976. Simple mathematical models with very complicated dynamics. Nature 261 (5560), 459–467. 2, 33

McGuffie, K., Henderson-Sellers, A., 2005. A climate modelling primer. Vol. 1. Wiley, Chichester, UK. 31, 49

Milgram, S., 1967. The small world problem. Psychology today 2 (1), 60–67. 21

Mirollo, R. E., Strogatz, S. H., 1990. Synchronization of pulse-coupled biological oscillators. SIAM Journal on Applied Mathematics 50 (6), 1645–1662. 111

Mishne, G., Glance, N. S., 2006. Predicting movie sales from blogger sentiment. In: AAAI Spring Symposium: Computational Approaches to Analyzing Weblogs. pp. 155–158. 142

Mitchell, M., 2009. Complexity: a guided tour. Oxford University Press. 1

Mitleton-Kelly, E., 2003. Complex systems and evolutionary perspectives on organisations: the application of complexity theory to organisations. Elsevier Science Ltd. 2

Moran, P. A. P., 1950. Notes on continuous stochastic phenomena. Biometrika 37 (1/2), 17–23. 43

Murray, J. D., 2008. Mathematical Biology II: Spatial models and biomedical applications, 3rd Edition. Vol. 2. Springer. 25, 27

Naess, A., 1973. The shallow and the deep, long-range ecology movement. Inquiry 16, 95–100. 30

Nakao, H., Mikhailov, A. S., 2010. Turing patterns in network-organized activator-inhibitor systems. Nature Physics 6 (7), 544–550. 27

Newman, M. E. J., 2001. The structure of scientific collaboration networks. Proceedings of the National Academy of Sciences 98 (2), 404. 21

Newman, M. E. J., Watts, D. J., 1999. Renormalization group analysis of the small-world network model. Physics Letters A 263 (4-6), 341–346. 9, 22, 103

Nishimori, H., Ouchi, N., 1993. Formation of ripple patterns and dunes by wind-blown sand. Physical Review Letters 71 (1), 197–200. 37

Nofsinger, J. R., 2005. Social mood and financial economics. The Journal of Behavioral Finance 6 (3), 144–160. 142

Nowak, M. A., 2006. Evolutionary dynamics: exploring the equations of life. Belknap Press. 75

Nowak, M. A., Komarova, N. L., Niyogi, P., 2001. Evolution of universal grammar. Science 291 (5501), 114. 34

Odling-Smee, F. J., Laland, K. N., Feldman, M. W., 2003. Niche Construction: the Neglected Process in Evolution. Vol. 37 of Monographs in Population Biology. Princeton Univ. Press. 73

Olfati-Saber, R., 2007. Evolutionary dynamics of behavior in social networks. In: Decision and Control, 2007 46th IEEE Conference on. Ieee, pp. 4051–4056. 34

Ozawa, H., Ohmura, A., Lorenz, R. D., Pujol, T., 2003. The second law of thermodynamics and the global climate system: a review of the maximum entropy production principle. Reviews of Geophysics 41 (4), 1018. 31

Page, K. M., Nowak, M. A., 2002. Unifying evolutionary dynamics. Journal of theoretical biology 219 (1), 93–98. 78

Pang, B., Lee, L., 2008. Opinion mining and sentiment analysis. Foundations and trends in information retrieval 2 (1-2), 1–135. 142

Perera, L., Russell, J. R., Provan, J., Powell, W., 2000. Use of microsatellite DNA markers to investigate the level of genetic diversity and population genetic structure of coconut (*Cocos nucifera* L.). Genome 43 (1), 15–21. 9

Prigogine, I., 1997. The end of certainty. SimonandSchuster. com. 2

Prigogine, I., Stengers, I., Pagels, H. R., 1985. Order out of chaos. Physics Today 38, 97. 19

Punithan, D., Kim, D. K., McKay, R. I., 2011. Daisyworld in two dimensional small-world networks. Database Theory and Application, Bio-Science and Bio-Technology, 167–178. 10, 118

Punithan, D., Kim, D. K., McKay, R. I., 2012. Spatio-temporal dynamics and quantification of daisyworld in two-dimensional coupled map lattices. Ecological Complexity, 43–57. 7, 8, 9

Punithan, D., McKay, B., 2013a. Collective dynamics and homeostatic emergence in complex adaptive ecosystem. In: Advances in Artificial Life, ECAL. Vol. 12. pp. 332–339. 11

Punithan, D., McKay, R., 2012a. Evolutionary dynamics and ecosystems feedback in two dimensional daisyworld. In: Artificial Life. Vol. 13. pp. 91–98. 9

Punithan, D., McKay, R. I., 2012b. Self-organizing spatio-temporal pattern formation in two-dimensional daisyworld. Self-Organizing Systems, 72–83. 8, 80

Punithan, D., McKay, R. I., 2013b. Phase transitions in two-dimensional daisyworld with small-world effects: A study of local and long-range couplings. Future Generation Computer Systems. 10, 39, 118, 122

Rogers, E. M., 2010. Diffusion of innovations. Simon and Schuster. 150

Saunders, P. T., Koeslag, J. H., Wessels, J. A., 1998. Integral rein control in physiology. Journal of theoretical biology 194 (2), 163–173. 31, 32

Saunders, P. T., Koeslag, J. H., Wessels, J. A., 2000. Integral rein control in physiology ii: a general model. Journal of theoretical biology 206 (2), 211–220. 31, 32

Simon, H. A., 1957. Models of man; social and rational. 139

Smith, A., 2008. The Invisible Hand. Great ideas. Penguin Adult. URL http://books.google.co.kr/books?id=qBgAb0EsQv8C 140

Strogatz, S., 2001. Nonlinear dynamics and chaos: with applications to physics, biology, chemistry and engineering. Perseus Books Group. 20

Strogatz, S. H., 2003. Sync: The emerging science of spontaneous order. Hyperion. 19

Surowiecki, J., 2005. The wisdom of crowds. Random House Digital, Inc. 151

Taleb, N. N., 2010. The black swan: The impact of the highly improbable. Random House Trade Paperbacks. 129

Tregonning, K., Roberts, A., 1979. Complex systems which evolve towards homeostasis. 2

Turing, A. M., 1952. The chemical basis of morphogenesis. Philosophical Transactions of the Royal Society of London. Series B, Biological Sciences 237 (641), 37–72. 8, 25, 27

Turner, J. S., 2009a. The extended organism: the physiology of animal-built structures. Harvard University Press. 18

Turner, J. S., 2009b. The tinkerer's accomplice: how design emerges from life itself. Harvard University Press. 18

Vernadski, V. I., McMenamin, M. A., 1998. The Biosphere. A Peter N. Nevraumont book. Copernicus.
URL http://books.google.co.kr/books?id=nUWsbRh5c7cC 29

Von Bertalanffy, L., 1968. General system theory: Foundations, development, applications. George Braziller New York. 2, 14

von Bloh, W., Block, A., Schellnhuber, H. J., 1997. Self-stabilization of the biosphere under global change: a tutorial geophysiological approach. Tellus B 49 (3), 249–262. 3, 4, 6, 7, 9, 31, 55

Walsh, T., 1999. Search in a small world. In: International Joint Conference on Artificial Intelligence. Vol. 16. Lawrence Erlbaum Associates Ltd, pp. 1172–1177. 39

Ward, M., 2002. Beyond chaos: The underlying theory behind life, the universe, and everything. Thomas Dunne Books. 157

Watson, A. J., Lovelock, J. E., 1983. Biological homeostasis of the global environment: the parable of daisyworld. Tellus B 35 (4), 284–289. 3, 7, 29, 45, 55, 75

Watts, D. J., 1999. Networks, dynamics, and the small-world phenomenon. American Journal of Sociology 105 (2), 493–527. 39, 40

Watts, D. J., 2003. Small worlds: the dynamics of networks between order and randomness. Princeton University Press, Princeton, NJ, USA. 40

Watts, D. J., 2004. Six degrees: The science of a connected age. WW Norton & Company. 24, 130

Watts, D. J., Strogatz, S. H., 1998. Collective dynamics of small-world networks. Nature 393 (6684), 440–442. 9, 21, 38, 103, 122

White, C., Selkoe, K. A., Watson, J., Siegel, D. A., Zacherl, D. C., Toonen, R. J., 2010. Ocean currents help explain population genetic structure. Proceedings of the Royal Society B: Biological Sciences 277 (1688), 1685. 9

Wilkinson, D. M., 2003. The fundamental processes in ecology: a thought experiment on extraterrestrial biospheres. Biological Reviews 78 (2), 171–179. 31

Wood, A. J., Ackland, G. J., Dyke, J. G., Williams, H. T. P., Lenton, T. M., 2008. Daisyworld: a review. Reviews of Geophysics 46 (1). 32, 45, 51, 76, 100, 118

Wright, D., Meadows, D. H., 2012. Thinking in systems: a primer. Routledge. 14

Yanagita, T., Kaneko, K., 1993. Coupled map lattice model for convection. Physics Letters A 175 (6), 415–420. 37

Yanagita, T., Kaneko, K., 1997. Modeling and characterization of cloud dynamics. Physical Review Letters 78 (22), 4297–4300. 37

Acknowledgements

First of all, I am extremely thankful to my supervisor Prof. Robert Ian Mckay for offering me the opportunity to pursue PhD. at Structural Complexity Lab. I am very greatly indebted to him for giving me the freedom to engage in research which has changed the way I look at the world. I also extend my sincere thanks to Prof. Byoung-Tak Zhang and Prof. Akira Namatame for their advice.

I would like to acknowledge the support provided by Basic Science Research Program of the National Research Foundation of Korea (NRF), Brain Korea 21 (BK21) program of Ministry of Education, Science and Technology (MEST), the Institute for Computer Technology (ICT) at Seoul National Univ. and the scholarship provided by the Computer Science Dept. of Seoul National Univ. I also would like to thank Ilun Science and Technology Foundation for their generous support especially the CEO of JUSUNG Engineering Co.,Ltd., Mr. Sang-Hoon Jung and Mr. An Sung-Moo.

A very special thanks to Dr. Kim MinHyeok for all his extremely wonderful support during my research period. I thank Dr. Kim Dong-Kyun for his mentorship during the initial phase of my research. I thank Dr. Lee Yun-Geun for informing about Ilun scholarship. I thank Dr. Kim Kang Il for his unique friendship.

I gratefully acknowledge all my other colleagues at SC lab Mr. Cho Hanggjun, Mr. Noh Junhyug, Mr. Shin Haisoo, Mr. Song Jinho, Mr. Hong Changwan, Mr. Kim Juho, Mr. Hong Won Wook, Mr. Park Namyong, Mr. Oh In Soo and Mr. Pham Minh Tuan for their kindness and assistance.

creative commons
COMMONS DEED

저작자표시-비영리-동일조건변경허락 2.0 대한민국

이용자는 아래의 조건을 따르는 경우에 한하여 자유롭게

- 이 저작물을 복제, 배포, 전송, 전시, 공연 및 방송할 수 있습니다.
- 이차적 저작물을 작성할 수 있습니다.

다음과 같은 조건을 따라야 합니다:

저작자표시. 귀하는 원저작자를 표시하여야 합니다.

비영리. 귀하는 이 저작물을 영리 목적으로 이용할 수 없습니다.

동일조건변경허락. 귀하가 이 저작물을 개작, 변형 또는 가공했을 경우에는, 이 저작물과 동일한 이용허락조건하에서만 배포할 수 있습니다.

- 귀하는, 이 저작물의 재이용이나 배포의 경우, 이 저작물에 적용된 이용허락조건을 명확하게 나타내어야 합니다.
- 저작권자로부터 별도의 허가를 받으면 이러한 조건들은 적용되지 않습니다.

저작권법에 따른 이용자의 권리는 위의 내용에 의하여 영향을 받지 않습니다.

이것은 이용허락규약(Legal Code)을 이해하기 쉽게 요약한 것입니다.

Disclaimer

dCollection

Coupled Map Lattice based Homeostatic Complex Systems

Dharani Punithan
Department of Computer Science & Engineering
Seoul National University

A thesis submitted for the degree of
Doctor of Philosophy
February, 2014

Abstract

Homeostasis is the ability to regulate the essential variables of a complex system within a viability zone in the face of perturbations. It is a core complexity phenomenon for understanding real or artificial life. In this thesis, we explore the interplay between nonlinear system dynamics and complex topologies in such homeostatic (self-regulating) systems.

We investigate the self-causing nature of homeostasis in artificial and real-world complex systems. We analyse planetary and ecological homeostasis using daisyworld system – a cybernetic proof of Gaia hypothesis and apply those principles to demonstrate the social homeostasis in stock market. We reconstruct the formulations of the original daisyworld based on Coupled Map Lattice (CML) which enable us to investigate a wide range of rich features of complex systems covering different arenas such as system science, nonlinear science and network science.

Our study reveals that daisyworld is a self-oganizing system and a reaction-diffusion (activator-inhibitor) system exhibiting an array of fascinating pattern formations – complex patterns, Turing-like structures, cyclic patterns, random patterns and uniform dispersed patterns for different parameter settings. The phenomenon governing the self-organizing pattern formation in our system is observed in biological systems (schooling of fish, animal coat formation, etc.) as well as in non-living systems (Turing's reaction-diffusion system, Belousov-Zhabotinsky reaction, Bénard convection, etc.).

We incorporate evolutionary interactions in our system via replicator-mutator mechanisms. The results underline the importance of balance between ecosystem feedback and ecosystem disturbance in

generating spatially coexistence of domains of dominance among the original daisies and their mutants and adaptants.

We inspect our system based on small-world graphs (complex topologies) embodying realistic couplings via the Watts-Strogatz (WS), Newman-Watts models and Smallest-world (SW) models. We examine our system on an adaptive topology (adding connections with more realistic mechanisms) where there exists a feedback between the local dynamics and the topology. We introduce scale-freeness into our system with high clustering.

We thus perturb our system through system parameters, system topologies and evolutionary changes. In all scenarios, our system self-regulates the environment and thus life persists, and thereby demonstrating robustness. We also introduce metrics Moran's I and permutation entropy to measure the spatio-temporal dynamics of the system.

Our remarkable finding is that by applying the dynamical linking mechanisms to our system on regular lattice can self-organise to a lattice with small-world phenomenon. We observe 'completely coherent (homogeneous) short-lived cyclical dominance' even with a small fraction of long-range couplings in complex and adaptive topologies. This apparent behaviour is seen in social, political and economical realms.

Our system yields profound insights and implications, from which we derive an analogy with stock market. Based on an "Ecosystem Approach", we analyse the feedback between market sentiment and stock price. We collect $\$APPL$ tweets from twitter and stock data from Yahoo finance and demonstrate their homeostatic nature. We compare stock market with other social homeostatic systems in nature such as termite colonies. Thus our study on self-causing systems helps both in understanding existing self-regulating systems and in modelling new artificial homeostatic system.

Keywords: complex systems, system thinking,
nonlinear thinking, network thinking,
collective dynamics, pattern formation,
self-organization, emergence,
reaction-diffusion system,
Turing instabilities, activator-inhibitor system,
Moore neighbourhood, Laplacian diffusion,
logistic growth model (Verhulst model),
chaos, bifurcation, attractors,
Coupled Map Lattice (CML),
Gaia hypothesis, daisyworld,
homeostasis, cybernetics, feedbacks,
graph theory,
small-world network, small-world phenomena,
Watts-Strogatz, Newman-Watts, Smallest-world,
adaptive network, scale-free network,
degree distribution, Poisson distribution,
power law distribution, long-fat-tail distribution,
clustering coefficient, characteristic path length,
proximity ratio,
phase transition and critical phenomenon,
Moran's I, permutation entropy,
replicator-mutator mechanisms,
sentiment analysis, machine learning,
Naive Bayes, Support Vector Machine,
Granger causality,
Engle–Granger two-step method,
Phillips–Ouliaris cointegration test

Student Number: 2008-30708

Contents

Contents v

List of Figures xi

List of Tables xix

1 Introduction 1

1.1 Homeostatic Complex Systems 2
1.2 Daisyworld 3
1.3 Limitations of Daisyworld Models 4
1.4 Motivation 4
1.5 Inspirations from Nature 5
1.6 Contribution 5
1.6.1 Incorporation of Complex Spatio-temporal Dynamics . . 6
1.6.2 Demonstration as Complex Systems 7
1.6.3 Incorporation of Evolutionary Mechanisms 8
1.6.4 Introduction of Spatio-temporal Quantification 9
1.6.5 Incorporation of Complex and Adaptive Topological Properties 9
1.6.6 Applications (Demonstration of Social Homeostasis in Stock Market) 11
1.7 Outline 11

2 Background **13**

2.1 Complexity Science : A Means to Understanding Complex Systems . . . 13

2.1.1 Systems Thinking . . . 14

2.1.2 Nonlinear Thinking . . . 19

2.1.3 Network Thinking . . . 20

2.1.4 Collective Behaviour . . . 25

2.1.5 Pattern Formation . . . 26

2.2 Modelling Tools . . . 28

2.2.1 Daisyworld Model (Life-Environment Bidirectional Feedback Model) . . . 28

2.2.2 Logistic Growth Model (Verhulst Model) . . . 32

2.2.3 Replicator Mutator Model . . . 34

2.2.4 Neighbourhood Models . . . 34

2.2.5 Diffusion Models . . . 35

2.2.6 Spatio-temporal Model – Coupled Map Lattice (CML) . . . 35

2.2.7 Graph (Network) Models . . . 37

2.3 Quantification of Spatio-Temporal Dynamics . . . 42

2.3.1 Permutation Entropy (PE): . . . 42

2.3.2 Moran's I (MI): . . . 43

3 Homeostatic Complex System based on Daisyworld Modelling **45**

3.1 Reconstructed Core Daisyworld Model . . . 46

3.1.1 Solar Insolation . . . 50

3.1.2 Albedo . . . 50

3.1.3 Growth . . . 50

3.1.4 Temperature . . . 51

3.1.5 Population Size . . . 51

3.2 Limiting Similarity (Temperature Overlap) . . . 52

3.3 Incorporation of Complex Topological Properties . . . 54

3.4 Experimental Setup . . . 55

3.4.1 Parameter Settings . . . 55

3.4.2 Initializations . . . 56
3.4.3 Visualisations . . . 56

4 Daisyworld with Local Couplings 57
4.1 Self-Organizing Spatio-temporal Patterns . . . 57
4.1.1 Variable Parameter Settings . . . 58
4.1.2 Self-organized Complex Pattern . . . 58
4.1.3 Turing-like Structure . . . 59
4.1.4 Cyclical Pattern . . . 60
4.1.5 Random Pattern . . . 61
4.1.6 Dispersed Pattern . . . 62
4.1.7 Discussion . . . 62
4.1.8 Summary . . . 65
4.2 Locally Chaotic and Globally Stable Dynamics (Temporal Fluctuations and Spatial Stability) . . . 67
4.2.1 Spatial Stability . . . 70
4.2.2 Temporal Fluctuations . . . 71
4.2.3 Summary . . . 72
4.3 Homeostasis with Evolutionary Dynamics . . . 73
4.3.1 Modification to Core Model . . . 77
4.3.2 Variable Parameter Settings . . . 80
4.3.3 Baseline Scenario: No Mutation . . . 81
4.3.4 Phenotypic Variability – Mutation . . . 85
4.3.5 Adaptation – Exploring New Environments . . . 90
4.3.6 Summary . . . 94
4.4 Quantification of the Daisyworld Model . . . 95
4.4.1 Statistical Measures and Spatio-Temporal Dynamics . . . 95
4.4.2 Parameter Space Analysis of the Daisyworld Model . . . 97

5 Daisyworld with Complex Couplings 99
5.1 Variable Parameter Settings . . . 99
5.2 Benchmark Graph Models . . . 100

5.2.1 Degree Distribution of Benchmark Models 100
5.2.2 Regular Graph 101
5.2.3 Random Graph 102
5.2.4 Fully Connected Graph 102
5.3 Small-world Phenomenon 103
5.3.1 Indentifying the Small-world Regime 105
5.3.2 Degree Distribution of Small-world Models 105
5.3.3 Daisyworld with Static Local and Non-local Couplings . 107
5.3.4 Possible Critical Point of Phase Change 111
5.3.5 Topology and Criticality 113
5.3.6 Without Life-Environment Feedback 116
5.3.7 Summary 117
5.4 Adaptive Couplings 118
5.4.1 Daisyworld with Dynamic Local and Non-local Couplings 119
5.4.2 Topological Properties of NW-CML and Adaptive CML 120
5.4.3 Topological Evolution 122
5.4.4 Summary 125
5.5 Scale-freeness 125
5.5.1 Degree Distribution of Scale-free Graph 126
5.5.2 Daisyworld with Hubs 126
5.5.3 Summary 127
5.6 Behaviour Study 127
5.6.1 Daisyworld Behaviour in Complex and Adaptive Topologies 127
5.6.2 Social Collective Behaviour 128
5.6.3 Analogies with Popular Metaphors 129
5.6.4 A Comparative Study 129

6 Applications – Demonstration of Social Homeostasis in Stock Market 139
6.1 Introduction 139
6.2 Daisyworld - Stock Market Analogy 140

6.2.1 Daisyworld Behaviour . . . 141
6.2.2 Stock Market Behaviour . . . 141
6.2.3 Comparison of Behaviours – An Ecosystem Approach . 142
6.3 Background . . . 142
6.3.1 Sentiment Analysis and Microblogging Services . . . 142
6.3.2 Supervised Classification . . . 143
6.3.3 Twitter API . . . 145
6.4 Sentiment Analysis on Apple ($*AAPL*) Stock Market Tweets . 145
6.4.1 Data Collection . . . 145
6.4.2 Tweet Text Pre-Processing . . . 146
6.4.3 Training the Classifier . . . 147
6.4.4 Sentiment Score . . . 148
6.5 Demonstration of Social Homeostasis . . . 148
6.6 Discussion . . . 149
6.6.1 Social Mood Trends - A Psychological Perspective . . . 149
6.6.2 Stock Market - A Termite Colony . . . 150
6.7 Summary . . . 151

7 Conclusion **153**
7.1 Summary . . . 153
7.2 Conclusion . . . 156
7.3 Future Directions . . . 156

Bibliography **159**

List of Figures

2.1 Linear Cause-and-Effect : A system consisting of components A, B and C 14

2.2 Circular Cause-and-Effect : A system consisting of components A, B and C 14

2.3 System with Feedback Mechanisms 15

2.4 Reinforcing Process 15

2.5 Balancing Process 15

2.6 Adaptive Network (Source : [Gross and Blasius, 2008]) 24

2.7 Neighbourhood Models 34

3.1 Overlap of Growth Curves of Black and White Daisies 53

4.1 Maze like Organization for 10% Overlap, $D_c = 0.001$, $D = 0.2$, $r = 1$ and NL= 0.001 in 2D 100×100 Lattice 59

4.2 Local Dynamics of Maze : 10% Overlap, $D_c = 0.001$, $D = 0.2$, $r = 1$ and NL= 0.001 in 2D 100×100 Lattice 60

4.3 Global Dynamics of Maze : 10% Overlap, $D_c = 0.001$, $D = 0.2$, $r = 1$ and NL= 0.001 in 2D 100×100 Lattice 61

4.4 Turing-like Structure for 100% Overlap, $D_c = 0.01$, $D = 0.2$, $r = 1$, $NL = 1$ in 2D 100×100 Lattice 62

4.5 Local Dynamics of Turing-like Structure : 100% Overlap, $D_c = 0.01$, $D = 0.2$, $r = 1$ and NL= 1 in 2D 100×100 Lattice 63

4.6 Global Dynamics of Turing-like Structure : 100% Overlap, $D_c = 0.01$, $D = 0.2$, $r = 1$ and NL= 1 in 2D 100×100 Lattice 64
4.7 Cyclical Pattern : 10% overlap, $D_c = 0.2$, $D = 0.2$, $r = 1$ and NL= 0.05 in 2D 100×100 Lattice 65
4.8 Local Dynamics of Cyclical Pattern : 10% overlap, $D_c = 0.2$, $D = 0.2$, $r = 1$ and NL= 0.05 in 2D 100×100 Lattice 66
4.9 Global Dynamics of Cyclical Pattern : 10% overlap, $D_c = 0.2$, $D = 0.2$, $r = 1$ and NL= 0.05 in 2D 100×100 Lattice 67
4.10 Random Pattern : 10% Overlap, $D_c = 0$, $D = 0.2$, $r = 1$ and $NL = 0.01$ in 2D 100×100 Lattice 68
4.11 Local Dynamics of Random Pattern : 10% Overlap, $D_c = 0$, $D = 0.2$, $r = 1$ and $NL = 0.01$ in 2D 100×100 Lattice 69
4.12 Global Dynamics of Random Pattern : 10% Overlap, $D_c = 0$, $D = 0.2$, $r = 1$ and $NL = 0.01$ in 2D 100×100 Lattice 70
4.13 Uniformly Dispersed Pattern : Overlap=10%, $D_c = 0$, $D = 0.2$, $r = 1$ and $NL = 0.5$ in 2D 100×100 Lattice 71
4.14 Local Dynamics of Uniformly Dispersed Pattern : 10% Overlap, $D_c = 0$, $D = 0.2$, $r = 1$ and $NL = 0.5$ in 2D 100×100 Lattice . 72
4.15 Global Dynamics of Uniformly Dispersed Pattern : 10% Overlap, $D_c = 0$, $D = 0.2$, $r = 1$ and $NL = 0.5$ in 2D 100×100 Lattice 73
4.16 Bifurcation Diagram of Daisyworld – Black Daisy Population . 74
4.17 Bifurcation Diagram of Daisyworld – White Daisy Population . 74
4.18 Population Dynamics in 100×100 2D CML with 10% Overlap, $D_c = 0.01$, $D = 0.2$, $r = 1$ and $NL = 1$ 75
4.19 Global Dynamics of Daisyworld in 100×100 2D CML with 10% Overlap, $D_c = 0.01$, $D = 0.2$, $r = 1$ and $NL = 1$ 76
4.20 Local Dynamics at a specific location (row 54 and column 54) with 10% Overlap, $D_c = 0.01$, $D = 0.2$, $r = 1$ and $NL = 1$ . . . 77
4.21 Cobweb Plot of Local Dynamics at a specific location (row 54 and column 54) with $D_c = 0.01$, $D = 0.2$, $r = 1$ and $NL = 1$ over 5000 Steps 77

4.22 Population abundance without mutation : $D_c = 0.2$, $D = 0.2$, $r = 1$ and $NL = 0.05$ 81
4.23 Local dynamics at habitat (55, 41) without mutation and $NL = 0.05$ 82
4.24 Global dynamics without mutation, $NL = 0.05$ 82
4.25 Population abundance without mutation : $D_c = 0.2$, $D = 0.2$, $r = 1$ and $NL = 3$ 82
4.26 Local dynamics at habitat (55, 50) without mutation, $NL = 3$. 83
4.27 Global dynamics without mutation, $NL = 3$ 83
4.28 Population abundance without mutation : $D_c = 0.2$, $D = 0.2$, $r = 1$ and $NL = 5$ 83
4.29 Local dynamics at habitat (56, 50) without mutation, $NL = 5$. 84
4.30 Global dynamics without mutation, $NL = 5$ 84
4.31 Population abundance with Grey daisies : $D_c = 0.2$, $D = 0.2$, $r = 1$ and $NL = 0.05$ 85
4.32 Local dynamics at habitat (57, 49) with Grey and $NL = 0.05$. 86
4.33 Global dynamics with Grey, $NL = 0.05$ 86
4.34 Population abundance with Grey daisies : $D_c = 0.2$, $D = 0.2$, $r = 1$ and $NL = 2$ 87
4.35 Local dynamics at habitat (54, 43) with Grey and $NL = 2$ . . . 87
4.36 Global dynamics with Grey, $NL = 2$ 88
4.37 Population abundance with Grey daisies : $D_c = 0.2$, $D = 0.2$, $r = 1$ and $NL = 3$ 88
4.38 Local dynamics at habitat (51, 53) with Grey and $NL = 3$ . . . 89
4.39 Global dynamics with Grey, $NL = 3$ 89
4.40 Population abundance without feedback : $D_c = 0.2$, $D = 0.2$ and $r = 1$ at epoch 5000 90
4.41 Population abundance with Warm Black and Cool White daisies : $D_c = 0.2$, $D = 0.2$, $r = 1$ and $NL = 0.05$ 91
4.42 Local dynamics at habitat (51, 50) with Warm Black and Cool White, $NL = 0.05$ 92
4.43 Global dynamics with Warm Black and Cool White, $NL = 0.05$ 92

4.44 Population abundance with Warm Black and Cool White daisies : $D_c = 0.2$, $D = 0.2$, $r = 1$ and $NL = 2$ 92
4.45 Local dynamics at habitat (57, 55) with Warm Black and Cool White, $NL = 2$ 93
4.46 Global dynamics with Warm Black and Cool White, $NL = 2$. 93
4.47 Population abundance with Warm Black and Cool White daisies : $D_c = 0.2$, $D = 0.2$, $r = 1$ and $NL = 3$ 94
4.48 Local dynamics at habitat (52, 61) with Warm Black and Cool White, $NL = 3$ 94
4.49 Global dynamics with Warm Black and Cool White, $NL = 3$. 95
4.50 Moran's I (section 4.2) 96
4.51 Moran's I and PE on 100×100 2D CML with 10% overlap and $r = 1$ 98

5.1 2-lattice Benchmark Models (with $k = 8$ except for fully-connected graph). We omit periodic boundary conditions for clarity, and also show some connections superimposed.
(a) Regular graph ($p = 0$) (b) Random graph ($p = 1$) (c) Fully-connected graph 101
5.2 Degree Distribution of Benchmark Models 101
5.3 Regular CML ($p = 0$) : Overlap=10%, $D_c = 0.2$, $D = 0.2$, $r = 1$ and $NL = 0.001$ in 2D 100×100 102
5.4 Random Lattice($p = 1$) : Overlap=10%, $D_c = 0.2$, $D = 0.2$, $r = 1$ and $NL = 0.001$ in 2D 100×100 103
5.5 Fully Connected Lattice : Overlap=10%, $D_c = 0.2$, $D = 0.2$, $r = 1$ and $NL = 0.001$ in 2D 100×100 103
5.6 2-lattice Small-world Models
(a) Watts-Strogatz (WS) ($p = 0.05$) (b) Newman-Watts (NW) ($p = 0.05$) (c) Smallest World (SW) ($p = 0.05$) 104
5.7 Watts-Strogatz model in 2D 100×100 lattice: Clustering Coefficient, Characteristic Path Length and Proximity Ratio . . . 106

5.8 Newman-Watts model in 2D 100×100 lattice: Clustering Coefficient, Characteristic Path Length and Proximity Ratio . . . 106
5.9 Smallest World model in 2D 100×100 lattice: Clustering Coefficient, Characteristic Path Length and Proximity Ratio . . . 107
5.10 Degree Distribution of Small-world Models . . . 107
5.11 Watts-Strogatz Model ($p = 0.05$) : Overlap=10%, $D_c = 0.2$, $D = 0.2$, $r = 1$ and $NL = 0.001$ in 2D 100×100 Small-world Lattice . . . 108
5.12 Newman-Watts ($p = 0.05$) : Overlap=10%, $D_c = 0.2$, $D = 0.2$, $r = 1$ and $NL = 0.001$ in 2D 100×100 Small-world CML . . . 109
5.13 Smallest-World Model ($p = 0.05$) : Overlap=10%, $D_c = 0.2$, $D = 0.2$, $r = 1$ and $NL = 0.001$ in 2D 100×100 Small-world Lattice . . . 109
5.14 WS close to phase change : Overlap=10%, $D_c = 0.2$, $D = 0.2$, $r = 1$ and $NL = 0.001$ in 2D 100×100 Small-world Lattice ($p = 0.01$) . . . 112
5.15 NW close to phase change : Overlap=10%, $D_c = 0.2$, $D = 0.2$, $r = 1$ and $NL = 0.001$ in 2D 100×100 Small-world Lattice ($p = 0.01$) . . . 112
5.16 SW close to phase change : Overlap=10%, $D_c = 0.2$, $D = 0.2$, $r = 1$ and $NL = 0.001$ in 2D 100×100 Small-world Lattice at epoch $5,000$ . . . 112
5.17 Regular without life-environment feedback: $p = 0$, $D = 0.2$ and $NL = 0.001$ in 2D 100×100 . . . 116
5.18 WS without life-environment feedback: $D = 0.2$ and $NL = 0.001$ in 2D 100×100 Small-world Lattice ($p = 0.05$) . . . 116
5.19 NW without life-environment feedback: $D = 0.2$ and $NL = 0.001$ in 2D 100×100 Small-world Lattice ($p = 0.05$) . . . 116
5.20 SW without life-environment feedback: $D = 0.2$ and $NL = 0.001$ in 2D 100×100 Small-world Lattice ($p = 0.05$) . . . 117
5.21 Adapted Reciprocal Couplings . . . 119

5.22 Adaptive CML : Overlap=10%, $D_c = 0.2$, $D = 0.2$, $r = 1$ and $NL = 0.001$ in 2D 100×100 120
5.23 Degree Distribution 121
5.24 Adapted Reciprocal Couplings 122
5.25 Degree Distribution 123
5.26 Global Temperature dynamics : Overlap=10%, $D_c = 0.2$, $D = 0.2$, $r = 1$ and $NL = 0.001$ 123
5.27 Quick Adaptation : Overlap=10%, $D_c = 0.2$, $D = 0.2$, $r = 1$ and $NL = 0.001$ in 2D 100×100 124
5.28 Slow Adaptation : Overlap=10%, $D_c = 0.2$, $D = 0.2$, $r = 1$ and and $NL = 0.001$ in 2D 100×100 124
5.29 Scale-free Graph 125
5.30 Scale-free Degree Distribution 126
5.31 $D = 0.2$ and $NL = 0.001$ in 2D 100×100 Scale-free CML . . . 126
5.32 Regular CML : Temperature dynamics; $p = 0$, Overlap=10%, $D_c = 0.2$, $D = 0.2$, $r = 1$ and $NL = 0.001$ in 2D 100×100 . . . 131
5.33 Regular CML: Local population dynamics at habitat (57, 50); $p = 0$, Overlap=10%, $D_c = 0.2$, $D = 0.2$, $r = 1$ and $NL = 0.001$ in 2D 100×100 131
5.34 Regular CML : Global population dynamics; $p = 0$, Overlap=10%, $D_c = 0.2$, $D = 0.2$, $r = 1$ and $NL = 0.001$ in 2D 100×100 . . . 131
5.35 Random Lattice: Temperature dynamics; $p = 1$, Overlap=10%, $D_c = 0.2$, $D = 0.2$, $r = 1$ and $NL = 0.001$ in 2D 100×100 . . . 132
5.36 Random Lattice: Local population dynamics at habitat (53, 53); $p = 1$, Overlap=10%, $D_c = 0.2$, $D = 0.2$, $r = 1$ and $NL = 0.001$ in 2D 100×100 132
5.37 Random Lattice: Global population dynamics; $p = 1$, Overlap=10%, $D_c = 0.2$, $D = 0.2$, $r = 1$ and $NL = 0.001$ in 2D 100×100 . . . 132
5.38 Fully Connected Lattice: Temperature dynamics; Overlap=10%, $D_c = 0.2$, $D = 0.2$, $r = 1$ and $NL = 0.001$ in 2D 100×100 . . . 133

5.39 Fully Connected Lattice: Local population dynamics at habitat (50, 46); Overlap=10%, $D_c = 0.2$, $D = 0.2$, $r = 1$ and $NL = 0.001$ in 2D 100×100 133

5.40 Fully Connected Lattice: Global population dynamics; Overlap=10%, $D_c = 0.2$, $D = 0.2$, $r = 1$ and $NL = 0.001$ in 2D 100×100 . . . 133

5.41 Watts-Strogatz Model ($p = 0.05$): Temperature dynamics; Overlap=10%, $D_c = 0.2$, $D = 0.2$, $r = 1$ and $NL = 0.001$ in 2D 100×100 . . . 134

5.42 Watts-Strogatz Model ($p = 0.05$): Local population dynamics at habitat (53, 62); Overlap=10%, $D_c = 0.2$, $D = 0.2$, $r = 1$ and $NL = 0.001$ in 2D 100×100 134

5.43 Watts-Strogatz Model ($p = 0.05$): Global population dynamics; Overlap=10%, $D_c = 0.2$, $D = 0.2$, $r = 1$ and $NL = 0.001$ in 2D 100×100 134

5.44 Newman-Watts CML ($p = 0.05$): Temperature dynamics; Overlap=10%, $D_c = 0.2$, $D = 0.2$, $r = 1$ and $NL = 0.001$ in 2D 100×100 . . . 135

5.45 Newman-Watts CML ($p = 0.05$): Local population dynamics at habitat (52, 58); Overlap=10%, $D_c = 0.2$, $D = 0.2$, $r = 1$ and $NL = 0.001$ in 2D 100×100 135

5.46 Newman-Watts CML ($p = 0.05$): Global population dynamics; Overlap=10%, $D_c = 0.2$, $D = 0.2$, $r = 1$ and $NL = 0.001$ in 2D 100×100 135

5.47 Smallest-World Model ($p = 0.05$): Temperature dynamics; Overlap=10%, $D_c = 0.2$, $D = 0.2$, $r = 1$ and $NL = 0.001$ in 2D 100×100 . . . 136

5.48 Smallest-World Model ($p = 0.05$): Local population dynamics at habitat (54, 44); Overlap=10%, $D_c = 0.2$, $D = 0.2$, $r = 1$ and $NL = 0.001$ in 2D 100×100 136

5.49 Smallest-World Model ($p = 0.05$): Global population dynamics; Overlap=10%, $D_c = 0.2$, $D = 0.2$, $r = 1$ and $NL = 0.001$ in 2D 100×100 136

5.50 Adaptive CML: Temperature dynamics; Overlap=10%, $D_c = 0.2$, $D = 0.2$, $r = 1$ and $NL = 0.001$ in 2D 100×100 137

5.51 Adaptive CML: Local population dynamics at habitat (56, 57); Overlap=10%, $D_c = 0.2$, $D = 0.2$, $r = 1$ and $NL = 0.001$ in 2D 100×100 137
5.52 Adaptive CML: Global population dynamics; Overlap=10%, $D_c = 0.2$, $D = 0.2$, $r = 1$ and $NL = 0.001$ in 2D 100×100 . . . 137
5.53 Scale-free CML ($p = 0.05$): Temperature dynamics; Overlap=10%, $D_c = 0.2$, $D = 0.2$, $r = 1$ and $NL = 0.001$ in 2D 100×100 . . . 138
5.54 Scale-free CML ($p = 0.05$): Local population dynamics at habitat (52, 58); Overlap=10%, $D_c = 0.2$, $D = 0.2$, $r = 1$ and $NL = 0.001$ in 2D 100×100 138
5.55 Scale-free CML ($p = 0.05$): Global population dynamics; Overlap=10%, $D_c = 0.2$, $D = 0.2$, $r = 1$ and $NL = 0.001$ in 2D 100×100 . . . 138

6.1 Self-causing Feedback in Daisyworld 140
6.2 Self-causing Feedback in Stock Market 140
6.3 Supervised Classification (Source : [Bird et al., 2009]) 143
6.4 Sentiment Vs. Price 148

List of Tables

3.1 Basic Equations 48
3.2 Daisyworld Model Equation Set 48
3.3 Optimal Temperature (of black and white daisies with respect to overlap) 53
3.4 Daisyworld Parameter Settings (last six rows are variable parameters, others are fixed) 55

4.1 Variable Parameter Settings 58
4.2 Optimal temp. and albedo of original daisies and their mutants 80
4.3 Evolutionary Dynamics : Representative Parameter Set 81
4.4 Permutation Entropy Regimes 95
4.5 Moran's I Regimes 96
4.6 Local PE (section 4.2) 96
4.7 Global PE (section 4.2) 97

5.1 Representative Parameter Set 100
5.2 $\bar{C}$, $\bar{L}$ and μ; $p = 0.05$ is qualitatively compared with $p = 1$ and quantitatively compared with μ 108
5.3 Possible Critical Point (p) 111
5.4 Spatial Emergence and Std. Dev. of States 113
5.5 Temporal Dynamics and Permutation Entropy 113
5.6 Spatio-temporal Patterns 113

5.7 The range of std. dev. of states and PE of daisies for 25 realizations . . . 114
5.8 Typical Clustering Coefficients and Characteristic Path Lengths 120
5.9 Average($\pm Std.Dev.$) Clustering Coefficients and Characteristic Path Lengths . . . 121
5.10 Adaptation : Clustering Coefficients and Characteristic Path Lengths . . . 122
5.11 Scale-free Graph : Clustering Coefficient and Characteristic Path Length . . . 126

6.1 Parametric Analogy of Daisyworld and Stock Market . . . 141
6.2 p-values of Granger Causality Analysis . . . 149
6.3 p-values of Cointegration Tests . . . 149

Chapter 1

Introduction

> "I think the next century will be the century of complexity."
> Stephen Hawking, *San Jose Mercury News, January 2000*

> "...the nations and people who master the new sciences of complexity will become the economic, cultural, and political superpowers of the next century."
> Heinz Pagels, *The Dreams of Reason: The Computer and the Rise of the Sciences of Complexity(1988)*

In recent decades, the complex system studies have revealed the paradigm shift in our worldviews [Bar-Yam, 2003; Mitchell, 2009] from linear thinking to complexity thinking. Before the world was described by command and control, linear cause-and-effect, centralised control, etc. But today the fundamental nature of the world is described by instability, disorder, chaos theory, bifurcations, turbulence, tipping points, butterfly effects, etc.

Traditional science focuses on simple cause-and-effect relationships – linear worldview in which the output of a system is proportional to its input. For example, the ideal gas law, $PV = nRT$ where P is the pressure of the gas, V is the volume of the gas, n is the amount of substance of gas, T is the temperature of the gas and R is the ideal gas constant. This reductionist approach of an "additive model", where "the composite whole is the sum of its component parts", enables us to predict the outcome based on the initial

conditions. For instance, the ideal gas law enables us to predict pressure given the initial temperature, volume, and quantity of a gas.

But our complex world is dynamic and unpredictable, exhibiting nonlinear patterns. Examples include unpredictability of weather, epidemics, economic, political and cultural behaviours of societies, stock price movement, etc. Complexity science reframes our worldview as "holistic" – where "the whole is more than the sum of the parts" [Von Bertalanffy, 1968]. The logistic equation $x_{t+1} = rx_t(1 - x_t)$ where x is a dynamical variable, r is bifurcation parameter and t is time. This simple (nonlinear) equation, when iterated, results in very complex forms – logistic map. By altering the value of r in the logistic equation, we can generate a variety of complex patterns, including fixed-point attractors, periodic attractors (bifurcations), and strange (chaotic) attractors [May, 1976].

Complexity emerge from simple rules and feedback mechanisms. Examples include climate change, stock market behaviour, human immune system, World Wide Web, Wood Wide Web, human brain, termite colony, etc. Complexity is an approach to problems in many diverse disciplines including artificial intelligence, artificial life, agent-based modelling, computer science, economics, evolutionary computation, sociology, etc.

1.1 Homeostatic Complex Systems

Complex system comprises of a network of nonlinear interactions involving multiple positive and negative feedback loops among huge number of lower-level components (agents) resulting in a higher-level emergence which is manifested as collective behaviours, self-organization and self-regulation [Mitleton-Kelly, 2003; Prigogine, 1997]. Complex systems can evolve towards homeostasis [Tregonning and Roberts, 1979] where the complex dynamics rest on balance between positive and negative feedbacks. Examples of such cybernetic systems include daisyworld, stock market, predator-prey system, etc. In this thesis, we investigate daisyworld where self-regulation of the physical environment emerge by the influence of biota.

1.2 Daisyworld

Daisyworld[Watson and Lovelock, 1983] model imitates the real feedback structure of the earth and captures the characteristic behaviour especially self-regulation. It provides mathematical justification for Lovelock's well-known Gaia hypothesis [Lovelock, 1972]. It is an imaginary planet where only two types of species live – black and white daisies. These biotic components interact stigmergically via an abiotic component – temperature. The different colours of the daisies influence the albedo (reflectivity) – environment-altering trait – of the planet.

In the beginning, the atmosphere of the daisyworld is cooler and only black daisies thrive as they absorb all the energy. As the black daisy population expands, it warms the planet. When it is too warm for black daisies to survive, white daisies start to bloom since they reflect all the energy back into space. As the white daisy cover spreads, it cools the planet. When it is too cold for the survival of white daisies, again black daisies thrive. This emergence leads to an infinite dance of black and white daisies. This endless cycle, owing to the bi-directional feedback loop between life and the environment, self-regulates the temperature and thereby allows life to persist.

Thus, it demonstrates the emergence of homeostasis as a consequence of the feedback loop between life and its environment. This ecosystems model has subsequent application in a number of fields (refer 2.2.1). The original daisyworld was modelled on a one-point (0D) world. It was subsequently extended to a one-dimensional (1D) world by Adams et al. [2003], to a flat two-dimensional (2D) world by von Bloh et al. [1997] and to a curved 2D world by Ackland et al. [2003] and Ackland and Wood [2010]. We have taken daisyworld as our base model and reconstruct formulations to incorporate complex dynamical features.

1.3 Limitations of Daisyworld Models

- All 2D spatial extension of Daisyworld in the literature are based on Cellular Automata [Ackland et al., 2003; Ackland and Wood, 2010; Lenton and Van Oijen, 2002; von Bloh et al., 1997]. In these, the new state of a cell is determined by a set of predetermined local rules and previous state of the randomly chosen cell in the neighbourhood.

- The original paper on Daisyworld pays only limited attention to population dynamics. But population dynamics may also lead to the regulation of resources and population.

- Stable coexistence of species in Daisyworld can be achieved either by temporal fluctuations or by spatial extension. Von Bloh and others used only spatial extensions for their study and not temporal fluctuations.

- The regular 1D or 2D lattice is not a real-world topology. In particular, non local dispersion or diffusion has not yet been studied in Daisyworld.

- The species diffusion approach used in Daisyworld modelling in the literature is not realistic, because the previous state of the neighbourhood alone determines the new state of a cell. There is no reflection of population density, and hence limited possibility to study population diffusion effects based on density gradient.

- The principles underlying complex systems are not deeply analysed with daisyworld.

1.4 Motivation

Future engineering systems are to be designed with long-term self-maintenance and self-organization which implies that the systems have to be homeostatic – they have to self-regulate their internal states by themselves to cope up with their changing environment without any external intervention. This urges

us to investigate self-regulating systems. If our systems implement the self-regulating principles of nature, they will be more close to nature and more reliable. Otherwise they will be alienated from nature and we have to engineer our systems again and again endlessly. By analysing homeostatic principles based on nature will give complete understanding of our problems.

Daisyworld is the mathematical proof of Gaia hypothesis [Lovelock, 1972] which illustrates how our earth works. Daisyworld model demonstrates the emergence of homeostasis (by and for the biosphere) as a consequence of the feedback loop between life and its environment. Identifying the feedback mechanisms which lead to homeostasis in a system is a very challenging research area. We apply daisyworld principles in deriving the analogies with stock market and we demonstrate social homeostasis.

1.5 Inspirations from Nature

Our behavioural studies of our daisyworld system is based on the following listed inspirations from nature.

- Life-environment Feedback Systems (Rock formation of bacteria)
- Complex Interacting Self-organizing Systems (Schooling of fish)
- Reaction-Diffusion Systems (Animal coats)
- Connections (Wood Wide Web)
- Super-organism (Termite colonies)
- Adaptive Networks (Brain)

1.6 Contribution

We analyse daisyworld as a paradigm shift from a mechanistic world view to a holistic ecological view. To study the complexity phenomena in daisyworld, we reconstruct some of the daisyworld formulations based on Coupled Map

Lattice (CML)(refer the chapter 3). We examine the emergence of complexity phenomena. We also incorporate complex and adaptive topological changes to our system. We observe the cyclical coexisting dominance of daises in complex and adaptive systems exemplifying behaviours of social, political and economical systems. We perceive the analogy between daisyworld and stock market as they both are complex systems giving rise to homeostatic behaviour (self-regulation, self-organization, self-causing, etc.).

1.6.1 Incorporation of Complex Spatio-temporal Dynamics

1.6.1.1 Coupled Map Lattice (CML) Modelling

Most 2D spatial extensions of daisyworld (life-environmental feedback system) in the literature are based on Cellular Automata (CA) [Ackland et al., 2003; Ackland and Wood, 2010; Lenton and Van Oijen, 2002; von Bloh et al., 1997]. In these CA based models, the new state of each cell is determined by a set of predetermined local rules and previous state of the randomly chosen cell in the neighbourhood. The discrete set of state values represents the presence or absence of a species at a cell.

In almost any real ecosystem, the population dynamics include both temporal reproduction processes and spatial diffusion processes. Hence we propose Coupled Map Lattices (CML) based spatio-temporal computational modelling tool which is convenient for simulation, interpretation of results, and analysis of spatio-temporal dynamics [Kaneko and Tsuda, 2001]. CML (also known as continuous cellular automata) are dynamical models in which discrete space and time are combined with a continuous state. The new state of a cell is updated with difference equations (maps) which depend on the current value of the cell itself, and a coupling (diffusion) term, which depends on the neighbourhood values. CMLs are CA in which the states of the cells are real values in [0, 1], and the update rule is in the form of a real function. Thus, they differ from CA primarily in the state value representations. In CA, each variable at a lattice point represents a microscopic state; in contrast, in CML, each variable represents a semi-macroscopic (mesoscopic) state. In this research,

we analyse the daisyworld dynamics through such mesoscopic modelling.

The basic CML incorporates both a nonlinear local map for temporal fluctuations, and a discretised diffusion process for spatial extension; due to these combined effects, it displays rich local and global dynamics.
(Publication : Punithan et al. [2012])

1.6.1.2 Detailed Population Dynamics

Daisyworld models in the literature lack detailed population dynamics, owing to their primary focus on environmental regulation. But population dynamics, with density dependent factors such as resource limitation and influence, crowding, dispersion, competition, disease, predation, etc., may lead to homeostasis at an ecosystem level. The regulation due to density dependence is a well known emergent ecological phenomenon.

This research studies the detailed symbiotic population dynamics of daisyworld in CML, in an alternative approach reconstructing some of the mathematical equations of the original Daisyworld models [von Bloh et al., 1997; Watson and Lovelock, 1983] adapted to coupled maps. The ecological homeostasis of our system is determined by the biotic and abiotic components of the system and the density-dependent nature of the growth due to overcrowding. These two regulatory mechanisms shape the dynamics and behaviour of our daisyworld model.
(Publication : Punithan et al. [2012])

1.6.2 Demonstration as Complex Systems

Based on our computations, we exemplify daisyworld as a complex dynamical system, self-organizing system and reaction-diffusion system. A large scale of identical habitats (components) in a 2D daisyworld interact with their neighbours produce complex and robust global behaviour. Our system combines spatial Laplacian diffusion, nonlinear local dynamics via logistic growth equation, noisy fluctuations in influencing the physiological, behavioural rules and physical constraints which cause a wide range of patterns formation such as

complex patterns, Turing-like structures, cyclic patterns, random patterns and uniform dispersed patterns emerge from our system. The emergence of such complex behaviours from our model serve to illuminate the complex mosaic of patterns that we observe in real-world biosystems.

1.6.2.1 Complex Dynamical System

From our results at a one point world, we infer daisyworld – a system with life-environment feedback – exerts stationary, periodic and strange attractors. (refer sub-section 4.1.7)

1.6.2.2 Self-organizing System

The combined effect of positive and negative feedback couplings result in a negative feedback loop, which stabilises the physiological processes and leads to homeostasis. We observe that life and their environment together organize themselves.
(Publications : Punithan and McKay [2012b] and Punithan et al. [2012])

1.6.2.3 Reaction-diffusion (Activator-inhibitor System)

In our nonlinear reaction-diffusion system, symmetry-breaking is induced by species dispersion, temperature diffusion and noise. Same as morphogens in Turing's experiments [Turing, 1952], black and white daisies locally react and spatially diffuse to give rise to complex behaviours and pattern formation.
(Publications : Punithan and McKay [2012b] and Punithan et al. [2012])

1.6.3 Incorporation of Evolutionary Mechanisms

We introduce replicator-mutator mechanisms from evolutionary dynamics into our core two-dimensional daisyworld model, thereby coupling evolutionary change with daisyworld's bi-directional feedback between biota and environment. Daisyworld continues to self-regulate in the presence of these evolutionary forces. The most interesting behaviours, exhibiting a complex and dynamic

dance through space and time in species' abundance, emerges through the introduction of additive spatio-temporal random perturbations in the form of thermal noise. The balance between ecosystem feedback and fluctuations in the ecosystem determines the spatial coexistence of dominance between daisy species and their mutants or adaptants.
(Publication : Punithan and McKay [2012a])

1.6.4 Introduction of Spatio-temporal Quantification

We introduce metrics for quantifying the behaviour of daisyworld, and used them to analyse the spatio-temporal dynamics: Permutation Entropy to measure the temporal dynamics, standard deviation to measure the scale of fluctuation, and Moran's I to measure the spatial auto correlation and pattern formation. PE and MI quantify the spatio-temporal dynamics accurately, demonstrating their reliability in quantifying a wide range of dynamics.
(Publication : Punithan et al. [2012])

1.6.5 Incorporation of Complex and Adaptive Topological Properties

1.6.5.1 Small-world Phenomena

All 2D versions of daisyworld [Ackland et al., 2003; Ackland and Wood, 2010; Lenton and Van Oijen, 2002; von Bloh et al., 1997] are of regular lattice structure – in which all neighbourhoods are isomorphic – with fixed numbers of nearest neighbours. However, in planetary ecodynamics, some species may have a mix of local and global dispersal patterns – for example, coconuts [Perera et al., 2000] or shellfish [White et al., 2010] – which can dramatically alter their ecological behaviour. This motivates us to study the effects of global interactions on daisyworld.

We study the dynamics of daisyworld using 2D versions of the Watts-Strogatz (WS) model [Watts and Strogatz, 1998] – in which a small fraction of the existing edges are rewired as random couplings, of the Newman-Watts (NW) model [Newman and Watts, 1999] – in which a few new random edges

are added and of Smallest-World (SW) model [Dorogovtsev and Mendes, 2002] – in which new nodes and random edges from them are added. These rewired or added edges are known as 'shortcuts', and they give rise to the small-world properties in which even a quite small numbers of shortcuts can dramatically change many characteristics of the network behaviour and can exhibit dramatic effect on the system dynamics.

We recognize that even a few long-range connections dramatically affect the population dynamics of daisyworld, but it is still able to self-regulate the environment (temperature) and thus sustain life (daisies). The introduction of non-local long-range connectivities into a highly locally structured daisy population lattice permits the rapid and homogeneous spread of a dominant daisy type, invading the whole coexisting daisyworld. Although the proportion of long-range connections is small, the pattern of interaction is changed from entirely local to almost entirely global.

If a system exhibits such a dramatic change in its characteristic properties under the perturbations of small changes in some of its model parameters, the system is said to have changed phase. Such phase transitions are very common in physical, social and technical systems. For example, a magnet exhibits magnetism up to a critical temperature, above which the magnetic properties are suddenly destroyed. In the same way, when we perturb the connectivity of our daisyworld graph while leaving all other parameters fixed, it exhibits periodic behaviour while the unaltered system forms static self-organised patterns.
(Publications : Punithan et al. [2011] and [Punithan and McKay, 2013b])

1.6.5.2 Topology-Dynamics Feedback (Adaptive Graphs)

We investigate the behaviour of the daisyworld on an adaptive graph [Gross and Blasius, 2008; Gross and Sayama, 2009] – a class of dynamical graphs whose topologies and states coevolve, comparing it to previous studies on a fixed topology grid, and a fixed small-world graph. Here, we consider the small-world graph based on Newman-Watts (NW) model as baseline for com-

parison. The adaptive graphs eventually generate topologies with small-world phenomenon behaving similarly to the NW model – and radically different from the grid world. Under the same parameter settings, static but complex patterns emerge in the grid world. In the NW model, we see the emergence of completely coherent periodic dominance. In the adaptive-topology world, the systems may transit through varied behaviours, but can self-organise to a small-world graph structure with similar cyclic behaviour to the NW model. (Publication : Punithan and McKay [2013a])

1.6.5.3 Scale-freeness (Power law or Fat-tailed Distribution)

We incorporate scale-freeness into our system possessing power law distribution, high clustering and small-world effect. The daisyworld dynamics exert the homeostatic emergent property even with the presence of additional topological properties. The system is shown to be able to precisely coordinate behaviour with internal dynamics.

1.6.6 Applications (Demonstration of Social Homeostasis in Stock Market)

We derive the parametric and functional analogies between daisyworld and stock market. The life-environment feedback mechanisms in daisyworld self-regulate the planet. The very same way the feedback between market sentiment (investors' opinion) and stock price cause the self-regulation in stock market. We apply our analysis from daisyworld (an imaginary world) to real-world stock market.

1.7 Outline

First we describe the background materials in the chapter 2. In chapter 3, we present our reconstructed mathematical modelling of daisyworld that is developed based on Coupled Map Lattice (CML) and other modelling tools provided in the background materials, and we detail our experimental set-up

that we use for our investigations. In the chapter 4, we analyse daisyworld in CML with only local couplings. In chapter 5, we examine daisyworld in CML with complex couplings based on small-world phenomenon, scale-freeness and adaptive networks. In chapter 6, we demonstrate stock market as a collective social homeostatic system by analysing stock tweets and stock price. Finally, we conclude by summarising our contribution and findings in the chapter 7.

Chapter 2

Background

In this chapter, we provide the background materials on complex systems (section 2.1), modelling tools (section 2.2) – that we use for our modelling, and quantifiers (section 2.3) – that we use to analyse the spatio-temporal dynamics of our model.

2.1 Complexity Science : A Means to Understanding Complex Systems

By etymology, the term complex roots from Latin *plectere*, which means interwoven. That implies a complex system is inseparable due to the interactions and the interdependencies between their the components. A complex system is a large network of components interacting according to simple rules and exhibit an emergent complex behaviour, adaptation via learning or evolution; or non-trivial information without central control. Complex systems covers many core areas such as system theory, nonlinearity theory, network theory, game theory, evolution and adaptation, collective behaviour and pattern formation, etc. There are numerous examples of complex systems in nature, society, man made technological systems– human brain (neurons), stock market (investors), insect colonies (termites), the internet (computers) and World Wide Web (pages), social networks (humans or animals), etc.

2.1.1 Systems Thinking

A system consists of components, interconnections, and a function or purpose [Wright and Meadows, 2012] – a set of interacting, interrelated or interdependent components interconnected to produce a specific pattern of behaviour over time. The system maintains its existence through the mutual interactions of its parts [Von Bertalanffy, 1968]. Example include societies, ecosystem, nervous system, etc.

Systems thinking is the science of how things are connected. It emphasizes the relationships among a system's parts rather than the parts themselves. It provides a way of thinking based on whole and relationship rather than parts. A system is more than sum of its parts that may exhibit adaptive, dynamic, self-regulating and evolutionary behaviour. In traditional thinking, a problem is broken into a set of simpler sub-problems and solving each of them individually. In contrast, systems thinking emphasizes the interconnections between parts of a system and external environment. Systems thinking signifies circular feedback (Figure 2.2) rather then linear cause and effect (Figure 2.1).

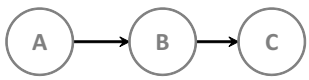

Figure 2.1: Linear Cause-and-Effect : A system consisting of components A, B and C

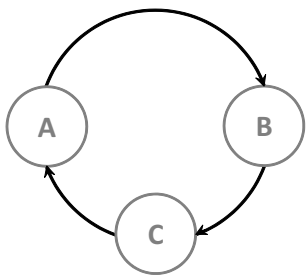

Figure 2.2: Circular Cause-and-Effect : A system consisting of components A, B and C

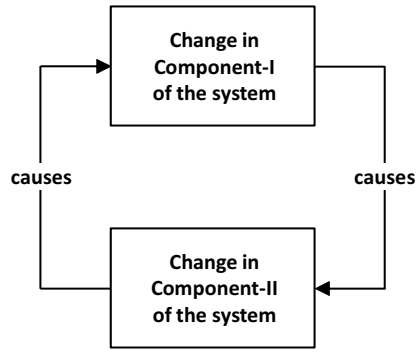

Figure 2.3: System with Feedback Mechanisms

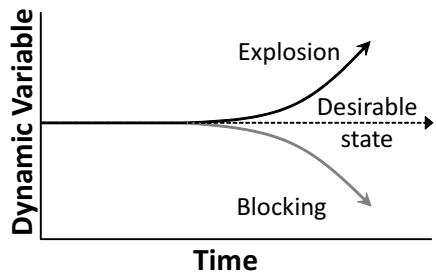

Figure 2.4: Reinforcing Process

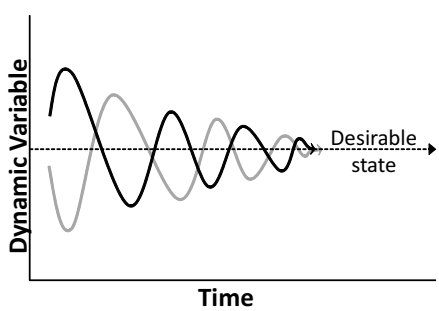

Figure 2.5: Balancing Process

Interactions : The *interactions* lead to shift from perception of objects to perception of relationships [Capra, 2004]. They play a vital rule in the system and can generate novel dynamics. Interactions trigger complexity in the system. When interactions of the system are dependent, feedback enters the system and alters the dynamics of the system (Figure 2.3). With the positive coupling, changes get amplified leading to instability. With the negative coupling, changes get quickly absorbed and the system gain stability. Thus the system behaviour is described by both reinforcing and balancing processes – bipolar feedback couplings.

Driving Positive Coupling Positive coupling (runaway or amplifying or escalating) is self-reinforcing. It generates exponential growth (virtuous) or collapse (vicious) (Figure 2.4). This brings changes (difference or innovation) in the system. If there is no positive coupling, the system will be monotonous and uninteresting. Examples include fashion crazes, reproduction cycle, etc.

Regulating Negative Coupling Negative Coupling (homeostatic or self-maintaining or dampening) is balancing – self-correct (Figure 2.5). It controls (counters) the change and exhibit self-maintenance, robustness and stability. Examples include thermostat, immune system, etc.

Dynamical Systems : Dynamical systems are systems that change over time. Examples include brain, heart, stock market, global economy, global climate, etc. Dynamical systems theory characterises the system behaviour in terms of attractors, bifurcations and universal properties of the ways systems can change.

Cybernetics : Cybernetics (from the Greek word for *steersman*) is the study of complex systems and processes, their modelling, feedback, control, information, communication and purpose. Examples include robots (technological), human body temperatures (biological), Gaia hypothesis-daisyworld (environmental), stock market (economical), etc. Artificial intelligence, artificial life,

neural networks are the offsprings of cybernetics.

Homeostasis - Adapting to change :

> "... a form of behaviour is **adaptive** if it maintains the essential variables within physiological limits"
> Ashby, W.R, *Design for a Brain: The Origin of Adaptive Behaviour, 1952*

Homeostasis is derived from the word *homoios* (Greek) meaning same, like, resembling and *stasis* (Greek) meaning to stand, posture. The term homeostasis was introduced by Claude Bernard, who founded the principle of the internal environment [Bernard, 1878]. Cannon suggested homeostasis as the coordinated physiological processes which maintain most of the steady states in the organism [Cannon, 1929]. Ashby stated that the process of homeostasis is directly related to intelligence [Ashby, 1952].

A well known example of homeostasis is the regulation of body temperature. Homeostasis is a fundamental property of living systems which tends to maintain the internal conditions of living organisms stable (within a normal range), regardless of the external environment. These internal conditions include body temperature, blood pressure, pH level, glucose level, etc. Hence it is essential for survival.

Adaptation is the maintenance of system variables within predetermined (normal) limits either by evolutionary changes, physiological reactions, sensory adjustment, or by learning novel behaviours. Hence adaptive behaviour is equivalent behaviour of a stable system. Homeostasis is the ability of a system to adapt to a continuously changing and unpredictable environment. It corresponds to an adaptive reaction to maintain "essential states" within a range [Ashby, 1952].

Through adaptation, a system or an organism functions within a "viability zone" – the lower and upper bounds of the essential states. When perturbations or environmental changes occur, the system adapts to face the changes within the viability zone, i.e. without the system "breaking" [Ashby, 1947]. The system remain in the viability zone owing to homeostasis. It is the active

regulation which differs from mere inertia – stagnant state. It also emphasises on the resistance to the change.

Homeostatic systems (either living or technical) maintain the balance through complex interacting feedback control processes. For instance, the brain keeps the living organisms in physical and emotional balance by its highly intricated physical, chemical and neurological processes. In order to understand real or artificial life, it is necessary to understand the conceptual framework and basic mechanisms of homeostasis [Dyke and Harvey, 2006]. The corrective behaviour in a system can be innate (pre-programmed) or learned. Hence, homeostasis is an important tool for adaptation in dynamic environments.

Homeostasis can exist at any scale of biological organization–from the cellular to the biospheric. Individual organisms can exhibit homeostasis and the assemblages of organisms can also co-operate to maintain the dynamic orderliness that is characteristic of life [Turner, 2009a]. Homeostatic systems provide high levels of stability, adaptation, coordination, self-organization, robustness, survivability, viability, sustainability, corrective behaviour, etc. Some of different forms of homeostasis are listed below.

Organismal Homeostasis The cells of an organism coordinate their activities to regulate the body's internal environment.

Ecological Homeostasis Ecosystem has the power of self-maintenance and self-regulation. Ecological homeostasis is referred as balance of nature. The ecological balance is maintained by the number of factors. The carrying capacity is one among them. The ecosystem also exhibits organism-like behaviours.

Social Homeostasis Social homeostasis is a phenomenon of social insect colonies. The environment of the colony is regulated by the collective activities of the colony's inhabitants. The colony is a superorganism [Turner, 2009b]. Examples include termite colony, bee hive, etc.

2.1.2 Nonlinear Thinking

In linear systems (proportional), the behaviour of the whole is the sum of the behaviour of its parts, while in nonlinear systems, the behaviour of the whole is more than the sum of its parts. Recursion (iterations) and feedback loops cause nonlinear effect.

Linear system obeys the principle of superposition and homogeneity. Any system that does not satisfy these properties is nonlinear. Linear system can be understood by analysing its parts in isolation. While nonlinear system can be understood by analysing the interactions between parts, rather than parts themselves [Langton et al., 1989]. Examples include our nervous system, laws of ecology, immune response of patients, viral population dynamics, human psychology, etc [Strogatz, 2003].

In nonlinear systems, cause and effect are disproportionate because of feedback loops. Interactions among the components are nonlinear and hence a very small perturbations or fluctuations can become amplified into gigantic, structure-breaking waves Prigogine et al. [1985]. These systems are of tipping points (systems tip from one state to another), stable regimes that collapse, butterfly effects, avalanches, etc. But linear systems are incapable of rich behaviour [Strogatz, 2003].

Dynamical Behaviours : The dynamics of the systems can evolve towards single stable steady state, multistability (several stable steady states), limit cycles (sustained oscillations), chaos (strange attractors), etc. Bistability (a particular case of multistability) is the coexistence of two steady states. Bistability plays a critical role in biological systems (genetic switch, memory effect, etc) and limit cycle in biological rhythms. The system can exhibit complex behaviours (such as chaos– multiple instability mechanisms) due to multiple feedback loops. Other complex behaviours include quasi-periodic oscillations, bursting (alternance between oscillatory and non-oscillatory phases), synchronization, and excitability.

Chaos : If the trajectories of the two realizations of the same dynamical system with an infinitesimal difference in the initial conditions diverge exponentially, then the system has sensitive dependence on initial conditions. "Chaos is aperiodic long-term behaviour in a deterministic system that exhibits sensitive dependence on initial conditions" [Strogatz, 2001]. In a chaotic system small disturbances grow exponentially, causing long-term prediction drastically inaccurate [Lorenz, 1963]. This is known as butterfly effect. An appropriate system of this sort of behaviour of is stock market. As the value of a stock rises or falls, people make their decisions to buy or sell that stock. This in turn further affects the price of the stock, causing it to rise or fall chaotically. Chaos has been observed in electronic circuits, cardiac disorders, etc.

Iterative Systems : The logistic map is the most popular equation in the science of dynamical systems and chaos, which exhibits the fundamental properties of complex systems in nature. This extremely simple nonlinear iterative system is astounding. The behaviours of such iterative systems are characterized by bifurcations, attractors and universal properties such as period-doubling route to chaos and Feigenbaum's constant is same for all unimodal maps. Other nonlinear iterative systems are growth and decay of biological populations, predator-prey interactions, spread of communicable diseases, etc.

2.1.3 Network Thinking

> "Whenever we look at life, we look at networks."
> Fritjof Capra, *The Web of Life*

> "Networks are present everywhere. All we need is an eye for them."
> Albert-László Barabasi, *Linked*

"Networks are prerequisite for describing any complex system, indicating that complexity theory must inevitably stand on the shoulders of network" [Barabasi, 2003]. Thinking networks is about how networks emerge, what they look like, and how they evolve [Barabasi, 2003]. The components of

living systems–organisms, parts of organisms, and communities of organisms–are arranged in network fashion [Capra, 1997]. Network thinking focuses on the relationships or connections or interactions among entities rather than the entities themselves.

The key features of networks are pattern of organization (holistic view), interconnectivity, nonlinearity, unpredictability, contingency, etc.

Random Networks : Paul Erdos and Alferd Renyi made first breakthrough in network science. They modelled networks by selecting n number of nodes and connecting every pair of nodes with a probability p – Poisson random network or Bernoulli network [Bollobás, 2001]. These random networks exhibits small-world effect but fail to display other topological characteristics of real world networks. One of the most characteristic of social networks that random networks cannot model is social cliques.

Small-world Complex Networks : Watts and Strogatz [1998] in their seminal paper proposed that real-world networks lie between regular and random networks and are usually highly locally clustered (cliquish), as in regular lattices, yet have low characteristic path lengths, in which they resemble random networks. These properties are found across a wide spectrum of sciences – in social, biological and technological networks such as neural networks, electronic power grids, networks of movie actors [Watts and Strogatz, 1998], the world wide web [Albert et al., 1999], scientific collaborations networks [Newman, 2001], and so on.

The small-world property was first investigated in the pioneering empirical work of social psychologist Milgram [1967]. He showed that any two randomly chosen people on the planet were likely to be linked by a chain of six intermediate acquaintances. His notion has been widely accepted, and is referred to as the "small-world phenomenon" (more popularly known as the "six degrees of separation"). More precisely, the underlying social network is a superposition of high local clustering and short global chains, possessing the small-world property.

Watts and Strogatz [1998] (WS) in their ground-breaking work first modelled the small-world phenomenon by randomly rewiring a fraction of the connections of regular networks. These 'shortcuts' drastically decreased the diameter of the network (the longest shortest path between two nodes) and created the small-worlds. The measure of connectedness of a network is the average minimum path length between any two points. This is known as degree of separation. Due to the shortcuts, networks have low degrees of separation and thus they make small-world small. They are highly connected as fully-connected network (one degree of separation).

Other variants exhibiting the small-world phenomenon include the Newman-Watts (NW) model of Newman and Watts [1999] and the Smallest World (SW) model of Dorogovtsev and Mendes [2002].

Since a small-world network realises both high local clustering and high connectivity simultaneously, it exhibits properties from regular lattices and random networks: with regular lattices, it shares local coherence, while with random networks, it shares rapid diffusion. Thus it shares interesting properties of two opposed topologies.

In turn, the structural properties of networks exhibiting small-world phenomenon can have dramatic effect on the dynamics of systems acting on them. Well known examples include the dynamics of epidemics, biological evolution and of diffusion processes. For further reading, see Boccaletti et al. [2006].

Scale-free Complex Networks : Watts and Strogatz model does not capture all topological properties of real networks. In WS model, each node begins with the same number of links and are rewired with a uniform distribution. The distribution of the number of links that a node has follow a peaked distribution. Albert-Laszlo Barabasi found that the distribution of links in real world networks follow a power law or fat-tailed distribution. Majority of nodes have very few links while a few have majority of links. Barabasi referred to these popular (high degree) nodes as hubs and coined complex networks exhibiting power law distribution as scale-free networks as they exhibit self-similarity (parts of network show the same statistical properties at many

scales) or a fractal. No single node can characterize the population of nodes and thus there is no scale in these networks. Hubs are exceptionally massive nodes in terms of the number of other nodes they are connected to. Hubs ('keystone species' in ecology and 'connectors' in sociology) are nodes with an anomalously large number of links. They present in very diverse complex systems ranging from economy to a cell. The emergence of hubs allows the small-world effect to occur.

"90% of all documents on the web have 10 or fewer links pointing to them, while a few, about 3, are referenced by close to a million other pages" [Barabasi, 2003].

Most real networks are formed by just a few nodes and a few links. The original links may be random or may not, but as the network grows – more and more links are added. However, they are not added completely randomly or at least not uniformly. Barabasi hypothesized that they are added with preferential attachment. ie., each link would be more likely to be added to those nodes which already have more links (older more established (popular) nodes). This allows the rich to get richer – "Matthew effect". The combination of allowing a network to grow and allowing it to grow with preferential attachment, forms the power distribution characteristic of scale-free networks.

There are two kinds of small-world networks :
egalitarian (those without hubs) and aristocratic (those with hubs) or also called scale-free networks [Buchanan, 2003]. In egalitarian networks, most of the nodes have approximately the same number of connections. Examples are synchronising fireflies, human brain and road, rail and air networks.

In aristocratic networks a few nodes (hubs) have a disproportionally large number of connections. Examples are the Internet, WWW, ecosystems, food webs, the networks of airline companies, citation networks, etc.

Adaptive Complex Networks (dynamics *on* the network interacting with dynamics *of* the network) : The key features in network theory are topologies and dynamics. The complex networks in nature, society and technology are adaptive and dynamic, in that they exhibit feedback between

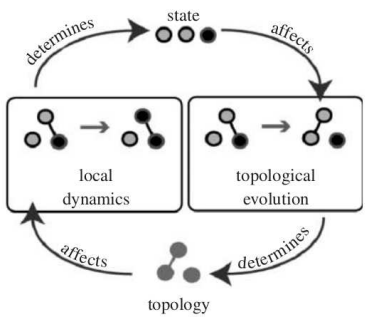

Figure 2.6: Adaptive Network (Source : [Gross and Blasius, 2008])

the local dynamics of nodes (state) and the evolution of the topological structure (Figure 2.6). Examples include genetic, neural, immunity, ecological, economic, organic, social networks, complex game interactions, etc.

Dynamics has two meanings:
"The first meaning is what we might call dynamics of the network. In this sense of the word, dynamics refers to the evolving structure of the network itself, the making and breaking of network ties. ... A dynamical view of networks, claims that existing structure can only be properly understood in terms of the nature of the processes that led to it. The second meaning, is what we might call dynamics on the network. From this perspective, we can imagine the network as a fixed substrate linking a population of individuals, but now the individuals are doing something – the outcome of which is influenced by what their neighbors are doing and, therefore, the structure of the network. ... In the real world, both kinds of dynamics are going on all the time. ... The structure of the network could change, but so could the pattern of activity on the network" [Watts, 2004].

In most real-world networks, the topology itself is a dynamical system which changes in time and in response to the dynamics of the states of the nodes (dynamics *of* the network). The evolved topology in turn influences the dynamics of the states of the nodes (dynamics *on* the network), creating a feedback loop between the dynamics of the nodes and the evolution of the topology. Networks exhibiting such a feedback loop (mutual evolution of struc-

ture and state values) are called adaptive or coevolutionary networks [Gross and Blasius, 2008; Gross and Sayama, 2009].

In road networks, the topology of the road influences the traffic flow, while traffic congestion influences the construction of new roads. In the vascular system, the topology of the blood vessels controls blood flow, while restrictions in blood flow influence the formation of new arteries (arteriogenesis). The internet respond to the addition and removal of nodes by re-routing messages via new nodes. The neuroplastic brain compensates the brain damage by re-routing, rewiring and with the growth of new neurons. Thus complex adaptive networks are intelligent.

2.1.4 Collective Behaviour

A collective behaviour (bottom-up behaviour or decentralization) is a fascinating phenomenon, in which the low-level components have the ability to self-organize themselves and emerge into a higher-level system of sophistication and intelligence [Johnson, 2012]. Examples include ant colonies, social web (a disorganized entity self-organize itself into a bottom-up intelligence), Linux open-source software (intelligent crowd in action), etc.

Self-Organization : The components comprising the system are able to self-organize and the interaction of the components comprising the system can exhibit emergence. In other words, self-organization is a processes, which exhibits emergences at global scale due to the short-range local interactions of the system, with no external intervention [Camazine et al., 2003]. A wide range of pattern formation processes have been observed in fields from chemistry (Turing's reaction-diffusion system [Turing, 1952], Belousov-Zhabotinsky reaction [Belousov, 1958]) and fluid dynamics (Bénard convection cells [Bénard, 1900]) to biology (patterns on animals' coats [Murray, 2008]). A large numbers of relatively simple entities organize themselves, without any central control, into a collective whole as patterns, information, learning and evolution.

Self-organizing systems produce global pattern from the interaction of their components. Classic examples include flocking of birds, colony of insects,

schooling of fishes, etc. A dynamical system can exhibit self-organizing property as they tend to attractors.

Emergence : The emergence is a phenomenon whereby well-formulated aggregate behaviour arises from localised individual behaviour. It is the property observed only at high scale and is not present at the lower scale. For example, the colour, conductivity, malleability of gold is not present in the properties of gold atoms [Anderson et al., 1972]. The properties of a system are emergent if they are not present in their components.

Phase Transition and Critical Phenomenon : Lev Landau invented theory of phase transition – how substances of all kinds change their forms – by focusing on the abstract elements of molecular and atomic organization. His visionary idea leads modern physics about discovering the law of forms in networks of interacting things and not the matter. The interacting things are not only atoms and molecules, but also bacteria and people. The small-world idea is just a part of this larger theory of networks – a collection of interacting elements often has properties that depend no crucial way on the nature of the elements themselves [Ball, 2004; Buchanan, 2003].

When solid ice melts into liquid or dry ice turns into smoky vapour – substances change from one form to another, the atoms or molecules remain the same. Only the collective organization of the atoms or molecules changes. The modern version of Landau's theory is called the theory of critical phenomena. When water is neither liquid nor vapour, it is in critical state. The new form of Landau's theory applies not only to changes in organization but also to the changes in the activity. Nothingness (static) changes to dynamism is called tipping point.

2.1.5 Pattern Formation

Positive and negative feedback are the two basic modes of interactions among components of self-organizing systems [Camazine et al., 2003]. Self-enhancing

positive feedback coupled with antagonistic negative feedback leads to the formation of striking patterns in nature (ripples in sand dunes, schooling of fish, flocking of birds, coat of animals). A stationary state becomes unstable due to amplification, and this provokes pattern in the system. Since amplification purely in one direction leads to destruction, negative feedback takes control of the system and plays a critical role in inhibiting amplification and shaping the process and pattern, for example in colonial nesting of male bluegill sunfish [Camazine et al., 2003].

Turing instabilities : Turing instability of a homogeneous steady state in a two-species reaction-diffusion system provides theoretical mechanisms for pattern formation. Generally diffusion is perceived as an homogenising process. By contrast, Turing, in his remarkable paper(1952 [Turing, 1952]), demonstrated that a simple system of coupled reaction-diffusion equations could give rise to spatial patterns in chemical concentrations, through a process of chemical instability. The chemicals (morphogens or species), characterised as activator and inhibitor, react and diffuse throughout the tissue, and due to this physico-chemical process patterns such as spots and stripes can form in an animal's coat. These spatial patterns emerge from a homogeneous equilibrium state, due to symmetry-breaking via diffusion. This diffusion-driven instability forms the basis of pattern formation in physics, chemistry and biology. A wide spectrum of complex self organized patterns such as stationary, waves, spirals or turbulence emerge from reaction-diffusion systems.

Turing pattern formation in activator-inhibitor systems forms the paradigm of self-organization [Nakao and Mikhailov, 2010], and provides a theoretical explanation of animal coat patterns [Murray, 2008]. The activator and inhibitor species destabilize the homogeneous state of the system due to diffusion, and lead to the spontaneous emergence of spatial patterns.

2.2 Modelling Tools

A mathematical model is the simplified representation of a real world principle or a phenomenon. We study nature through modelling tools. In this chapter, we describe the background material on computational modelling tools.

2.2.1 Daisyworld Model (Life-Environment Bidirectional Feedback Model)

Gaia Hypothesis :

> "Living organisms and their material environment are tightly coupled. The coupled system is a superorganism, and as it evolves there emerges a new property, the ability to self-regulate climate and chemistry ."
> James Lovelock, *The Ages of Gaia, 1988*

> ...[Gaia can be defined] as a complex entity involving the Earths biosphere, atmosphere, oceans, and soil; the totality constituting a feedback of cybernetic systems which seeks an optimal physical and chemical environment for life on this planet." James Lovelock, *Gaia - A New Look at Life on Earth*

The Gaia hypothesis, was conceived by James E lovelock, posits that earth and its biological systems behave as a huge single entity. This entity comprises of closely controlled self-regulatory negative feedback loops that keep the conditions on the plant within the boundaries that are favourable to life. The self-regulation of physical variables around a narrow range and resistance to perturbation via cybernetic feedback loops leads the earth to be homeostatic. This new perception of global ecology differs from the classical ecology owing to the biological response to physical conditions [Jrgensen and Fath, 2010].

A wide range of fascinating examples have been observed in nature, portraying the influence of life on its environment. Examples include the formation of lakes, dams and canals by those so-called ecosystem engineers, beavers; chemical changes in soil by earthworms; cloud formation by marine phytoplankton; carbon sinks in terrestrial plants via photosynthesis and in the

oceans via physicochemical and biological processes; stromatolite formation by microbial mats, etc.

Daisyworld Model : Hutton et al. [1987], father of modern geology, emphasised that the Earth was a superorganism and its study should be viewed as physiology. Lamarck, Goethe, Humboldt, and Suess espoused similar holistic system views [Capra, 1997; Harding, 2006]. Vernadski and McMenamin [1998], influenced by Y. Korolenko, hypothesized that life is the geological force that shapes the earth and popularised the term 'biosphere'. Lotka [1925] recognised that species and environment are inseparable. However Lovelock and Margulis were the first to explore the self-regulating earth beyond these preliminary speculative ideas [Harding, 2006]. Watson and Lovelock [1983] devised a model known as 'daisyworld', which demonstrates homeostasis by and for the biosphere.

Daisyworld is a cybernetic model which demonstrates that a biosphere can regulate a planetary environment without external guidance, providing mathematical justification for Lovelock's well-known Gaia hypothesis [Lovelock, 1972]. This simple self adaptive system consists of two dominant life forms (absorptive black and reflective white daisies) and an environmental variable (surface temperature). The petal colour (phenotype) of the daisies influences the environment-altering trait, albedo (i.e. the reflectivity of the surface) of the planet, and thus the temperature which in turn determines the daisy cover; thus life and environment are tightly coupled in this model. The homeostasis emerges from the biosphere's tuning of the planetary albedo. The daisies do not interact with each other directly but via the temperature of the environment. Thus the biotic components (black and white daisies) interact stigmergically via an abiotic component (temperature).

In the beginning, the planet is lifeless, cold ($278K$) and equally seeded with black and white daisies(=agents). At this lower temperature, black daisies are favoured as they absorb more sun light. As the growth of black daisies increases, it lowers the surface albedo (negative coupling). The decrease in surface albedo cause an increase in the surface temperature (negative coupling).

The increase in temperature increases the growth (positive coupling).This positive feedback amplifies the growth and daisyworld becomes hotter. Eventually highly reflective white daisies are favoured to prevent the system from overheating as they are good at reflecting the sunlight. As the growth of white daisies increases, it increases the surface albedo (positive coupling) which in turn decreases the surface temperature (negative coupling). The decrease in temperature increases the growth (negative coupling). Due to this positive feedback, daisyworld becomes cooler and black take advantage, re-warming the system. This cycle goes on continuously.

The behaviour of one type of daisies modifies the temperature, which affects the behaviour of the other, and vice versa. In general, increased growth of a particular type of daisy alters the temperature in a direction which is unfavourable for itself, but suitable to the other type. When black daisies start spreading more, the local temperature rises. Conversely, when white daisies spread, the temperature drops.

Due to the complementary tendencies of the species, the planet remains in homeostasis, the temperature is self-regulated and hence the planet remains habitable without any explicit mechanism for cooperation. This is the key emergent property of the system.

Daisyworld as Deep Ecological System Deep ecology, as introduced in Naess [1973], is a contemporary ecological view emphasising the interdependence and connectedness of organisms within ecosystems, and ecosystems within the biosphere. Capra [1983] emphasised that the planetary ecosystem is an integrated web of living and nonliving forms, and encouraged a paradigm shift from a mechanistic world view to a holistic ecological view. Anima Mundi [Harding, 2006], a similar perspective, emphasised the intrinsic connection between all living things on the planet. Daisyworld reflects all these perspectives and recognises life and environment as a single coupled, self-regulating and self-organising system.

Daisyworld Models in Literature : This mathematical model has inspired interpretations and analogies in many fields such as social science, politics, religion etc. There have been many offshoots to other area of science, including ecology [Wilkinson, 2003], food web theory [Ackland and Gallagher, 2004; Harding, 1999], evolutionary theory[Lenton and Lovelock, 2000, 2001; Lenton et al., 1998; Lovelock, 1992], physiology [Saunders et al., 1998, 2000], maximum entropy production [Dewar, 2003, 2005; Ozawa et al., 2003], artificial life [Harvey, 2004], cybernetics [Andrew, 1996], earth system science [Ford, 1999; Kump et al., 2010; McGuffie and Henderson-Sellers, 2005] and Information Technology. Daisyworld has been applied in information technology and robotics [Dyke and Harvey, 2005, 2006] and inherent rein control mechanism [Saunders et al., 1998, 2000].

Variants of Daisyworld on Spatial Structures : The original model was based on a zero-dimensional world. It was extended to a one-dimensional (1D) world by Adams et al. [2003], to a two-dimensional (2D) world by von Bloh et al. [1997] and to a curved 2D world by [Ackland et al., 2003; Ackland and Wood, 2010].

Adams et al. [2003] examined a 1D Daisyworld with curvature on a spherical planet. The global regulatory properties of the original model are retained. The introduction of heat diffusion destabilizes the coexistence equilibrium of the two daisy types. As a result, a striped pattern consisting of blocks of all black or all white daisies emerges. Because of curvature, this model exhibits desert formation, the equatorial or polar regions being denuded of biota.

von Bloh et al. [1997] extended the Daisyworld to a 2D Cellular Automata (CA). This is the most studied and basic 2D model and includes multiple daisy types with regrowth rules as follows: At a given time step, one cell is chosen at random. If the neighbouring cell is empty, there is no colonization. If the neighbouring cell is vegetated, the chosen cell is colonized with growth rate. During successful colonization the albedo of the colonizing vegetation is allowed to mutate by a small random change.

A two-dimensional Daisyworld model with curvature was developed by Ack-

land et al. [2003]; Ackland and Wood [2010] to further study spatial effects. They found that catastrophic collapse of life can occur under gradual forcing of environmental feedback. This model predicts that large desert formation will be a sudden phenomenon, foreshadowed by large but temporary fluctuations, rather than the gradual growth of a small, expanding desert.

Daisyworld Applications : Although Daisyworld was originally introduced as an ecosystems model, it has seen subsequent application in a number of fields.

The regulation of some human physiological systems is analogous to Daisyworld. For example in the blood glucose regulation analogy, black and white daisies are replaced by the hormones insulin and glucagon, and temperature is replaced with blood glucose. Saunders et al. [1998] used this analogy to predict salient feature of type I and type II diabetes. Saunders et al. [2000] extended this to model the control of ionized calcium by parathyroid hormone and calcitonin.

Harvey used Daisyworld to model a sensing system [Harvey, 2004]. A circular body agent rotates around its centre by a force from a tentacle with sensor. Many tentacles on the surface work cooperatively and rotate the agent towards a light source over a range of positions just as daisies maintain global temperature over a range of luminosities.

Having intrinsic self-regulating behaviour, daisyworld system concept can be applied to a wide range of problems especially decision making under changing environmental conditions such as stock market, autonomous robot navigation, smart vehicles, etc. For further reading on daisyworld literature and applications, please see Wood et al. [2008].

2.2.2 Logistic Growth Model (Verhulst Model)

Populations grow at geometric or exponential (Malthusian) rates in unconstrained ecological systems. In realistic worlds, this cannot continue indefinitely. Verhulst proposed an extension of the Malthusian growth model with

an additional negative quadratic term $-r\frac{P^2}{\kappa}$, which decreases the population growth due to over-crowding. An Euler discretisation of Verhulst's equation (equation 2.1), also known as the discrete logistic equation, is key to theoretical population ecology. This density dependent population growth also models a form of ecological homeostasis.

$$P_{(t+1)} = P_t \left[1 + r\left(1 - \frac{P_t}{\kappa}\right)\right]; \quad r > 0, \kappa > 0 \tag{2.1}$$

where $P \in [0, \kappa]$ is the population size (at times t and $t+1$), and ranges from 0 (extinction) to κ (maximum conceivable population); r is the intrinsic rate of natural increase (growth coefficient) or bifurcation parameter; κ is the carrying capacity: the maximum sustainable population beyond which P cannot increase; and $\left(1 - \frac{P_t}{\kappa}\right)$ is known as the 'biotic resistance'. The parameter r enhances the growth (positive coupling) and the component $[1 - \frac{P_t}{\kappa}]$ dampens the growth (negative coupling), with their combined effect regulating the population.

The logistic map was originally studied in the context of population dynamics. May [1976], through his pioneering studies, showed that deterministic chaos emerges in population dynamics due to non-linearity and density-dependence. He proved that the above simple, density-dependent, non-linear, iterative, discrete map gives rise to a wide range of complex dynamics. It exhibits three types of attractors, namely static or fixed point attractors, limit cycles or periodic attractors, and chaotic or strange attractors. Although this equation has a built in regulatory mechanism based on κ, it forms the paradigm for the period-doubling bifurcation route to deterministic chaos, the basis of modern chaos theory.

2.2.3 Replicator Mutator Model

Replicator-mutator (aka selection-mutation) dynamics are embodied in the RME (equation 2.2):

$$\dot{P}_c = \sum_{c'=1}^{\mathfrak{n}} P_{c'} \mathfrak{f}_{c'} \mathfrak{q}_{c'c} - \phi P_c, c = 1, ..., \mathfrak{n} \tag{2.2}$$

Here P_c is the population proportion of type c, $\mathfrak{n}$ is the total species, $\mathbb{Q} = [\mathfrak{q}_{cc'}]$ is the mutation matrix, $\mathfrak{f}_{c'}$ defines the selection dynamics $\mathfrak{f}_{c'} = \mathfrak{f}_0 + \sum_{c'} \mathfrak{a}_{c'c} P_{c'}$ and $\phi = \sum_c P_c \mathfrak{f}_c$ is the average fitness. $\mathfrak{f}_0$ is the intrinsic fitness and $\mathbb{A} = [\mathfrak{a}_{cc'}]$ is a reward matrix.

In addition to biological evolution [Bürger, 1998], RME has been used to model evolution in language [Nowak et al., 2001], culture, behaviour in social networks [Olfati-Saber, 2007] and evolutionary game theory [Brenner, 1998].

2.2.4 Neighbourhood Models

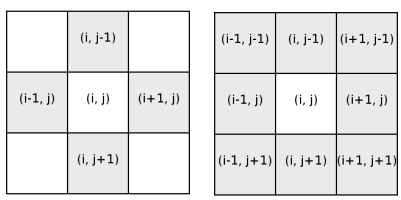

(a) von Neumann (b) Moore

Figure 2.7: Neighbourhood Models

The choice of neighbourhood models can be von Neumann (right, left, up, down); refer sub figure 2.7(a) or Moore (orthogonal (right, left, up, down) and diagonal vertices); refer sub figure 2.7(b). In the sub figures of Figure 2.7, the shaded grey cells indicate the neighbours of the central cell (i, j).

2.2.5 Diffusion Models

Spatial effects come into play in any system via diffusion, and this coupling effect is defined by the neighbourhood structure. In our model, we use the discretised version of the Laplacian operator. This is simple passive diffusion, requiring no catalyst. Diffusion is one of the key ingredients in our system to break symmetry and spread effects to the entire system. In the absence of diffusion, the ecosystem is uncoupled, and each habitat functions independently leading to an unrealistic world. Unlike other models, we do not have an explicit reseeding mechanism; instead the dispersal of daisies achieves the same function implicitly. Dispersal also reduces the likelihood of global extinction of daisies.

2.2.6 Spatio-temporal Model – Coupled Map Lattice (CML)

The Coupled Map Lattice (CML), introduced by Kaneko [1985], is one of the most widely used models for investigating the non linear dynamics of a spatially extended system. CML incorporates discrete time evolution (map) in a discrete space (lattice or network) as in cellular automata (CA), but can take arbitrary state values in the range $[0, 1]$ as in partial differential equation (PDE) models. In our model, we permit a range of population size from $[0, \kappa]$, where κ is the carrying capacity at a particular habitat (cell), for population dynamics and a range of temperature values from $[270, 330]K$ in the case of planetary energy dynamics.

The dynamics of a CML is governed by two terms: the temporal nonlinear reaction (maps - difference equation - f) and the spatial diffusion (coupling - ϵ). The evolution rules for a system in two-dimensional space with periodic conditions are defined as follows. The local variables $x_{(i,j,t)}$ diffuse to their neighbours, and the local weighted average value after diffusion is iterated over a local map.

Discrete Laplacian diffusion model is defined by:

$$x'_{(i,j,t)} = (1-\epsilon)x_{(i,j,t)} + \frac{\epsilon}{k}\sum_{<l,m>}^{n} x_{(l,m,t)} \tag{2.3}$$

where $x_{(i,j,t)}$ is the spatio-temporal distribution of a dynamical variable, t is the time step: $t \in \mathbb{Z}$; (i,j) indicates a 2D lattice point: $i,j \in \mathbb{Z}$; x is a dynamical variable: $x_{(i,j,t)} \in \mathbb{R}$; $x'_{(i,j,t)}$ is an intermediate local value after diffusion; $\epsilon \in [0,1]$ is the coupling parameter (diffusion rate); and k is the coordination number, specifying the number of interacting neighbours. It is derived from the neighbourhood model, in which $< l,m >$ ranges over the immediate neighbours of (i,j).

Discrete Laplacian diffusion in a regular graph with Moore neighbourhoods $(k=8)$ is formulated as:

$$\begin{aligned} x'_{(i,j,t)} = (1-\epsilon)x_{(i,j,t)} + \frac{\epsilon}{8}\Big[&x_{(i+1,j,t)} + x_{(i-1,j,t)} + x_{(i,j+1,t)} + x_{(i,j-1,t)} \\ &+x_{(i-1,j-1,t)} + x_{(i+1,j-1,t)} + x_{(i-1,j+1,t)} + x_{(i+1,j+1,t)}\Big] \end{aligned} \tag{2.4}$$

The local map function is defined as: $f(x)$ can be any nonlinear function of a dynamical variable. In our work, we use logistic maps.

Combining local reaction and spatial diffusion terms

$$x_{(i,j,t+1)} = f\Big(x'_{(i,j,t)}\Big) \tag{2.5}$$

where f is the local non-linear function – logistic map in the case of population dynamics and temperature update function in the case of planetary energy dynamics.

Equation 2.5 can be rewritten as:

$$\begin{aligned} x_{(i,j,t+1)} = f\Big((1-\epsilon)x_{(i,j,t)} + \frac{\epsilon}{8}\Big[&x_{(i+1,j,t)} + x_{(i-1,j,t)} + x_{(i,j+1,t)} + x_{(i,j-1,t)} \\ &+x_{(i-1,j-1,t)} + x_{(i+1,j-1,t)} + x_{(i-1,j+1,t)} + x_{(i+1,j+1,t)}\Big]\Big) \end{aligned} \tag{2.6}$$

And is simplified as :

$$x_{(i,j,t+1)} = f\Big((1-\epsilon)x_{(i,j,t)} + \frac{\epsilon}{k}\sum_{<l,m>}^{k} x_{(l,m,t)}\Big) \tag{2.7}$$

CML is a widely used tool in numerous fields such as physics, biology, mathematics, ecology and engineering; specific simulation of phenomena include convection [Yanagita and Kaneko, 1993], chemical waves [Kaneko, 1993], formation of sand dunes [Nishimori and Ouchi, 1993] and cloud formation [Yanagita and Kaneko, 1997]. CML has also been used as an alternative to other spatially explicit models such as IBM [Brännström and Sumpter, 2005].

2.2.7 Graph (Network) Models

A graph is a compact mathematical representation of the connectivity topology of complex systems. It consists of an ordered pair of disjoint sets $G = \langle V(G), E(G)\rangle$ such that $V(G) \neq \phi$ and $E(G) \subseteq \{\{u, v\} : u \neq v \in V(G)\}$, i.e. $E(G)$, the edge set, is a subset of the set of the unordered pairs of a nonempty vertex set $V(G)$ [Bollobás, 1979], implying that $|E(G)| \leq \binom{n}{2}$; $n = |V(G)|$[1].

G is called *regular (k-regular)* if each of its vertices has the same degree (k). It is *fully connected* ($k = n - 1$) if $|E(G)| = \binom{n}{2}$ and *random* if $kn/2$ out of all possible $\binom{n}{2}$ edges are chosen uniformly randomly with equal probability [Bollobás, 2001].

Structural properties : The most commonly used metrics to characterise structural properties of graphs are the characteristic path length and the clustering coefficient.

Characteristic path length ($\bar{L}$) The characteristic path length is a measure of the global structure of a graph (how well connected a graph is). In general, a path (a walk in which no vertex is visited more than once) from

[1] In graph theory, the size of the graph is generally denoted by $|E(G)|$ and the order of the graph by $|V(G)|$; however in complex systems theory, the size usually refers to the vertex set $|V(G)|$.

a vertex u to another vertex v in a graph G is a sequence of edges that are traversed from u to v with no edge traversed more than once (trail). There may exist more than one path from u to v in G. The length of a path is the number of edges. The shortest path (or geodesic) between two vertices u and v is the path between them with the smallest length. The Characteristic Path Length is the length of the shortest path $d_{uv} = \min_{l \in \text{paths}(u,v)} \text{length}(l) : u, v \in V(G)$ between any two vertices u and v, averaged over all pairs of vertices:

$$\bar{L} = \frac{1}{\binom{n}{2}} \sum_{u=1}^{n} \sum_{v>u}^{n} d_{uv} \tag{2.8}$$

where n is the order of the graph.

Clustering coefficient ($\bar{C}$) The clustering coefficient [Watts and Strogatz, 1998] is a measure of local graph structure – the "cliquishness" of a neighbourhood (how locally clustered a graph is). The open neighbourhood of a vertex v is $\Gamma_v = \{u \mid d(u,v) = 1\} \setminus \{v\}$, i.e. the set of vertices directly connected to v, but excluding v itself. The clustering coefficient of vertex v is the ratio of the actual number of edges realised in Γ_v to the number of possible edges:

$$C_v = \frac{|E(\Gamma_v)|}{\binom{k_v}{2}} \tag{2.9}$$

where $C_v \in [0,1]$, Γ_v is the neighbourhood of the vertex v, $|E(\Gamma_v)|$ is the number of actual edges in the neighbourhood of v, k_v is the number of vertices in the subgraph Γ_v (or equivalently $|\Gamma_v|$) and $\binom{k_v}{2}$ is the number of possible edges in Γ_v since a vertex v with k_v neighbours can have have at most $k_v(k_v-1)/2$ edges between them (the fully connected graph). $C_v = 1$ if every vertex in the neighbourhood of v is connected to every other vertex in the neighbourhood of v. $C_v = 0$ if no vertices in the neighbourhood of v are connected.

The clustering coefficient of the graph G, ($\bar{C}$) is the average neighbourhood clustering coefficient, or equivalently, the number of actual edges normalised

by number of possible edges and averaged over all the vertices $v \in V(G)$:

$$\bar{C} = \frac{1}{n} \sum_{v=1}^{n} C_v \tag{2.10}$$

where $\bar{C} \in [0, 1]$, n is the order of the graph and C_v is the clustering coefficient of vertex v in graph G.

For a complete graph we have $(k = n - 1)$, $\bar{C} = 1$, and for an empty graph $(k = 0)$, $\bar{C} = 0$ [Watts, 1999].

Proximity ratio Walsh [1999] introduced a quantitative measure of "small-worldliness" known as the proximity ratio, defined as the ratio $\bar{C}(p)/\bar{L}(p)$ normalised by $\bar{C}(1)/\bar{L}(1)$:

$$\mu = \frac{\bar{C}(p)}{\bar{L}(p)} \frac{\bar{L}(1)}{\bar{C}(1)} \tag{2.11}$$

where $\bar{L}(1)$ and $\bar{C}(1)$ are the characteristic path length and clustering coefficient of random graphs and $0 < p < 1$ is the randomness probability which introduces long range edges in the graph. Random graphs have a proximity ratio of 1, while lattice graphs have smaller proximity ratios. For graphs with a small world effect, $\mu \gg 1$.

Degree Distribution The degree of a node is the number of neighbours it is connected to. The degree distribution is defined as the normalised frequency distribution of degrees over the whole network. The degree distribution of a network is a simple property which helps to classify networks. The regular network with Moore neighbourhoods have the same degree $(k = 8)$ for all the nodes. The degree distribution of small-world networks (p in the small-world regime [Punithan and McKay, 2013b] follows a Poisson distribution with exponential tail. Networks in which most nodes have approximately the same number of neighbours are known as "egalitarian" networks [Buchanan, 2003].

Regular graphs have high local clustering ($\bar{C} \approx 3/4$ for $k \gg 2d$; where d is the dimension of the graph), but large global separation ($\bar{L} \approx n/2k$) [Watts, 1999, 2003]. Random graphs have low local clustering ($\bar{C} \approx k/n$) and short paths ($\bar{L} \approx \ln(n)/\ln(k)$) [Watts, 1999, 2003]. Fully connected (all-to-all) graphs have the maximum clustering coefficient of 1 and no spatial relations. Although fully connected graphs have large $\bar{C}$ and small $\bar{L}$, they are not sparse, with the number of edges being quadratic in the number of vertices. But real world graphs typically have the properties of high local clustering (large $\bar{C}$) as in regular graphs, and low characteristic path length (small $\bar{L}$) as in random or fully connected graphs. In addition, they are sparse: the number of edges is comparable to the number of vertices.

Small-world graph : Many real-world graphs are characterised by large size ($n \gg 1$), sparseness ($|E(G)| \ll \binom{n}{2}$), decentralisation ($n \gg k_{max} \gg 1$ – where k_{max} is the maximal degree over all vertices), and rich local clustering ($\bar{C} \gg \bar{C}_{random}$), but still show short paths ($\bar{L} \approx \bar{L}_{random}$) between pairs of vertices [Watts, 1999, 2003]. This structure derives from the existence of a few non-local long range connections. Such a graph is said to exhibit the 'small-world phenomenon'.

Small-world graphs can be created in a multitude ways. We use three methods: randomly rewiring the edges of a regular graph (WS), adding new edges to a regular graph (NW) and adding both new vertices and random edges to a regular graph (SW). In more detail:

Watts-Strogatz model The existing edges between the vertices in a d-dimensional k-regular graph are rewired uniformly randomly with probability $p \in [0, 1]$; that is, approximately $pnk/2$ edges are randomly removed, and the same number of new edges are added, where n is order of the graph and k is the number of neighbours. When the existing edge from a vertex is removed, a new edge is added from the same vertex to a randomly chosen vertex in the graph. After the rewiring process, each vertex has a varying number of edges (degree). The random rewiring does not change the size of the graph,

maintaining it as $nk/2$. Though this WS procedure preserves the number of connections in the original graph, it suffers from one deficiency: it does not guarantee that the resulting graph is connected.

As p increases, the properties of the graph change. When $p = 0$, no existing edge has been rewired, so the graph remains a regular graph. For small values of p, the graph remains highly clustered and highly connected. When $p = 1$, all the existing edges have been rewired, and the graph is similar to a random graph. In the WS model, the connectivity topology can be set anywhere between a completely regular graph and a random graph, through tuning the rewiring probability p.

Newman-Watts model Newman and Watts adapted the WS model to guarantee connectivity, by introducing a variant in which instead of rewiring the edges, additional long range edges are added with probability $p \in [0, 1]$ between randomly chosen vertices in the regular graph with k neighbours. In contrast to WS, no edges are removed, which means the local connectivity is not altered. After the addition of the extra edges, the number of neighbours at each vertex may vary, but it remains at least k. Thus we can guarantee that there are no disjoint vertices. This process changes the size of the graph.

When $p = 0$, no non local connections are added. When $p = 1$, k extra non local edges are added to each vertex in the graph. When p is between 0 and 1, [0, k] edges are added. Thus the linkage density increases over that for $p = 0$. With 0 or small values of p, the graph will be close to a regular graph. When $p = 1$ and $k = n - 1$, the resultant graph is fully connected.

Smallest-World model In this model, (np) new vertices are added and are connected to randomly chosen (k) vertices in the initial graph. No edges are deleted from the initial lattice. This process changes both the order and size of the graph. When $p = 0$, no new vertices and edges are added. When $p = 1$, n new vertices are added and nk edges are added.

The rewired or added edges are built independent of their spatial locations. As more are added, so-called small-world properties emerge; the region in which this occurs is known as the small-world regime. Within this regime, the graph is ordered locally but randomised globally.

Adaptive graph : The adaptive nature of the system is modelled via Dynamic Linking (DL), which is the key feature of adaptive networks and can be modelled in a number of ways:

1. Active vertices grow and inactive vertices lose edges
2. Active vertices lose edges and inactive vertices grow them
3. Vertices never lose edges; the graph evolves by either:
   (a) Adding new edges to active vertices from inactive vertices
   (b) Adding new edges to inactive vertices from active vertices
   (c) Adding reciprocal edges between vertices and inactive vertices

2.3 Quantification of Spatio-Temporal Dynamics

2.3.1 Permutation Entropy (PE):

Bandt and Pompe [2002] introduced Permutation Entropy (PE) as a measure to detect stationary, periodic, chaotic and random behaviour of a complex time series. Other metrics, for example the Lyapunov exponent, have been used to characterise a chaotic time series; we chose PE due to its conceptual simplicity and computational efficiency. Importantly, it is robust to noise and does not require any preprocessing of the data such as noise elimination. The PE of order $q \geq 2$ is defined as:

$$H_p(q) = -\sum p(\pi) \ln p(\pi) \tag{2.12}$$

where the sum is over all $q!$ permutations π of order q.

A normalised form, H_p, can be computed by:

$$0 \leq H_p = \frac{H_p(q)}{\ln(q!)} \leq 1 \tag{2.13}$$

where the lower bound denotes regularity in a time series and the upper bound represents a completely random system. In general, smaller values of q, such as 1 or 2, are not appropriate due to the small number of distinct states and larger values of q, such as 12 or 15, are also inappropriate since the aim is to detect the changes in the system [Cao et al., 2004]. Bandt and Pompe used $q = 3, ..., 7$ in their experiments. Hence we have chosen 7 as the order in our experiments.

2.3.2 Moran's I (MI):

Moran's I [Moran, 1950] is a measure of spatial autocorrelation, and is also used to analyse spatial patterns. It is defined as:

$$I = \frac{U}{\sum_i \sum_j w_{ij}} \frac{\sum_i \sum_j w_{ij}(P_i - \bar{P})(P_j - \bar{P})}{\sum_i (P_i - \bar{P})^2} \tag{2.14}$$

where U is the number of spatial units, indexed by i and j; P is the population size; $\bar{P}$ is the mean population; and w_{ij} is a spatial weight matrix. In our work, we use a binary weight matrix with $w_{ij} = 1$ if i and j are neighbours and 0 otherwise. The Moran's I value ranges from -1 to $+1$. Positive values indicate high spatial autocorrelation, while negative values indicate negative spatial autocorrelation, with 0 indicating no spatial correlation. In the context of pattern analysis, negative, 0 and positive values indicate spatially dispersed, random, and clustered patterns respectively.

Chapter 3

Homeostatic Complex System based on Daisyworld Modelling

Homeostasis is resistance to change. The most studied homeostatic systems are Ashby's homeostat [Ashby, 1962] (physical device) and Lovelock's daisyworld (a planetary mathematical model). Homeostat demonstrated ultrastability by maintaining the essential variables within a viability ranges in the face of externally imposed perturbations. Daisyworld model demonstrated homeostatic regulation of the environment by the biota. Daisyworld is an approach to design and analyse robust artificial homeostatic systems. Hence we take daisyworld as our base model for further investigations.

In this chapter, we reconstruct the original daisyworld model [Watson and Lovelock, 1983] based on Coupled Map Lattice (CML). We model life-environment feedback in diffusively coupled logistic systems in a 2D tordoidal regular lattice with chaotic local dynamics. Then we incorporate small-world phenomenon, scale-freeness and topology-dynamics feedback.

Our model differs from previous work [Wood et al., 2008, section 3] primarily in the following areas:

- Previous work generally used only presence/absence of daisies in a cell (hence the population model functioned as a form of cellular automaton). We use a finite population with a logistic carrying capacity model, permitting more detailed examination of population dynamics and of diffusion effects using Coupled Map Lattice(CML).
- As a result, previous work extending daisyworld spatially could only observe boom and bust temporal behaviour; because of the more detailed population dynamics in our model, we can observe other kinds of temporal fluctuations (including chaos) arising from spatial extension, and can analyse new and interesting spatio-temporal interactions in daisyworld.
- Previous work analysed the dynamics of daisyworld qualitatively. We use statistical quantifiers to measure the spatio-temporal dynamics of the daisyworld.
- We study the variation of the spatio-temporal dynamics with changes in the model parameters both qualitatively and quantitatively.
- We allow limiting similarity (sub section 3.2).
- Previous work are only based on regular lattice, we incorporate characteristics of complex and adaptive networks (sub section 3.3), such as
  - Small-world phenomenon
  - Adaptiveness
  - Scale-freeness

3.1 Reconstructed Core Daisyworld Model

Our version of daisyworld is a 2-lattice graph $G_{N,N}$ ($N = 100$ is the lattice length) of coupled dynamic units. We first construct a square regular lattice in a two-dimensional Euclidean space ($N \times N$) of unit-distance, each vertex having the same degree k. The k vertices are based on the Moore neighbourhood model ($k = 8$) and hence our graph is sufficiently sparse ($k \ll N * N$)

and also sufficiently dense ($k \gg 1$). We enforce periodic boundary conditions in this lattice to eliminate edge effects by wrapping the edges around, resulting in a torus.

Each vertex in the lattice represents a habitat (dynamical unit) and is constrained with a maximum vegetation (carrying capacity κ) of $10,000$ daisies to avoid unbounded behaviours, while each edge supports interactions between the units – the neighbourhood connectivities. There are k habitats in the neighbourhood Γ. Each such habitat (*discrete space*) contains real-valued attributes ($0 < P_b, P_w < 10,000$ and $278 < T < 313$K; P_b, P_w and T are *continuous states* representing black and white daisy population size and temperature respectively). The states are updated in *discrete time* by real-valued functions. Thus our constructed system is a complex dynamic system in which the continuous state habitats diffusively interact with their neighbours (coupled), evolve in discrete time (map) and are distributed on a discrete space (lattice) – a Coupled Map Lattice (CML). The attribute values evolve according to deterministic rules, depending both on their own value and those of their neighbours.

Each habitat (interating component) in our ecosystem is a system. The elements such as life (black and white daisies) and environment (temperature) are interconnected and interdependent via reinforcing and balancing feedback loops. The interaction rules among these system components are based only on local information (microscopic level) and not on the global emergence (macroscopic level). The black and white daisies, along with the temperature, diffuse around the world via their neighbourhood. At each succession of a habitat, we compute the population of black and white daisies, and the temperature, based on equation 2.7.

Our daisyworld model has two terms:

- A *reaction term* describing the growth of daisies and temperature change at a particular habitat
- A *coupling term* describing the dispersion of daisies and diffusion of temperature in their neighbourhood

These local components and their interaction rules at the microscopic level give rise to global emergence at the system level.

Table 3.1: Basic Equations

Name of the equation	**Equation**
Energy balance	$\sigma_B T^4 = SL(1-A)$
Logistic population growth	$P_{(t+1)} = P_t \left[1 + r\left(1 - \frac{P_t}{\kappa}\right)\right]$
Logistic population growth with temperature feedback	$P_{(t+1)} = P_t \left[1 + r\left(\beta(T) - \frac{P_t}{\kappa}\right)\right]$
Discrete Laplacian diffusion	$x'_{(i,j,t)} = (1-\epsilon)x_{(i,j,t)} + \frac{\epsilon}{k}\sum_{<l,m>}^{k} x_{l,m,t)}$
Reaction diffusion of a dynamic variable (x)	$x_{(i,j,t+1)} = f\left(x'_{(i,j,t)}\right)$
Reaction diffusion extended form	$x_{(i,j,t+1)} = f\left((1-\epsilon)x_{(i,j,t)} + \frac{\epsilon}{k}\sum_{<l,m>}^{k} x_{l,m,t)}\right)$

Table 3.2: Daisyworld Model Equation Set

Parameter Name	**Equation**
Albedo	$A_{(i,j,t)} = A_b(\alpha_b)_{(i,j,t)} + A_w(\alpha_w)_{(i,j,t)} + A_g(\alpha_g)_{(i,j,t)}$
Growth rate	$\beta_c(T_{(i,j,t)}) = \max\left(1 - \left[\frac{(T_{\mathrm{opt}_c} - T_{(i,j,t)})^2}{17.5^2}\right], 0\right)$
Temperature	$T_{(i,j,t+1)} = g\left((1-D)T_{(i,j,t)} + \frac{D}{k}\sum_{<l,m>}^{k} T_{(l,m,t)}\right)$ $g\left(T'_{(i,j,t)}\right) = T'_{(i,j,t)} + \left[\frac{\left(SL(1-A_{(i,j,t)}) - \sigma_B (T'_{(i,j,t)})^4\right)}{C}\right] + \xi$
Population size	$P_{c(i,j,t+1)} = h\left((1-D_c)P_{c(i,j,t)} + \frac{D_c}{k}\sum_{<l,m>}^{k} P_{c(l,m,t)}\right)$ $h\left(P'_{c(i,j,t)}\right) = P'_{c(i,j,t)}\left[1 + r\left(\beta_c(T_{(i,j,t)}) - \frac{P'_{c(i,j,t)}}{\kappa}\right)\right]$

Reaction Term

Population Dynamics The local population dynamics at each location is computed using Verhulst dynamics (logistic equation with carrying capacity); it is of interest due to its chaotic behaviour over a specific range of bifur-

cation parameter values. The logistic population growth model with carrying capacity can lead to a density dependent population regulation (equation 2.1).

We also incorporate the temperature feedback effect in the logistic equation. The computation of population size with temperature feedback uses a difference equation based on Maddock [1991]:

$$P_{(t+1)} = P_t \left[1 + r\left(\beta(T) - \frac{P_t}{\kappa}\right)\right] \tag{3.1}$$

where $\beta(T)$ is temperature feedback; refer equation 3.4.

Temperature Dynamics The emitted radiation is defined by the Stefan-Boltzmann law as $E_{out} = \sigma_B T^4$ where σ_B is the Stefan-Boltzmann constant, and T is the temperature. The absorbed energy is computed as $E_{in} = SL(1 - A)$ where S is the solar constant, L is the luminosity and A is the albedo. At equilibrium, absorbed and emitted radiation follows Kirchhoff's law. Thus we can compute the temperature change at each location based on the planetary energy balance equation [McGuffie and Henderson-Sellers, 2005]:

$$\sigma_B T^4 = SL(1 - A) \tag{3.2}$$

Coupling Term

The interaction pattern of daisyworld is determined by the neighbourhood and the diffusion model.

Neighbourhood Model Since cliques are not captured in an open von Neumann neighbourhood, we choose Moore neighbourhoods. In any ecosystem, both species and temperature of our model diffuse around the world via their neighbourhood.

Diffusion Model We use a Laplacian diffusion model (or Turing diffusion). The diffusion model is detailed in the section 2.2.6.

The population and temperature update functions in our daisyworld model are based on the above basic equations (equation 3.1 and equation 3.2) from population dynamics and thermodynamics combining the spatio-temporal modelling (equations in the section 2.2.6). The basic set of equations is tabulated in Table 3.1.

3.1.1 Solar Insolation

Let us assume that there is no life in a Daisyworld. In this case, the albedo of the planet is that of bare ground, i.e. 0.5. The desired environmental temperature is $295.5K$ with solar luminosity 1.0. Substituting these values in equation 3.2 (energy balance), the required solar insolation is $864.65Wm^{-2}$; we use this value in all our experiments.

3.1.2 Albedo

The albedo (A) at a lattice point (i, j) and at time (t) is

$$A_{(i,j,t)} = A_b\alpha_{b_{(i,j,t)}} + A_w\alpha_{w_{(i,j,t)}} + A_g\alpha_{g_{(i,j,t)}} \tag{3.3}$$

i.e. the average of the albedos A_b of ground covered by black daisies, A_w of ground covered by white daisies and A_g of bare ground, weighted by $\alpha_b, \alpha_w, \alpha_g (= 1 - \alpha_w - \alpha_b) \in [0, 1]$, the relative areas occupied by black, white daisies and bare ground at time t. We assume that $A_w > A_g > A_b$, with corresponding values of 0.75, 0.5, 0.25. In our experiments, bare ground is completely occupied within the first few epochs.

3.1.3 Growth

The growth curve of daisies (β_c) is an inverted parabola:

$$\beta_c(T_{(i,j,t)}) = \max\left(1 - \left[\frac{(T_{\text{opt}_c} - T_{(i,j,t)})^2}{17.5^2}\right], 0\right) \tag{3.4}$$

$T_{(i,j,t)}$ is the local temperature and T_{opt_c} is the optimal temperature of the species. The optimal temperature of the daisies depends on their petal colour 'c' (phenotype). The optimal temperature for black daisies is lower than for white; the mean optimal temperature is assumed to be $295.5K$.

3.1.4 Temperature

The temperature $(T_{(i,j,t+1)})$ is computed as the sum of temperature after Laplacian diffusion $(T'_{(i,j,t)})$, the difference between solar absorption and heat radiation incorporating $T'_{(i,j,t)}$, and Gaussian white noise:

$$T_{(i,j,t+1)} = g\Big((1-D)T_{(i,j,t)} + \frac{D}{k}\sum_{<l,m>}^{k} T_{(l,m,t)}\Big) \tag{3.5}$$

where $T_{(i,j,t)}$ is local temperature , $< l, m >$ represents the set of neighbours of (i, j) and $D = D_T/C$ is the thermal diffusion constant normalised by heat capacity C. $g(T'_{(i,j,t)})$ is the temperature update function [Wood et al., 2008], in which $T'_{(i,j,t)}$ is the temperature after diffusion:

$$g\Big(T'_{(i,j,t)}\Big) \quad = \quad T'_{(i,j,t)} + \left[\frac{\Big(SL(1-A_{(i,j,t)}) - \sigma_B(T'_{(i,j,t)})^4\Big)}{C}\right] + \xi \tag{3.6}$$

where S is the solar constant, L is the luminosity, $A_{(i,j,t)}$ is the albedo, σ_B is the Stefan-Boltzmann constant and ξ is additive Gaussian white noise (with mean 0 and standard deviation 1.0) multiplied by the noise level (NL).

3.1.5 Population Size

The local population update depends on dispersion, density-dependant growth rate and the feedback coefficient:

$$P_{c_{(i,j,t+1)}} = h\Big((1-D_c)P_{c_{(i,j,t)}} + \frac{D_c}{k}\sum_{<l,m>}^{k} P_{c_{(l,m,t)}}\Big) \tag{3.7}$$

where $P_{c_{(i,j,t)}}$ is the population size at location (i, j) and time step t, D_c is the fraction of the population being dispersed to its neighbours, c stands for colour of daisies and k is number of neighbours. $h(P'_{c_{(i,j,t)}})$ is the population growth function and $P'_{c_{(i,j,t)}}$ is population size after dispersion:

$$h\left(P'_{c_{(i,j,t)}}\right) = P'_{c_{(i,j,t)}}\left[1 + r\left(\beta_c(T_{(i,j,t)}) - \frac{P'_{c_{(i,j,t)}}}{\kappa}\right)\right] \tag{3.8}$$

where r is population increase rate, $\beta_c(T_{(i,j,t)})$ is the feedback due to temperature and κ is the carrying capacity. Thus the population density at a habitat is controlled by the density dependence at that location and dispersal to its nearest neighbours. In general simulations, deterministic chaos is observed only at high values for the increase rate. But deterministic chaos can also be induced by diffusion, so our system does not require high intrinsic growth rates to exhibit interesting behaviours.

The above set of equations (from 3.3 to 3.8) from thermodynamics and population dynamics integrate well and generate the couplings between life and the environment. Daisy population size (P) depends on the growth rate (β) which depends on the environmental variable temperature (T) which depends on the environment altering trait albedo (A) which is influenced by the daisy cover (P). These interdependencies among the physical variables of interest form a tightly coupled system with an endless feedback loop. The computation of these variable are tabulated in the Table 3.2 for easy understanding.

3.2 Limiting Similarity (Temperature Overlap)

Limiting similarity defines a level of overlap between any two species that allows them to coexist. The range of temperature regimes in which daisies can survive is the viability constraint of our model, and is based on the overlap between the optimal temperatures of black and white daisies as in Table 3.3. We define the optimal temperature of black daisies within the range $[278, 295.5]K$

Table 3.3: Optimal Temperature (of black and white daisies with respect to overlap)

Overlap(%)	**Opt. temp. (K) black daisies**	**Opt. temp. (K) white daisies**
0	278	313
10	284.5	306.5
25	288	303
50	291.5	299.5
100	295.5	295.5

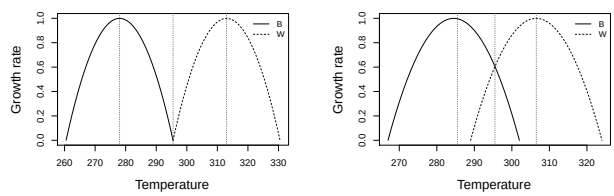

(a) Overlap0

(b) Overlap10

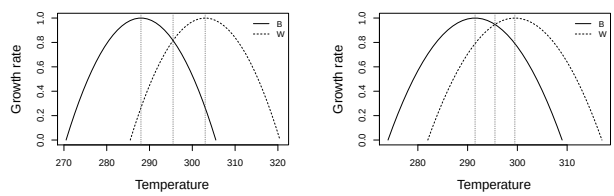

(c) Overlap25

(d) Overlap50

Figure 3.1: Overlap of Growth Curves of Black and White Daisies

and of white in the range $[295.5, 313]K$ so as to have an overlap in the range $[0, 100]\%$ (Figure 3.1). When the overlap is 100%, the two growth curves superimpose on each other.

3.3 Incorporation of Complex Topological Properties

We have investigated daisyworld phenomenon in regular (chapter 4 and sub section 5.2.2), random (sub section 5.2.3), fully-connected (sub section 5.2.4), small-world (section 5.3), adaptive topologies (section 5.4) and scale-free (section 5.5). The changes to the underlying topology (regular) are described in their corresponding chapters.

1. We start with an ecosystem where habitats are only locally connected (regular CML with Moore neighbourhood). The experiments described in the chapter 4 are based on regular lattice.

2. We rewire or add random non-local couplings to the underlying regular lattice, which introduces small-world effects in system (Watts-Strogatz model, Newman-Watts model and Smallest World model in CML). The experiments described in the section 5.3 incorporate small-world phenomenon.

3. Each frozen vertex in the underlying regular lattice is dynamically and reciprocally coupled to a randomly chosen active vertex (adaptive CML). The experiments described in section 5.4 are adaptivly acquire connections based on the local dynamics.

4. Each vertex in the lattice reciprocally connected to hub vertices or to local vertices or to non-local vertices. The experiments described in section 5.5 incorporate scale-freeness.

In complex and adaptive topologies, species (black and white daisies) –through the mix of local and long range couplings– can disperse quickly around the daisyworld but temperature diffuses only via the local neighbours to other parts of the world. The inclusion of even a few long-range interactions in the underlying topology leads to highly interconnected dynamical units, exhibiting a significant effect on daisyworld dynamics.

3.4 Experimental Setup

3.4.1 Parameter Settings

Table 3.4: Daisyworld Parameter Settings (last six rows are variable parameters, others are fixed)

Parameter	**Value(s)**
Fixed	
Number of cells ($N \times N$)	100×100
Bare ground Albedo (A_g)	0.5
Albedo of black daisies (A_b)	0.25
Albedo of white daisies (A_w)	0.75
Heat capacity (C)	2500 $Wm^{-2}K^{-1}$
Diffusion constant (D_T)	500 $Wm^{-2}K^{-1}$
Stefan-Boltzmann constant (σ_B)	5.67 $E^{-8}Wm^{-2}K^{-4}$
Solar constant (S)	$864.65Wm^{-2}$
Luminosity (L)	1
Mean growth temperature	$295.5K$
Carraying capacity (κ)	10000
Time step (t)	1
Horizontal grid size (i)	1
Vertical grid size (j)	1
Variable	
Opt. temp. of black daisies (T_{opt_b})	$[278, 295.5]K$
Opt. temp. of white daisies (T_{opt_w})	$[295.5, 313]K$
Diffusion rate of black daisies (D_b)	$[0, 1]$
Diffusion rate of white daisies (D_w)	$[0, 1]$
Noise level (NL)	$[0, 10]K$
Natural rate of increase (r)	$[1, 4]$

The model parameters for the simulation are shown in Table 3.4. They are adapted from the parameter values used in the wider daisyworld literature, modified to fit a CML model [von Bloh et al., 1997; Watson and Lovelock, 1983]. The last six rows in Table 3.4 are variable parameters, while the rest are the fixed parameters. As we have a huge parameter space, we have restricted

our experiments to an increase rate of $r = 1$. We have used the same diffusion constant for both black and white daisies in all our experiments. We have limited our focus to studying the effects of species diffusion (which influences the species distribution) and noise (which influences the temperature) in detail. The range of temperatures in which daisies can survive is the viability constraint of our model, and is based on the overlap between the optimal temperatures of black and white daisies as in Table 3.3. We define the optimal temperature of black daisies within the range $[278, 295.5]$K and of white in the range $[313, 295.5]$K so as to have an overlap in the range $[0, 100]\%$. The variable parameter differs for different set of experiments and are tabulated in their corresponding chapters.

3.4.2 Initializations

All habitats in the lattice are randomly initialised with a population size in $[0, 100]$ for both black and white daisies. The temperature is initialised randomly depending on the overlap between the optimal temperatures of black and white daisies (Table 3.3).

3.4.3 Visualisations

We capture snapshots from the evolution of daisyworld to inspect its spatio-temporal dynamics. Each snapshot represents the population structure of the ecosystem at the particular epoch. As it is impractical to show all the snapshots over $5,000$ epochs, we plot the temporal dynamics of daisy populations and temperature at a particular habitat as well as the temporal dynamics of the average daisy populations and temperature of the whole ecosystem. These plots reflect the local and global behaviours of the daisyworld. In the visualisations, a habitat is shown as black if black daisies alone occupy that habitat and correspondingly for white. If both daisies coexist at a habitat but black dominates, it is shown as dark grey; if white dominates, it is presented as light grey; and if the populations are equal, it is represented as medium grey.

Chapter 4

Daisyworld with Local Couplings

In this chapter, we investigate two-dimensional (2D) CML based daisyworld with only local couplings. In the section 4.1, we analyse daisyworld as self-organizing system, reaction-diffusion system (activator-inhibitor system), complex dynamical system and pattern formation system based on biological inspirations from nature. In section 4.2, we investigate local chaoticity and global stability dynamics of daisyworld. We examine the evolutionary dynamics of daisyworld in the section 4.3. In section 4.4, we introduce methods to analyse a huge parameter space with spatio-temporal quantifiers.

4.1 Self-Organizing Spatio-temporal Patterns

In this section, we examine self-organized, spatio-temporal patterns from our 2D CML based daisyworld with only local couplings. We investigate the self-organizing properties of daisyworld, and qualitatively analyse pattern formation in daisyworld. We also quantify the emergence of vegetation patterns using a statistical measure, Moran's I. We show that the surface temperature of planet is self-regulated around the mean 295.5K by the daisyworld dynamics regardless of the varied self-organized pattern formations.

In our daisyworld model, depending on model parameter values we observe a variety of behaviours, such as 1) complex patterns, 2) Turing-like structures, 3) cyclical patterns, 4) random patterns and 5) uniformly dispersed patterns.

4.1.1 Variable Parameter Settings

Table 4.1: Variable Parameter Settings

Parameter	**Value**
Overlap	$\{0, 5, 10, 25, 50, 100\}\%$
Natural rate of increase (r)	$[1, 4]$
Noise level (NL)	$\{0, 0.001, 0.005, 0.01, 0.05,$ $0.1, 0.2, 0.5, 1, 2.5, 5, 7.5, 10\}$
Temperature diffusion (D)	$\{0, 0.05, 0.1, 0.2, 0.3, 0.5, 1\}$
Dispersion rate (D_c)	$\{0, 0.001, 0.01, 0.1, 0.2, 0.5, 1\}$

We have run over $15,000$ experiments on this CML based daisyworld model, with each experiment running for 5000 epochs. The ranges for the various parameters are shown in Table 4.1. The results presented in the following sub sections are samples from over 15,000 experiments with different variable parameter settings. We have examined the results for the emergence of interesting patterns both qualitatively (by capturing snapshots of each experiment and inspecting visually and by plotting cobwebs) and quantitatively (using the value of Moran's I).

4.1.2 Self-organized Complex Pattern

A maze-like self-organizing pattern (Figure 4.1) emerge from our system with a temperature overlap of 10%, species dispersion rate of 0.001, and a noise level of 0.001. After some cyclical behaviour, the system finally converged to a stationary maze-like structure. The global spatial behaviour is plotted in the Figure 4.3. The sub Figure 4.3 (a) shows that the global temperature fluctuates initially, but converges to $295.5K$ and the sub Figure 4.3 (b) displays a static average population of black and white daisies, exhibiting a stationary

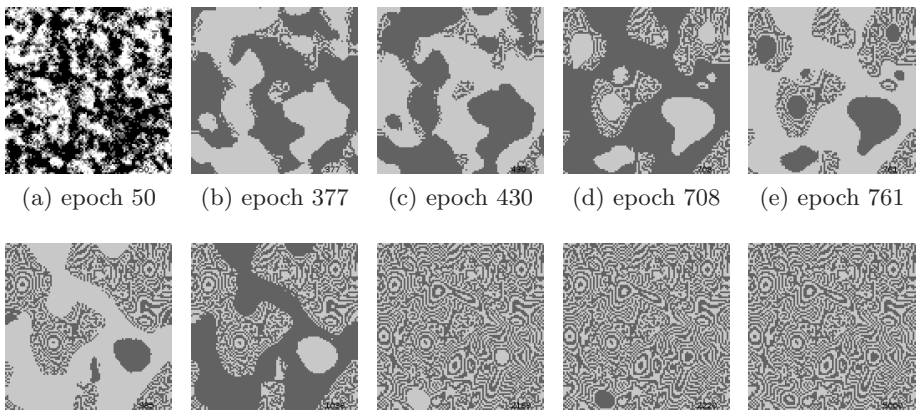

(a) epoch 50 (b) epoch 377 (c) epoch 430 (d) epoch 708 (e) epoch 761

(f) epoch 985 (g) epoch 1036 (h) epoch 2169 (i) epoch 2220 (j) epoch 5000

Figure 4.1: Maze like Organization for 10% Overlap, $D_c = 0.001$, $D = 0.2$, $r = 1$ and NL= 0.001 in 2D 100×100 Lattice

pattern formation. Initially the Moran's I is very high (sub Figures 4.3 (c) and 4.3 (d)), indicating the formation of very large clusters, but it finally drops below 0, indicating a uniformly dispersed pattern. In between, the fluctuations show complex dynamics. The local behaviours at a particular habitat is depicted in the Figure 4.2. The local temperature (sub Figure 4.2 (a)) and population (sub Figure 4.2 (b)) confirms stationary dynamics. The straight lines in coweb plots 4.2 (c) and 4.2 (d) also indicate the static dynamics (stationarity) of black and white daisy populations.

4.1.3 Turing-like Structure

Turing-like patterns emerge with a diffusion constant of 0.01 for both species, a noise level of 1 and an overlap of 100% – refer to Figure 4.4. This clearly shows self-organized pattern emerge with time. The patterns which emerge look like an animal's coat (e.g. Holstein cow). The corresponding global dynamics are plotted in Figure 4.6. The fluctuations in global temperature in sub Figure 4.6 (a) shows the dynamicity (non-stationary) of pattern formation. The sub Figure 4.6 (b) depicts the global population dynamics. The high

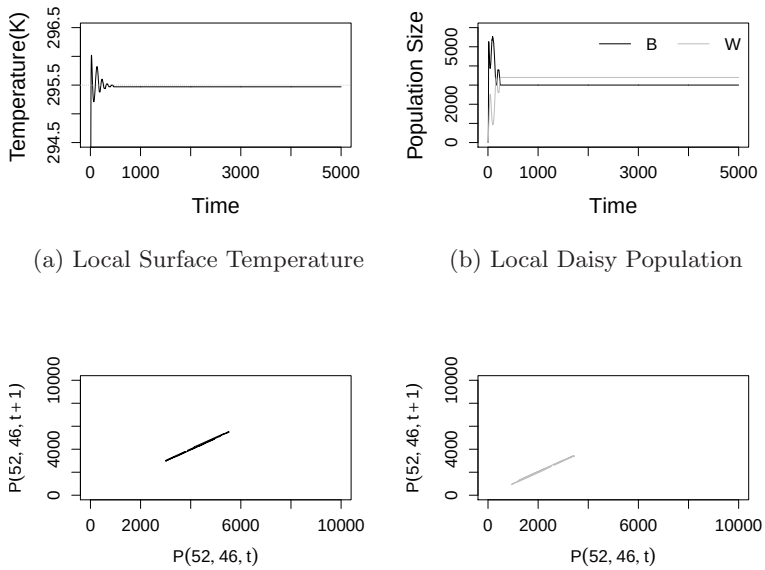

(a) Local Surface Temperature

(b) Local Daisy Population

(c) Local Black Daisy Cobweb

(d) Local White Daisy Cobweb

Figure 4.2: Local Dynamics of Maze : 10% Overlap, $D_c = 0.001$, $D = 0.2$, $r = 1$ and NL= 0.001 in 2D 100×100 Lattice

Moran's I throughout the run (except the initial transitions) corresponds to the emergence of large clusters in the patterns (sub Figures 4.6 (c) and 4.6 (d)). The local dynamics can be observed in the Figure 4.5. The cowebs displays chaoticity within the range $[4000, 6000]$ – population size.

4.1.4 Cyclical Pattern

Cyclical patterns are formed (Figure 4.7) from the system with a temperature overlap of 10%, dispersion rate of 0.2 for both the species, and noise level of 0.05. The corresponding global dynamics are plotted in Figure 4.9. The cycles in the global temperature (sub Figure 4.9 (a)) indicate the cyclical dynamics of the daisy population (sub Figure 4.9 (b)). Except for the initial states, Moran's I is high throughout the run, confirming the formation of large clusters (sub

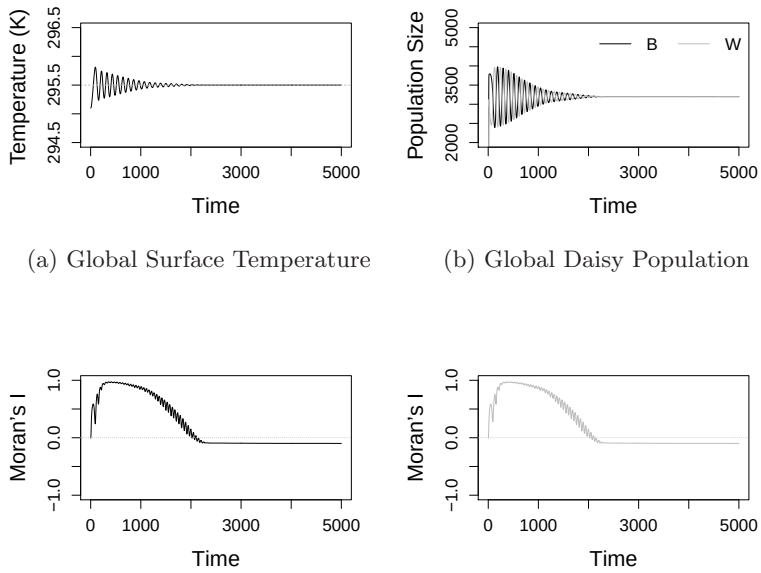

(a) Global Surface Temperature

(b) Global Daisy Population

(c) MI Black Daisy

(d) MI White Daisy

Figure 4.3: Global Dynamics of Maze : 10% Overlap, $D_c = 0.001$, $D = 0.2$, $r = 1$ and NL= 0.001 in 2D 100×100 Lattice

Figures 4.9 (c) and 4.9 (d)). The local dynamics are plotted in the Figure 4.8. The cobweb plots 4.8 (c) and 4.8 (d) depict cyclical abundance of black and white daisies. The cycles seen in local temperature and population plots (sub Figures 4.8 (a) and 4.8 (b)) confirm the cyclical pattern formation.

4.1.5 Random Pattern

Figure 4.10 depicts the global dynamics of random pattern formation in the daisyworld system for a noise level of 0.01 and with no species dispersion. The global temperature dynamics is shown in sub Figure 4.12 (a) and corresponding daisy abundance is plotted in sub Figure 4.12 (b). The near-zero value of Moran's I in sub Figures 4.12 (c) and 4.12 (d) confirm the formation of random patterns. The local dynamics are plotted in the Figure 4.11.

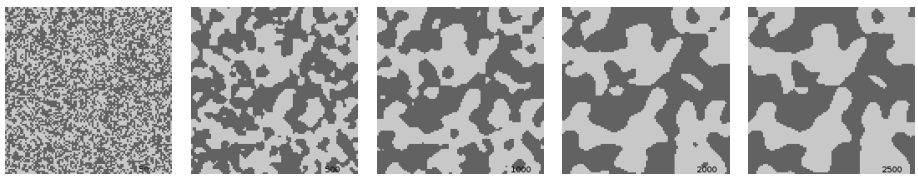

(a) epoch 50 (b) epoch 500 (c) epoch 1000 (d) epoch 2000 (e) epoch 2500

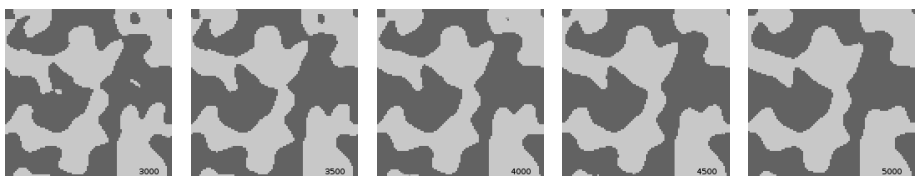

(f) epoch 3000 (g) epoch 3500 (h) epoch 4000 (i) epoch 4500 (j) epoch 5000

Figure 4.4: Turing-like Structure for 100% Overlap, $D_c = 0.01$, $D = 0.2$, $r = 1$, $NL = 1$ in 2D 100×100 Lattice

4.1.6 Dispersed Pattern

Uniformly dispersed patterns emerge at a of noise level 0.5 with no species diffusion (Figure 4.13); the corresponding global dynamics are depicted in Figure 4.15. Moran's I in sub Figures 4.15 (c) and 4.15 (d) lie below zero, indicating dispersed patterns. Interestingly, we do see the emergence of a hint of a large scale grid in this setting, presumably resulting from the effects of temperature diffusion. The local dynamics are depicted in the Figure 4.14.

4.1.7 Discussion

Global Emergence: The behavioural rules in the system specify that black daisies grow better in colder temperatures, while white daisies grow better in hotter temperatures, both diffusing to their nearest neighbours. These simple components at the local level generate complicated dynamics at the global level due to the collective behaviour of the whole system, without the influence of any external forces. The interaction pattern is determined by the neighbourhood topology and the diffusion term. The key ingredients leading to global emergence are the local nonlinear interactions among the components,

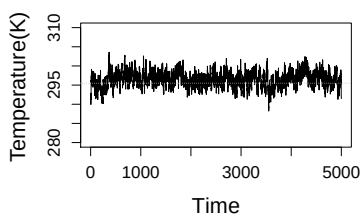

(a) Local Surface Temperature

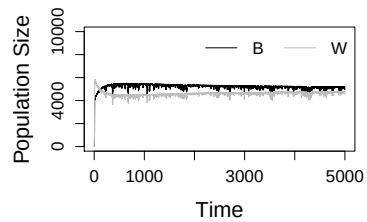

(b) Local Daisy Population

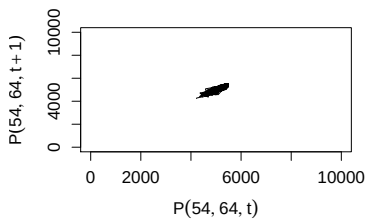

(c) Local Black Daisy Cobweb

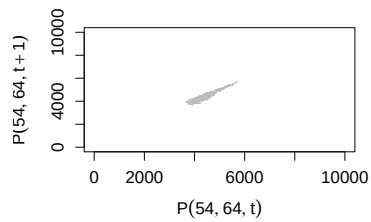

(d) Local White Daisy Cobweb

Figure 4.5: Local Dynamics of Turing-like Structure : 100% Overlap, $D_c = 0.01$, $D = 0.2$, $r = 1$ and NL= 1 in 2D 100×100 Lattice

physiological and behavioural rules, and physical constraints. The inhibition of self-growth can also arise from the physical constraints, due to the self-limiting factor of carrying capacity.

Daisyworld as a Dynamical System We examine our formulation at a point with NL=0.1 and 100% overlap. The corresponding bifurcation plots in the Figures 4.16 and 4.17 illustrate that the reconstructed daisyworld system is a dynamical system. The plots show fixed point attractors, bifurcations and strange attractors.

Daisyworld as Self-organizing System In daisyworld, an initial growth of black daisies, due to positive feedback, increases the temperature of system

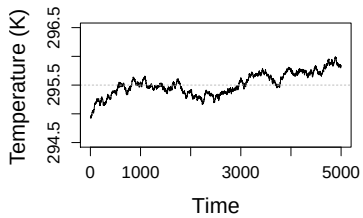

(a) Global Surface Temperature

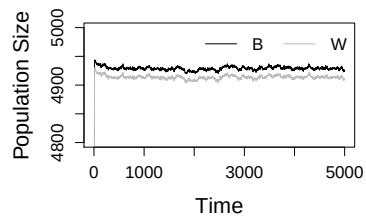

(b) Global Daisy Population

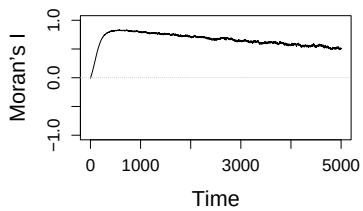

(c) MI Black Daisy

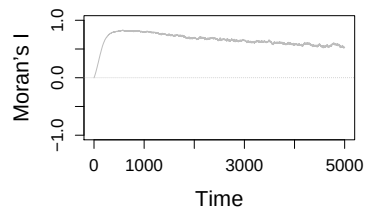

(d) MI White Daisy

Figure 4.6: Global Dynamics of Turing-like Structure : 100% Overlap, $D_c = 0.01$, $D = 0.2$, $r = 1$ and NL= 1 in 2D 100×100 Lattice

and thus reinforces the change in the same direction. Hence it has the potential to explode the system. But in daisyworld, at a higher temperature, white daisies bloom and keep the positive feedback under control. In the same manner, the growth of white daisies, due to positive feedback, decreases the temperature in the same direction. But at a colder temperature, black daisies bloom and inhibit the system behaviour. The initial growth of daisies promotes new changes in the system state but on the other hand, increased growth counteracts the changes. The combined effect of positive and negative feedback couplings result in a negative feedback loop, which stabilises the physiological processes and leads to homeostasis. Due to this behaviour, we can see that daisyworld is a self-organizing system.

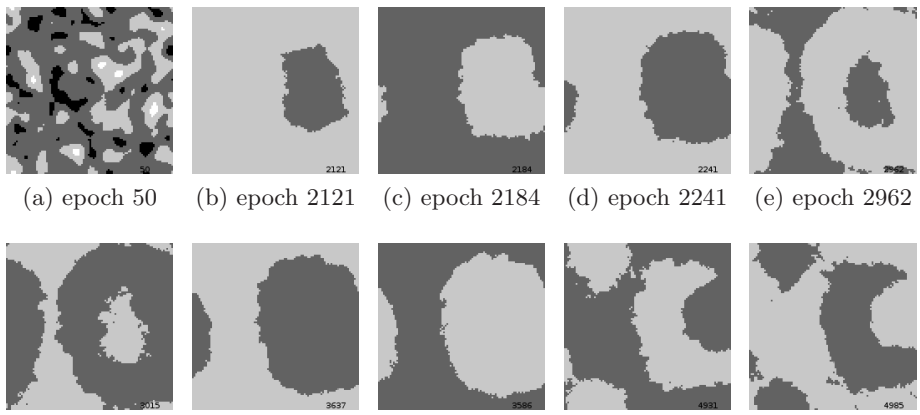

(a) epoch 50 (b) epoch 2121 (c) epoch 2184 (d) epoch 2241 (e) epoch 2962

(f) epoch 3015 (g) epoch 3637 (h) epoch 3586 (i) epoch 4931 (j) epoch 4985

Figure 4.7: Cyclical Pattern : 10% overlap, $D_c = 0.2$, $D = 0.2$, $r = 1$ and NL= 0.05 in 2D 100×100 Lattice

Daisyworld as Reaction-Diffusion System We can view daisyworld as a Turing reaction-diffusion system of two morphogens: black and white daisies. In cooler temperatures, black daisies absorb the available sun light and amplify their growth, functioning as activators (autocatalysis) because they activate their own production. But further increase in black daisies increases the surface temperature to the level at which cooler white daisies grow well, thereby acting as an inhibitor (self-suppression) because they inhibit their own production. This process is reversed for white daisies. Depending on the temperature, black and white daisies act both as inhibitor and as activator. Here, the diffusion of the two species, coupled by nonlinear local rules, result in the generation of patterns and spatial self-organization due to symmetry-breaking instability.

4.1.8 Summary

The results in this section illustrate that the underlying dynamics of daisyworld are not restricted to stationary patterns but extend to periodic and chaotic behaviour. We see stability as well as complexity emerge. The fig-

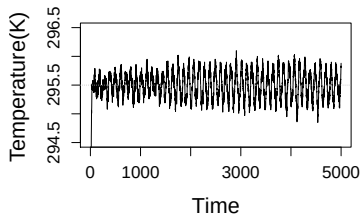

(a) Local Surface Temperature

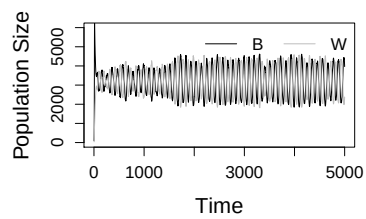

(b) Local Daisy Population

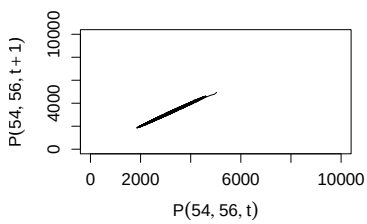

(c) Local Black Daisy Cobweb

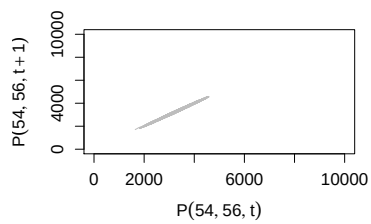

(d) Local White Daisy Cobweb

Figure 4.8: Local Dynamics of Cyclical Pattern : 10% overlap, $D_c = 0.2$, $D = 0.2$, $r = 1$ and NL= 0.05 in 2D 100×100 Lattice

ures clearly show the spatial patterns and temporal behaviour of daisyworld. Moran's I quantifies the pattern formation accurately, demonstrating its reliability in spatially quantifying a wide spectrum of patterns. The global temperature in all cases is self-regulated around $295.5K$.

The localised interaction of species (black and white daisies) in our daisyworld model generate an array of fascinating spatio-temporal patterns, due to endogenous self-organization resulting from "symmetry-breaking instability". In our nonlinear reaction-diffusion system, symmetry-breaking is induced by species dispersion, temperature diffusion and noise. A low species dispersion rate combined with noise leads to complex self-organized patterns (Figure 4.1). As species dispersion and noise increase, periodic (Figure 4.7) and dynamic chaotically evolving patterns (Figure 4.4) emerge. In the absence of species

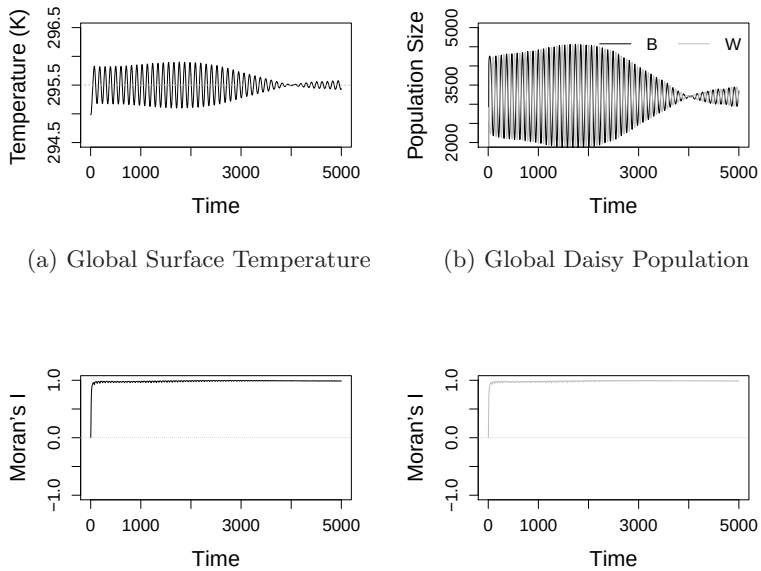

(a) Global Surface Temperature

(b) Global Daisy Population

(c) MI Black Daisy

(d) MI White Daisy

Figure 4.9: Global Dynamics of Cyclical Pattern : 10% overlap, $D_c = 0.2$, $D = 0.2$, $r = 1$ and NL= 0.05 in 2D 100×100 Lattice

dispersion, random (Figure 4.10) and dispersed (Figure 4.13) patterns emerge. We thus see the constructive roles of spatial diffusion, nonlinear local rules and noisy fluctuations in influencing the physiological, behavioural rules and physical constraints and thereby self-organizing the daisyworld. In addition, we have also demonstrated that our system as dynamical system and reaction-diffusion (activator-inhibitor) system.

4.2 Locally Chaotic and Globally Stable Dynamics (Temporal Fluctuations and Spatial Stability)

We first visually inspect the spatial dynamics of the system. We have collected snapshots from the evolution of Daisyworld in order to characterise the

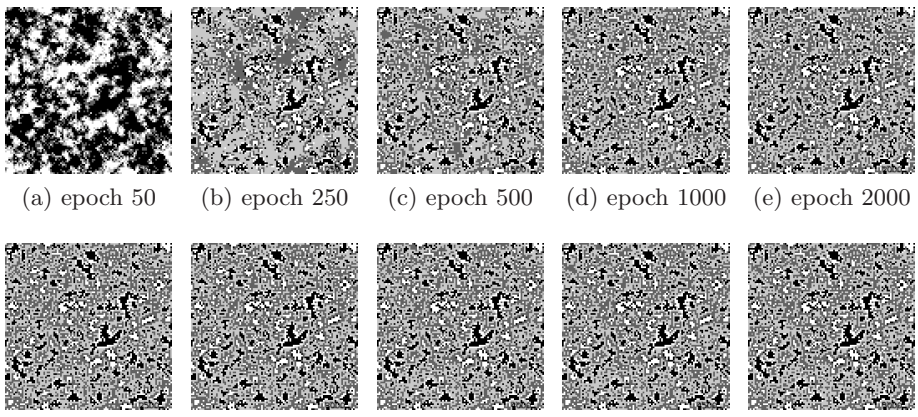

(a) epoch 50 (b) epoch 250 (c) epoch 500 (d) epoch 1000 (e) epoch 2000

(f) epoch 2500 (g) epoch 3000 (h) epoch 4000 (i) epoch 4500 (j) epoch 5000

Figure 4.10: Random Pattern : 10% Overlap, $D_c = 0$, $D = 0.2$, $r = 1$ and $NL = 0.01$ in 2D 100×100 Lattice

dynamics. For illustration purposes, we show the state of the Daisyworld at time step 1 (initial), 500 (i.e. after the system's behaviour has stabilised from any initial behaviours), 1000 (so that the system's behaviour can be compared over a long period), 1010 (so that we can see any short-term dynamicity), 2000, 2500, 3000, 3500 and 4000 (as intermediate epochs) and 5000 (the limit of the epochs).

Figure 4.18 depicts a typical succession of the ecosystem over time. We observe that black or white daisies form individual dominant clumped/patchy clusters, and coexistence of black and white occurs only at the boundaries. These boundary zones expand and contract depending on the local temperature and local population density of each daisy type. This is an example of a community that has a distinct boundaries which are driven by physical conditions that influence them. The boundaries of the daisy populations form patterns, and these patterns define the community structures. The communities are dynamic, changing over time. Though the initial frame appears greyish, the system breaks symmetry and evolves to more spatially heterogeneous coexisting dissipative patches, due to the recolonisation of the population from neighbouring patches via short-range dispersal.

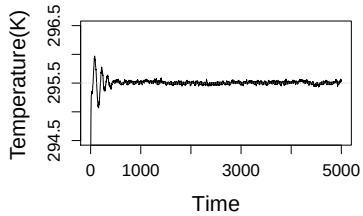

(a) Local Surface Temperature

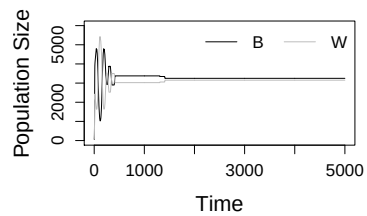

(b) Local Daisy Population

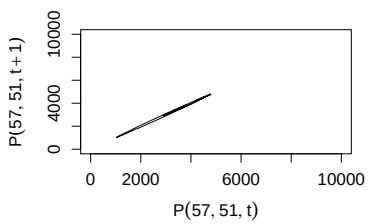

(c) Local Black Daisy Cobweb

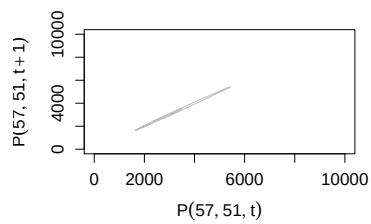

(d) Local White Daisy Cobweb

Figure 4.11: Local Dynamics of Random Pattern : 10% Overlap, $D_c = 0$, $D = 0.2$, $r = 1$ and $NL = 0.01$ in 2D 100×100 Lattice

Once daisies start germinating at a location, they spread to the neighbourhood, and hence the neighbouring environment is modified and a set of micro-environments is formed. Thus the daisy population creates a form of distributive patchy landscape, separating the habitable sites and inhospitable sites, due to environmental heterogeneity. These microclimates are then modified by the increased growth of a particular type of daisy. Such mosaic occurrence of species in patchy environments is an ubiquitous feature in ecological communities.

The changes appear essentially random to the naked eye. While there is persistence over short timespans (epochs 1000 and 1010 closely resemble each other), there is essentially no persistence over long timespans (it is difficult to detect any hint of previous clusters from a particular epoch when one examines

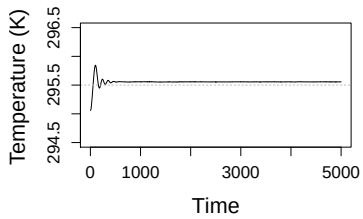

(a) Global Surface Temperature

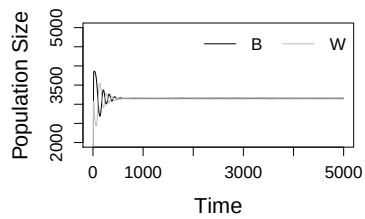

(b) Global Daisy Population

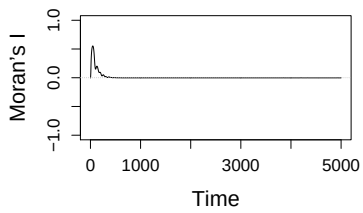

(c) MI Black Daisy

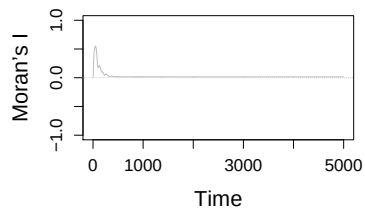

(d) MI White Daisy

Figure 4.12: Global Dynamics of Random Pattern : 10% Overlap, $D_c = 0$, $D = 0.2$, $r = 1$ and $NL = 0.01$ in 2D 100×100 Lattice

the population 500 epochs later).

4.2.1 Spatial Stability

To fill in the gaps between the spatial snapshots, we show the temporal trajectory of global dynamics (the temperature averaged over all lattice points) over the 5000 epochs in Figure 4.19 (a). The figure clearly captures the emergence of temperature self-regulation by the daisy population. The global temperature is regulated around the mean temperature ($295.5K$), ideal for daisy growth. This self-regulation of surface temperature arises from, but also gives rise to, a globally stable daisy population (average black or white population of the whole ecosystem), an emergent property of daisyworld, as seen in Figure 4.19 (b). In these figures, we discard the first 20 epochs (which would

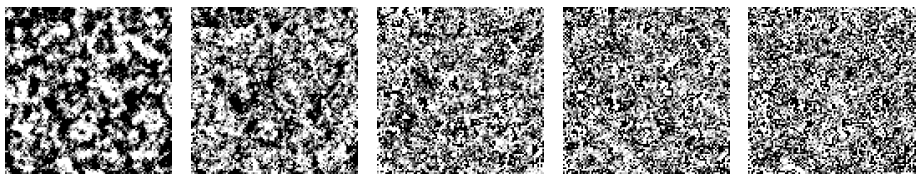

(a) epoch 50 (b) epoch 100 (c) epoch 200 (d) epoch 300 (e) epoch 500

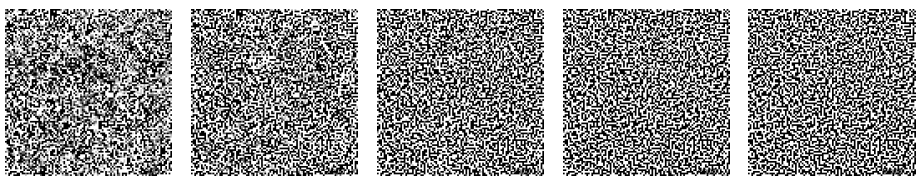

(f) epoch 1000 (g) epoch 2000 (h) epoch 3000 (i) epoch 4000 (j) epoch 5000

Figure 4.13: Uniformly Dispersed Pattern : Overlap=10%, $D_c = 0$, $D = 0.2$, $r = 1$ and $NL = 0.5$ in 2D 100×100 Lattice

otherwise generate off-scale behaviours) to concentrate on the long-term behaviour.

4.2.2 Temporal Fluctuations

The environmental fluctuations arise from temporal heterogeneity: different environmental conditions occur at different times at the same habitat. Figure 4.20 plots the local temporal series of temperature 4.20 (a), black 4.20 (b) and white 4.20 (c) daisies at a specific location (arbitrarily chosen as row 54 and column 54), showing the aperiodic dynamics arising from the deterministic chaos of the system. Although we used an increase rate of 1 (which in a non-diffusive world would not generate such dynamics), we observe deterministic temporal chaos. This is induced by the diffusion, an alternate route to chaos. Thus the network topologies and neighbourhood (structural properties) play a key role in determining the ecosystem complexity.

Figure 4.21 presents the cobweb plots (Verhulst diagrams) corresponding to Figure 4.20. In these, the value at a particular location (54, 54) and time step (x-axis) is plotted against the value at the same location but the next

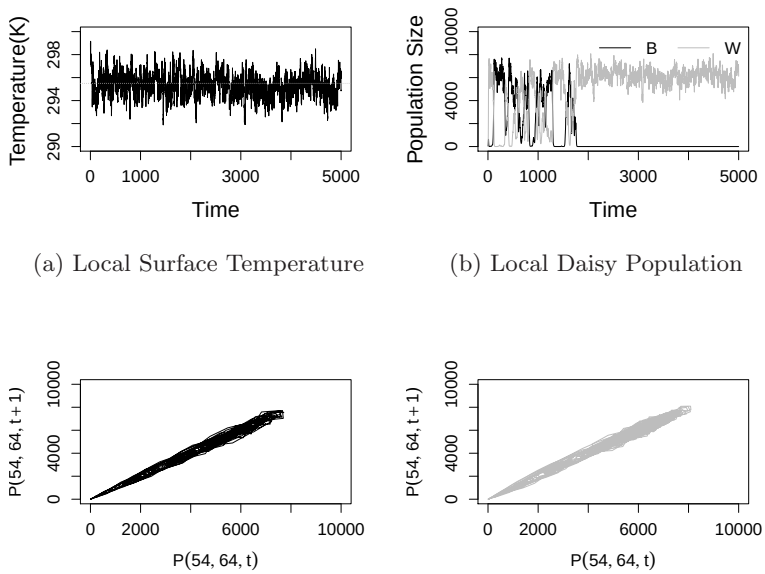

(a) Local Surface Temperature

(b) Local Daisy Population

(c) Local Black Daisy Cobweb

(d) Local White Daisy Cobweb

Figure 4.14: Local Dynamics of Uniformly Dispersed Pattern : 10% Overlap, $D_c = 0$, $D = 0.2$, $r = 1$ and $NL = 0.5$ in 2D 100×100 Lattice

time step (y-axis). We show plots for surface temperature 4.21 (a), black daisies 4.21 (b) and white daisies 4.21 (c). We clearly see the fluctuating but chaotic, aperiodic behaviour of the temporal dynamics in these plots.

4.2.3 Summary

The daisyworld model exhibits local temporal aperiodicity and global spatially-stabilised dynamics. We also see that spatial heterogeneity and temporal heterogeneity create a set of microclimates, which determine the existence of daisies. In our model, daisies' spread in a patchy environment is influenced by various factors such as overlap, dispersion, noise level and increase rate.

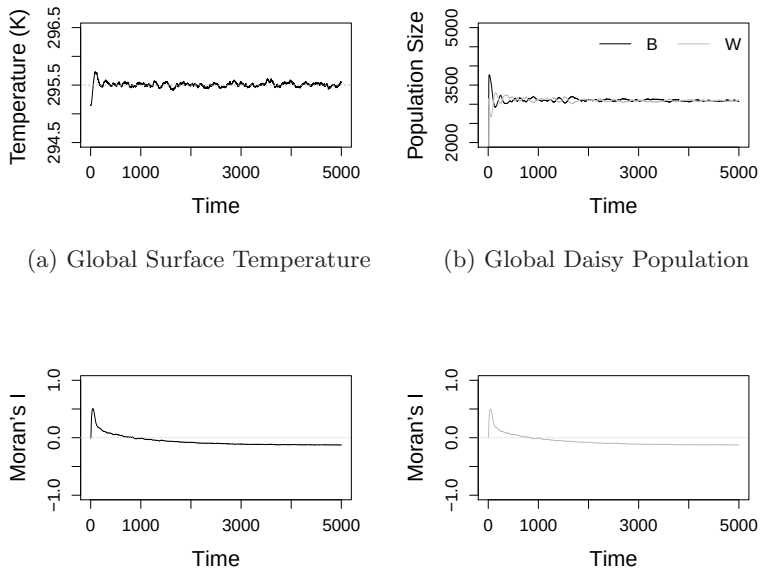

(a) Global Surface Temperature

(b) Global Daisy Population

(c) MI Black Daisy

(d) MI White Daisy

Figure 4.15: Global Dynamics of Uniformly Dispersed Pattern : 10% Overlap, $D_c = 0$, $D = 0.2$, $r = 1$ and $NL = 0.5$ in 2D 100×100 Lattice

4.3 Homeostasis with Evolutionary Dynamics

Evolutionary studies have highlighted the importance of biota-environment feedback in evolutionary dynamics, for example, niche construction [Odling-Smee et al., 2003], extended phenotypes [Dawkins, 1999]. Biota-environment feedback is inherent in daisyworld models, so we have chosen to extend the basic daisyworld model with evolutionary dynamics based on the replicator-mutator equation (RME) [Hofbauer and Sigmund, 2003].

The three fundamental factors in Darwinian evolution are replication (entities reproducing themselves), mutation (producing small variations in transforming to a new entity) and selection (passing the fitter entities to later generations). These factors determine the population dynamics: changes in population size and evolution of new populations. Populations are the funda-

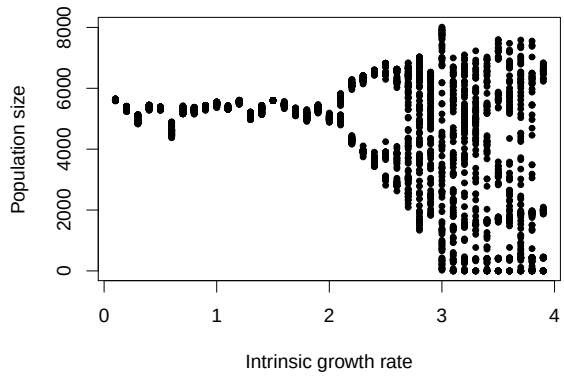

Figure 4.16: Bifurcation Diagram of Daisyworld – Black Daisy Population

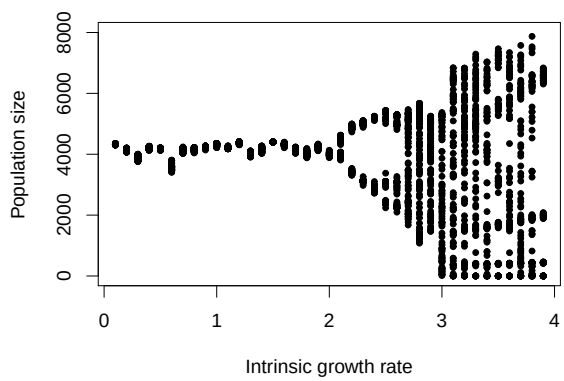

Figure 4.17: Bifurcation Diagram of Daisyworld – White Daisy Population

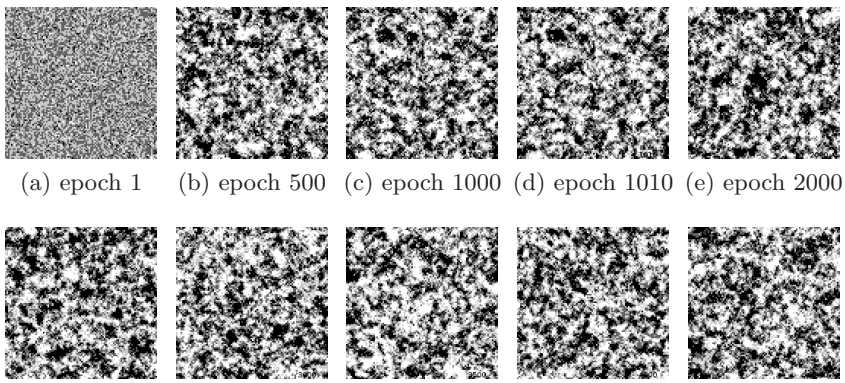

(a) epoch 1 (b) epoch 500 (c) epoch 1000 (d) epoch 1010 (e) epoch 2000

(f) epoch 2500 (g) epoch 3000 (h) epoch 3500 (i) epoch 4000 (j) epoch 5000

Figure 4.18: Population Dynamics in 100×100 2D CML with 10% Overlap, $D_c = 0.01$, $D = 0.2$, $r = 1$ and $NL = 1$

mental basis of evolution; individuals can change over time, but only populations evolve [Nowak, 2006]. We focus our attention on population dynamics in daisyworld with evolutionary change.

Generally, selection arises as a consequence of competition, commonly due to prey-predator relationships or resource limits. In the daisyworld of Watson and Lovelock [1983], daisies compete for space and hence for light. Daisyworld also incorporates a feedback mechanism: different daisy species affect the temperature, and the temperature in turn affects daisy survival, and hence selection. Thus the classic daisyworld realises the competition and natural selection of an evolutionary framework.

What is less studied in classical Darwinian evolution is the global feedback between biota and environment; conversely, the components that are omitted in the original daisyworld model are mutation and adaptation. In this field, it is common to distinguish between evolution of the daisies in ways which change their effect on the environment (in this case, albedo), which is referred to simply as mutation; and evolution of the daisies in ways which change their response to the environment (growth curve with temperature), generally referred to as adaptation. Thus a simple evolutionary daisyworld can incor-

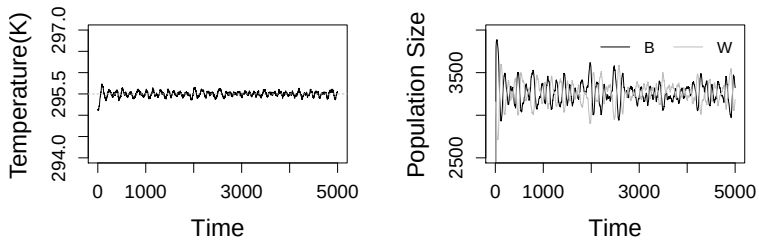

(a) Average Surface Temperature of all habitats

(b) Average Daisy Population of all habitats

Figure 4.19: Global Dynamics of Daisyworld in 100×100 2D CML with 10% Overlap, $D_c = 0.01$, $D = 0.2$, $r = 1$ and $NL = 1$

porate all these factors, through 1) influence of temperature on daisies, 2) influence of daisies on temperature, 3) mutation of daisies and 4) adaptation of daisies to the temperature.

A number of researchers have studied evolution in daisyworld. Mutation was introduced into daisyworld by Lovelock [1992] and expanded by Lenton and Lovelock [2001]; Lenton et al. [1998]. Adaptation in daisyworld was studied by Lenton and Lovelock [2000]. For a more detailed survey, please see Wood et al. [2008, section 4].

In this section, we model the population dynamics of daisies using the replicator-mutator equation (RME) of evolutionary dynamics, in a diffusively coupled logistic lattice of daisyworld - a model which has not been studied previously. RME has the advantage of expressing replication, mutation and selection mechanisms within a single framework; these evolutionary changes can be influenced by external environment factors such as temperature or abundance of species. Also, the interaction with the environment affects the survival of daisies and changes their adaptive fitness.

We have analysed the population dynamics of our daisyworld model through allowing a range of fluctuations in temperature, studying its effects on the evolutionary behaviour of the daisyworld. We have done this by introducing

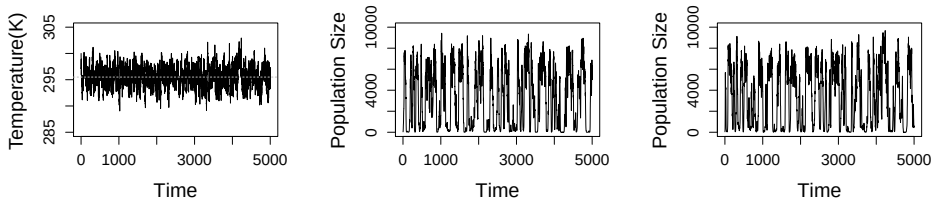

(a) Surface Temperature (b) Black Daisy Population (c) White Daisy Population

Figure 4.20: Local Dynamics at a specific location (row 54 and column 54) with 10% Overlap, $D_c = 0.01$, $D = 0.2$, $r = 1$ and $NL = 1$

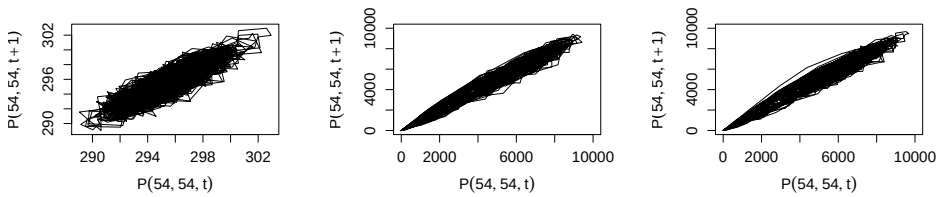

(a) Surface Temperature (b) Black Daisy Population (c) White Daisy Population

Figure 4.21: Cobweb Plot of Local Dynamics at a specific location (row 54 and column 54) with $D_c = 0.01$, $D = 0.2$, $r = 1$ and $NL = 1$ over 5000 Steps

ecosystem disturbance in the form of additive spatio-temporal Gaussian white noise [García-Ojalvo and Sancho, 1999]. The scale of fluctuation is controlled by the noise level.

4.3.1 Modification to Core Model

Patch Temperature: Daisies at a location (i, j) are divided (by species) into patches, whose temperature may vary from the local temperature $T_{(i,j,t)}$. The albedo of the daisies in the patch determines the patch temperature:

$$T_{c_{(i,j,t)}} = q(A_{(i,j,t)} - A_{c_{(i,j,t)}}) + T_{(i,j,t)} \tag{4.1}$$

where $T_{c_{(i,j,t)}}$ is the patch temperature of a habitat (i, j) at time t; c (phenotype) is the color of the daisies, $q = 20$ is a constant; refer [Lovelock, 1992], $A_{(i,j,t)}$ is the albedo of a habitat (i, j) at time t, $A_{c_{(i,j,t)}}$ is the albedo of each daisy type 'c' of a habitat (i, j) at a time t and $T_{(i,j,t)}$ is the local temperature of a habitat at a time t.

Density Dependent Fitness: We use absolute numbers for population size (P) rather than the relative frequencies of the classical form (equation 2.2). To prevent unrealistic exponential growth or decay, we formulated our fitness $(\mathfrak{f})$ based on a carrying capacity (κ) such that $\mathfrak{f} < 0$ for $P > \kappa$ and $\mathfrak{f} > 0$ for $P < \kappa$. The death rate of each daisy type is dependent on the total density of daisies. The corresponding fitness function is (equation 4.2):

$$\mathfrak{f}_{c_{(i,j,t)}} = \beta_{c_{(i,j,t)}} * \left(1 - \frac{P_{c_{(i,j,t)}}}{\kappa}\right) - \gamma * \left(\frac{P_{c_{(i,j,t)}}}{\kappa}\right) \tag{4.2}$$

β is the growth rate from equation 3.4, $\gamma = 0.3$ is the death rate, P is total population size and κ the carrying capacity.

Population Size: The local population abundance is based on replicator-mutator dynamics. We start from a variant of the discrete form [Page and Nowak, 2002] of RME (equation 2.2) shown in equation 4.3:

$$P\prime_{c(i,j,t)} = \frac{\sum_{c'=1}^{\mathfrak{n}} P_{c'(i,j,t)} \mathfrak{f}_{c'(i,j,t)} \mathfrak{q}_{c'c}}{\phi}, c = 1, ..., \mathfrak{n} \tag{4.3}$$

where P_c is the proportion of the population of type c, (i, j) represents a spatial location, $\mathfrak{n}$ is the number of phenotypes, and $\mathfrak{f}_{c'}$ defines the selection dynamics. Rather than separate reward (payoff) and mutation matrices, we use a combined replicator-mutator matrix $\mathbb{Q} = [\mathfrak{q}_{cc'}]$ – a doubly stochastic matrix – defining the evolutionary properties and satisfying $\sum_c \mathfrak{q}_{cc'} = \sum_{c'} \mathfrak{q}_{cc'} = 1$. The diagonal of the matrix defines the replication rate, while other entries

defines the mutation rates. $\phi = \sum_c P_c \mathfrak{f}_c$ is the average fitness, and is used as a normalisation term to ensure the population doesn't exceed its bounds.

Since our fitness function is density dependent and directly ensures the orbits are bounded in the region $P \leq \kappa$, the term ϕ is not needed. However we need to incorporate diffusion of individuals. Combining this, we can define the change in population as in equation 4.4:

$$h\left(P'_{c_{(i,j,t)}}\right) = P'_{c_{(i,j,t)}} + \sum_{c=1}^{\mathfrak{n}} P_{c_{(i,j,t)}} \mathfrak{f}_{c_{(i,j,t)}} \mathfrak{q}_{cc} + \sum_{c' \neq c}^{\mathfrak{n}} P_{c'_{(i,j,t)}} \mathfrak{f}_{c'_{(i,j,t)}} \mathfrak{q}_{c'c} \tag{4.4}$$

D is the Laplace-diffused population. Since we don't use a reward matrix, the discrete time fitness (selection coefficient) is just the intrinsic fitness, leading to equation 4.2.

The fitness of a particular type of daisies changes, depending on the abundance of both itself and the other species because of the life-environment feedback. Here, $\mathfrak{f}$ affects P and depends on β which depends on T which depends on A which in turn depends on P, thus forming a tightly coupled system with an indefinite feedback loop. The model incorporates two types of feedback: from the life-environment effect of daisyworld and from the density-dependent nature of population dynamics. This model covers all the main ingredients of evolutionary population dynamics – reproduction, mutation, selection and spatial dispersion – with a bi-directional life-environment feedback effect.

Importance to Study Noise Modelling nonlinear dynamics in a noisy world is very common in population ecology. The two key factors in studying population dynamics are the internal feedback which inhibits the exploding population and the external environmental (abiotic) variability which determines the population fluctuations [Begon et al., 1996]. In our model, the first factor (internal feedback) results from the imposition of a carrying capacity and the second (external variability) from Gaussian noise. These external perturbations can cause the system to deviate from equilibrium. The noise level controls the scale fluctuations in the environment. Noise helps to intro-

duce sufficient nonlinearity to observe complex dynamics such as limit cycles, quasi-periodicity and chaos (nonlinear attractors). Diffusion of temperature and dispersion of daisies also allow the system to break symmetry and generate interesting patterns in daisyworld [Punithan and McKay, 2012b]. In this section, we focus on the evolutionary population dynamics of daisyworld, so we study the impact of the external variability in detail. In the absence of noise, the dynamics of the world is stationary (static attractor). But with the imposition of noise, we observe evolving patterns of life – so long as there is not too much. With higher levels, noise completely dominates the feedback, and the behaviour becomes random and uninteresting.

4.3.2 Variable Parameter Settings

We analyse the changes in dominance by specific phenotypes (petal colour) under the effect of environmental perturbations (temperature). In our experiments, the optimal temperature and albedo of the original black, white daisies, their mutants and adaptants are tabulated in the Table 4.2; please refer Lenton and Lovelock [2001], and other parameter settings are tabulated in the Table 4.3. In all analyses, we first examine the spatio-temporal population patterns (using snapshots of the system status over the 5000 epochs). We focus on the local dominance of species. We plot the local (temporal) behaviour at a single habitat, and the global dynamics (average temporal behaviour of the whole ecosystem).

Table 4.2: Optimal temp. and albedo of original daisies and their mutants

	T_{opt}(K)	Albedo	Colours in Figures
Black	295.5	0.25	black
White	295.5	0.75	white
Grey	295.5	0.5	grey
Warm Black	300.5	0.25	dark grey
Cool White	290.5	0.75	light grey

Table 4.3: Evolutionary Dynamics : Representative Parameter Set

Parameter	**Value**
Diffusion rate of black daisies (D_b)	0.2
Diffusion rate of white daisies (D_w)	0.2
Noise Level (NL)	$[0, 3]$
Natural Rate of Increase (r)	1

4.3.3 Baseline Scenario: No Mutation

In this subsection, we present the behaviour of the system with no evolutionary change, as a baseline for comparisons. Since the level of noise is an important control in determining the effect of evolutionary change, we present results for different levels of noise.

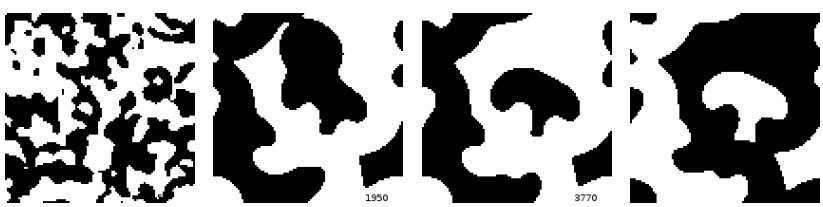

(a) epoch 50 (b) epoch 1950 (c) epoch 3770 (d) epoch 4885

Figure 4.22: Population abundance without mutation : $D_c = 0.2$, $D = 0.2$, $r = 1$ and $NL = 0.05$

Noise Level $= 0.05$ With low noise levels ($NL = 0.05$), periodic behaviour emerges from the system (Figure 4.22). The cycles in the local dynamics (Figure 4.23) for both patch temperature and population confirm this. At the global level, the temperature (Figure 4.24) is regulated around $295.5K$.

Noise Level $= 3$ With increased noise, rough turing like structures form – Figure 4.25, and the periodic behaviour becomes less regular – Figures 4.26 and 4.27.

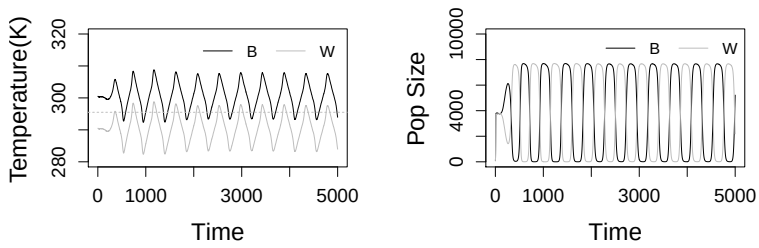

(a) Patch Temperature (b) Population abundance

Figure 4.23: Local dynamics at habitat (55, 41) without mutation and $NL = 0.05$

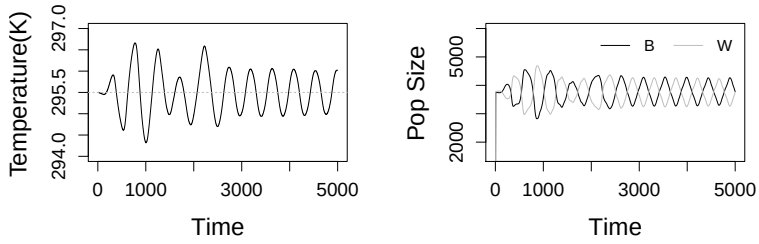

(a) Surface Temperature (b) Population abundance

Figure 4.24: Global dynamics without mutation, $NL = 0.05$

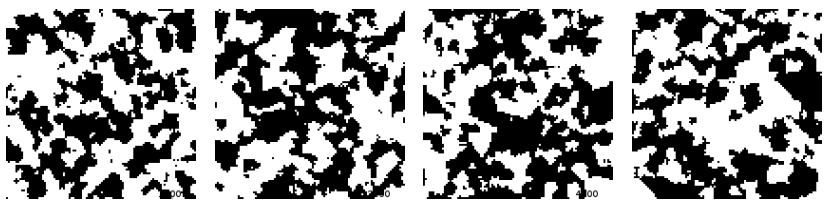

(a) epoch 1000 (b) epoch 2000 (c) epoch 4000 (d) epoch 5000

Figure 4.25: Population abundance without mutation : $D_c = 0.2$, $D = 0.2$, $r = 1$ and $NL = 3$

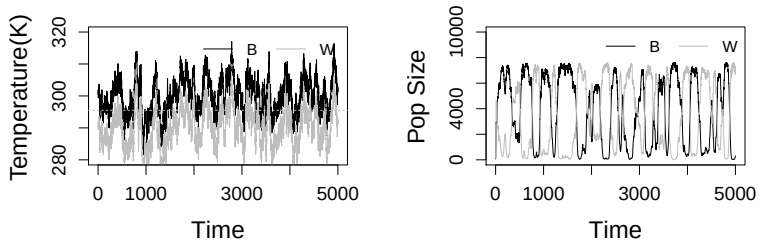

(a) Patch Temperature (b) Population abundance

Figure 4.26: Local dynamics at habitat (55, 50) without mutation, $NL = 3$

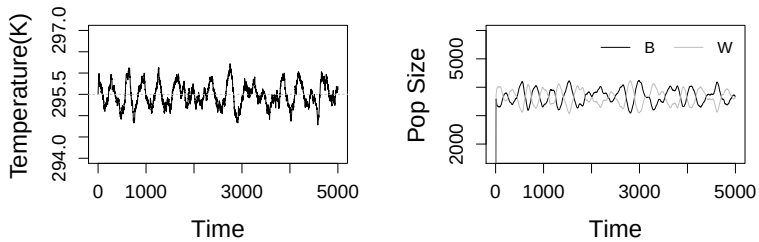

(a) Surface Temperature (b) Population abundance

Figure 4.27: Global dynamics without mutation, $NL = 3$

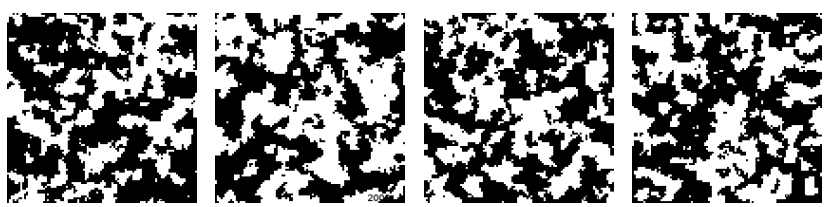

(a) epoch 1000 (b) epoch 2000 (c) epoch 4000 (d) epoch 5000

Figure 4.28: Population abundance without mutation : $D_c = 0.2$, $D = 0.2$, $r = 1$ and $NL = 5$

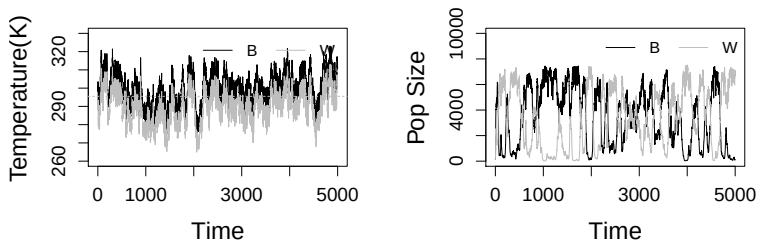

(a) Patch Temperature (b) Population abundance

Figure 4.29: Local dynamics at habitat (56, 50) without mutation, $NL = 5$

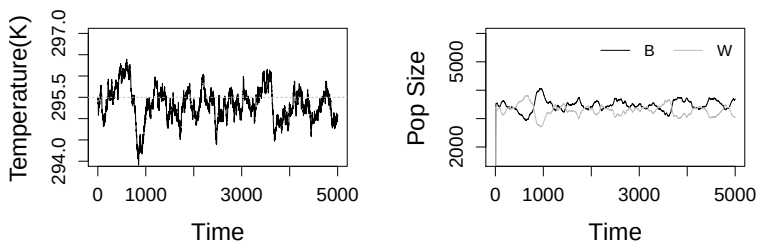

(a) Surface Temperature (b) Population abundance

Figure 4.30: Global dynamics without mutation, $NL = 5$

Noise Level = 5 With further increase in noise, rough clusters ceaselessly form and dissolve (Figure 4.28), and the periodic behaviour almost entirely disappears as in Figures 4.29 and 4.30. We have reached the less interesting region in which noise dominates the environmental feedback; behaviours in this region are little affected by other parameters, so we omit it from consideration in the rest of the section.

4.3.4 Phenotypic Variability – Mutation

The ability of mutations to generate new phenotypes is one of the hallmarks of Darwinian evolution. The black and white daisies in the model undergo random mutation, introducing a new phenotypic state – grey daisies (T_{opt} = 295.5 and albedo = 0.5). The evolutionary relationships between the species are defined in the replicator-mutator matrix (μ is the rate of random mutation and B, W, G denote Black, White and Grey daisies):

$$Q = \begin{array}{c} \\ B \\ W \\ G \end{array} \begin{array}{c} \begin{array}{ccc} B & W & G \end{array} \\ \begin{pmatrix} (1-0.1\mu) & 0 & 0.1\mu \\ 0 & (1-0.1\mu) & 0.1\mu \\ 0.1\mu & 0.1\mu & (1-2(0.1\mu)) \end{pmatrix} \end{array}$$

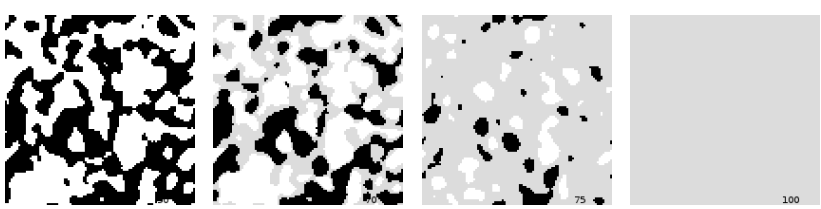

(a) epoch 50 (b) epoch 70 (c) epoch 75 (d) epoch 100

Figure 4.31: Population abundance with Grey daisies : $D_c = 0.2$, $D = 0.2$, $r = 1$ and $NL = 0.05$

Noise Level = 0.05 Grey daisies quickly dominate (Figure 4.31) when the noise level is very low ($NL = 0.05$). Both local (Figure 4.32 (b)) and global (Figure 4.33 (b)) populations of the original black and white daisies drop very low, almost disappearing. This happens because the patch temperatures of

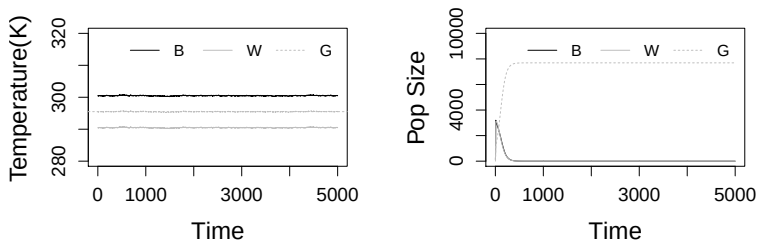

(a) Patch Temperature (b) Population abundance

Figure 4.32: Local dynamics at habitat (57, 49) with Grey and $NL = 0.05$

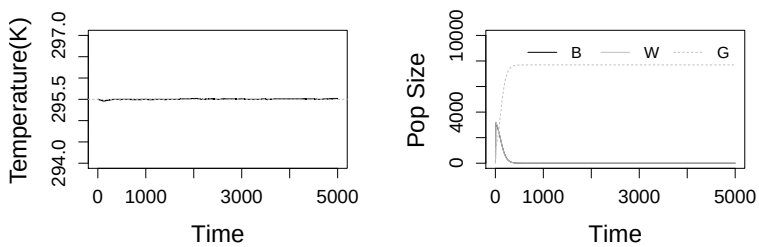

(a) Surface Temperature (b) Population abundance

Figure 4.33: Global dynamics with Grey, $NL = 0.05$

black and white daisies are almost constant, above and below $295.5K$, so the growth of grey daisies is favoured: refer to Figure 4.32 (a). Since there is not much fluctuation in the local temperature due to the low noise level, grey daisies dominate the whole space. The temperature is regulated to $295.5K$ (Figure 4.33 (a)).

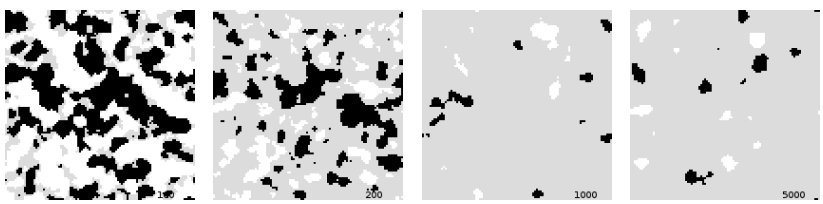

(a) epoch 100 (b) epoch 200 (c) epoch 1000 (d) epoch 5000

Figure 4.34: Population abundance with Grey daisies : $D_c = 0.2$, $D = 0.2$, $r = 1$ and $NL = 2$

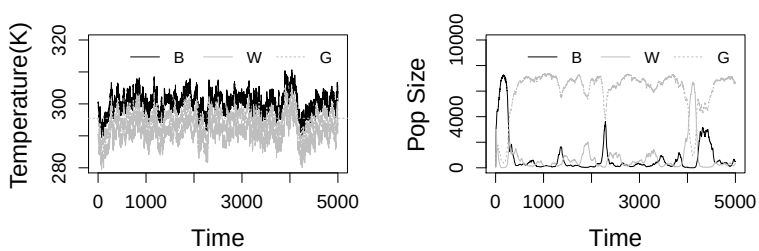

(a) Patch Temperature (b) Population abundance

Figure 4.35: Local dynamics at habitat (54, 43) with Grey and $NL = 2$

Noise Level = 2 When the noise level increases to 2, although the world is still rapidly dominated by grey daisies, the original black and white species can form distinct groups and dominate smaller regions (Figure 4.34). All three species coexist locally as well as globally, mainly to due the patch temperatures. Black patches mostly fluctuate above $295.5K$, and white mostly below,

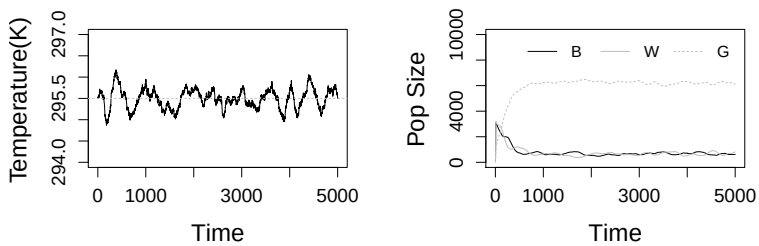

(a) Surface Temperature (b) Population abundance

Figure 4.36: Global dynamics with Grey, $NL = 2$

with only grey fluctuating around the favoured $295.5K$ (Figure 4.35 (a)). The global temperature is regulated around $295.5K$ (Figure 4.36 (a)) with coexisting populations (Figures 4.35 (b) and 4.36 (b)) but a majority of grey.

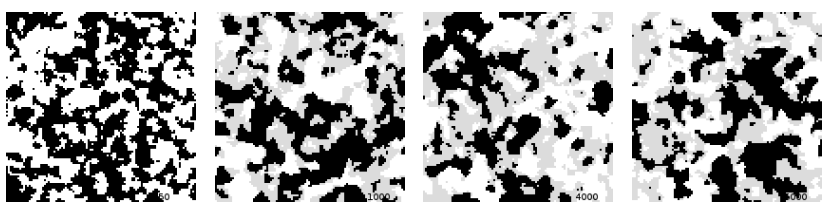

(a) epoch 50 (b) epoch 1000 (c) epoch 4000 (d) epoch 5000

Figure 4.37: Population abundance with Grey daisies : $D_c = 0.2$, $D = 0.2$, $r = 1$ and $NL = 3$

Noise Level = 3 Further increasing the noise level to 3 results in all species dominating local regions, with highly evolving and dynamic (Figure 4.37) behaviours. The local patch temperatures fluctuate widely around the mean $295.5K$ (Figure 4.38 (a)). The global temperature is regulated to around $295.5K$ (Figure 4.39 (a)) with all species coexisting locally (Figure 4.38 (b)) and globally (Figure 4.39 (b)).

To summarise, the grey mutant form dominates the whole ecosystem when

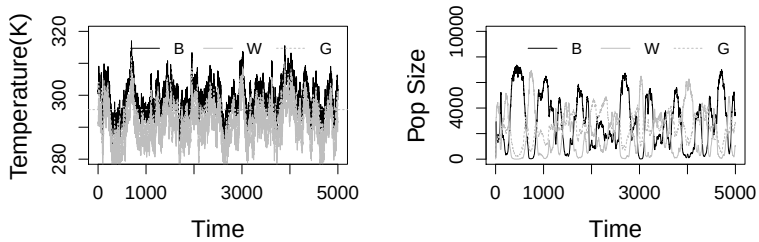

(a) Patch Temperature (b) Population abundance

Figure 4.38: Local dynamics at habitat (51, 53) with Grey and $NL = 3$

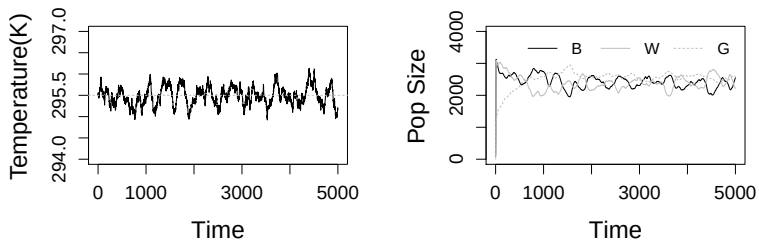

(a) Surface Temperature (b) Population abundance

Figure 4.39: Global dynamics with Grey, $NL = 3$

there are small temperature fluctuations ($NL = 0.05$). As the noise level increases to ($NL = 2$), the black and white daisies form distinct population groups. Further increase in noise level ($NL = 3$), allow all three species to dominate locally, and they coexist both locally and globally. Thus we see the determination of evolutionary dominance through environmental influences.

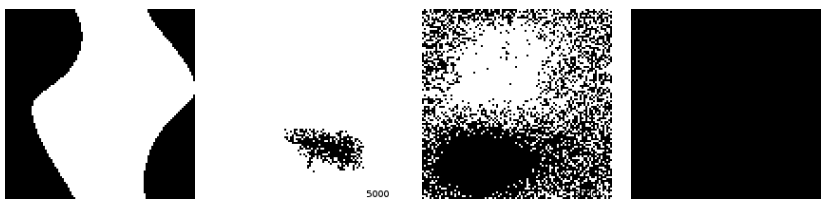

(a) $NL = 0$ (b) $NL = 2$ (c) $NL = 3$ (d) $NL = 5$

Figure 4.40: Population abundance without feedback : $D_c = 0.2$, $D = 0.2$ and $r = 1$ at epoch 5000

Mutation without Life-Environment Feedback We observed population spatial structures with mutation but excluding life-environment feedback (i.e. temperature is not influenced by the daisies at all) for different noise levels (Figure 4.40). When we compare these snapshots (no grey dominance) with Figures 4.31 and 4.37, we can see that the balance between feedback and noise plays a vital role in the coexistence of dominance of the original daisies and their mutants. The dynamics we see, for example, in Figure 4.37 is due to the interplay of noise and feedback, rather than either alone.

4.3.5 Adaptation – Exploring New Environments

In the absence of other species, black daises will generate a very hot environment unsuited to them. Instead of mutating to reduce their environmental effect, they can also adapt to tolerate these higher temperatures, generating "warm black daisies". Similarly, white daisies may adapt to a cold environment, giving "cool white daisies". We explore the effects of warm black ($T_{opt} = 300.5$, $albedo = 0.25$) and cool white daisies ($T_{opt} = 290.5$,

albedo = 0.75). In all patch temperature plots, the patch temperature trajectories of black and warm black daisies superimpose and similarly for white and cool white – inevitably, because the originals and their adaptants have the same albedo.

The evolutionary properties are by the following replicator-adapter matrix (WB and CW stand for warm black and cool white daisies):

$$Q = \begin{array}{c} \\ B \\ W \\ WB \\ CW \end{array} \begin{array}{c} \begin{array}{cccc} B & W & WB & CW \end{array} \\ \begin{pmatrix} (1-0.1\mu) & 0 & 0.1\mu & 0 \\ 0 & (1-0.1\mu) & 0 & 0.1\mu \\ 0.1\mu & 0 & (1-0.1\mu) & 0 \\ 0 & 0.1\mu & 0 & (1-0.1\mu) \end{pmatrix} \end{array}$$

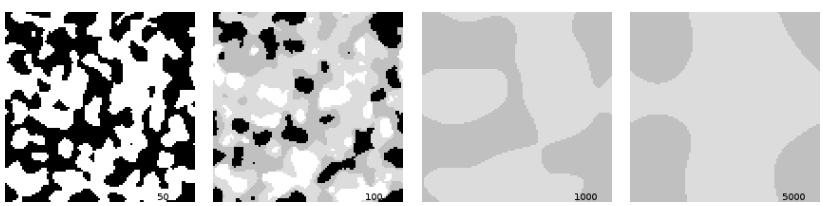

(a) epoch 50 (b) epoch 100 (c) epoch 1000 (d) epoch 5000

Figure 4.41: Population abundance with Warm Black and Cool White daisies : $D_c = 0.2$, $D = 0.2$, $r = 1$ and $NL = 0.05$

Noise Level = 0.05 When the noise level is low (0.05), the original daisies almost disappear (Figures 4.42 (b) and 4.43 (b)) and the warm black and cool white self-organise, forming patterns with huge clusters that dominate the ecosystem (Figure 4.41). The global surface temperature is regulated to 295.5K (Figure 4.43 (a)). Though the patch temperatures of black and warm black are identical (also for white and cool white) (Figure 4.42 (a)), the adaptants are superior to the existing phenotypes, and rapidly dominate.

Noise Level = 2 At a noise level of 2, both warm black and cool white, self-organise to form Turing-like patterns, while the originals, black and white, dominate in smaller regions here and there (Figure 4.44). The local and global dynamics are shown in Figures 4.45 and 4.46.

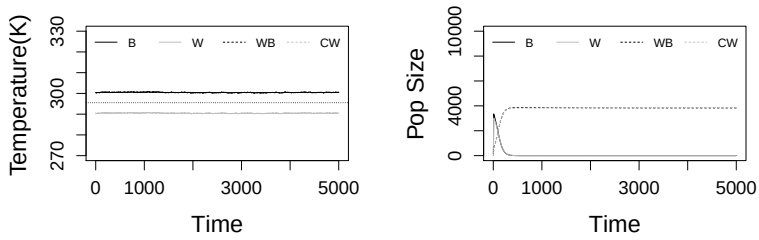

(a) Patch Temperature (b) Population abundance

Figure 4.42: Local dynamics at habitat (51, 50) with Warm Black and Cool White, $NL = 0.05$

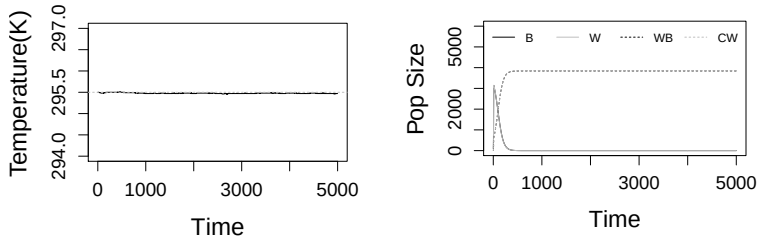

(a) Surface Temperature (b) Population abundance

Figure 4.43: Global dynamics with Warm Black and Cool White, $NL = 0.05$

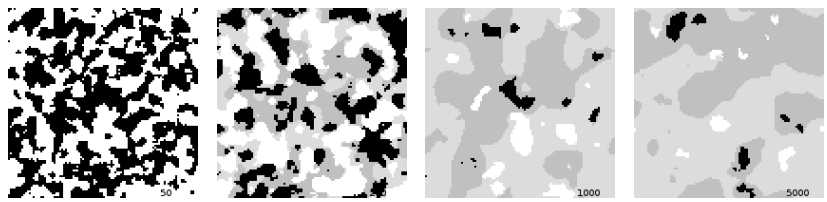

(a) epoch 50 (b) epoch 200 (c) epoch 1000 (d) epoch 5000

Figure 4.44: Population abundance with Warm Black and Cool White daisies : $D_c = 0.2$, $D = 0.2$, $r = 1$ and $NL = 2$

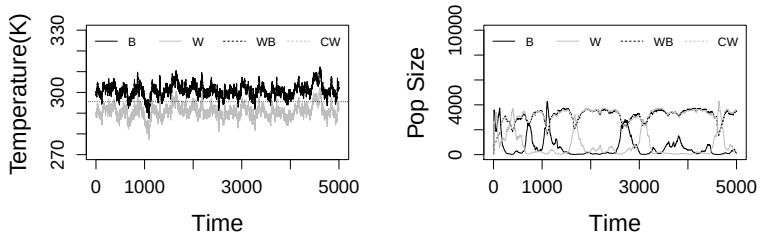

(a) Patch Temperature (b) Population abundance

Figure 4.45: Local dynamics at habitat (57, 55) with Warm Black and Cool White, $NL = 2$

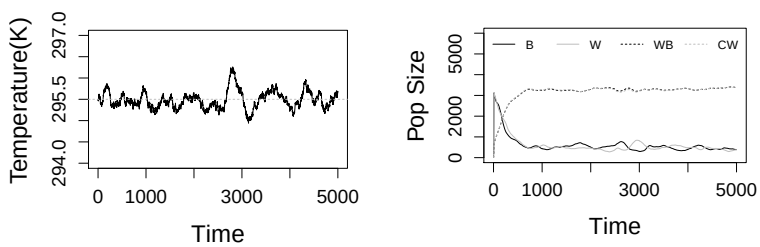

(a) Surface Temperature (b) Population abundance

Figure 4.46: Global dynamics with Warm Black and Cool White, $NL = 2$

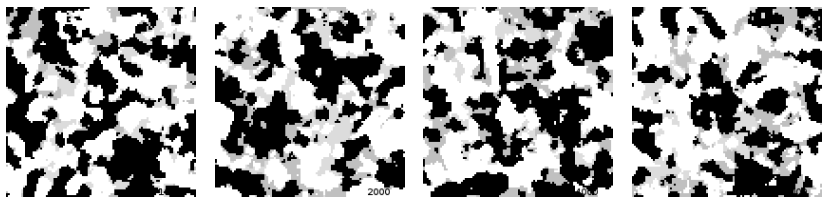

(a) epoch 1000 (b) epoch 2000 (c) epoch 4000 (d) epoch 5000

Figure 4.47: Population abundance with Warm Black and Cool White daisies : $D_c = 0.2$, $D = 0.2$, $r = 1$ and $NL = 3$

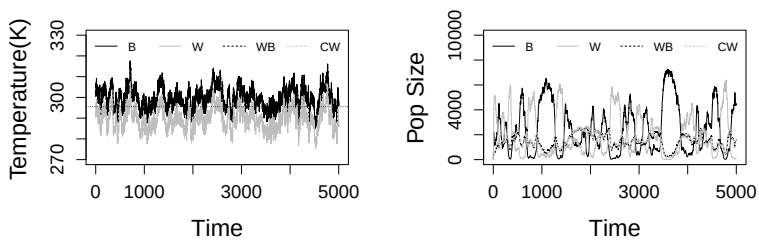

(a) Patch Temperature (b) Population abundance

Figure 4.48: Local dynamics at habitat (52, 61) with Warm Black and Cool White, $NL = 3$

Noise Level = 3 All four phenotypes coexist, each dominating the ecosystem locally (Figure 4.47). The overall behaviour is revealed in Figures 4.48 and 4.49.

4.3.6 Summary

The evolutionary daisyworld model – replication with mutation and adaptation – presented in this section illustrates global surface temperature regulation around $295.5K$ as in the original models. Thus demonstrating its robustness in homeostatic self-regulation in scenarios such as evolution of the environment altering trait (albedo) and adaptive evolution of optimal temperature. Tem-

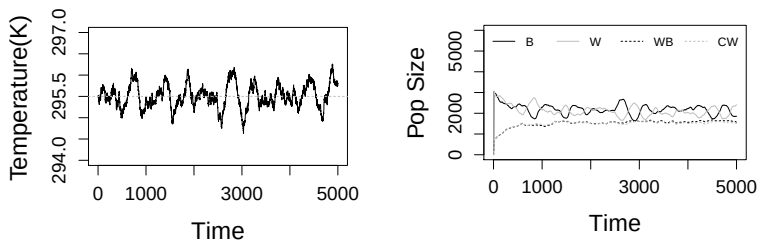

(a) Surface Temperature

(b) Population abundance

Figure 4.49: Global dynamics with Warm Black and Cool White, $NL = 3$

poral fluctuation in temperature, due to ecosystem disturbance, introduces nonlinearity into the daisyworld, leading to the most interesting behaviours. With very low noise, we observe monotonous life (quiescent daisy dominance states). Without feedback or with very high noise, we observe suppression of mutants. Thus, these results underline the importance of balance between ecosystem feedback and ecosystem disturbance in generating spatially coexistence of domains of dominance among the original daisies and their mutants.

4.4 Quantification of the Daisyworld Model

4.4.1 Statistical Measures and Spatio-Temporal Dynamics

Table 4.4: Permutation Entropy Regimes

Temporal Dynamics (Local or Global)	**PE value**
Static	< 0.1
Periodic	$[0.1, 0.2]$
Chaotic	$[0.3, 0.7]$
Random	near 1

We analyse the temporal and spatial dynamics of our daisyworld model us-

Table 4.5: Moran's I Regimes

Global Spatial Distribution	**MI value**
Uniform	$-ve$
Random	0
Clustered	$+ve$

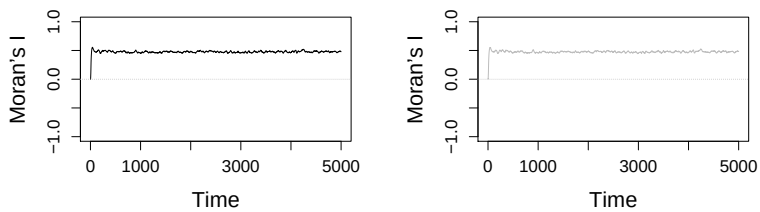

(a) MI Black Daisy (b) MI White Daisy

Figure 4.50: Moran's I (section 4.2)

ing Permutation Entropy (PE) and Moran's I (MI) (defined in subsection 2.3), along with standard deviation metrics. We are particularly interested in settings which lead to a chaotically stable (locally chaotic and globally stable (section 4.2)) system with self-regulation and interesting spatio-temporal dynamics, so we aim to characterise the values of PE and MI at which we are likely to find such behaviours. We have studied over $15,000$ experiments delineated in subsection 3.4.1, to find suitable regimes for local and global dynamics. The dynamics of our interest (chaotic stability with evolving patches) are observed for systems with local dynamics (dynamics at a specific habitat in the ecosystem) characterised by a local permutation entropy (PE computed

Table 4.6: Local PE (section 4.2)

	Local PE	Std Dev
Black Population	0.435	2783
White Population	0.424	2800

Table 4.7: Global PE (section 4.2)

	Global PE	Std Dev
Black Population	0.365	132
White Population	0.365	130

on temporal trajectory of daisies at a specific habitat in the ecosystem) in the range $[0.3, 0.7]$ with high standard deviation, and global dynamics (mean population dynamics of the whole ecosystem) characterised by Moran's I in the range $[0.4, 0.9]$ and global permutation entropy (PE computed on temporal trajectory of mean daisy populations of the whole ecosystem) in the range $[0.3, 0.7]$ with low standard deviation. We also observe that large clumped/patchy patterns tend to emerge as Moran's I increases towards $+1$. The overall regimes of PE and MI that we observed are shown in Tables 4.4 and 4.5. However these are not enough to characterise the dynamics. We use the standard deviation to measure the scale of fluctuation in both local and global dynamics. For example, a given value of PE for both local and global dynamics tells us only about the shape of fluctuations, not their scale. We use the standard deviation to measure the range of fluctuation. If it is high, the behaviour is characterised as chaotic, otherwise not.

As an example of such an analysis, consider the daisyworld presented in the section 4.2. The figure 4.50 shows the time evolution of MI (4.50 (a) and 4.50 (b)) of daisy population. The global permutation entropy and standard deviation of daisy population are listed in the table 4.7. The local permutation entropy and standard deviation of daisy population are tabulated in the table 4.6. Although the global PE would indicate a globally chaotic world, the small standard deviation indicates instead a stable world.

4.4.2 Parameter Space Analysis of the Daisyworld Model

Two of the most influential factors on daisyworld behaviour are the noise level (which influences temperature) and the dispersion rate of daisies (which influences the distribution of daisies). In this section, we study the effects

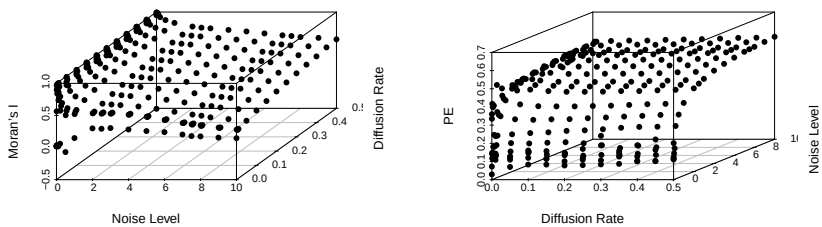

(a) (b)

Figure 4.51: Moran's I and PE on 100×100 2D CML with 10% overlap and $r = 1$

of noise and diffusion rate on our two key metrics; Moran's I (average of Moran's I of the whole ecosystem over 5000 epochs) and permutation entropy (average of permutation entropy of N randomly selected habitats with their neighbours (ecological aggregate), from the ecosystem of $N \times N$ habitats, over 5000 epochs).

From sub Figure 4.51 (a), we observe low MI values when both the dispersion rate of species and noise are very low, indicating the formation of uniform (MI < 0) and random (MI is nearly 0) patterns. The noise level has the largest overall effect, especially at very low values where we see very high MI values (even as high as 1), indicating the formation of huge patches. As noise increases and diffusion decreases, we see the MI values decrease, indicating the formation of patches of decreasing size.

The diffusion rate has almost no effect on the permutation entropy (sub Figure 4.51 (b)). However the effect of noise level is very substantial. Low noise results in very low PE (less than 0.1), indicating static attractors. With little increase in noise, PE also increases in the range $[0.1, 0.2]$, indicating periodic attractors. PE rises rapidly with increasing noise level at first, but saturates from noise levels of around 4. High PE in $[0.3, 0.7]$ indicates strange attractors.

Chapter 5

Daisyworld with Complex Couplings

In this chapter, we investigate two-dimensional (2D) CML based daisyworld with local couplings and non-local couplings (added either statically or dynamically). In section 5.2, daisyworld dynamics in different baseline graph models such as regular, random and fully-connected graphs are discussed which we use to compare other complex and adaptive topologies in the following sections 5.3, 5.4 and 5.5. In section 5.3, we introduce and examine the small-world phenomenon in daisyworld. In section 5.4, we examine adaptive topology of the system based on the local daisyworld dynamics. We study scale-freeness in daisyworld in section 5.5. In section 5.6, we discuss the behaviour study of the daisyworld with the additional connections (added either statically or dynamically).

5.1 Variable Parameter Settings

The parameter settings for the experiments described in this chapter are shown in Table 5.1 to have consistency for analyses. We have chosen a low noise level, increase rate and overlap so that we can study topological effect on the system behaviour without undue influences from other model system parameters.

Table 5.1: Representative Parameter Set

Parameter	**Value**
Opt. temp. of black daisies (T_{opt_b})	$284.5K$
Opt. temp. of white daisies (T_{opt_w})	$306.5K$
Diffusion rate of black daisies (D_b)	0.2
Diffusion rate of white daisies (D_w)	0.2
Noise Level (NL)	0.001
Natural Rate of Increase (r)	1

In the daisyworld literature [Wood et al., 2008, section 3], the connectivities for both species (black and white), and for the environmental resource (temperature), are the same – local connections. In our system, we use different connectivity topologies for species and the resource. Black and white daisies disperse via both local and long-range connections (by water, air, animal pollinator transport etc.), while temperature diffuses only locally. All the rewired or added connections are reciprocal.

5.2 Benchmark Graph Models

We have taken regular (sub Figure 5.1 (a)) and random graphs (sub Figure 5.1 (b)) as our benchmarks, as the interactions are purely local in former and purely global in the latter. For completeness, we also compare with fully-connected graphs (sub Figure 5.1 (c)) in which there is no notion of spatial relationship.

5.2.1 Degree Distribution of Benchmark Models

The degree distributions of regular graph having constant degree distribution (sub Figure 5.2 (a)) and random graph having Poisson distribution (sub Figure 5.2 (b)) are depicted in the Figure 5.2. Both graphs are constructed in 100×100 lattice.

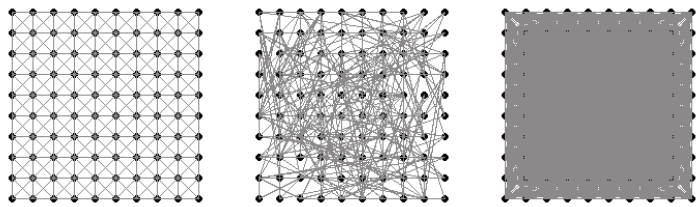

(a) (b) (c)

Figure 5.1: 2-lattice Benchmark Models (with $k = 8$ except for fully-connected graph). We omit periodic boundary conditions for clarity, and also show some connections superimposed.
(a) Regular graph ($p = 0$) (b) Random graph ($p = 1$) (c) Fully-connected graph

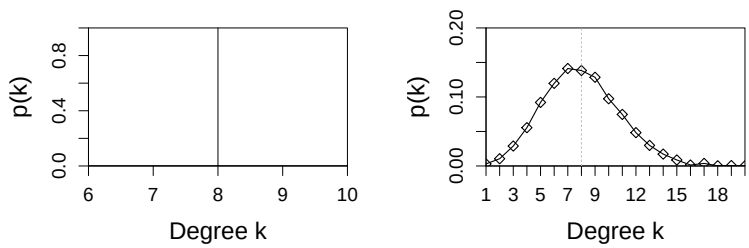

(a) Regular (b) Random

Figure 5.2: Degree Distribution of Benchmark Models

5.2.2 Regular Graph

With only local couplings, we observe the formation of complex static patterns. The whole ecosystem freezes after epoch 1710. This scenario is clearly seen in the snapshots (Figure 5.3), in global population dynamics (Figure 5.34) and in global temperature dynamics (sub Figure 5.32 (b)). The local population dynamics (Figure 5.33) and local temperature (sub Figure 5.32 (a)) at a typical habitat $(57, 50)$ shows that the dynamics freezes even quicker (epoch 1055). All trajectories show initial fluctuations but evolve to complete stationarity.

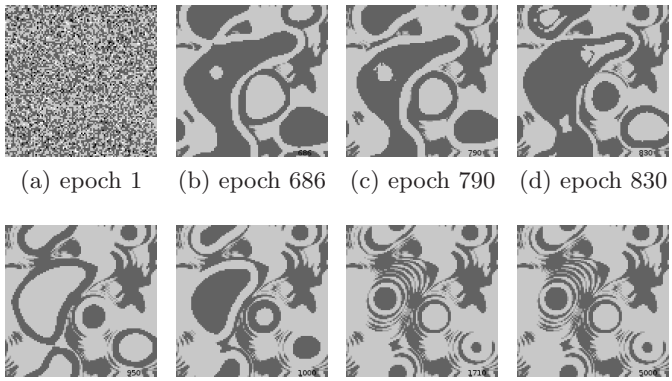

(a) epoch 1 (b) epoch 686 (c) epoch 790 (d) epoch 830

(e) epoch 950 (f) epoch 1000 (g) epoch1710 (h) epoch5000

Figure 5.3: Regular CML ($p = 0$) : Overlap=10%, $D_c = 0.2$, $D = 0.2$, $r = 1$ and $NL = 0.001$ in 2D 100×100

5.2.3 Random Graph

In the random connectivity case, $N^2k/2$ random connections are made, independent of the spatial structure. We observe a periodic behaviour. Both daisy types coexist, both locally and globally. But one type homogeneously dominates the world for some epochs, while the other type takes over completely for others. The transition from one type to the other is extremely rapid – see epoch numbers in the visuals (Figure 5.4). The top row shows a change from dark grey (coexistence dominated by black daisies) to light grey (coexistence dominated by white daisies); the bottom row shows the reverse. The periodic behaviour is confirmed by the local and global temperature dynamics (Figure 5.35) and by the local (Figure 5.36) and global (Figure 5.37) population dynamics.

5.2.4 Fully Connected Graph

We see a similar behaviour to a random lattice (Figure 5.5). The cycles in the local population dynamics (Figure 5.39), global population dynamics (Figure 5.40) and temperature dynamics (Figure 5.38) reflect the periodicity.

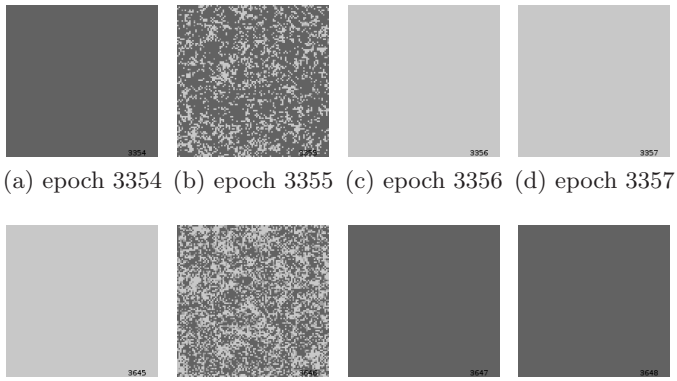

(a) epoch 3354 (b) epoch 3355 (c) epoch 3356 (d) epoch 3357

(e) epoch 3645 (f) epoch 3646 (g) epoch 3647 (h) epoch 3648

Figure 5.4: Random Lattice($p = 1$) : Overlap=10%, $D_c = 0.2$, $D = 0.2$, $r = 1$ and $NL = 0.001$ in 2D 100×100

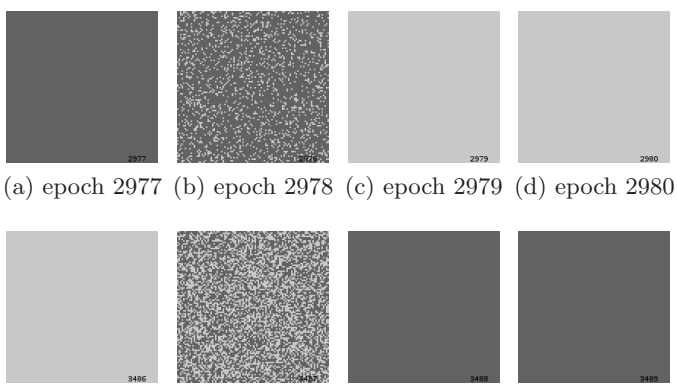

(a) epoch 2977 (b) epoch 2978 (c) epoch 2979 (d) epoch 2980

(e) epoch 3486 (f) epoch 3487 (g) epoch 3488 (h) epoch 3489

Figure 5.5: Fully Connected Lattice : Overlap=10%, $D_c = 0.2$, $D = 0.2$, $r = 1$ and $NL = 0.001$ in 2D 100×100

5.3 Small-world Phenomenon

Small-world graphs can be modelled in various ways – Watts and Strogatz [1998] (WS) model, Newman and Watts [1999] (NW) model, Dorogovtsev and Mendes [2002] (SW) model, etc. We introduce small-world effects to the underlying 2-lattice graph by applying either the WS, NW or SW model to

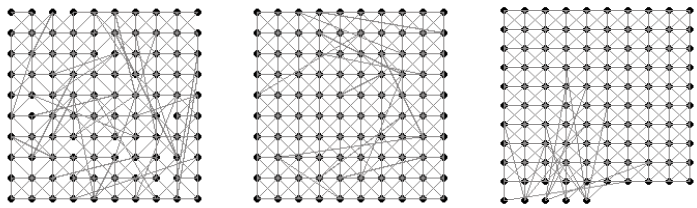

(a) (b) (c)

Figure 5.6: 2-lattice Small-world Models
(a) Watts-Strogatz (WS) ($p = 0.05$) (b) Newman-Watts (NW) ($p = 0.05$)
(c) Smallest World (SW) ($p = 0.05$)

introduce non-local long-range shortcuts. These processes may change the size and order of the neighbourhood (Γ) of each vertex depending on a random probability $0 < p < 1$. WS maintains the order ($N * N$) and size ($N * N * k/2$) of the graph, NW changes the size of the graph but not the order and SW alters both the size and order of the graph. Hence in the visualisations, the snapshots of the smallest-world (SW) lattice are a little taller than for WS and NW because its order (and size) grow with increasing randomness. The newly added habitats are shown at the bottoms of the snapshot.

WS model In the WS model, for each edge (u, v) in the underlying square lattice with k-sized neighbourhood (sub Figure 5.1 (a)), the selected edge is rewired with probability p. In other words, a new edge (u, w) is added to a randomly chosen vertex $w \notin (u \cup \Gamma(u))$ in the rest of the lattice, and the existing edge (u, v) is removed (sub Figure 5.6 (a)). When $p = 1$, the graph is completely rewired into a random graph (sub Figure 5.1 (b)).

NW model In the NW model, for each edge (u, v) in the underlying square lattice with k nearest neighbours (sub Figure 5.1 (a)), an extra short cut (u, w) is added, joining u to a randomly chosen vertex $w \notin (u \cup \Gamma(u))$ with probability p (sub Figure 5.6 (b)).

SW model In the SW model, N^2p new vertices (V') are added and are connected to k randomly chosen vertices in the initial regular lattice (sub Figure 5.6 (c)).

The small-world graphs generated from the above models conform to simple graph properties. ie., the added or rewired edges are undirected without self loops ($(v, v) \notin E$) and without parallel edges (multiple or duplicate). In WS, re-created copies of previously removed edges are discarded. The three models exhibit the small-world effect to varying degrees but they are generally connected (there is a path between any two distinct vertices) with short paths and have low average vertex degree ($k \ll n$ and $k \gg 1$) with high degrees of clustering.

5.3.1 Indentifying the Small-world Regime

The small world regime is identified as the region where $\bar{L}(p) \gtrsim \bar{L}(1)$ and $\bar{C}(p) \gg \bar{C}(1)$, or in other words where the proximity ratio $\mu \gg 1$. Starting from randomness probability $p = 0$, the average path length rapidly drops with increasing p for all three models, as can be observed in Figures 5.7, 5.8 and 5.9.[1] In the small world regime (the shaded regions in these Figures), the observed structural properties of the graphs are similar to real-world topologies – we see a coexistence of small path length and high cliquishness.

5.3.2 Degree Distribution of Small-world Models

The Figure 5.10 shows the degree distribution of small-world graphs (in 100×100 lattice) generated via WS (5.10 (a)), NW (5.10 (b)) and SW (5.10 (c)) models. All possessing Poisson distribution with tails reaching 0.

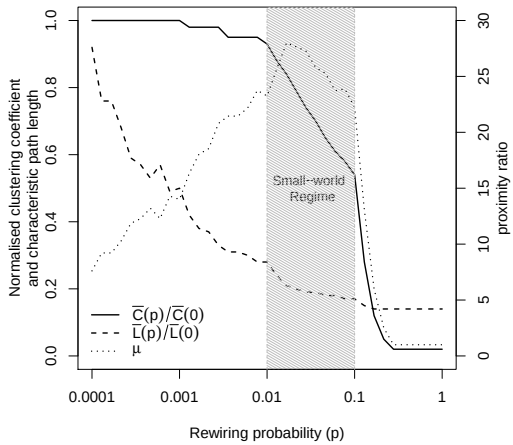

Figure 5.7: Watts-Strogatz model in 2D 100×100 lattice: Clustering Coefficient, Characteristic Path Length and Proximity Ratio

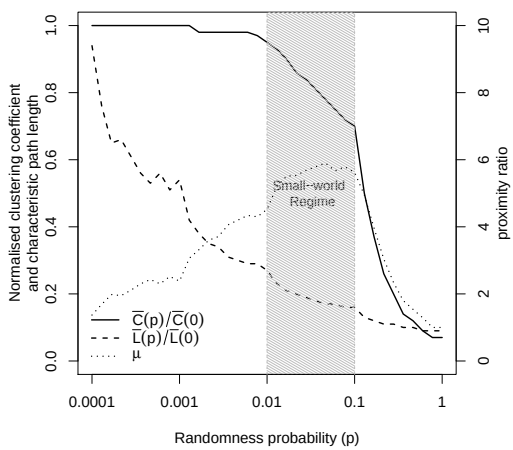

Figure 5.8: Newman-Watts model in 2D 100×100 lattice: Clustering Coefficient, Characteristic Path Length and Proximity Ratio

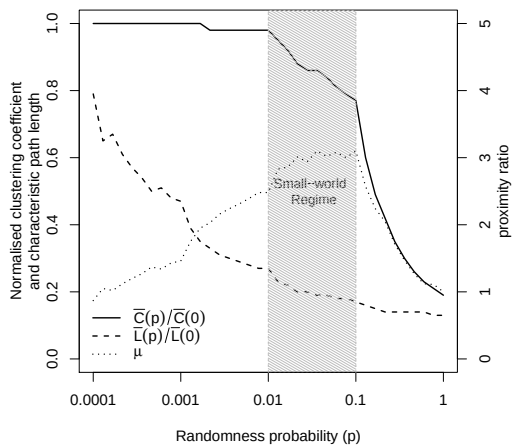

Figure 5.9: Smallest World model in 2D 100×100 lattice: Clustering Coefficient, Characteristic Path Length and Proximity Ratio

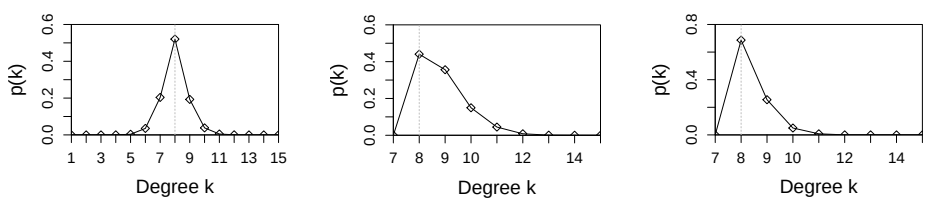

(a) WS (b) NW (c) SW

Figure 5.10: Degree Distribution of Small-world Models

5.3.3 Daisyworld with Static Local and Non-local Couplings

We observe a phase change in daisy population dynamics, from static self-organised patterns to periodic behaviour, when small-world effects are introduced by any of the three models – WS, NW, SW.

[1]In these Figures, the values of $\bar{L}(p)$ and $\bar{C}(p)$ are normalised by the respective values of a regular lattice $\bar{L}(0)$ and $\bar{C}(0)$.

Table 5.2: $\bar{C}$, $\bar{L}$ and μ; $p = 0.05$ is qualitatively compared with $p = 1$ and quantitatively compared with μ

	$\bar{L}(0.05)$	$\bar{L}(1)$	$\bar{C}(0.05)$	$\bar{C}(1)$	$\mu(0.05)$
WS	0.19	0.14	0.74	0.02	27.26
NW	0.19	0.09	0.84	0.07	5.68
SW	0.2	0.13	0.86	0.19	2.94

We fix 0.05 as the randomness probability for all the three models (WS, NW and SW) in our experiments for easy comparison. At $p = 0.05$, we have tabulated the corresponding values of characteristic path length, clustering coefficient and proximity ratio for all models (Table 5.2). We can conclude that all graphs exhibit small-world effects. The μ values for NW and SW greatly differ from those for WS for the obvious reasons: WS maintains the graph size and order even up to probability ($p = 1$), whereas the other models do not.[1]

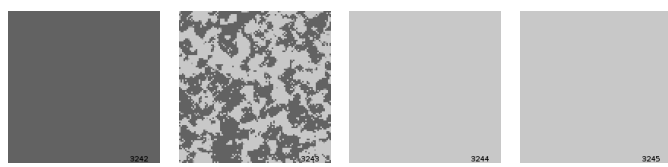

(a) epoch 3242 (b) epoch 3243 (c) epoch 3244 (d) epoch 3245

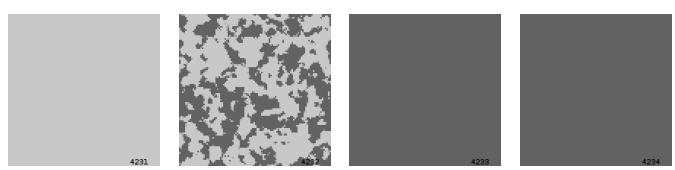

(e) epoch 4231 (f) epoch 4232 (g) epoch 4233 (h) epoch 4234

Figure 5.11: Watts-Strogatz Model ($p = 0.05$) : Overlap=10%, $D_c = 0.2$, $D = 0.2$, $r = 1$ and $NL = 0.001$ in 2D 100×100 Small-world Lattice

[1]We picked the probability $p = 0.05$ by inspecting the visuals and by analysing the results of quantifiers; please see section 5.3.4 for more details.

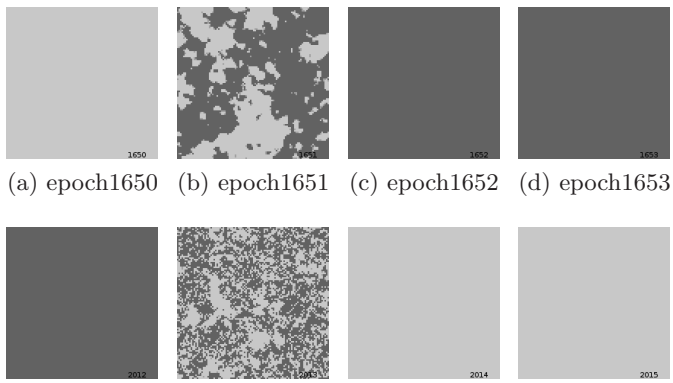

(a) epoch1650 (b) epoch1651 (c) epoch1652 (d) epoch1653

(e) epoch2012 (f) epoch2013 (g) epoch2014 (h) epoch2015

Figure 5.12: Newman-Watts ($p = 0.05$) : Overlap=10%, $D_c = 0.2$, $D = 0.2$, $r = 1$ and $NL = 0.001$ in 2D 100×100 Small-world CML

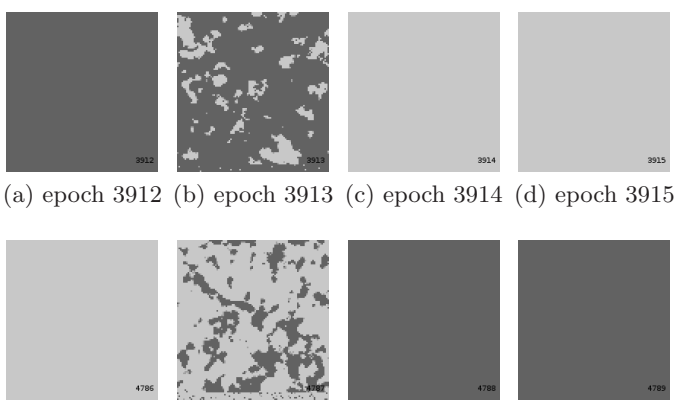

(a) epoch 3912 (b) epoch 3913 (c) epoch 3914 (d) epoch 3915

(e) epoch 4786 (f) epoch 4787 (g) epoch 4788 (h) epoch 4789

Figure 5.13: Smallest-World Model ($p = 0.05$) : Overlap=10%, $D_c = 0.2$, $D = 0.2$, $r = 1$ and $NL = 0.001$ in 2D 100×100 Small-world Lattice

Watts-Strogatz (WS) model: We observe that the periodic behaviour we saw in random and fully connected graphs is also exhibited in WS-based small-world graphs (Figure 5.11). The transition between the daisy type dominance is also very rapid (see the epoch numbers in the visuals), even though most connectivities are still local. The periodicity in the daisyworld dynamics

is confirmed by the temporal trajectories of the local population abundance (Figure 5.42), global population abundance (Figure 5.43) and temperature dynamics (Figure 5.41).

Newman-Watts (NW) model: Each dynamic unit (habitat) is coupled through a small-world topology initialised through the NW mechanism. The topology remains static but the states of the habitats change dynamically. This ecosystem exhibits a periodic behaviour (Figure 5.12). The cyclic behaviour is understood by observing the trajectories in temperature dynamics (Figure 5.44), local population dynamics (Figure 5.45) and global population dynamics (Figure 5.46). This shows that a small change in the underlying topology drastically influences the dynamical properties of the ecosystem, and the transition is very abrupt. Within a single time frame, black dominance may change to white dominance, or vice versa (Figure 5.12).

Smallest-World (SW) model: Periodic behaviour again emerges from the small-world SW lattice (Figure 5.13), and we see similar periodicity in local population (Figure 5.48), global population (Figure 5.49) and temperature dynamics (Figure 5.47).

The result section 5.3.3 illustrates the collective dynamic behaviour (behaviour in a large system of similar interacting units) of a set of coupled life-environmental feedback oscillators with direct short-cuts chosen randomly between oscillators by either WS or NW or SW. Due to the introduction of the non-local connections, the range of interaction grows. But even a small degree of randomness in topological connectivity plays a constructive role in determining the dynamics of the system. This can be understood clearly by comparing the spatio-temporal trajectories of our daisyworld with only local connectives (Figures 5.32, 5.33 and 5.34) and daisyworld with both local and few non-local connectives by WS (Figures 5.41, 5.42 and 5.43), NW (Figures 5.44, 5.45 and 5.46) and SW (Figures 5.47, 5.48 and 5.49). The trajectories in regularly connected daisyworld are static with initial fluctuations

and the ones in smallworld-daisyworld are periodic in nature, which is obviously due to the random perturbation in connectivity, as in trajectories of fully connected daisyworld (Figures 5.38, 5.39, and 5.40).

In general, though the overall dynamics looks the same for random, fully-connected and small-world lattices, a detailed examination shows some differences. If we observe the transition frames, those between black dominance and white dominance or vice versa, they differ depending on the nature of the connectivity. However the main conclusion we can draw is that even quite low levels of long-range connection make daisyworld behave like a fully-connected world: the static emergent patterns of the grid world depend on the almost complete absence of long-range connections. With short-cuts, the emergent spatio-temporal pattern of the daisyworld is completely coherent in space and periodic in time. This sort of behavioural patterns can be observed in nature, for example in firing pattern of neurons [Goel and Ermentrout, 2002], flashing of fire flies [Mirollo and Strogatz, 1990], etc.

5.3.4 Possible Critical Point of Phase Change

Table 5.3: Possible Critical Point (p)

Model	**Probability** p
WS	0.02
NW	0.02
SW	0.04

If there is a phase transition in daisyworld behaviour between grid-like worlds ($p = 0$) and small-world graphs ($p = [0.01, 1]$), then it is of interest to examine the critical point: the point at which the new behaviour emerges. In this context, the relevant parameter is that controlling graph randomness, the probability parameter p (often known as the rewiring probability, as that is its role in the original WS model). The possible critical points for WS, NW and SW are tabulated in Table 5.3.

We examined the behaviour in the transition region of the small-world

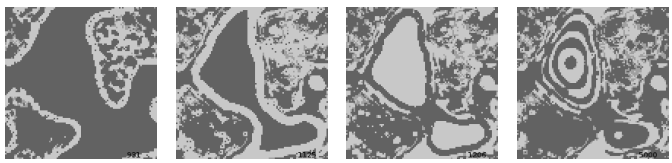

(a) epoch 931 (b) epoch 1125 (c) epoch 1206 (d) epoch 5000

Figure 5.14: WS close to phase change : Overlap=10%, $D_c = 0.2$, $D = 0.2$, $r = 1$ and $NL = 0.001$ in 2D 100×100 Small-world Lattice ($p = 0.01$)

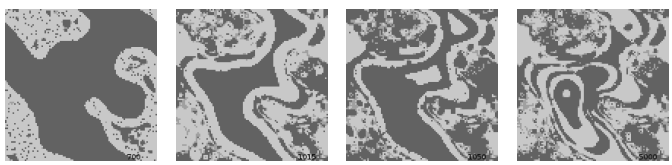

(a) epoch 700 (b) epoch 1015 (c) epoch 1050 (d) epoch 5000

Figure 5.15: NW close to phase change : Overlap=10%, $D_c = 0.2$, $D = 0.2$, $r = 1$ and $NL = 0.001$ in 2D 100×100 Small-world Lattice ($p = 0.01$)

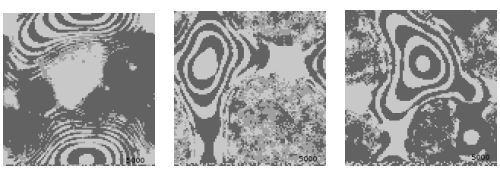

(a) p=0.01 (b) p=0.02 (c) p=0.03

Figure 5.16: SW close to phase change : Overlap=10%, $D_c = 0.2$, $D = 0.2$, $r = 1$ and $NL = 0.001$ in 2D 100×100 Small-world Lattice at epoch $5,000$

effect regime for each of the three small-world mechanisms. In each case, we see a mix of self-organised patterns (as in regular lattices) and partially collapsed patterns (as in random or fully-connected graphs). We show the dynamics for WS (Figure 5.14) and NW (Figure 5.15) at ($p = 0.01$). For SW, we show only the final system state, but at different probability parameter values ($p = 0.01, 0.02, 0.03$ – Figure 5.16). The coexistence of order and disorder indicates that the system behaviour is in transition. The small dots or patches

that we see in the visuals are due to the shortcuts, which tend to destroy the static patterns that we see in regular lattice.

Table 5.4: Spatial Emergence and Std. Dev. of States

Spatial emergence	**Std. dev.**
Mix of states	> 0.25
Dominance of a state	< 0.25

Table 5.5: Temporal Dynamics and Permutation Entropy

Temporal dynamics	**PE**
Static	< 0.1
Periodic	$[0.1, 0.2]$

Table 5.6: Spatio-temporal Patterns

Patterns	**Std. dev.**	**PE**
Self-organised	> 0.25	< 0.1
Static distorted	> 0.25	< 0.1
Periodic distorted	> 0.25	$[0.1, 0.2]$
Periodic complete dominance	< 0.25	$[0.1, 0.2]$

5.3.5 Topology and Criticality

Topology explains how the habitats of the ecosystem are connected and criticality explains how the ecosystem behaves. The topological connectivity affects the critical behaviour of the ecosystem. Since identifying the critical points by inspecting the visuals is laborious, we computed the standard deviation of the local states (spatial dynamics; refer Table 5.4) and permutation entropy (PE) (temporal dynamics; refer Table 5.5). We also used standard deviation of states and PE to analyse the spatio-temporal pattern formation in our daisyworld – (1)static complex self-organised or (2)periodic complete dominance or (3)static distorted patterns or (4)periodic distorted patterns; re-

Table 5.7: The range of std. dev. of states and PE of daisies for 25 realizations

Model	p	**Std. dev.**	**PE**
WS	0.01	$[0.474, 0.649]$	$[0.062, 0.086]$
WS	0.02	$[0.028, 0.595]$	$[0.116, 0.073]$
WS	0.03	$[0.019, 0.589]$	$[0.119, 0.058]$
WS	0.04	$[0.015, 0.504]$	$[0.117, 0.074]$
WS	0.05	$[0.011, 0.563]$	$[0.118, 0.035]$
NW	0.01	$[0.462, 0.647]$	$[0.126, 0.080]$
NW	0.02	$[0.032, 0.618]$	$[0.116, 0.068]$
NW	0.03	$[0.018, 0.586]$	$[0.119, 0.058]$
NW	0.04	$[0.015, 0.516]$	$[0.116, 0.067]$
NW	0.05	$[0.011, 0.524]$	$[0.117, 0.058]$
SW	0.01	$[0.556, 0.682]$	$[0.071, 0.095]$
SW	0.02	$[0.514, 0.691]$	$[0.062, 0.101]$
SW	0.03	$[0.415, 0.647]$	$[0.146, 0.068]$
SW	0.04	$[0.035, 0.646]$	$[0.116, 0.058]$
SW	0.05	$[0.024, 0.622]$	$[0.116, 0.059]$

fer 5.6. Daisyworlds with only local connections exhibit self-organised patterns (Figure 5.3). Periodic complete dominance patterns emerge from daisyworld with local and a few long range connections at critical points (Figures 5.11, 5.12 and 5.13) and from fully connected daisyworld (Figure 5.5). In the transition regions, we observe static or periodic distorted patterns (Figures 5.14, 5.15 and 5.16).

Though we see a collective behaviour of the whole ecosystem (a snapshot) in the visuals, each habitat falls into one of the six states of life. They are (1) no life (dead state) (2) only the presence of black daisies (complete black dominance state) (3) only the presence of white daisies (complete white dominance state) (4) presence of both black and white daisies in equal numbers (coexistence state with equality) (5) presence of both but with black abundance (coexistence state with black abundance) and (6) presence of both but with white abundance (coexistence state with white abundance). In our experiments, the states (1) and (4) are rare; the other four states indicate the

dominance of a particular daisy type with coexistence or otherwise.

If we analyse the states of all habitats and compute their standard deviation, we can understand the behaviour of the ecosystem spatially at a particular epoch – mix of states or a dominance of a particular state. If we compute the standard deviation of states for all the $5,000$ epochs, we can understand the behaviour of the system over a period of time. Obviously the standard deviation of states is 0 if all the habitats in the ecosystem have the same state – dominance of a particular state. Hence if the average standard deviation of the whole ecosystem over $5,000$ epochs is very low in the range $[0, 0.25]$, our daisyworld system exhibits complete dominance patterns. In our experiments, we see values are little over 0 because the computation includes the initial and transition epochs.

We used permutation entropy (PE) to measure the periodicity in the temporal trajectory of both black and white daisies of a habitat (with its ecological aggregates) in the ecosystem. We sampled N out of $N * N$ habitats and compute PE for each of the sample and then averaged them. If the averaged PE is in the range $[0.1, 0.2]$, it indicates the presence of periodic attractors in the temporal series of daisies (population size).

A configuration of an experiment is defined how a small-world graph is constructed – by which of the mechanisms (WS or NW or SW) and which randomness probability $p = [0.01, 0.05]$ is used. All other parameters such as $D = 0.2$ and $NL = 0.001$ are same for all the configurations. For each of the topological configurations, we run 25 realizations. The spatio-temporal behaviour for each realization of the same configuration can be different due to the randomness in the connectivity and ecosystem disturbance in the form of additive spatio-temporal Gaussian white noise controlled by the noise level. If any one of 25 realizations of a configuration has both the standard deviation of the states in $[0, 0.25]$ and PE in $[0.1, 0.2]$, we consider that p as the critical point for that configuration. The range of standard deviation of states and permutation entropy values are listed in Table 5.7 with the corresponding small-world construction model and p for all the 25 realizations.

The standard deviation of states and PE for the configurations WS($p =$

0.01), NW($p = 0.01$), SW($p = 0.01, 0.02, 0.03$) and for all their 25 realizations (Table 5.7) are not in the specified ranges (Tables 5.4 and 5.5). Hence, the possible critical points are chosen as listed in Table 5.3.

5.3.6 Without Life-Environment Feedback

(a) epoch 50 (b) epoch 1000 (c) epoch 3000 (d) epoch 5000

Figure 5.17: Regular without life-environment feedback: $p = 0$, $D = 0.2$ and $NL = 0.001$ in 2D 100×100

(a) epoch 50 (b) epoch 1000 (c) epoch 5000 (d) epoch 10000

Figure 5.18: WS without life-environment feedback: $D = 0.2$ and $NL = 0.001$ in 2D 100×100 Small-world Lattice ($p = 0.05$)

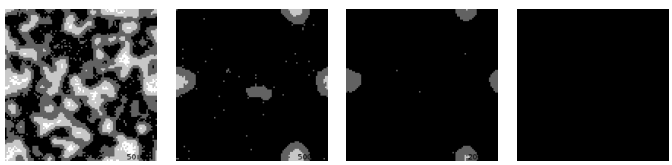

(a) epoch 50 (b) epoch 5000 (c) epoch 20000 (d) epoch 35175

Figure 5.19: NW without life-environment feedback: $D = 0.2$ and $NL = 0.001$ in 2D 100×100 Small-world Lattice ($p = 0.05$)

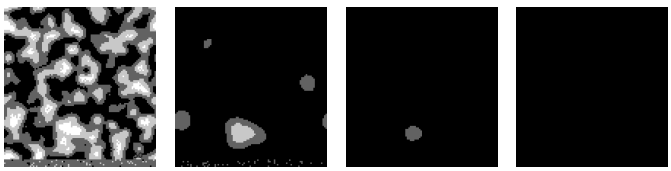

(a) epoch 50 (b) epoch 5000 (c) epoch 50000(d) epoch 61010

Figure 5.20: SW without life-environment feedback: $D = 0.2$ and $NL = 0.001$ in 2D 100×100 Small-world Lattice ($p = 0.05$)

In this section, we validate the system dynamics with no closed loop. To investigate this, we disrupt the feedback: the environment still influences the life (daisies' growth depends on temperature), but there is no feedback from the life to the environment, the daisies do not influence the temperature. We examine the dynamics of system without such feedback in a regular lattice (Figure 5.17) and in small-world lattices – WS (Figure 5.18), NW (Figure 5.19), SW (Figure 5.20). We observe that there is no dynamicity in the behaviour, simply a steady increase in the black daisy cover. The feedback from ecosystem to environment is essential to the rich dynamics of daisyworld, and in the absence of feedback, the qualitative behaviours of regular and small-world lattices are similar. However the long-distance connectivities do change the quantitative behaviour: small-world networks take far longer to converge to a completely black cover (see the epoch numbers in sub Figures 5.18 (d), 5.19 (d) and 5.20 (d) – the final frame is sampled soon after the first emergence of a complete black cover for each model).

5.3.7 Summary

We have explored the implications of small-world phenomena in two-dimensional coupled map daisyworld – a superposition of regular and random graphs. The small fraction of introduced fluctuations in the daisyworld grid structure dramatically affects the dynamics of the system. Proportionally, fewer connections are required for almost full interconnectivity. A few random long range connections to the underlying regular lattice (with high degree of separation)

improves the overall connectivity. Thus adding more and more connections will not increase the connectivity of the lattice. We see an emergence of collective dynamical behaviours, exemplified by homogeneous invasion of a particular daisy type. The daisyworld system in a small-world graphs evolves toward a critical state, where small perturbation are amplified and affect the whole system.

With changes in the level of random connections, we noted a phase transition in the daisyworld, from a self-organised static world to a periodic (seasonal) world in which black or white daisies spread rapidly dominating the whole world. Small alterations to the local structure of daisyworld heavily impact the global emergence. Nevertheless, despite these great variations in behaviour, the temperature is still regulated around 295.5K even in the presence of external perturbations to its connectivity.

5.4 Adaptive Couplings

We examine connectivity changes in a complex adaptive ecosystem based on the daisyworld model, combining coupled map lattice (CML) and complex adaptive graph models. Daisyworld topologies in the literature are static, with only local connections [Wood et al., 2008]. In the previous section 5.3, we have investigated ecological homeostasis in preconstructed static topologies with local and non-local long range couplings –small-world graphs [Punithan et al., 2011; Punithan and McKay, 2013b]. But complex topologies in nature and society are adaptive, in that they exhibit feedback between the local dynamics of nodes (state) and the evolution of the topological structure [Gross and Blasius, 2008; Gross and Sayama, 2009]. Examples include genetic, neural, immunity, ecological, economic and social graphs, complex game interactions etc.

The topology of our ecosystem evolves in response to local habitat states, and the evolved topology in turn impacts the habitat states. Our adaptive and self-maintaining ecosystem, based on CML consists of a set of diffusively coupled habitats incorporating logistic growth of life with bi-directional biota-

environment influences. Thus our ecosystem incorporates three kinds of feedback:

1. Life-environment feedback via the daisyworld model
2. State-topology feedback via an adaptive graph model
3. Density-growth feedback via a logistic growth model

The topology of the our ecosystem evolves with a simple local rule – a frozen habitat is reciprocally linked to an active habitat – and self-organises to complex topologies with small-world effect. In this section, we focus on the emergent collective phenomena and properties that arise in egalitarian small-world ecosystems, constructed from a large number of interacting adaptively linked habitats.

5.4.1 Daisyworld with Dynamic Local and Non-local Couplings

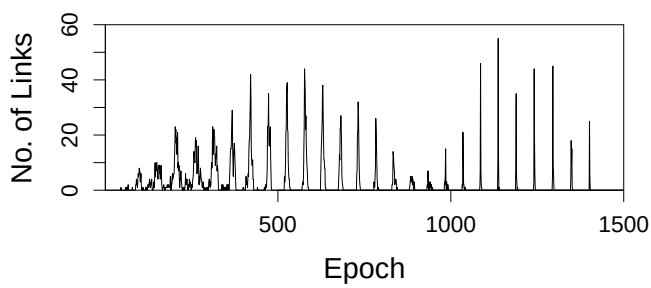

Figure 5.21: Adapted Reciprocal Couplings

The local dynamical linking rule (when a node becomes frozen, we allow that habitat to reciprocally connect to a random active habitat) generates topologies with small-world effect (low characteristic path length (CP)) – here we show topologies with high clustering coefficient (CC) (approximately 50% of runs) to compare to NW-CML ($p = 0.05$). It can also generate topologies with

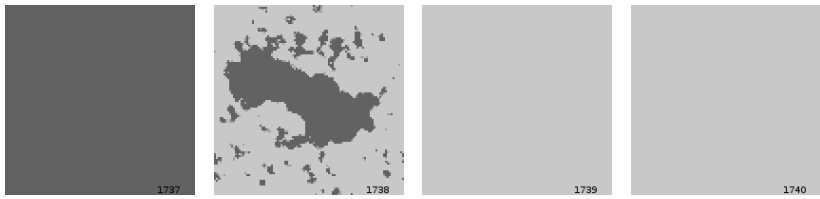

(a) epoch1737 (b) epoch1738 (c) epoch1739 (d) epoch1740

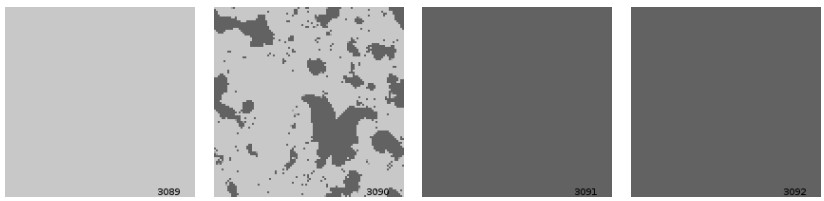

(e) epoch3089 (f) epoch3090 (g) epoch3091 (h) epoch3092

Figure 5.22: Adaptive CML : Overlap=10%, $D_c = 0.2$, $D = 0.2$, $r = 1$ and $NL = 0.001$ in 2D 100×100

low CC. It depends on the random initialization of the temperature of each habitat and random dynamic linking. Typically we observe periodic behaviour (Figure 5.22) similar to NW-CML. In the corresponding time series plots, the dynamics of both local and global temperature (Figure 5.50), local population (Figure 5.51) and global population (Figure 5.52) exhibit cyclic behaviour. The dynamically adapted reciprocal links are shown in Figure 5.21.

5.4.2 Topological Properties of NW-CML and Adaptive CML

Table 5.8: Typical Clustering Coefficients and Characteristic Path Lengths

Model	$\bar{C}(p)/\bar{C}(0)$	$\bar{L}(p)/\bar{L}(0)$
NW-CML	0.837	0.185
Adaptive CML	0.837	0.189

We saw very similar limit behaviours from CML based small-worlds (section 5.3 and adaptive CML (sub section 5.4.1). For comparison and analysis, we take NW-CML results with adptive CML. We can gain understanding

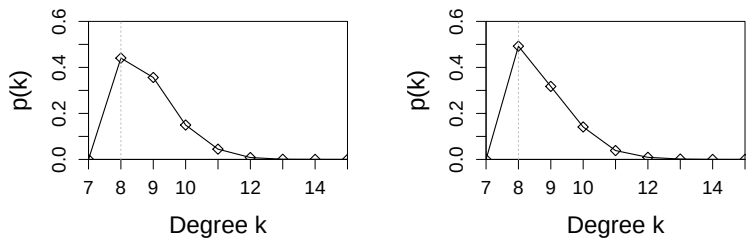

(a) NW-CML (b) Adaptive CML

Figure 5.23: Degree Distribution

through analysing the topological quantifiers (degree distribution, clustering coefficient and characteristic path length) for their network topologies.

The degree distribution of the small-world CML constructed via the NW model in sub section 5.3.3 ranges over $[8, 14]$ and has an exponential tail reaching zero, as shown in the Figure 5.10 (b). The degree distribution reached by adaptive CML in sub section 5.4.1, which dynamically linked with reciprocal links, also ranges over $[8, 14]$ and has an exponential tail reaching zero as shown in the Figure 5.23 (b).

The CC for NW-CML, and that for the final epoch of adaptive CML are almost the same, as are CPs. Figure 5.23 and Table 5.8 show the results. The finally-converged adaptive CML is an egalitarian small-world network. This is why we observe a drastic change in the dynamics of the system compared to the regular lattice. It also shows that the topology, constructed statically or dynamically, influences the collective behaviour of the system: relatively small changes in the linkage structure can generate vastly different dynamics.

Table 5.9: Average($\pm Std.Dev.$) Clustering Coefficients and Characteristic Path Lengths

Model	$\bar{C}(p)/\bar{C}(0)$	$\bar{L}(p)/\bar{L}(0)$
NW-CML	0.8412 ± 0.0024	0.1868 ± 0.001
Adaptive CML	0.8928 ± 0.0639	0.2204 ± 0.0392

The sub section 5.3.3 and sub section 5.4.1 illustrate typical scenarios of NW-CML and adaptive CML. Table 5.9 shows averages over 25 realisations of adaptive CML model and 25 of NW-CML ($p = 0.05$) model. We ran 100 realizations of adaptive CML and picked 25 that fell in small-world regime [Punithan and McKay, 2013b] for comparison purposes – CC in $[0.98, 0.7]$ and CP in $[0.3, 0.16]$. CC and CP are normalised by the values for a regular lattice as proposed in [Watts and Strogatz, 1998].

5.4.3 Topological Evolution

Table 5.10: Adaptation : Clustering Coefficients and Characteristic Path Lengths

Adaptation	$\bar{C}(p)/\bar{C}(0)$	$\bar{L}(p)/\bar{L}(0)$
Quick	0.977	0.295
Slow	0.837	0.238

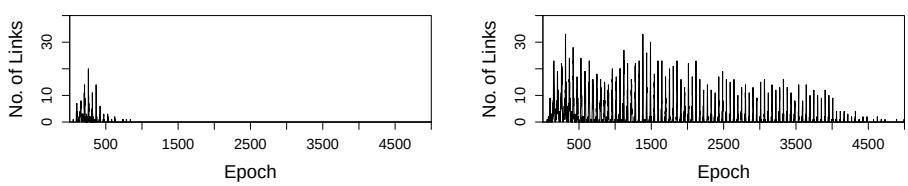

(a) Quick Adaption

(b) Slow Adaptation

Figure 5.24: Adapted Reciprocal Couplings

The evolution of the topology continues until the stationary attractor (frozen local dynamics) of all habitats reach a dynamical attractor – here a limit cycle. Some samples adapt quickly, reaching a stable topology around the 500th epoch (Figure 5.24 (a) – Quick Adaptation), while a few evolve almost until the 5000th epoch (Figure 5.24 (b) – Slow Adaptation). Their degree distribution (Figure 5.25), clustering coefficient and characteristic path (Ta-

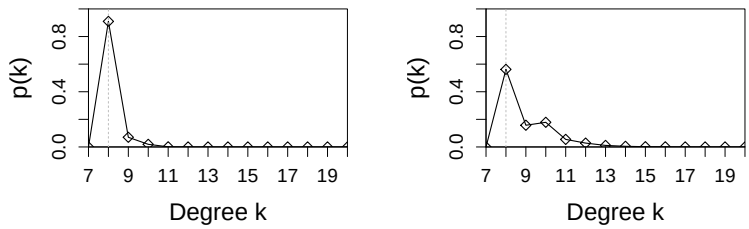

(a) Quick Adaption (b) Slow Adaptation

Figure 5.25: Degree Distribution

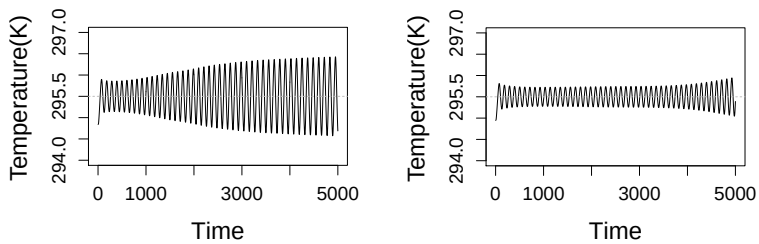

(a) Quick Adaptation (b) Slow Adaptation

Figure 5.26: Global Temperature dynamics : Overlap=10%, $D_c = 0.2$, $D = 0.2$, $r = 1$ and $NL = 0.001$

ble 5.10) show that both evolve to small-world networks, although at different rates.

The collective dynamics in both quick and slow adaptations (Figures 5.27 and 5.28) show the shift in dominance is not so abrupt as in Figures 5.12 and 5.22 (see epoch nos.). The emergent property – the temperature cycles – depicted in Figure 5.26 (in both adaptations) have different limit ranges. In sub Figure 5.26 (b), the shift in dominance takes more time initially, eventually speeding up owing to the increasing limit height. The abruptness is clear in the corresponding global temperature plots – compare the limits in sub

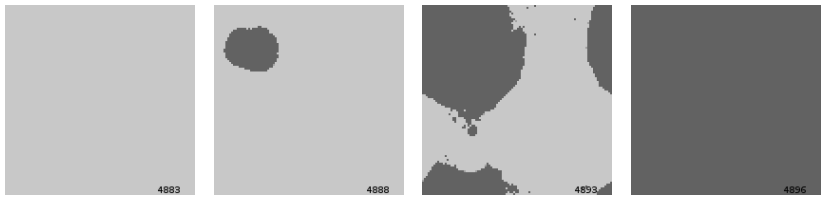

(a) epoch4883 (b) epoch4888 (c) epoch4893 (d) epoch4896

(e) epoch4942 (f) epoch4947 (g) epoch4951 (h) epoch4954

Figure 5.27: Quick Adaptation : Overlap=10%, $D_c = 0.2$, $D = 0.2$, $r = 1$ and $NL = 0.001$ in 2D 100×100

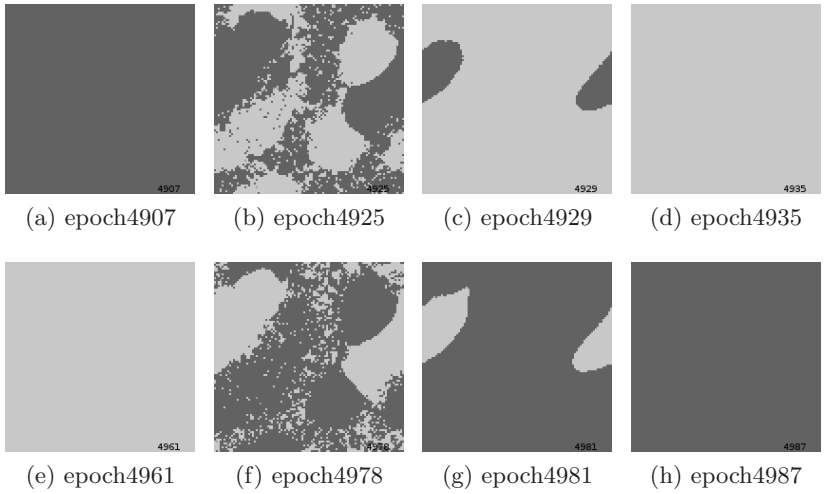

(a) epoch4907 (b) epoch4925 (c) epoch4929 (d) epoch4935

(e) epoch4961 (f) epoch4978 (g) epoch4981 (h) epoch4987

Figure 5.28: Slow Adaptation : Overlap=10%, $D_c = 0.2$, $D = 0.2$, $r = 1$ and and $NL = 0.001$ in 2D 100×100

Figures 5.44 (b), 5.50 (b), 5.26 (a) and 5.26 (b). The degree distribution shows that relatively few reciprocal links are added (sub Figure 5.25 (a)).

This confirms even a few long-distance links – if they are the right links – lead to drastic behaviours changes.

5.4.4 Summary

We have analysed the connectivity changes in a complex adaptive ecosystem combining life-environment, state-topology and density-growth feedback loops. The results illustrate the capacity of the adaptive ecosystem to self-organise to a complex ecosystem (small-world network) through a simple dynamical rule – frozen habitats (nodes) gain reciprocal non-local neighbours (links). Though the collective dynamics change in varying ways, we still observe the emergent property – self-regulation of the temperature at around $295.5K$.

5.5 Scale-freeness

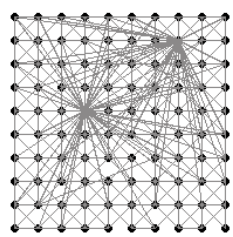

Figure 5.29: Scale-free Graph

We incorporate scale-freeness by pre-defining a set of hub nodes. A node, in a 2-lattice, is assigned a set of $k = 8$ neighbours. The neighbours are added either to local nodes or to hub nodes or to a non-local long-range nodes. Each node is added to any of the hub nodes with probability p, to non-local nodes with probability q and the remaining are added to the local neighbours (Figure 5.29).

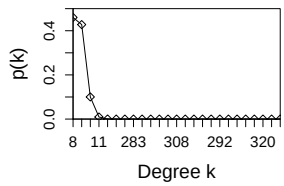

Figure 5.30: Scale-free Degree Distribution

5.5.1 Degree Distribution of Scale-free Graph

Figure 5.30 depicts the degree distribution of the constructed scale-free graph which has a long tail.

5.5.2 Daisyworld with Hubs

Table 5.11: Scale-free Graph : Clustering Coefficient and Characteristic Path Length

$\bar{C}(p)/\bar{C}(0)$	0.79
$\bar{L}(p)/\bar{L}(0)$	0.115

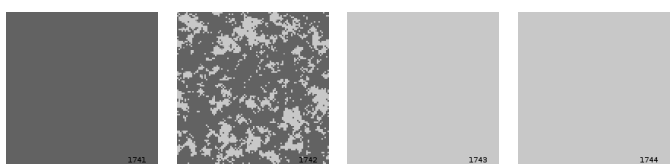

(a) epoch1741 (b) epoch1742 (c) epoch1743 (d) epoch1744

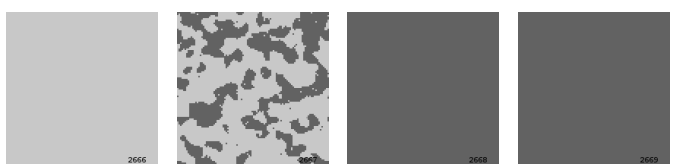

(e) epoch2666 (f) epoch2667 (g) epoch2668 (h) epoch2669

Figure 5.31: $D = 0.2$ and $NL = 0.001$ in 2D 100×100 Scale-free CML

Cyclical behaviour emerges from the lattice with scale-freeness (Figure 5.31), and we see cycles in local population (Figure 5.54), global population (Figure 5.55) and temperature dynamics (Figure 5.53). The degree distribution has a long-tail (Figure 5.30). The corresponding clustering coefficient and characteristic path length are represented in the Table 5.11.

5.5.3 Summary

The results in this section show that the temperature is regulated around $295.5K$ with the hubs and high clustering coefficient. The system behaviour is very similar to daisyworld with small-world phenomenon – 'completely coherent (homogeneous) short-lived cyclical dominance'.

5.6 Behaviour Study

5.6.1 Daisyworld Behaviour in Complex and Adaptive Topologies

Each habitat in the grid daisyworld is confined to a local environment. The inclusion of a few long-range connections, generating a small world networks, brings the whole world close: information is able to disseminate rapidly (ie., dispersion of both daisy types is very rapid). The presence of this global information at a local scale significantly affects the dynamics of daisyworld. Daisyworld with small-world shortcuts in a locally structured networks greatly speeds up the migration of the daisy populations, overcoming the formation of static patterns. The population dynamics in a small-world daisyworld is similar to that of a fully-connected world: just a few long-range connections rapidly disseminating information can completely change the behaviour of the daisyworld. Even a small perturbation in connections are enough for the transition of the system state from a static patterns to dynamic recurrent homogeneous dominance. This recurrent global emergence of complete domination of a particular type of daisies leads to analogies not just in ecosystems dynamics, but in real-world scenarios such as social collective behaviour.

5.6.2 Social Collective Behaviour

In sociology, collective behaviour is defined as "...voluntary, often spontaneous activity that is engaged in by a large number of people and typically violates dominant-group norms and values" [Kendall, 2012]. A contemporary example of collective social behaviour is "flash mobs". Rumours and gossip, crazes and mania, mass hysteria and panic, fads and fashions, public opinion and propaganda are different forms of mass (collective) behaviour [Kendall, 2012; Macionis, 2009] – a dispersed "collective behaviour among people spread over a wide geographic area" [Macionis, 2009]. Fashions are accepted "cultural forms but are periodically subject to change" such as clothing and hair styles, furniture styles, cars, sports, dog breeds, etc. Among varied mass behaviour forms, fads, crazes and mania are similar to fashion but have more extreme rise and fall in their behavioural pattern – a large group of people catch on and adopt very quickly but also give up abruptly.

Fads ("unconventional social patterns" [Macionis, 2009]) emerge out of nowhere and abruptly vanish as fast they appeared. Sometimes, fads that have disappeared reappear and are embraced enthusiastically by a large number of people, even though they are not in one another's immediate vicinity. This phenomenon presumably results from nostalgia. For example, disco music originally emerged in the 1970s and re-emerged in the late 1990s [Malnig, 2008]. Hula hoop, yo-yos, pokemon cards [Andersen and Taylor, 2007] are other examples of the rise and fall of fads from pop culture – reappearing from time to time [Macionis, 2009]. This is due to 'bandwagon effect' – a form of the psychological phenomenon known as 'groupthink'.

Economic bubbles are similar to fads, but profit is the motivator. An example is the high-tech stock boom of the late 1990s, with the corresponding "bubble burst" in the early 2000s. The boom and the burst phases of the economic bubble are result from positive feedback. In dot-com frenzy, a large number of investors purchased technology and e-commerce stocks in the hope of a short-term profit (herd mentality). The stocks reached a higher price than could be supported by the fundamental market value, and subsequently

crashed in value. The Dutch tulip mania, the British south sea bubble and nineteenth century railroad manias are other examples of economic bubbles in history [Mackay, 2004].

Both these examples, the quasi-manic behaviour of fads, with their rapid rise and fall and the boom and bust cycles of markets exhibit similar dynamics, often analogised by a simple model, periodic ups and downs of hemlines. Their behavioural patterns consist of four phases – a rising transition, a positive peak, a falling transition and a negative peak – a behaviour we see clearly modelled in daisyworld.

In the past, with few or no long-distance connections, fads and bubbles were localised, so that a spatially stabilised equilibrium could be reached. Thus tulip mania dramatically affected the Netherlands, but had limited effect on other economies; crinolines could cripple the women of Europe without in the least affecting fashion in East Asia. Nowadays, mass behaviour can propagate beyond physical proximity via telecommunications, viral emails, social media, etc. Hence, the observed behavioural pattern of our small-word daisyworld model – recurrent dominance of black and white daisies and sudden emergence followed by sudden collapse – is reminiscent of more globalised fads and crazes.

5.6.3 Analogies with Popular Metaphors

This "small cause, large effect" behaviour draws analogies with popular metaphors black swan (low probable but high-impact events) [Taleb, 2010], butterfly effect (sensitive dependence on initial conditions) [Hilborn, 2004] and tipping point (little things make a big difference) [Gladwell, 2006].

5.6.4 A Comparative Study

This ecosystem exhibits similar behaviour to contagion systems such as memes or virus – cyclic behaviours – without any external intervention, requiring only the adding of new reciprocal connections under certain locally-defined conditions. Even a small change in the connectivity, with almost no effect on the mean degree of the ecosystem, leads to a drastic behaviour change from

the grid network. It is much more like the real-world behaviour we see in social systems (seasonal rise and fall of fads), economic systems (cyclical booms and busts) etc.. A Flash crash is the quick drop and recovery in stock prices – few recent crashes are May 6, 2010 flash crash and April 23, 2013 flash crash.

The high interconnectivity (same as fully-connected network), owing to the addition of extra connections, of the small-world networks cause the butterfly effect and tipping points. The shortcuts are both change-propagating and change-restraining. Mathematical physics guarantees that there is always a sharp tipping point [Buchanan, 2003] (phase transitions or critical points) – implying that there are always conditions under which a group of social agents or an ecosystem is susceptible to change. When a system goes beyond a threshold, changes occur – a breakthrough or a breakdown. A cascade (contagion or chain-reaction or domino-effect) propagates the effect of the new change across the network. Thus, the individuals in the group act as a coherent mass [Watts, 2004]. This spread can be very rapid and become universal. Example market bubble burst, epidemic of disease, fads, memes, etc.

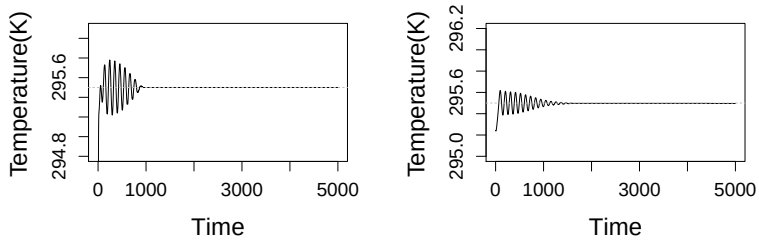

(a) Local Temp. at habitat (57, 50) (b) Global Surface Temp.

Figure 5.32: Regular CML : Temperature dynamics; $p = 0$, Overlap=10%, $D_c = 0.2$, $D = 0.2$, $r = 1$ and $NL = 0.001$ in 2D 100×100

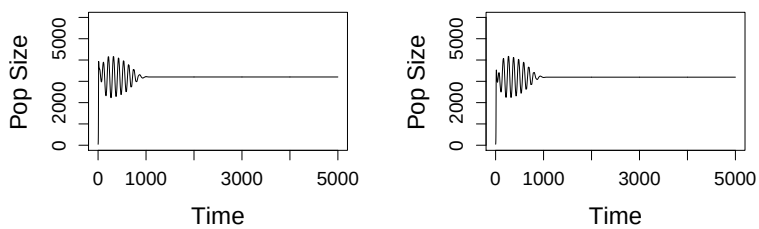

(a) Black Daisy Population (b) White Daisy Population

Figure 5.33: Regular CML: Local population dynamics at habitat (57, 50); $p = 0$, Overlap=10%, $D_c = 0.2$, $D = 0.2$, $r = 1$ and $NL = 0.001$ in 2D 100×100

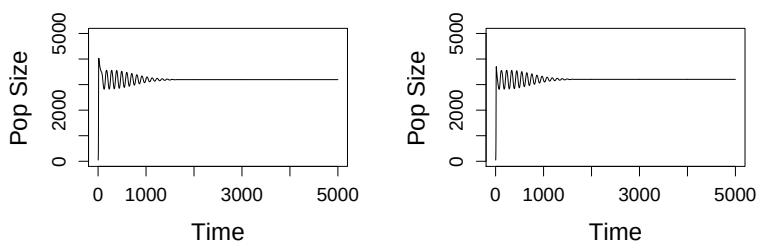

(a) Black Daisy Abundance (b) White Daisy Abundance

Figure 5.34: Regular CML : Global population dynamics; $p = 0$, Overlap=10%, $D_c = 0.2$, $D = 0.2$, $r = 1$ and $NL = 0.001$ in 2D 100×100

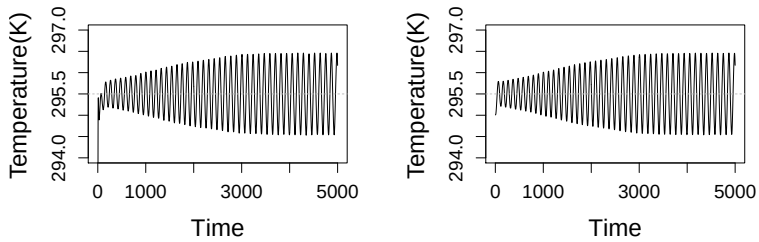

(a) Local Temperature at habitat (53, 53)

(b) Global Surface Temperature

Figure 5.35: Random Lattice: Temperature dynamics; $p = 1$, Overlap=10%, $D_c = 0.2$, $D = 0.2$, $r = 1$ and $NL = 0.001$ in 2D 100×100

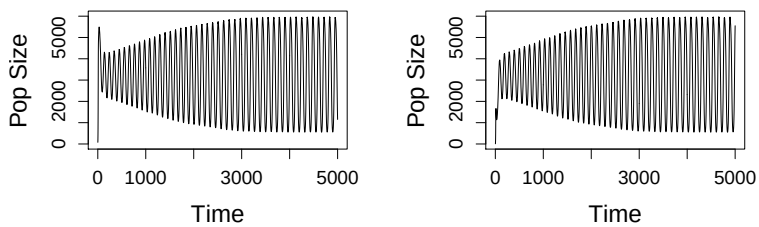

(a) Black Daisy Population

(b) White Daisy Population

Figure 5.36: Random Lattice: Local population dynamics at habitat (53, 53); $p = 1$, Overlap=10%, $D_c = 0.2$, $D = 0.2$, $r = 1$ and $NL = 0.001$ in 2D 100×100

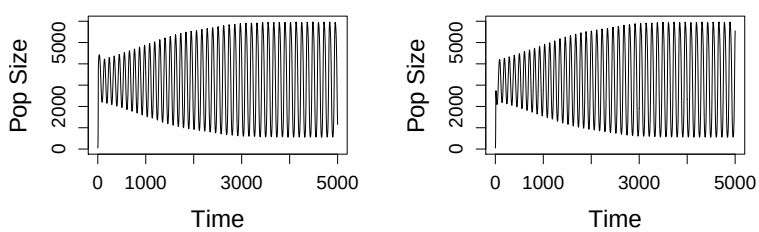

(a) Black Daisy Abundance

(b) White Daisy Abundance

Figure 5.37: Random Lattice: Global population dynamics; $p = 1$, Overlap=10%, $D_c = 0.2$, $D = 0.2$, $r = 1$ and $NL = 0.001$ in 2D 100×100

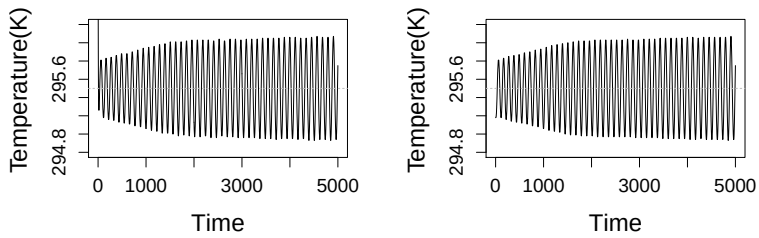

(a) Local Temperature at habitat (50, 46)

(b) Global Surface Temperature

Figure 5.38: Fully Connected Lattice: Temperature dynamics; Overlap=10%, $D_c = 0.2$, $D = 0.2$, $r = 1$ and $NL = 0.001$ in 2D 100×100

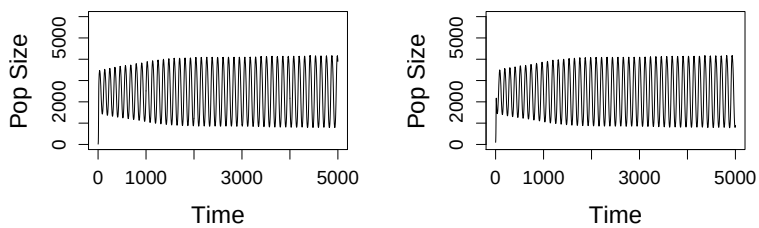

(a) Black Daisy Population

(b) White Daisy Population

Figure 5.39: Fully Connected Lattice: Local population dynamics at habitat (50, 46); Overlap=10%, $D_c = 0.2$, $D = 0.2$, $r = 1$ and $NL = 0.001$ in 2D 100×100

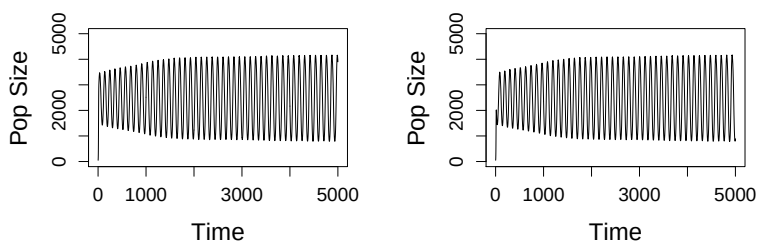

(a) Black Daisy Abundance

(b) White Daisy Abundance

Figure 5.40: Fully Connected Lattice: Global population dynamics; Overlap=10%, $D_c = 0.2$, $D = 0.2$, $r = 1$ and $NL = 0.001$ in 2D 100×100

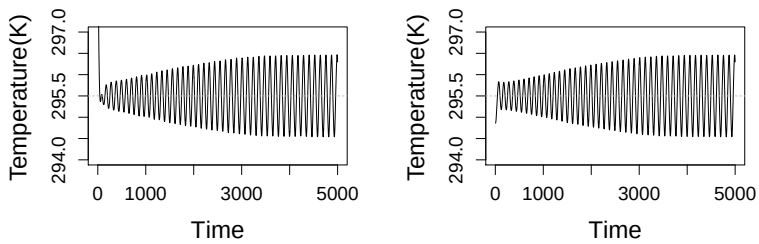

(a) Local Temperature at habitat (53, 62)

(b) Global Surface Temperature

Figure 5.41: Watts-Strogatz Model ($p = 0.05$): Temperature dynamics; Overlap=10%, $D_c = 0.2$, $D = 0.2$, $r = 1$ and $NL = 0.001$ in 2D 100×100

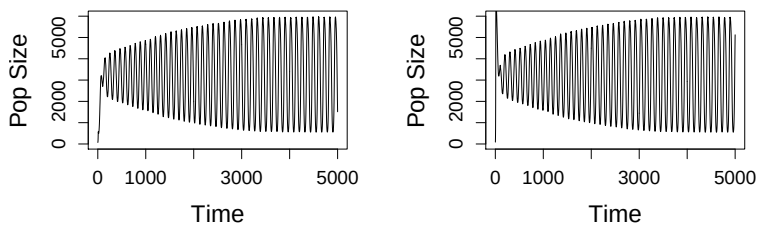

(a) Black Daisy Population

(b) White Daisy Population

Figure 5.42: Watts-Strogatz Model ($p = 0.05$): Local population dynamics at habitat (53, 62); Overlap=10%, $D_c = 0.2$, $D = 0.2$, $r = 1$ and $NL = 0.001$ in 2D 100×100

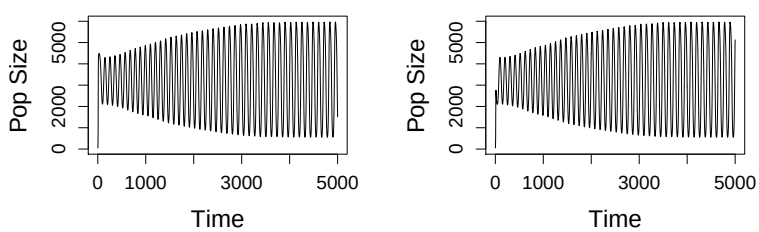

(a) Black Daisy Abundance

(b) White Daisy Abundance

Figure 5.43: Watts-Strogatz Model ($p = 0.05$): Global population dynamics; Overlap=10%, $D_c = 0.2$, $D = 0.2$, $r = 1$ and $NL = 0.001$ in 2D 100×100

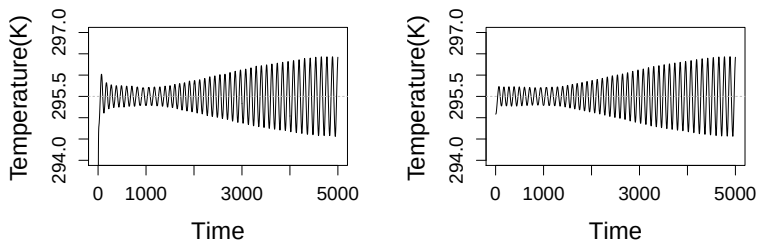

(a) Local Temp. at habitat (52, 58) (b) Global Surface Temp.

Figure 5.44: Newman-Watts CML ($p = 0.05$): Temperature dynamics; Overlap=10%, $D_c = 0.2$, $D = 0.2$, $r = 1$ and $NL = 0.001$ in 2D 100×100

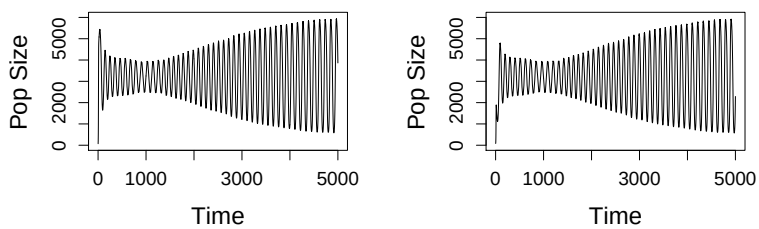

(a) Black Daisy Population (b) White Daisy Population

Figure 5.45: Newman-Watts CML ($p = 0.05$): Local population dynamics at habitat (52, 58); Overlap=10%, $D_c = 0.2$, $D = 0.2$, $r = 1$ and $NL = 0.001$ in 2D 100×100

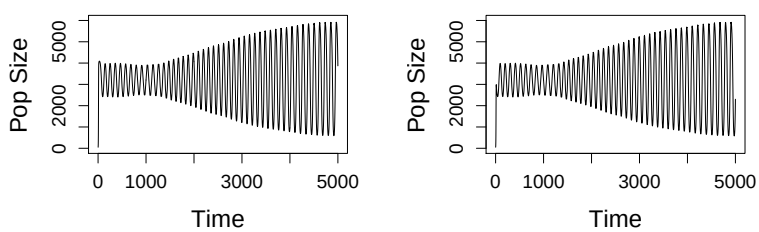

(a) Black Daisy Abundance (b) White Daisy Abundance

Figure 5.46: Newman-Watts CML ($p = 0.05$): Global population dynamics; Overlap=10%, $D_c = 0.2$, $D = 0.2$, $r = 1$ and $NL = 0.001$ in 2D 100×100

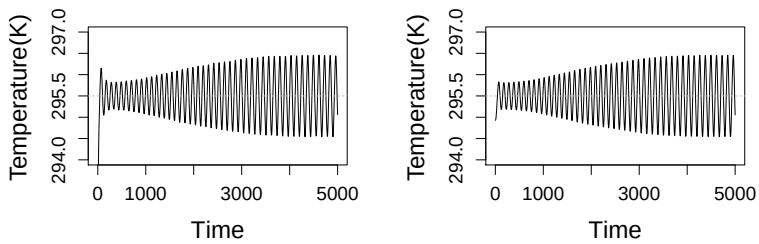

(a) Local Temperature at habitat (54, 44)

(b) Global Surface Temperature

Figure 5.47: Smallest-World Model ($p = 0.05$): Temperature dynamics; Overlap=10%, $D_c = 0.2$, $D = 0.2$, $r = 1$ and $NL = 0.001$ in 2D 100×100

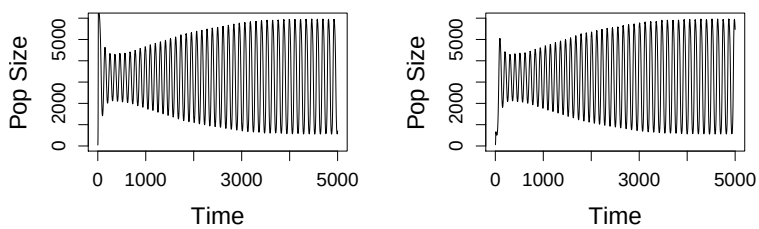

(a) Black Daisy Population

(b) White Daisy Population

Figure 5.48: Smallest-World Model ($p = 0.05$): Local population dynamics at habitat (54, 44); Overlap=10%, $D_c = 0.2$, $D = 0.2$, $r = 1$ and $NL = 0.001$ in 2D 100×100

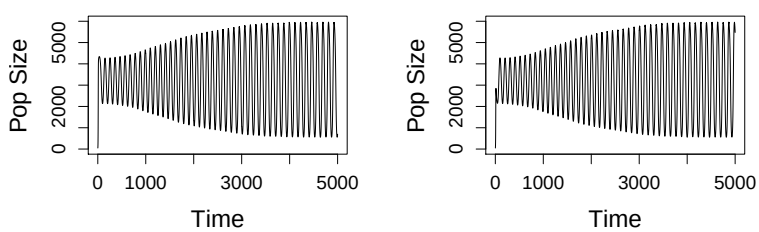

(a) Black Daisy Abundance

(b) White Daisy Abundance

Figure 5.49: Smallest-World Model ($p = 0.05$): Global population dynamics; Overlap=10%, $D_c = 0.2$, $D = 0.2$, $r = 1$ and $NL = 0.001$ in 2D 100×100

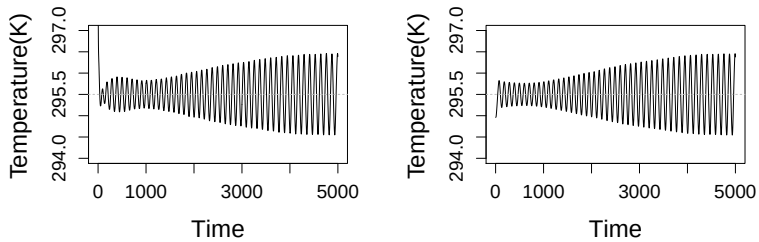

(a) Local Temp. at habitat (56, 57) (b) Global Surface Temp.

Figure 5.50: Adaptive CML: Temperature dynamics; Overlap=10%, $D_c = 0.2$, $D = 0.2$, $r = 1$ and $NL = 0.001$ in 2D 100×100

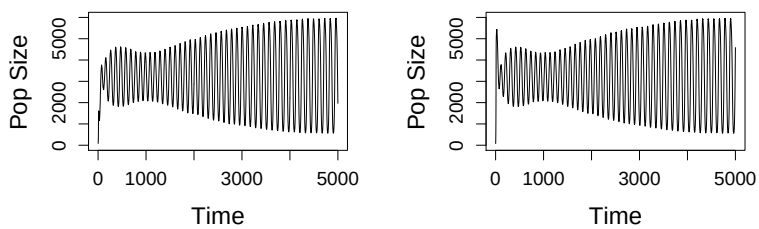

(a) Black Daisy Population (b) White Daisy Population

Figure 5.51: Adaptive CML: Local population dynamics at habitat (56, 57); Overlap=10%, $D_c = 0.2$, $D = 0.2$, $r = 1$ and $NL = 0.001$ in 2D 100×100

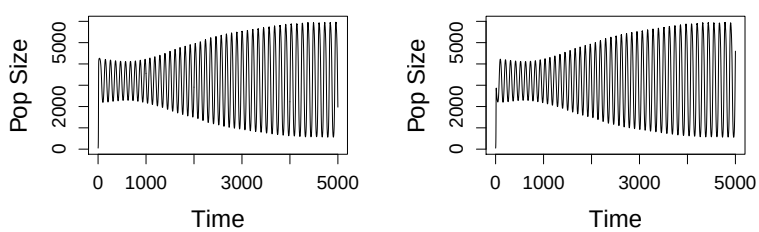

(a) Black Daisy Abundance (b) White Daisy Abundance

Figure 5.52: Adaptive CML: Global population dynamics; Overlap=10%, $D_c = 0.2$, $D = 0.2$, $r = 1$ and $NL = 0.001$ in 2D 100×100

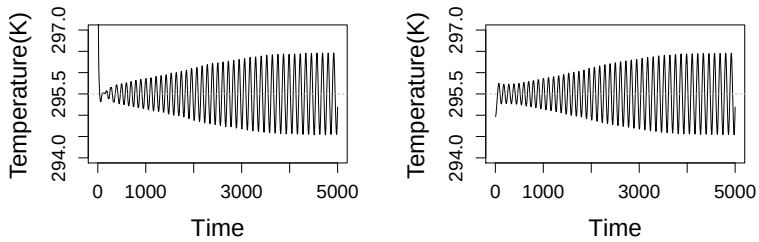

(a) Local Temp. at habitat (52, 58) (b) Global Surface Temp.

Figure 5.53: Scale-free CML ($p = 0.05$): Temperature dynamics; Overlap=10%, $D_c = 0.2$, $D = 0.2$, $r = 1$ and $NL = 0.001$ in 2D 100×100

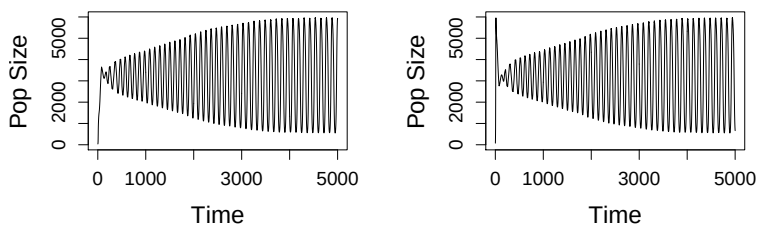

(a) Black Daisy Population (b) White Daisy Population

Figure 5.54: Scale-free CML ($p = 0.05$): Local population dynamics at habitat (52, 58); Overlap=10%, $D_c = 0.2$, $D = 0.2$, $r = 1$ and $NL = 0.001$ in 2D 100×100

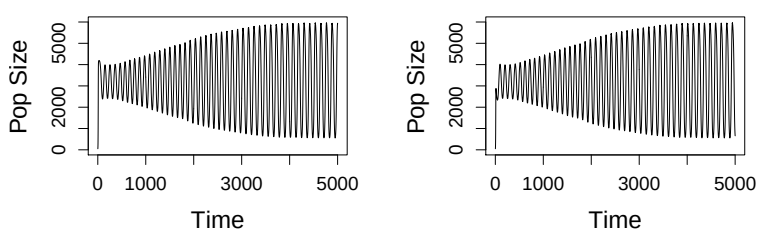

(a) Black Daisy Abundance (b) White Daisy Abundance

Figure 5.55: Scale-free CML ($p = 0.05$): Global population dynamics; Overlap=10%, $D_c = 0.2$, $D = 0.2$, $r = 1$ and $NL = 0.001$ in 2D 100×100

Chapter 6

Applications – Demonstration of Social Homeostasis in Stock Market

6.1 Introduction

Stock market is one of the examples of homeostatic complex system. This is one such system whose response is fedback autonomously into the system as a new cause. The (self-interested) investors' opinion affect the stock price, also the price causes investors to make those very same decision. Thus, the price is self-generated (self-affinity). This produces a feedback loop which is governed by an unconscious social nature of the investors [Frost and Prechter, 2005].

The nobel laureate, Herbert A. Simon, emphasises that most people are only partly rational and partly emotional/irrational in making their decisions [Simon, 1957]. This implies investors' emotions that are expressed can influence their fellow investors.

In this contemporary world, investors express their mood via social media such as Twitter. The tweets posted by the investors reflect their emotions and mood which affect stock price and vice versa. The opinions and emotional expressions are reflected by other traders involved in the market. Eventually,

the wax and wane of the emotions are reflected in the stock price. The stock price urges the traders to monitor themselves. The community feeds off its own emotion and thus self-maintains the stock price. This self-organizing behaviour of markets is called as "invisible hand" [Smith, 2008] which arises from the microscopic decisions of individual investors.

The investors' collective action (response) influence the stock price. The very same way stock price also influences the investors' decision (mood or opinion or sentiments). Thus, investors and stock price influence each other reciprocally. The stock price reflects and affects the pulse of investors. This scenario is very similar to organismic view of society, ecosystem, etc. In this chapter, we analyse the tweets (which reflects traders' emotions) and the stock price movement with the insights from daisyworld.

6.2 Daisyworld - Stock Market Analogy

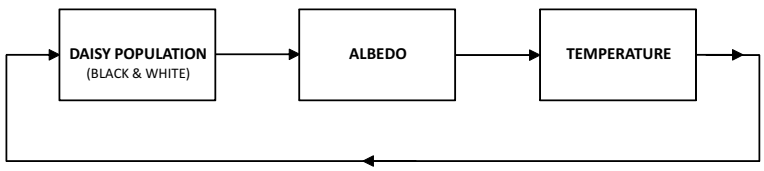

Figure 6.1: Self-causing Feedback in Daisyworld

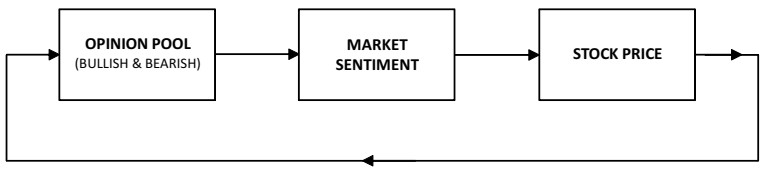

Figure 6.2: Self-causing Feedback in Stock Market

Daisyworld emphasises on reciprocal influence between living organisms and their environment, exemplifying deep ecology principles. The very same way, collective stock market investors' opinion and stock price influence each

Table 6.1: Parametric Analogy of Daisyworld and Stock Market

	Daisyworld	**Stock Market**
Species	Black and White Daisies	Bull and Bear Opinions
Environment	Temperature	Stock Price
Environment Altering Trait	Albedo (reflectivity)	Market Sentiment

other reciprocally. Each investor (at the microscopic level) buys the stocks by learning others' behaviour which pushes the price up in bull market or down in bear market as a whole (on the macroscopic level), and thereby self-organize themselves.

6.2.1 Daisyworld Behaviour

Initially daisyworld is cold and hence black daisies start to grow by absorbing the heat. An initial growth of black daisies increases the temperature of the system (positive coupling). But at a higher temperature, white daisies bloom and keep the positive feedback under control (negative coupling).

The growth of white daisies decreases the temperature further and further (positive feedback). But at a colder temperature, black daisies bloom and inhibit the system behaviour (negative coupling).

This cycle goes on and on demonstrating it as a homeostatic system – keeping the temperature in the viable range of the daisies.

6.2.2 Stock Market Behaviour

When stocks rise, the investors tempt to buy more stocks – bull market. The aggregate behaviour of traders gets amplified and the net buying lifts the prices up and higher (positive coupling). But the increased price of the stocks indicates a peak after which the market will fall and deter buyers (negative coupling).

Once the market begins to fall, investors refrain from buying and are induced to sell – bear market. The net selling pushes prices down and lower (positive coupling). But some may buy because stocks become more and more of a bargain (negative coupling).

Thus, the aggregate behaviour produces a cyclical trend consisting of accelerating growth and accelerating decline.

6.2.3 Comparison of Behaviours – An Ecosystem Approach

We can view stock market as an ecosystem, consisting of a collection of stock investors' bullish and bearish opinions as its biotic component (black and white daisies in daisyworld), stock price as its abiotic component (temperature in daisyworld) and market sentiment as environmental changing trait (albedo in daisyworld – influence factor). Refer Figures 6.1 and 6.2 for comparison. The parametric analogy is provided in Table 6.2. We also perceive stock market as a "superorganism" with "collective intelligence" where social homeostasis emerges similarly to termite colony, bee hives, etc.

6.3 Background

6.3.1 Sentiment Analysis and Microblogging Services

Microblogging is one of the popular contemporary communication tools. A large-scale of data is generated via microblogging web-sites such as Twitter, Tumblr, Facebook, etc. Internet users post their personal views on variety of topics. This huge collection of posts from online microblogging service can be used for social studies. In other words, microblogging is a rich source of data for opinion mining and sentiment analysis. Sentiment analysis detects the public's opinion – polarity (positive or negative) about a given topic in the corresponding document collection. Opinion mining and sentiment analysis on user created contents is relatively recent and a growing research field [Asur and Huberman, 2010; Bollen et al., 2011; Das and Chen, 2007; Gruhl et al., 2005; Mishne and Glance, 2006; Nofsinger, 2005]. Pang and Lee [2008] present

a wide overview of the existing work.

Recently, Twitter – the most popular microblogging platform – is used for sentiment analysis where the users create status messages (called "tweets"). A huge amount of tweets (over 400 million) are transmitted per day via Twitter. Each tweet has maximum of 140 characters and hence 56 billion characters are generated and transmitted via Twitter alone. An individual tweet may not be useful and interesting. But aggregation – collection of tweets – reflects the public mood (opinion) and sentiment of tweeples (people who use twitter.com).

In this chapter, we focus on Apple stock tweets for analysing the sentiments of the stock traders with the stock price fluctuations. By Twitter convention, developed by the users, $ symbol is used with the stock tickers to post the stock related tweets. For instance, $\$AAPL$ represents Apple stocks.

6.3.2 Supervised Classification

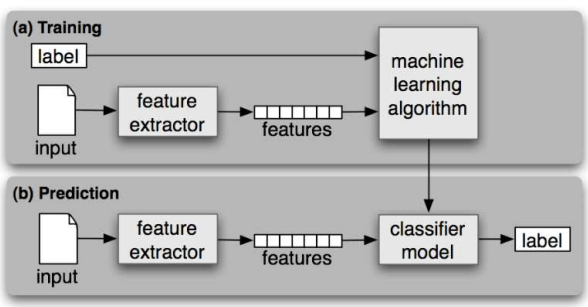

Figure 6.3: Supervised Classification (Source : [Bird et al., 2009])

Classification predicts the appropriate class label for a given input. A classifier is supervised if it is constructed on training corpora which contain correct label for each input. The framework used by supervised classification is depicted in the Figure 6.3. In this framework, features (domain specific words) play the key role. A feature extractor converts each input to a feature set. The feature sets and their corresponding labels are used to build the model. The model is built using the training corpora containing the label for each input

and thus the classifier learns from the training data. The same extractor is also used to convert unseen inputs to feature sets. These feature sets are fed into the model which predicts the possible labels [Bird et al., 2009].

6.3.2.1 Naive Bayes Classifier

A naive Bayes classifier assumes that the presence or absence of a particular feature is unrelated to the presence or absence of any other feature, given the class variable. It considers each of the features to contribute independently to the probability in choosing the class type, regardless of the presence or absence of the other features. The underlying probability model is an "independent feature model". Naive Bayes classifier calculates the prior probability of each label based on the frequency of each label occurring in the training data. The contribution from each feature is then combined with this prior probability, to get a likelihood estimate for each label. The label whose likelihood estimate is the highest is then assigned to the input value.

$$P(label|features) = \frac{P(label) * P(features|label)}{P(features)} \tag{6.1}$$

6.3.2.2 Support Vector Machine (SVM)

Given a training set of features-label pairs $(\mathbf{x}_i, y_i)$ where $i = 1, ..., l$, $\mathbf{x}_i \in R^n$ and $\mathbf{y} \in \{1, 1\}^l$, the support vector machine (SVM) solves the optimization problem:

$$\begin{aligned} \min_{\mathbf{w},b,\xi} \quad & \frac{1}{2}\mathbf{w}^T\mathbf{w} + C\sum_{i=1}^{l}\xi_i \\ \text{subject to} \quad & y_i(\mathbf{w}^T\phi(\mathbf{x}_i) + b) \geq 1 - \xi_i, \\ & \xi_i \geq 0. \end{aligned} \tag{6.2}$$

The training vectors $\mathbf{x}_i$ are mapped into a higher dimensional space by the function ϕ. SVM finds a linear separating hyperplane with the maximal

margin in this higher dimensional space. $C > 0$ is the penalty parameter of the error term. $K(\mathbf{x}_i, \mathbf{x}_j) \equiv \phi(\mathbf{x}_i)^T \phi(\mathbf{x}_j)$ is called the kernel function. The basic kernel functions are linear, polynomial, radia basis function (RBF) and sigmoid. We use linear kernel function: $K(\mathbf{x}_i, \mathbf{x}_j) = \mathbf{x}_i^T \mathbf{x}_j$.

6.3.3 Twitter API

We can collect tweets either via Streaming API or Search API.

Streaming API The Streaming API allows real-time access to tweets based on the input query – in our case, it is apple stock ticker symbol $\$AAPL$. We need to get authenticated and request for a connection to the stream of tweets from the server. After the server opens the streaming connection, the tweets are streamed.

Search API The Search API is a REST API which allows us to request specific queries of only the recent (last 6 days) tweets.

6.4 Sentiment Analysis on Apple ($\$AAPL$) Stock Market Tweets

We form the corpus for sentiment analysis from the tweets collected from Twitter. We use machine learning techniques in acquiring positive and negative sentiments of the tweet corpus. We mine the stock tweets using Twitter's search API and pre-process them for further analysis. We use Naive Bayes classification and Support Vector Machine machine learning techniques to determine the sentiment of the tweets. Then we carry out causality analyses between sentiment score and stock price collected from Yahoo finance.

6.4.1 Data Collection

Collection of Stock Market Domain Specific Words We have collected nearly 1200 stock market specific words. This is a very essential step in sen-

timent analysis. These words are used as features in the analysis. Domain specific words will improve the accuracy of the model.

Stock Data We have collected stock data from July, 2013 to October, 2013 from Yahoo finance data feed.

Training Dataset We form the training dataset by collecting the tweets using Twitter API. We use streaming API to collect the tweets. We have hand classified 1000 tweets as bullish and 1000 tweets as bearish. Each instance in the training dataset contains a tweet (collection of words) and its corresponding class label ("target value") – bullish or bearish. We used the tweets during June, 2013 as our training dataset.

Test Dataset We have streamed $\$AAPL$ tweets from July, 2013 to October, 2013 to form our test dataset.

6.4.2 Tweet Text Pre-Processing

We remove the extraneous words which do not affect the sentiment of the tweet. They are URLs, hash tags (#), user name (@), retweet notation (RT) etc. We pre-process the tweets by following the steps below :

1. converting the tweets to lower case
2. replacing urls with URL
3. replacing @username with AT_USER
4. replacing #hashtag with HASH_WD
5. removing punctuations at the start and at the end of the tweet
6. removing additional white spaces

6.4.3 Training the Classifier

The first step of creating a classifier is collecting the relevant features of the tweets. The feature extractor builds a dictionary containing relevant features in the given tweet. We first tokenize the tweets to list of words. Then we clean up the words, filter unnecessary words and then finally extract the relevant features.

Feature Extraction Feature extraction is the process of transforming a list of words into a feature set that is used by the classifier in learning and predicting. We have collected the domain (stock market) specific bullish and bearish words. The presence/absence of these words in a tweet are the features. Each tweet is splitted into words and each of those words are added to the feature vector. Before adding the words, we need to filter some unnecessary words which don't make any impact on the sentiment. Otherwise the feature vector will explode. We use the following procedure to filter the words:

1. removing stop words
2. removing repeating letters. Eg., woooow as wow
3. converting words starting with an alphabet and containing only alphabets
4. removing punctuation ' " ‘ ? , . ! : ; -

Model Generation The goal of classifiers is to generate a model based on the training data (labelled feature set) which predicts the target values of the unseen (test) tweet (unlabelled feature set) given only the features of the test tweet. We use the machine learning classifiers Naive Bayes Classifier (NB) and Support Vector Machines (SVM) to classify each of tweets. We use Natural Language Toolkit (nltk) [Bird et al., 2009] and LIBSVM [Chang and Lin, 2001] libraries to implement these classifiers.

6.4.4 Sentiment Score

In our approach, we measure the reflectivity of stock investors' mood by a sentiment score. After we classify each day's tweets, we compute the sentiment score on daily basis.

$sentiment = \frac{NumOfBulls - NumOfBears}{NumOfBulls + NumOfBears}$

6.5 Demonstration of Social Homeostasis

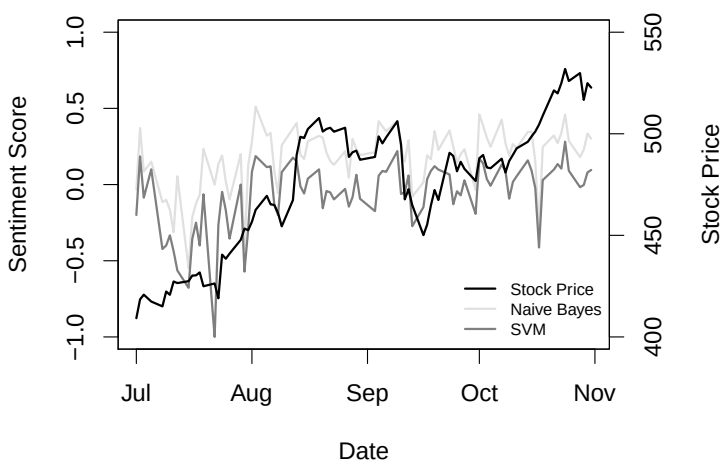

Figure 6.4: Sentiment Vs. Price

In the Figure 6.4, we have plotted the stock price (black line), sentiment score based on Naive Bayes classification (lighter grey line) and sentiment score based on SVM classification (darker grey line). These hemlines show that they are non-stationary time series. We observe that the peaks and troughs in all the three time series have common drifts.

Table 6.2: p-values of Granger Causality Analysis

	Naive Bayes	**SVM**
price causes sentiment	0.03788	0.00452
sentiment causes price	0.01109	0.04421

Causality Analysis The p-values in the Granger causality analysis for lag=1 show that stock price and sentiments cause each other reciprocally.

Table 6.3: p-values of Cointegration Tests

	Naive Bayes and Price	**SVM and Price**
Engle-Granger	0.01	0.01
Phillips-Ouliaris	0.04271	0.03024

Cointegration Tests Two or more time series are cointegrated if they share a common stochastic drift. We have performed Engle-Granger two-step method and Phillips-Ouliaris cointegration tests (Table 6.3). The p-values in the tests show that the time series are cointegrated.

6.6 Discussion

6.6.1 Social Mood Trends - A Psychological Perspective

Band wagon effect is a cognitive bias (tendencies to think in certain way). People tend to do (or believe) something because many other people do (or believe) the same. Herding mentality (gregarious behaviour) and group think are similar biases. This bias affects social, political and economic decisions and belief formation – human behaviour in general.

The evolutionary biologist Richard Dawkins suggests that as genes pass from generation to generation, memes also do the same – genes propagate themselves in the gene pool by leaping body to body via sperm or eggs and

memes propagate themselves in the meme pool by leaping brain to brain via imitation [Dawkins, 2006]. The neuron "mirrors" the behaviour of the others. Vilayanur S. Ramachandran (Marco Polo of neuroscience as called by Richard Dawkins) has speculated that role of mirror neurons will help explain a variety of human mental capacities such as empathy, imitation learning, and the evolution of language.

Human activity can be viewed as collections of many interacting agents (same fluid of interacting atoms or molecules) from which decision-making, learning and adaptation arise [Ball, 2004; Buchanan, 2008]. Then the decision or the innovation diffuses in the social system [Rogers, 2010]. The innovation must be widely adopted in order to self-sustain. Within the rate of adoption, there is a point at which an innovation reaches critical mass [Ball, 2004; Granovetter, 1978].

Herding in stock market is a collective irrationality of investors. Individual investors join the crowd to make decision (buy or sell). This unconscious herding impulse impels social mood trends and is reflected in the stock price. Though stock market face crashes, the system soon recovers due to sentiments of the investors on the stock price. Thus, owing to reflexism, investors act and reinforce and at criticality market crash occurs.

6.6.2 Stock Market - A Termite Colony

Colonies of social insects is the most mysterious complex system in nature. Every termite functions based on set of low level rules and feedback from its neighbours. We have analysed the emergence of stock price by applying the five fundamental principles as illustrated by Johnson [2012]. Here, we compare termites to investors and stock market to the termite colonies – both exhibiting social homeostasis.

More is different: A huge number of termites construct the colonies. Just one tweet does not contribute much to sentiment analysis. But an aggregation of tweets makes the stock market decision.

Ignorance is Useful: Each termite is not intelligent. Each investor does not required to be intelligent. The masses can be smarter than the solitary expert [Surowiecki, 2005]. Hence investor can be a mediocre.

Encourage random encounters: Termites use the feedback from encountering the activities of other termites to usefully modify their behaviour. The very same way investors watch their fellow investors to make their decisions.

Look for Patterns in the Signs: Termites follow trails of pheromones left by other termites. Investors follow the emotions left by other investors.

Pay Attention to Your Neighbours: Termites alter their behaviour by noticing a large number of other fellow termites. The investors in the stock market pay attention to other investors and express their emotions.

To sum up, "**Local information leads to global wisdom**" [Johnson, 2012].

6.7 Summary

The investors' emotions expressed via tweets can influence their fellow investors. This mass action is reflected by the stock price and affects the same. This cause is endogenous. We see a common drift both in the stock price movement and social sentiment trends. Thus Stock price movement is not random but nonlinear due to sentiments. We have analysed this self-causing nature using Granger causality analysis and cointegration tests. We have also touched upon the psychological reasons behind the price trends. We have demonstrated the social homeostasis in stock market is similar to social homeostasis in termite colonies.

Chapter 7

Conclusion

7.1 Summary

In our computational model presented (CML based daisyworld system), life undergoes fluctuations as local nonlinear chaotic oscillators, influenced by the ecological disturbance (noise) and the intrinsic increase rate; this effect is spread throughout the system via diffusion, and then amplified and controlled by the internal feedback mechanisms. We have noticed that the system self-organize itself owing to the combined effect of positive and negative couplings resulting in negative feedback loops, giving rise to the emergence of temperature self-regulation and sustainable population dynamics. This typical behaviour emerge without any tuning of the system from the outside. While the tuning happens from the internal mechanisms, ie., albedo (reflectivity) tunes the temperature (environment).

Thus the dynamics of life, together with temperature feedback, regulate the global temperature of the daisyworld homeostatically in our CML based daisyworld, as in the earlier CA versions. This regulatory behaviour emerges even in the presence of perturbations. The results envisage that daisyworld coordinate complex behaviours and has potential to cope up with disruptions with huge parameter space. Regardless of the varied and complex dynamical response of our system, depending on the parameter settings, the simplify-

ing aspect is that the homeostatic property is exhibited by the system in all scenarios.

The daisyworld models based on both CA and CML are spatially extended bottom-up approaches, in which globally emergent behaviours are generated by the local rules and bounded interactions. In the former model, daisy populations exhibit boom and bust local behaviour at a particular habitat in the ecosystem, and in the latter, chaotic local behaviour. CML represents mesoscopic daisy states, while deterministic CA represents the microscopic states of the daisies.

We have investigated that our system has exerted the following complexity features: • interconnected and interdependent components • simple rules of interaction • positive and negative feedbacks • nonlinearity • sensitivity to initial conditions • structured randomness • neighbour interactions • decentralized control • self-organization • self-regulation • pattern formation • co-evolution • adaptive dynamics

We have analysed life-environment feedback system (daisyworld) from different angles and aspects of complex system's phenomena. We have illustrated that our system exhibits stationary attractors, bifurcations and strange attractors and thereby signifying it as a dynamical system. Our system generates a wide spectrum of striking spatio-temporal patterns deriving insights from biological systems and non-living systems. In our nonlinear reaction-diffusion system, symmetry-breaking is induced by species dispersion, temperature diffusion and noise, which paves the pattern formation.

We have introduced metrics for quantifying the behaviour of daisyworld, and used them to analyse the spatio-temporal dynamics: Permutation Entropy to measure the temporal dynamics, standard deviation to measure the scale of fluctuation, and Moran's I to measure the spatial auto correlation and pattern formation. As we have seen in the analyses, PE and MI quantify the spatio-temporal dynamics accurately, demonstrating their reliability in quantifying a wide range of dynamics.

We have incorporated evolutionary mechanisms via replication with mutation and adaptation into our system which displays the robustness in self-

regulation. Noise plays vital in the system exhibiting different life forms – monotonous (quiescent daisy dominance states), suppression of mutants, etc.

We have explored the implications of topological effects in our system. Under the same parameter settings, the additional random connections to the grid, generating a small-world, destroys the heterogeneous static behaviour of grid to a homogeneous cyclical short-lived behaviours. The system (possessing small-world phenomena) evolves toward a critical state, where a small perturbation is amplified and affects the whole system. Even a small change in one part of the network propagate via the shortcuts, gets amplified (self-reinforcing feedback) and cause huge changes in the whole system. But the self-maintaining feedback counters the effect and the cycle start over. In spite of these variations, the system persists homeostasis.

In addition to life-environment and density-growth feedback loops, we have added up state-topology feedback (adaptive networks). This addition enables the capacity of grid to self-organize to complex topology (small-world) via simple dynamical linking rule – frozen habitats (nodes) gain reciprocal non-local neighbours (links). When the threshold of adding new connections is crossed, the system is switched from one network architecture (organization) to another and hence the behaviour changes. The system displays homogeneous cyclical short-lived behaviours and still self-regulates its environment.

We have incorporated scale-freeness into our system possessing power law distribution. The outcome shows similar behaviours as that of small-world and adaptive networks.

The complex and adaptive networks display 'completely coherent (homogeneous) short-lived cyclical dominance'. Our system represents social phenomena as in spread of memes, epidemics, etc. These behaviours are also seen in stock market – a man made complex adaptive system, which has led us to analyse the social homeostasis in stock market. We have collected $\$APPL$ stock tweets from twitter and stock data from Yahoo finance and examined that the sentiment causes the price reciprocally. We have analysed the chain of causality between investors' sentiment and stock price movement.

7.2 Conclusion

We have detailed how we have reconstructed the computational modelling of our life-environmental, self-regulating system and quantified its spatio-temporal behaviours. We have showed the robustness of our system in self-regulating its environment for the sustainability of life in the presence of various perturbations – parameter change, topological change and evolutionary change. We have analysed our system in different perspective of complexity phenomena. We have demonstrated our system as a complex dynamical system, self-organizing system and reaction-diffusion system. We have acquired insights from natural complex systems such as schooling of fish, flocking of birds, synchronization of fireflies, animal coat to understand the pattern formation principles in our system. Our system, with complex or adaptive topological properties, has displayed a dynamical phase transition both in system dynamics and network structures with significant emergent properties exhibiting interesting analogies with the dynamics of social, political and economical systems. We have related daisyworld behaviour to stock market behaviour. With our application of our behaviour study and its relation in sentiment analysis of stock tweets and stock price movement, we have manifested stock market as complex adaptive man-made system exhibiting social homeostasis. We have also explored the psychological and sociological reasons behind such apparent behaviours. We have compared stock market with other super-organism exhibiting social homeostasis – a termite colony. Thus, we have illustrated our system's utility in understanding self-regulating, self-causing and self-designed principles and systems.

7.3 Future Directions

- Further development of daisyworld model include :
  - Introducing one more feedback loop in the topology of the daisyworld system which dampens the growth of hubs and amplifies the growth of smaller nodes. For instance, we can observe this pattern

in citation networks where the first paper in any new area becomes richer and richer (gets more and more references). But after some time, when a review paper is published, researchers start citing to the new review paper.

- Investigating fractal attractors in the dynamics of daisyworld dynamics.

- The potential directions in sentiment analysis of stock market include :
  - Technical analysis of stock market trends using Elliott wave principle [Frost and Prechter, 2005].
  - Fractals and Fibonacci sequence analysis of human mentation for investigating their social mood swings.

The **theory of Universality** emphasises on fractal patterns to explain much of the world around us [Ward, 2002]. Hence, we are interested in exploring daisyworld model and sentiment analysis of stock market tweets based on fractals.

Bibliography

Ackland, G., Gallagher, I., 2004. Stabilization of large generalized lotka-volterra foodwebs by evolutionary feedback. Physical Review Letters 93 (15), 158701. 31

Ackland, G. J., Clark, M. A., Lenton, T. M., 2003. Catastrophic desert formation in daisyworld. Journal of theoretical biology 223 (1), 39–44. 3, 4, 6, 9, 31

Ackland, G. J., Wood, A. J., 2010. Emergent patterns in space and time from daisyworld: a simple evolving coupled biosphere-climate model. Philosophical Transactions of the Royal Society A: Mathematical, Physical and Engineering Sciences 368 (1910), 161. 3, 4, 6, 9, 31, 32

Adams, B., Carr, J., Lenton, T. M., White, A., 2003. One-dimensional daisyworld: spatial interactions and pattern formation. Journal of Theoretical Biology 223 (4), 505–513. 3, 31

Albert, R., Jeong, H., Barabási, A. L., 1999. The diameter of the world wide web. Arxiv preprint cond-mat/9907038. 21

Andersen, M. L., Taylor, H. F., 2007. Sociology: Understanding a diverse society. Wadsworth Publishing Company. 128

Anderson, P. W., et al., 1972. More is different. Science 177 (4047), 393–396. 26

Andrew, A. M., 1996. The challenge of daisyworld. Kybernetes 25 (7/8), 94–99. 31

Ashby, W. R., 1947. Iii.the nervous system as physical machine: With special reference to the origin of adaptive behaviour. Mind 56 (221), 44–59. 17

Ashby, W. R., 1952. Design for a brain. 17

Ashby, W. R., 1962. Principles of the self-organizing system. Principles of Self-organization, 255–278. 45

Asur, S., Huberman, B. A., 2010. Predicting the future with social media. In: Web Intelligence and Intelligent Agent Technology (WI-IAT), 2010 IEEE/WIC/ACM International Conference on. Vol. 1. IEEE, pp. 492–499. 142

Ball, P., 2004. Critical mass: How one thing leads to another. Macmillan. 26, 150

Bandt, C., Pompe, B., 2002. Permutation entropy: A natural complexity measure for time series. Physical Review Letters 88 (17), 174102. 42

Bar-Yam, Y., 2003. Dynamics of complex systems. 1

Barabasi, A.-L., 2003. Linked: How everything is connected to everything else and what it means. 20, 23

Begon, M., Harper, J. L., Townsend, C. R., 1996. Ecology: individuals, populations, and communities. Blackwell. 79

Belousov, B. P., 1958. A periodic reaction and its mechanism. Sbornik Referatov po Radiatsonno Meditsine (Medgiz, Moscow), 145–147 (in Russian). 25

Bénard, H., 1900. Les tourbillons cellulaires dans une nappe liquide. Revue générale des Sciences pures et appliquées 11, 1261–1271 and 1309–1328. 25

Bernard, C., 1878. Leçons sur les phénomènes de la vie commune aux animaux et aux végétaux. Baillière. 17

Bird, S., Klein, E., Loper, E., 2009. Natural language processing with Python. O'reilly. xviii, 143, 144, 147

Boccaletti, S., Latora, V., Moreno, Y., Chavez, M., Hwang, D. U., 2006. Complex networks: structure and dynamics. Physics reports 424 (4), 175–308. 22

Bollen, J., Mao, H., Zeng, X., 2011. Twitter mood predicts the stock market. Journal of Computational Science 2 (1), 1–8. 142

Bollobás, B., 1979. Graph theory, an introductory course. Springer-Verlag, New York, Heidelberg, Berlin. 37

Bollobás, B., 2001. Random graphs. Vol. 73. Cambridge university press. 21, 37

Brännström, Å., Sumpter, D., 2005. Coupled map lattice approximations for spatially explicit individual-based models of ecology. Bulletin of Mathematical Biology 67 (4), 663–682. 37

Brenner, T., 1998. Can evolutionary algorithms describe learning processes? Journal of Evolutionary Economics 8, 271–283. 34

Buchanan, M., 2003. Nexus: small worlds and the groundbreaking theory of networks. WW Norton. 23, 26, 39, 130

Buchanan, M., 2008. The social atom: Why the rich get richer, cheaters get caught, and your neighbor usually looks like you. Bloomsbury Publishing USA. 150

Bürger, R., 1998. Mathematical properties of mutation-selection models. Genetica 102-103, 279–298. 34

Camazine, S., Deneubourg, J.-L., Franks, N. R., Sneyd, J., Theraula, G., Bonabeau, E., 2003. Self-organization in biological systems, 2nd Edition. Princeton University Press. 25, 26, 27

Cannon, W. B., 1929. Organization for physiological homeostasis. Physiological Reviews 9 (3), 399–431. 17

Cao, Y., Tung, W., Gao, J., Protopopescu, V., Hively, L., 2004. Detecting dynamical changes in time series using the permutation entropy. Physical Review-Series E- 70 (4; PART 2), 46217–46217. 43

Capra, F., 1983. The Turning Point: Science, Society, and the Rising Culture. Bantam. 30

Capra, F., 1997. The Web of Life: A New Scientific Understanding of Living Systems. Anchor. 21, 29

Capra, F., 2004. The hidden connections: A science for sustainable living. Random House Digital, Inc. 16

Chang, C., Lin, C., 2001. Libsvm – a library for support vector machines. URL http://www.csie.ntu.edu.tw/~cjlin/libsvm/ 147

Das, S. R., Chen, M. Y., 2007. Yahoo! for amazon: Sentiment extraction from small talk on the web. Management Science 53 (9), 1375–1388. 142

Dawkins, R., 1999. The extended phenotype: The long reach of the gene. Oxford University Press, USA. 73

Dawkins, R., 2006. The selfish gene. Oxford university press. 150

Dewar, R., 2003. Information theory explanation of the fluctuation theorem, maximum entropy production and self-organized criticality in non-equilibrium stationary states. Journal of Physics A: Mathematical and General 36 (3), 631. 31

Dewar, R. C., 2005. Maximum entropy production and the fluctuation theorem. Journal of Physics A: Mathematical and General 38 (21), L371. 31

Dorogovtsev, S. N., Mendes, J. F. F., 2002. Evolution of networks. Advances in physics 51 (4), 1079–1187. 10, 22, 103

Dyke, J., Harvey, I., 2005. Hysteresis and the limits of homeostasis: from daisyworld to phototaxis. In: Advances in Artificial Life. Springer, pp. 241–251. 31

Dyke, J., Harvey, I., 2006. Pushing up the daisies. 18, 31

Ford, F. A., 1999. Modeling the environment: an introduction to system dynamics modeling of environmental systems. Island press. 31

Frost, A. J., Prechter, R. R., 2005. Elliott wave principle: key to market behavior. Elliott Wave International. 139, 157

García-Ojalvo, J., Sancho, J. M., 1999. Noise in spatially extended systems. Springer. 77

Gladwell, M., 2006. The tipping point: How little things can make a big difference. Little, Brown. 129

Goel, P., Ermentrout, B., 2002. Synchrony, stability, and firing patterns in pulse-coupled oscillators. Physica D: Nonlinear Phenomena 163 (3), 191–216. 111

Granovetter, M., 1978. Threshold models of collective behavior. American journal of sociology, 1420–1443. 150

Gross, T., Blasius, B., 2008. Adaptive coevolutionary networks: a review. Journal of the Royal Society Interface 5 (20), 259–271. xi, 10, 24, 25, 118

Gross, T., Sayama, H., 2009. Adaptive networks. Adaptive Networks, 1–8. 10, 25, 118

Gruhl, D., Guha, R., Kumar, R., Novak, J., Tomkins, A., 2005. The predictive power of online chatter. In: Proceedings of the eleventh ACM SIGKDD international conference on Knowledge discovery in data mining. ACM, pp. 78–87. 142

Harding, S., 1999. Food web complexity enhances community stability and climate regulation in a geophysiological model. Tellus B 51 (4), 815–829. 31

Harding, S., 2006. Animate Earth: Science, Intuition and Gaia. Chelsea Green. 29, 30

Harvey, I., 2004. Homeostasis and rein control: From daisyworld to active perception. In: Proceedings of the Ninth International Conference on the Simulation and Synthesis of Living Systems, ALIFE. Vol. 9. pp. 309–314. 31, 32

Hilborn, R. C., 2004. Sea gulls, butterflies, and grasshoppers: A brief history of the butterfly effect in nonlinear dynamics. American Journal of Physics 72, 425. 129

Hofbauer, J., Sigmund, K., 2003. Evolutionary game dynamics. Bulletin of the American Mathematical Society 40 (4), 479 – 519. 73

Hutton, J., Library, E. U., Society, E. G., 1987. The 1785 Abstract of James Hutton's Theory of the Earth. Scottish Academic Press.
URL http://books.google.co.kr/books?id=2WE7AQAAMAAJ 29

Johnson, S., 2012. Emergence: The connected lives of ants, brains, cities, and software. Simon and Schuster. 25, 150, 151

Jrgensen, Sven Erik, ., Fath, B. D., 2010. Global ecology : a derivative of Encyclopedia of ecology / editor-in-chief, Sven Erik Jrgensen ; associate editor-in-chief, Brian D. Fath. Amsterdam ; Boston : Elsevier/Academic Press, "Material in the text originally appeared in the Encyclopedia of ecology, edited by Sven Eric Jrgenson (Elsevier B.V. 2008)"–T.p. verso. 28

Kaneko, K., 1985. Spatiotemporal intermittency in coupled map lattices. Progress of Theoretical Physics 74 (5), 1033–1044. 35

Kaneko, K., Tsuda, I., 2001. Complex systems: chaos and beyond: a constructive approach with applications in life sciences. Springer Verlag. 6

Kaneko, K. *Ed.*, 1993. Theory and Applications of Coupled Map Lattices. John Wiley & Sons. 37

Kendall, D., 2012. Sociology in our times. Wadsworth Publishing Company. 128

Kump, L. R., Kasting, J. F., Crane, R. G., 2010. The Earth System, 3rd Edition. Prentice Hall. 31

Langton, C. G., et al., 1989. Artificial life. Addison-Wesley Publishing Company Redwood City, CA. 19

Lenton, T., Van Oijen, M., 2002. Gaia as a complex adaptive system. Philosophical Transactions of the Royal Society of London. Series B: Biological Sciences 357 (1421), 683. 4, 6, 9

Lenton, T. M., Lovelock, J. E., 2000. Daisyworld is darwinian: constraints on adaptation are important for planetary self-regulation. Journal of Theoretical Biology 206 (1), 109–114. 31, 76

Lenton, T. M., Lovelock, J. E., 2001. Daisyworld revisited: quantifying biological effects on planetary self-regulation. Tellus B 53 (3), 288–305. 31, 76, 80

Lenton, T. M., et al., 1998. Gaia and natural selection. Nature 394 (6692), 439–447. 31, 76

Lorenz, E. N., 1963. Deterministic nonperiodic flow. Journal of the atmospheric sciences 20 (2), 130–141. 20

Lotka, A. J., 1925. Elements of physical biology. Williams & Wilkins Baltimore. 29

Lovelock, J., 1992. A numerical model for biodiversity. Philosophical Transactions of the Royal Society of London. Series B: Biological Sciences 338 (1286), 383. 31, 76, 78

Lovelock, J. E., 1972. Gaia as seen through the atmosphere. Atmos. Environ. 6, 579–580. 3, 5, 29

Macionis, J. J., 2009. Sociology. Prentice Hall. 128

Mackay, C., 2004. Extraordinary popular delusions and the madness of crowds. Barnes & Noble Publishing. 129

Maddock, L., 1991. Effects of simple environmental feedback on some population models. Tellus B 43 (3), 331–337. 49

Malnig, J., 2008. Ballroom, boogie, shimmy sham, shake: a social and popular dance reader. University of Illinois Press. 128

May, R. M., 1976. Simple mathematical models with very complicated dynamics. Nature 261 (5560), 459–467. 2, 33

McGuffie, K., Henderson-Sellers, A., 2005. A climate modelling primer. Vol. 1. Wiley, Chichester, UK. 31, 49

Milgram, S., 1967. The small world problem. Psychology today 2 (1), 60–67. 21

Mirollo, R. E., Strogatz, S. H., 1990. Synchronization of pulse-coupled biological oscillators. SIAM Journal on Applied Mathematics 50 (6), 1645–1662. 111

Mishne, G., Glance, N. S., 2006. Predicting movie sales from blogger sentiment. In: AAAI Spring Symposium: Computational Approaches to Analyzing Weblogs. pp. 155–158. 142

Mitchell, M., 2009. Complexity: a guided tour. Oxford University Press. 1

Mitleton-Kelly, E., 2003. Complex systems and evolutionary perspectives on organisations: the application of complexity theory to organisations. Elsevier Science Ltd. 2

Moran, P. A. P., 1950. Notes on continuous stochastic phenomena. Biometrika 37 (1/2), 17–23. 43

Murray, J. D., 2008. Mathematical Biology II: Spatial models and biomedical applications, 3rd Edition. Vol. 2. Springer. 25, 27

Naess, A., 1973. The shallow and the deep, long-range ecology movement. Inquiry 16, 95–100. 30

Nakao, H., Mikhailov, A. S., 2010. Turing patterns in network-organized activator-inhibitor systems. Nature Physics 6 (7), 544–550. 27

Newman, M. E. J., 2001. The structure of scientific collaboration networks. Proceedings of the National Academy of Sciences 98 (2), 404. 21

Newman, M. E. J., Watts, D. J., 1999. Renormalization group analysis of the small-world network model. Physics Letters A 263 (4-6), 341–346. 9, 22, 103

Nishimori, H., Ouchi, N., 1993. Formation of ripple patterns and dunes by wind-blown sand. Physical Review Letters 71 (1), 197–200. 37

Nofsinger, J. R., 2005. Social mood and financial economics. The Journal of Behavioral Finance 6 (3), 144–160. 142

Nowak, M. A., 2006. Evolutionary dynamics: exploring the equations of life. Belknap Press. 75

Nowak, M. A., Komarova, N. L., Niyogi, P., 2001. Evolution of universal grammar. Science 291 (5501), 114. 34

Odling-Smee, F. J., Laland, K. N., Feldman, M. W., 2003. Niche Construction: the Neglected Process in Evolution. Vol. 37 of Monographs in Population Biology. Princeton Univ. Press. 73

Olfati-Saber, R., 2007. Evolutionary dynamics of behavior in social networks. In: Decision and Control, 2007 46th IEEE Conference on. Ieee, pp. 4051–4056. 34

Ozawa, H., Ohmura, A., Lorenz, R. D., Pujol, T., 2003. The second law of thermodynamics and the global climate system: a review of the maximum entropy production principle. Reviews of Geophysics 41 (4), 1018. 31

Page, K. M., Nowak, M. A., 2002. Unifying evolutionary dynamics. Journal of theoretical biology 219 (1), 93–98. 78

Pang, B., Lee, L., 2008. Opinion mining and sentiment analysis. Foundations and trends in information retrieval 2 (1-2), 1–135. 142

Perera, L., Russell, J. R., Provan, J., Powell, W., 2000. Use of microsatellite DNA markers to investigate the level of genetic diversity and population genetic structure of coconut (*Cocos nucifera* L.). Genome 43 (1), 15–21. 9

Prigogine, I., 1997. The end of certainty. SimonandSchuster. com. 2

Prigogine, I., Stengers, I., Pagels, H. R., 1985. Order out of chaos. Physics Today 38, 97. 19

Punithan, D., Kim, D. K., McKay, R. I., 2011. Daisyworld in two dimensional small-world networks. Database Theory and Application, Bio-Science and Bio-Technology, 167–178. 10, 118

Punithan, D., Kim, D. K., McKay, R. I., 2012. Spatio-temporal dynamics and quantification of daisyworld in two-dimensional coupled map lattices. Ecological Complexity, 43–57. 7, 8, 9

Punithan, D., McKay, B., 2013a. Collective dynamics and homeostatic emergence in complex adaptive ecosystem. In: Advances in Artificial Life, ECAL. Vol. 12. pp. 332–339. 11

Punithan, D., McKay, R., 2012a. Evolutionary dynamics and ecosystems feedback in two dimensional daisyworld. In: Artificial Life. Vol. 13. pp. 91–98. 9

Punithan, D., McKay, R. I., 2012b. Self-organizing spatio-temporal pattern formation in two-dimensional daisyworld. Self-Organizing Systems, 72–83. 8, 80

Punithan, D., McKay, R. I., 2013b. Phase transitions in two-dimensional daisyworld with small-world effects: A study of local and long-range couplings. Future Generation Computer Systems. 10, 39, 118, 122

Rogers, E. M., 2010. Diffusion of innovations. Simon and Schuster. 150

Saunders, P. T., Koeslag, J. H., Wessels, J. A., 1998. Integral rein control in physiology. Journal of theoretical biology 194 (2), 163–173. 31, 32

Saunders, P. T., Koeslag, J. H., Wessels, J. A., 2000. Integral rein control in physiology ii: a general model. Journal of theoretical biology 206 (2), 211–220. 31, 32

Simon, H. A., 1957. Models of man; social and rational. 139

Smith, A., 2008. The Invisible Hand. Great ideas. Penguin Adult. URL http://books.google.co.kr/books?id=qBgAb0EsQv8C 140

Strogatz, S., 2001. Nonlinear dynamics and chaos: with applications to physics, biology, chemistry and engineering. Perseus Books Group. 20

Strogatz, S. H., 2003. Sync: The emerging science of spontaneous order. Hyperion. 19

Surowiecki, J., 2005. The wisdom of crowds. Random House Digital, Inc. 151

Taleb, N. N., 2010. The black swan: The impact of the highly improbable. Random House Trade Paperbacks. 129

Tregonning, K., Roberts, A., 1979. Complex systems which evolve towards homeostasis. 2

Turing, A. M., 1952. The chemical basis of morphogenesis. Philosophical Transactions of the Royal Society of London. Series B, Biological Sciences 237 (641), 37–72. 8, 25, 27

Turner, J. S., 2009a. The extended organism: the physiology of animal-built structures. Harvard University Press. 18

Turner, J. S., 2009b. The tinkerer's accomplice: how design emerges from life itself. Harvard University Press. 18

Vernadski, V. I., McMenamin, M. A., 1998. The Biosphere. A Peter N. Nevraumont book. Copernicus.
URL http://books.google.co.kr/books?id=nUWsbRh5c7cC 29

Von Bertalanffy, L., 1968. General system theory: Foundations, development, applications. George Braziller New York. 2, 14

von Bloh, W., Block, A., Schellnhuber, H. J., 1997. Self-stabilization of the biosphere under global change: a tutorial geophysiological approach. Tellus B 49 (3), 249–262. 3, 4, 6, 7, 9, 31, 55

Walsh, T., 1999. Search in a small world. In: International Joint Conference on Artificial Intelligence. Vol. 16. Lawrence Erlbaum Associates Ltd, pp. 1172–1177. 39

Ward, M., 2002. Beyond chaos: The underlying theory behind life, the universe, and everything. Thomas Dunne Books. 157

Watson, A. J., Lovelock, J. E., 1983. Biological homeostasis of the global environment: the parable of daisyworld. Tellus B 35 (4), 284–289. 3, 7, 29, 45, 55, 75

Watts, D. J., 1999. Networks, dynamics, and the small-world phenomenon. American Journal of Sociology 105 (2), 493–527. 39, 40

Watts, D. J., 2003. Small worlds: the dynamics of networks between order and randomness. Princeton University Press, Princeton, NJ, USA. 40

Watts, D. J., 2004. Six degrees: The science of a connected age. WW Norton & Company. 24, 130

Watts, D. J., Strogatz, S. H., 1998. Collective dynamics of small-world networks. Nature 393 (6684), 440–442. 9, 21, 38, 103, 122

White, C., Selkoe, K. A., Watson, J., Siegel, D. A., Zacherl, D. C., Toonen, R. J., 2010. Ocean currents help explain population genetic structure. Proceedings of the Royal Society B: Biological Sciences 277 (1688), 1685. 9

Wilkinson, D. M., 2003. The fundamental processes in ecology: a thought experiment on extraterrestrial biospheres. Biological Reviews 78 (2), 171–179. 31

Wood, A. J., Ackland, G. J., Dyke, J. G., Williams, H. T. P., Lenton, T. M., 2008. Daisyworld: a review. Reviews of Geophysics 46 (1). 32, 45, 51, 76, 100, 118

Wright, D., Meadows, D. H., 2012. Thinking in systems: a primer. Routledge. 14

Yanagita, T., Kaneko, K., 1993. Coupled map lattice model for convection. Physics Letters A 175 (6), 415–420. 37

Yanagita, T., Kaneko, K., 1997. Modeling and characterization of cloud dynamics. Physical Review Letters 78 (22), 4297–4300. 37

Acknowledgements

First of all, I am extremely thankful to my supervisor Prof. Robert Ian Mckay for offering me the opportunity to pursue PhD. at Structural Complexity Lab. I am very greatly indebted to him for giving me the freedom to engage in research which has changed the way I look at the world. I also extend my sincere thanks to Prof. Byoung-Tak Zhang and Prof. Akira Namatame for their advice.

I would like to acknowledge the support provided by Basic Science Research Program of the National Research Foundation of Korea (NRF), Brain Korea 21 (BK21) program of Ministry of Education, Science and Technology (MEST), the Institute for Computer Technology (ICT) at Seoul National Univ. and the scholarship provided by the Computer Science Dept. of Seoul National Univ. I also would like to thank Ilun Science and Technology Foundation for their generous support especially the CEO of JUSUNG Engineering Co.,Ltd., Mr. Sang-Hoon Jung and Mr. An Sung-Moo.

A very special thanks to Dr. Kim MinHyeok for all his extremely wonderful support during my research period. I thank Dr. Kim Dong-Kyun for his mentorship during the initial phase of my research. I thank Dr. Lee Yun-Geun for informing about Ilun scholarship. I thank Dr. Kim Kang Il for his unique friendship.

I gratefully acknowledge all my other colleagues at SC lab Mr. Cho Hanggjun, Mr. Noh Junhyug, Mr. Shin Haisoo, Mr. Song Jinho, Mr. Hong Changwan, Mr. Kim Juho, Mr. Hong Won Wook, Mr. Park Namyong, Mr. Oh In Soo and Mr. Pham Minh Tuan for their kindness and assistance.